Wavefields and Reciprocity

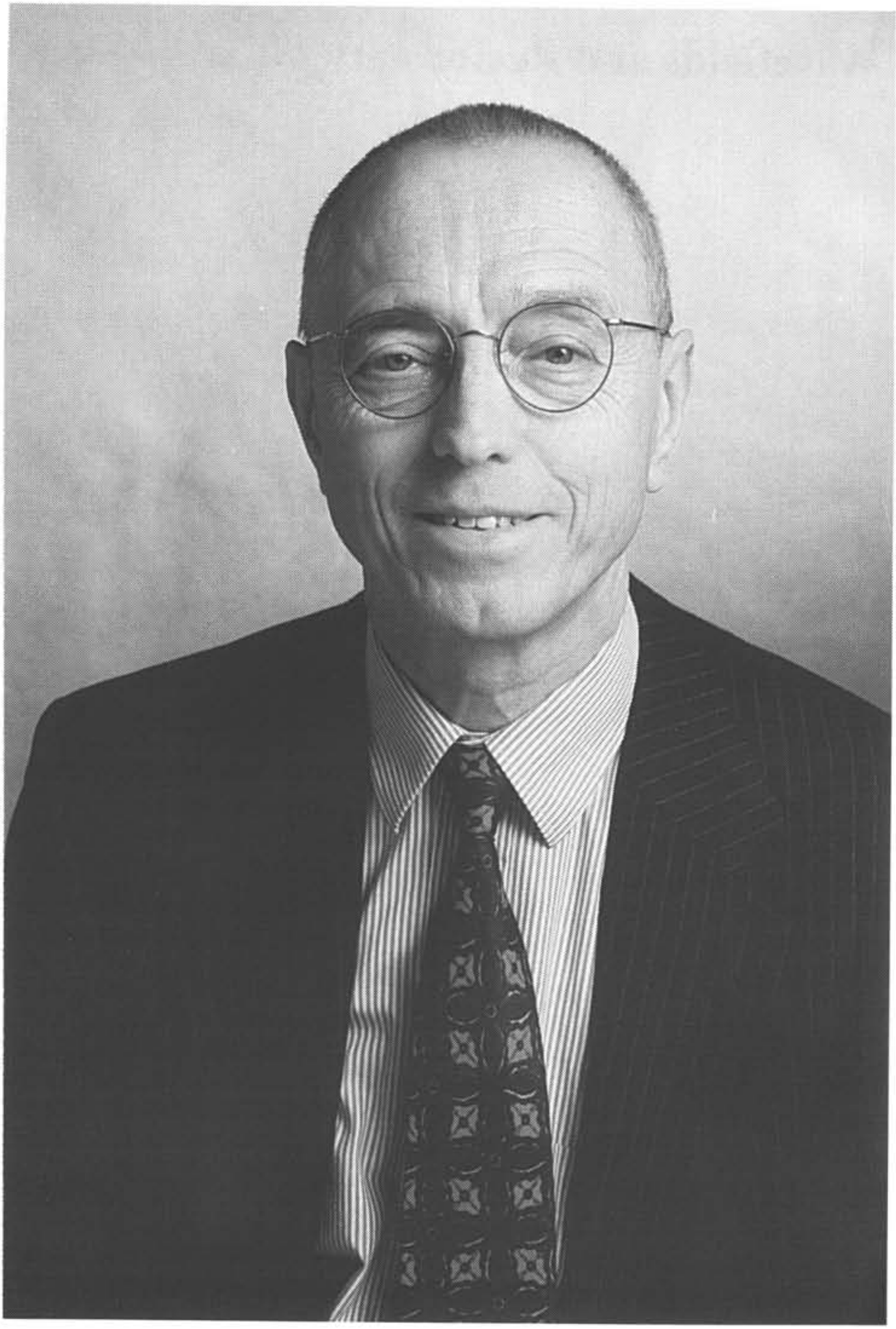

Adrianus T. de Hoop

Wavefields and Reciprocity

Proceedings of a Symposium held in honour of Professor dr. A.T. de Hoop November 20–21, 1996, Delft, the Netherlands

edited by

P.M. van den Berg, H. Blok and J.T. Fokkema
Centre for Technical Geoscience, Delft University of Technology
Delft, the Netherlands

1996

Delft University Press

Published and distributed by:
Delft University Press
Mekelweg 4, 2628 CD Delft,
the Netherlands
Telephone + 31 15 2783254
Fax + 31 15 2781661

By order of:
Laboratory of Electromagnetic Research
Faculty of Electrical Engineering
Delft University of Technology
P.O. Box 5031, 2600 GA Delft,
the Netherlands
Telephone + 31 15 2786620
Fax + 31 15 2786194

Cover: Illustration of H.A. Lorentz by Jan Veth del. 1899. Taken by permission from H.A. Lorentz, Collected papers, Volume IX, Martinus Nijhof, The Hague, the Netherlands, 1939.

CIP-DATA KONINKLIJKE BIBLIOTHEEK, DEN HAAG

Wavefields

Wavefields and Reciprocity / ed.: P.M. van den Berg, H. Blok, J.T. Fokkema.
- Delft : Delft University Press. - Ill.
Proceedings of a Symposium held in honour of Professor dr. A.T. de Hoop,
November 20-21, 1996, Delft, the Netherlands. With lit.
ISBN 90-407-1402-9
Subject headings: reciprocity; scattering; inversion.

Printed in the Netherlands

Preface

Adrianus Teunis de Hoop was born in Rotterdam, the Netherlands, on December 24, 1927. He studied at the Delft University of Technology, where he graduated in electrical engineering in 1950. In 1950 he joined the scientific staff of the Faculty of Electrical Engineering in Delft, interrupted for two years by his military service as reserve officer in the Royal Netherlands Navy. On a leave of absence during the academic year 1956–1957 as research assistant at the Institute of Geophysics, University of California, Los Angeles, California, U.S.A., the foundations of his celebrated work, part of which later became known as the Cagniard-De Hoop technique, were laid. This work became part of his doctoral thesis, which he completed under J.P. Schouten in 1958. In 1960, at the age of 32 years, he was appointed Professor of Electromagnetic Theory and Applied Mathematics at the Delft University of Technology. In 1966–1967, De Hoop was on leave of absence at Philips Research Laboratory, Eindhoven, the Netherlands, performing research on magnetic recording theory. During 1978 through 1980, he served as part-time professor at the Eindhoven University of Technology. From 1982 on, De Hoop has on a regular basis been Visiting Scientist at Schlumberger-Doll Research, Ridgefield, Connecticut, U.S.A., and Schlumberger Cambridge Research, Cambridge, U.K., involved in research on electromagnetic and acoustic borehole problems and seismic problems, respectively.

In 1982, the State University of Ghent, Belgium, conferred an honorary doctorate in applied sciences upon Professor De Hoop. In 1989, he was awarded the Gold Research Medal ("Speurwerkprijs") of the Royal Institution of Engineers in the Netherlands for his contributions to seismic wave theory. Since 1989, De Hoop has been a Member of the Royal Netherlands Academy of Arts and Sciences. In 1986, 1989 and 1990, he was recipient of awards from the Stichting Fund for Science, Technology and Research (a companion organization to the Schlumberger Foundation in the U.S.A.). He also obtained financial grants from Schlumberger-Doll Research, Ridgefield, Connecticut, U.S.A., Schlumberger Cambridge Research, Cambridge, U.K., and from Etudes et Production Schlumberger, Clamart, France.

Professor De Hoop has held many professional positions throughout his career: Member of the Council of the Netherlands Organization for the Advancement of Pure Research (Z.W.O.); from 1975 to 1982 a member of its Governing Board. He was a consultant of Philips Research Laboratories, Eindhoven. He has been and is a member of the editorial boards of Applied Scientific Research, Wave Electronics, Wave Motion and Inverse Problems.

Professor De Hoop was and is an excellent teacher. His lectures were clear, always firmly based on physical foundations with emphasis on proper mathematical formulations. De Hoop was able to make difficult problems look simple for students, without compromising on their mathematical and physical aspects. He produced a wide series of excellent lectures notes on many aspects of electromagnetics, acoustics and elastodynamics, also notes on special topics in mathematics and electrical engineering, such as Wiener-Hopf methods, asymptotics, magnetic recording and, more recently, electromagnetic compatibility and interference. He has published two books: a textbook for students in Dutch, "Theorie van het elektromagnetische veld", Delft University Press, 1975, and his magnum opus, *Handbook of Radiation and Scattering of Waves*, Academic Press, London, 1995, in which a lifetime of teaching and research on acoustic waves, elastic waves and electromagnetic waves has been presented in a very concise style using the subscript notation as an interdisciplinary notational tool.

Over the course of forty years, De Hoop has authored and co-authored around seventy papers in international journals. He has supervised a succession of (22) research students, whose research topics have been well chosen both for their applicability and their educational value, in a wide range of styles from heavily analytical to purely numerical, and mostly a well-balanced combination of the two.

Professor De Hoop is the founder of the Laboratory of Electromagnetics at the Faculty of Electrical Engineering of the Delft University of Technology. His outstanding scientific leadership has over the years gained the laboratory the status of one of the leading groups in electromagnetic research in Europe. On December 31, 1996, the official involvement of Professor A.T. de Hoop with the Delft University of Technology comes to an end. By then, he will have served for 36 years as a full Professor of Electromagnetic Theory and Applied Mathematics. His colleagues and former students want to give special meaning to this occasion by holding a symposium in his honour. A symposium dedicated to Adrianus T. de Hoop, an outstanding professor whose teaching and commitment inspired all the students he taught, within the university and beyond. Not only at the end of 1996 will Professor De Hoop be 69 years young, it will also then be 100 years ago that H.A. Lorentz published his famous paper on reciprocity. Knowing Professor De Hoop's fascination with this theorem and its consequences for the solution of wavefield problems, the theme of the symposium has been chosen to be *Wavefields and Reciprocity.*

Peter M. van den Berg
Hans Blok
Jacob T. Fokkema

Contents

Some uses (and abuses) of reciprocity in wavefield inversion

Michael L. Oristaglio and **Tarek M. Habashy**
Schlumberger-Doll Research
Old Quarry Road, Ridgefield, Connecticut 06877-4108, U.S.A.

Abstract

Fields and their partial derivatives interact in the reciprocity theorems of convolution and correlation type to produce not only elegant formulas, but also fast algorithms for wavefield inversion. Equations for the partial derivatives of the fields follow from differentiating Maxwell's equations with respect to material properties. When coupled with the fields themselves in a (global) reciprocity theorem, difference terms and the surface integral vanish leaving just the interaction of sources and fields in the two states. Convolutional reciprocity thus gives expressions for partial (or Frechet) derivatives of the field with respect to medium properties. A generalization gives partial derivatives with respect to parameters defining the geometry of the medium. Correlational reciprocity between the partial derivative field and a time-reversed adjoint state gives an expression for the gradient of an error functional, which is the sum of squared differences between measured and computed fields. This expression calculates the gradient from two forward modeling runs; it also resembles the formula for seismic migration. It *becomes* the formula for seismic migration when the functional is the flow of power (flux of the Poynting vector) in the residual (scattered) fields across the surface where measurements are made. Neither the gradient algorithm nor seismic migration inverts the equations of linearized scattering (Born approximation), but a small modification provides an approximate inverse.

1. Introduction

Reciprocity plays a curious role in the analysis and solution of inverse problems for wavefields. It is fundamental—as De Hoop and his colleagues have shown in a beautiful series of papers applying reciprocity theorems to (forward and) inverse problems for wavefields (De Hoop, 1987; De Hoop, 1991; De Hoop and Stam, 1988; Blok and Zeijlmans, 1987; De Hoop and De Hoop, 1995). And it is superfluous—as many others have shown by happily solving inverse problems for wavefields without any direct mention of reciprocity. It seems that wavefield reciprocity itself exists in two different states: its uses and its abuses![1] We aim here to help reconcile these states by considering some uses of reciprocity in wavefield inversion and pointing out what (we think) is its proper role and why it is often overlooked or misconstrued. We consider first the key component of any inverse method, the calculation of partial derivatives

[1]This situation, however, does not violate a reciprocity theorem because the two states never occupy the same space-time domain.

of field quantities with respect to model parameters (also called sensitivity functions or Frechet derivatives). Next we discuss how reciprocity leads to fast algorithms for computing the gradient of nonlinear least-squares functionals in the optimization method of wavefield inversion. Finally, we compare gradient methods with Born (or distorted-wave Born) inversion and seismic migration.

The examples draw on our work with electromagnetic fields in the earth, where conduction currents usually dominate in Maxwell's equations, but displacement currents can be important (and dispersion and anisotropy, though sometimes important, are usually ignored). The notation and conventions are, with minor changes, those of the *Handbook of Radiation and Scattering of Waves* (De Hoop, 1995). The inspiration is all Adrian's.

2. Basic equations and notation

To show our notation, we collect here basic formulas used in the sections that follow. We work mainly with Maxwell's equations in the time-domain,

$$\begin{aligned} \partial_t D_k - \varepsilon_{kij}\partial_i H_j &= -J_k, \\ \varepsilon_{kij}\partial_i E_j + \partial_t B_k &= -K_k, \end{aligned} \tag{1}$$

where $\partial_t = \partial/\partial t$ denotes the partial derivative with respect to time; $\partial_i = \partial/\partial x_i$ is the partial derivative with respect to a (Cartesian) spatial coordinate x_i (where $i = 1$, 2, or 3); ε_{kij} is the anti-symmetric Levi-Civita tensor; and the field symbols have their usual meaning (De Hoop, 1995). The summation convention applies over repeated indices (sometimes we write summations explicitly to avoid confusion).

In a linear, time-invariant, isotropic, and locally reacting medium, the constitutive relations are convolutions,

$$D_i(x,t) = \epsilon(x,t)*E_i(x,t) = \int_{-\infty}^{\infty} \hat{\epsilon}(x,t-t')E_i(x,t')\,dt', \tag{2}$$

$$B_i(x,t) = \mu(x,t)*H_i(x,t) = \int_{-\infty}^{\infty} \mu(x,t-t')H_i(x,t')\,dt', \tag{3}$$

where $\hat{\epsilon}$ is the medium's permittivity (or dielectric function) and μ is its permeability. (At the risk of some confusion, we do not use boldface characters for position vectors such as $x = \sum_i x_i \hat{e}^{(i)}$, where $\{\hat{e}^{(1)}, \hat{e}^{(2)}, \hat{e}^{(3)}\}$ are unit vectors in the three Cartesian coordinate directions.) We will consider media with constitutive parameters that vary in space, but have simple time-dependence: μ is instantaneously reacting, and $\hat{\epsilon}$ splits into pure dielectric and conductive parts,

$$\begin{aligned} \mu(x,t) &= \mu(x)\delta(t), \\ \hat{\epsilon}(x,t) &= \epsilon(x)\delta(t) + \sigma(x)\theta(t), \end{aligned} \tag{4}$$

where $\theta(t)$ is the Heaviside step-function. The time-dependent Maxwell's equations become

$$\begin{aligned} \epsilon(x)\partial_t E_k + \sigma(x)E_k - \varepsilon_{kij}\partial_i H_j &= -J_k, \\ \varepsilon_{kij}\partial_i E_j + \mu(x)\partial_t H_k &= -K_k. \end{aligned} \tag{5}$$

2.1. Green functions

Solutions of Maxwell's equations (5) can be formally written using dyadic (tensor) Green functions,

$$\begin{aligned} E_k(x,t) &= \int_V G^{EJ}_{kk'}(x,x',t)*J_{k'}(x',t)dx' + \int_V G^{EK}_{kk'}(x,x',t)*K_{k'}(x',t)dx', \\ H_k(x,t) &= \int_V G^{HJ}_{kk'}(x,x',t)*J_{k'}(x',t)dx' + \int_V G^{HK}_{kk'}(x,x',t)*K_{k'}(x',t)dx'. \end{aligned} \tag{6}$$

The meaning of each Green function is clear from these equations: for example, $G^{EJ}_{kk'}(x,x',t-t')$ is the k-th component of the electric field generated by an impulsive point electric-current dipole located at position x', pointing in the k'-direction, and acting at time t'. The Green functions satisfy

$$\begin{aligned} \epsilon(x)\partial_t G^{EJ}_{kk'} + \sigma(x)G^{EJ}_{kk'} - \varepsilon_{kij}\partial_i G^{HJ}_{jk'} &= -\delta_{kk'}\delta(x-x')\delta(t-t'), \\ \varepsilon_{kij}\partial_i G^{EJ}_{jk'} + \mu(x)\partial_t G^{HJ}_{kk'} &= 0, \end{aligned} \tag{7}$$

$$\begin{aligned} \epsilon(x)\partial_t G^{EK}_{kk'} + \sigma(x)G^{EK}_{kk'} - \varepsilon_{kij}\partial_i G^{HK}_{jk'} &= 0, \\ \varepsilon_{kij}\partial_i G^{EK}_{jk'} + \mu(x)\partial_t G^{HK}_{kk'} &= -\delta_{kk'}\delta(x-x')\delta(t-t'), \end{aligned} \tag{8}$$

and (for physical fields) are causal,

$$\left\{G^{EJ}_{kk'}, G^{HJ}_{kk'}, G^{EK}_{kk'}, G^{HK}_{kk'}\right\}(x,x',t-t') \equiv 0, \quad \text{if } t < t'. \tag{9}$$

2.2. Reciprocity theorems

We use global (integrated) forms of the two reciprocity theorems of "convolution" and "correlation" type. For derivation (and illumination!) of these theorems, see De Hoop (1987, 1995). The global reciprocity theorem of convolution type for Maxwell's equations (5) in domain V bounded by surface S is

$$\begin{aligned} \int_S dx\, \hat{\upsilon}_k \epsilon_{kij}\Big(E^a_i * H^b_j - E^b_i * H^a_j\Big) = \\ + \int_V dx\, \left[(\mu^b - \mu^a)\partial_t(H^b_j * H^a_j) - (\epsilon^b - \epsilon^a)\partial_t(E^b_i * E^a_i) - (\sigma^b - \sigma^a)E^b_i * E^a_i\right] \\ + \int_V dx\, \left[H^a_j * K^b_j - H^b_j * K^a_j - E^a_i * J^b_i + E^b_i * J^a_i\right], \end{aligned} \tag{10}$$

where $\{E^a_i, H^a_j\}$ and $\{E^b_i, H^b_j\}$ are two states occupying the space-time domain with corresponding material properties $\{\epsilon^a, \sigma^a, \mu^a\}$ and $\{\epsilon^b, \sigma^b, \mu^b\}$; $\hat{\upsilon}_k$ is the outward unit

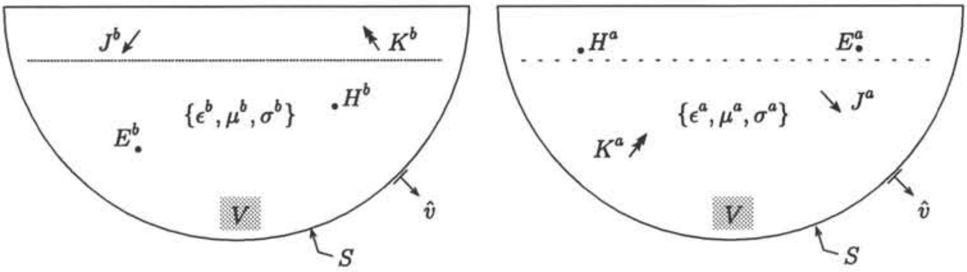

Figure 1. Two different states (fields, media, and sources) occupy the same space-time domain and interact in a reciprocity theorem.

normal to S (Figure 1). We will arrange states in our use of (10) so that the surface integral and the terms involving material properties vanish, leaving only the interaction of fields and sources in the two states:

$$\int_V dx \int_{-\infty}^{\infty} \left[H_j^a(x, t-t') K_j^b(x,t') - H_j^b(x,t-t') K_j^a(x,t') \right] dt' =$$

$$\int_V dx \int_{-\infty}^{\infty} \left[E_i^a(x, t-t') J_i^b(x,t') - E_i^b(x,t-t') J_i^a(x,t') \right] dt'. \qquad (11)$$

Although a reciprocity theorem of correlation type is easily derived for Maxwell's equations (5), it is more instructive to work first with the general Maxwell's equations (1). The global reciprocity theorem of correlation type for (1) is

$$\begin{aligned}\int_S dx\, \hat{v}_k\, \epsilon_{kij} \left(E_i^a * \overline{H_j^b} + \overline{E_i^b} * H_j^a \right) = \\ + \int_V dx\, \partial_t \left[\left(\overline{\mu^b} - \mu^a \right) * H_j^a * \overline{H_j^b} + \left(\overline{\hat{\epsilon}^b} - \hat{\epsilon}^a \right) * E_i^a * \overline{E_i^b} \right] \\ - \int_V dx \left[H_j^a * \overline{K_j^b} + K_j^a * \overline{H_j^b} + E_i^a * \overline{J_i^b} + J_i^a * \overline{E_i^b} \right], \qquad (12)\end{aligned}$$

where, as in De Hoop (1995), all time correlations appear as convolutions with the time-reversed state,

$$\overline{F}(x,t) = F(x,-t), \qquad (13)$$

since

$$G(x,t) * \overline{F}(x,t) = \int_T G(x, t-t') \overline{F}(x,t') dt' = \int_T G(x,t+t') F(x,t') dt'. \qquad (14)$$

When the terms not involving sources vanish (we will show below what this means in practice when one state satisfies Maxwell's equations (5), the reciprocity theorem (12) becomes

$$\int_V dx \int_{-\infty}^{\infty} \left[H_j^a(x,t+t') K_j^b(x,t') + K_j^a(x,t+t') H_j^b(x,t') \right] dt' =$$

$$- \int_V dx \int_{-\infty}^{\infty} \left[E_i^a(x, t+t') J_i^b(x, t') + J_i^a(x, t+t') E_i^b(x, t') \right] dt'. \quad (15)$$

3. Reciprocity and sensitivity

Give me a (partial) derivative and I will invert the world
—Newton (ca. 1670)

Early methods of inversion for electromagnetic fields in the earth (see Jupp and Vozoff, 1977; Oristaglio and Worthington, 1980; and Hohmann and Raiche, 1987, for a general review) were essentially applications of Newton's method for solving nonlinear equations. Models were defined by a small number (< 100) of parameters. Newton's method in outline is:

$$F_i(m) = d_i, \quad i = 1, \ldots, N; \quad (16)$$

$$F_i(m^{(0)}) + \sum_j \frac{\partial F_i}{\partial m_j} \delta m_j \simeq d_i; \quad (17)$$

$$J_{ij} \delta m_j \simeq \delta d_i; \quad (18)$$

$$\delta m_k \simeq J_{ki}^+ \delta d_i, \quad (19)$$

where $J_{ij} = \partial F_i / \partial m_j$ is the "Jacobian", the matrix of partial derivatives of model functions F_i with respect to parameters m_j, and J^+ indicates a generalized inverse of J. We use the shorthand notation,

$$F_i(m) \equiv F_i(m_1, m_2, \ldots, m_M); \quad (20)$$

$m^{(0)}$ is an initial model. For nonlinear inversion, the process is iterated in the standard way: $m^{(0)} \to m^{(0)} + \delta m$ and the steps are repeated.

The Jacobian J_{ij} is the heart of Newton's method; it is also useful in optimizing experimental designs and investigating the propagation of errors from data to model. Reciprocity theorems give elegant expressions for its elements (the partial derivatives). We follow the approach outlined by McGillivray et al. (1994). Let the medium parameters of the model be defined by expansions in basis functions:

$$\sigma(x) = \sum_n \sigma_n \phi_n(x), \quad \epsilon(x) = \sum_n \epsilon_n \phi_n(x), \quad \mu(x) = \sum_n \mu_n \phi_n(x). \quad (21)$$

All field quantities are then functions of the expansion coefficients (model parameters) $\{\sigma_n, \epsilon_n, \mu_n\}$. Equations for the partial derivatives of field quantities with respect to these parameters follow from differentiating Maxwell's equations. For example, partial derivatives of the electric and magnetic fields with respect to (conductivity) parameter σ_n,

$$\partial_{\sigma_n} E_i = \frac{\partial E_i}{\partial \sigma_n}, \quad \text{and} \quad \partial_{\sigma_n} H_j = \frac{\partial H_j}{\partial \sigma_n}, \quad (22)$$

Table 1. Partial (Frechet) derivative fields and their sources

Frechet Derivative		Source
$\partial_{\sigma(x')}\{H_i, E_j\}$	$\longleftrightarrow$	$J_k = E_k(x',t)\,\delta(x-x')$
$\partial_{\epsilon(x')}\{H_i, E_j\}$	$\longleftrightarrow$	$J_k = \partial_t E_k(x',t)\,\delta(x-x')$
$\partial_{\mu(x')}\{H_i, E_j\}$	$\longleftrightarrow$	$K_k = \partial_t H_k(x',t)\,\delta(x-x')$

satisfy

$$\begin{aligned} \epsilon(x)\partial_t(\partial_{\sigma_n}E_k) + \sigma(x)(\partial_{\sigma_n}E_k) - \varepsilon_{kij}\partial_i(\partial_{\sigma_n}H_j) &= -E_k\,\phi_n(x), \\ \varepsilon_{kij}\partial_i(\partial_{\sigma_n}E_j) + \mu(x)\partial_t(\partial_{\sigma_n}H_k) &= 0. \end{aligned} \tag{23}$$

These are just Maxwell's equations with new source terms (sources for the other partial derivative fields are given in Table 1). When the state $\{\partial_{\sigma_n}E_i, \partial_{\sigma_n}H_j\}$ is paired with a computational state $\{E_i^b, H_j^b\}$ (in the same medium) with general source terms,

$$\begin{aligned} \epsilon(x)\partial_t E_k^b + \sigma(x)E_k^b - \varepsilon_{kij}\partial_i H_j^b &= -J_k^b, \\ \varepsilon_{kij}\partial_i E_j^b + \mu(x)\partial_t H_k^b &= -K_k^b, \end{aligned} \tag{24}$$

all terms involving material properties in the reciprocity theorem vanish. The surface integral also vanishes if the states are taken to satisfy the same boundary conditions on a finite surface or causality (radiation) conditions in an unbounded medium (the boundary conditions on a finite surface can have very general form, see McGillivray et al., 1994). Only terms involving sources in the two states remain:

$$\begin{aligned} \int_V dx \int_{-\infty}^{\infty} \left[\partial_{\sigma_n}H_j(x,t-t')K_j^b(x,t') - \partial_{\sigma_n}E_i(x,t-t')J_i^b(x,t')\right] dt' = \\ -\int_V dx\,\phi(x) \int_{-\infty}^{\infty} E_k^b(x,t-t')E_k(x,t')dt'. \end{aligned} \tag{25}$$

The computational state can pick out specific partial derivatives. The partial derivative of the z-component (x_3-component) of the magnetic field at location[1] x_R is selected with the computational state of a point magnetic dipole at position x_R, pointing in the x_3-direction,

$$\begin{aligned} J_i^b(x,t) &= 0, \\ K_j^b(x,t) &= \delta_{j3}\delta(x-x_R)\delta(t), \\ E_k^b(x,t) &= G_{k3}^{EK}(x,x_R,t). \end{aligned} \tag{26}$$

[1]Lack of boldface can cause confusion here. The subscript on x_R labels receiver positions (vectors!), not coordinate components of the vector x; similarly, x_S will indicate different source positions. Subscript i or $\{1,2,3\}$ are used exclusively used for coordinate components of position vector x.

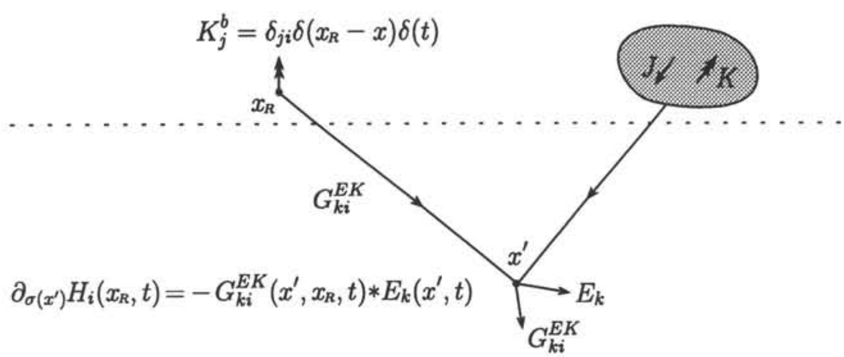

Figure 2. Physical picture in the reciprocal formula for the partial (Frechet) derivative: A magnetic current dipole source at the location of the receiver radiates an electric field into the medium which interacts (via an inner product and convolution) with the physical electric field.

Thus,

$$\partial_{\sigma_n} H_3(x_R, t) = -\int_V dx\, \phi(x) \int_{-\infty}^{\infty} G_{k3}^{EK}(x, x_R, t-t') E_k(x, t') dt'. \tag{27}$$

Equation (27) generalizes to any component ($3 \to i$). The derivation also applies when the (expansion) function $\phi(x)$ is a delta-function $\delta(x - x')$, and the partial derivative becomes a Frechet derivative,

$$\partial_{\sigma(x')} H_i(x_R, t) \equiv \frac{\delta H_i(x_R, t)}{\delta\sigma(x')} = -\int_{-\infty}^{\infty} G_{ki}^{EK}(x', x_R, t-t') E_k(x', t') dt'. \tag{28}$$

This formula for the partial derivative has a pleasing interpretation (Figure 2): The partial (or Frechet) derivative of the magnetic field at point x_R with respect to the conductivity at point x' is the "convolutional inner product" of two electric fields: the field E_k at x' in the model (produced by the physical sources) and the field at x' of a (fictious or computational) magnetic current source that is located at receiver position x_R and points in the same direction as the (magnetic field) receiver.

If the physical source itself is a magnetic dipole at position x_S, pointing in the j-direction, then

$$\partial_{\sigma(x')} H_i(x_R, t | x_S, \hat{e}^{(j)}) = -\int_{-\infty}^{\infty} G_{ki}^{EK}(x', x_R, t-t') G_{kj}^{EK}(x', x_S, t') dt', \tag{29}$$

a formula which is perfectly symmetric with respect to source and receiver (as required by reciprocity).

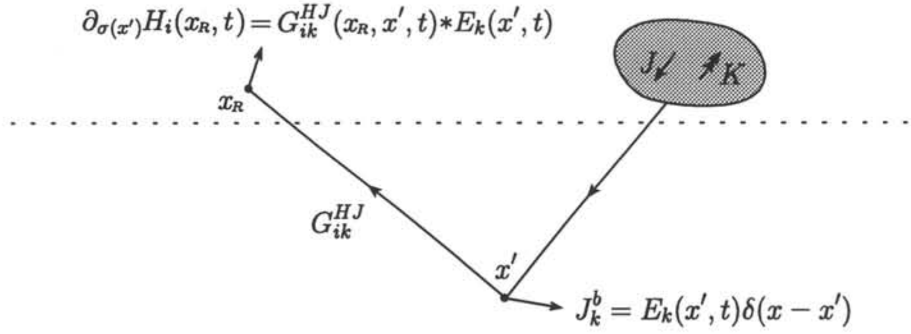

Figure 3. Physical picture in the direct formula for the partial derivative: A point electric current dipole with the amplitude, direction, and time-dependence of the physical electric field at a given point radiates a magnetic field equal to the partial (Frechet) derivative of the physical magnetic field.

Reciprocal formulas such as (28) were little used in the early years of electromagnetic inversion (but see Rodi, 1976). More popular was the "direct" form—e.g.,

$$\partial_{\sigma(x')}H_i(x_R,t) = \int_{-\infty}^{\infty} G_{ik}^{HJ}(x_R,x',t-t')E_k(x',t')dt' \tag{30}$$

—which can be obtained by using symmetry properties of the Green functions (De Hoop, 1995),

$$G_{kj}^{HJ}(x,x',t) = -G_{jk}^{EK}(x',x,t), \tag{31}$$

in (28) or by solving equations (23) directly using the appropriate Green function. Equation (30) also has a pleasing physical interpretation (Figure 3): The partial derivative of the magnetic field with respect to the conductivity at point x' is the field of a point electric current source at x' whose direction, amplitude, and time-dependence is that of the physical electric field at x' in the model.

One sometimes overhears (and gets drawn into!) semi-serious discussions about the relative merits of formulas (28) and (30). Both are (of course) absolutely correct theoretically. Which one is better practically depends on the type of experiment being inverted and the method of computation. Each formula implies that, after the fields in a given model have been computed, partial derivatives of the fields with respect to model parameters can be computed with more forward modeling: either compute the reciprocal field E_k^b (to use in 28) by placing an appropriate point source at position x_R, or compute directly the partial derivative field by placing an appropriate point source at x'. When modeling is done by a finite-difference (or finite-element) code, where each run gives the field at all locations in space, the yields of these two approaches are very different. On the one hand, computing the reciprocal state E_k^b will give everything needed to obtain the partial derivatives of the field at *one location* x_R

with respect to *all model parameters*. On the other hand, computing the partial derivative field directly (by solving 23) gives the partial derivative of the field at *all locations* with respect to *one model parameter* $\sigma(x')$. The direct form (30) is obviously "better" (in full-field modeling) when receivers outnumber model parameters—i.e., for overdetermined models (more data than unknowns), which were typical in early applications of inversion. The reciprocal form (28) is better when model parameters outnumber receivers—i.e., for over-parameterized models (more unknowns than data), which are now in fashion, along with sophisticated regularization (Van den Berg and Kleinman, 1995). It is worthwhile to master both ways of computing (and thinking).

3.1. Derivatives with respect to geometry

A further application of the above methods, which does not seem to be widely known, is calculating partial derivatives with respect to model geometry, such as the locations and shapes of interfaces between regions of constant material properties. This can be handled by taking derivatives of the basis functions in the expansions (21). Some care is needed in interpreting the results. For example, in a layered model, where only the conductivity changes across interfaces z_n (ϵ and μ are constant), we can write:

$$\sigma(x) = \sum_n \sigma_n \left[\theta(x_3 - z_{n-1}) - \theta(x_3 - z_n)\right] \tag{32}$$

where z_n is the interface between the layers $(n-1)$ and n, and

$$\partial_{z_n}\sigma = (\sigma_n - \sigma_{n-1})\delta(x_3 - z_n). \tag{33}$$

Proceeding (naively) as above gives

$$\begin{aligned} \partial_{z_n} H_i(x_R, t) &= -\int_V dx\, [\partial_{z_n}\sigma(x)]\, G_{ki}^{EK}(x, x_R, t) * E_k(x, t) \\ &= -(\sigma_n - \sigma_{n-1}) \int_V dx\, \delta(x_3 - z_n) G_{ki}^{EK}(x, x_R, t) * E_k(x, t). \end{aligned} \tag{34}$$

The delta-function picks out an integral over the interface $(x_1, x_2, x_3 = z_n)$,

$$\int_V dx\, \delta(x_3 - z_n) F(x) = \iint dx_1 dx_2\, F(x_1, x_2, x_3 = z_n).$$

Equation (34), however, is not well defined, because some fields are discontinous at the interface (normal components of the electric field, e.g., when conductivity is discontinous).

The problem with (34) is easier to fix in the frequency domain, with harmonic $\exp(-i\omega t)$ time dependence. First, write

$$\partial_{z_n} H_i(x_R, \omega) = -\int_V dx\, \left[\partial_{z_n}\hat{\sigma}(x, \omega)\right] G_{ki}^{EK}(x, x_R, \omega) E_k(x, \omega), \tag{35}$$

where $\hat{\sigma} = (\sigma - i\omega\epsilon)$ is the complex conductivity, whose real part is given by the expansion above. Next, separate terms that are continuous and those that are discontinous at the interface, and introduce the complex resistivity $\hat{\rho}(x, \omega) = 1/\hat{\sigma}(x, \omega)$

to remove the discontinuities, using $\hat\sigma^2\partial_{z_n}\hat\rho = -\partial_{z_n}\hat\sigma$,

$$\begin{aligned}
\partial_{z_n} H_i(x_R,\omega) &= -\sum_{k=1}^{2}\int_V dx\ [\partial_{z_n}\hat\sigma(x,\omega)]\, G^{EK}_{ki}(x,x_R,\omega)E_k(x,\omega) \\
&\quad + \int_V dx\ [\partial_{z_n}\hat\rho(x,\omega)]\left[\hat\sigma(x,\omega)G^{EK}_{3i}(x,x_R,\omega)\right][\hat\sigma(x,\omega)E_3(x,\omega)] \\
&= -(\sigma_n-\sigma_{n-1})\sum_{k=1}^{2}\int_V dx\,\delta(x_3-z_n)G^{EK}_{ki}(x,x_R,\omega)E_k(x,\omega) \\
+[\hat\rho_n(\omega)-\hat\rho_{n-1}(\omega)]&\int_V dx\,\delta(x_3-z_n)\left[\hat\sigma(x,\omega)G^{EK}_{3i}(x,x_R,\omega)\right][\hat\sigma(x,\omega)E_3(x,\omega)]\,. \quad (36)
\end{aligned}$$

Now all quantities in the integral over the interface (picked out by the delta function) are continuous.

We can generalize this result to give the Frechet derivative of the field with respect to variation of a point on an interface defined by the surface $x_3 = z(x_1,x_2)$, where the conductivity changes by

$$\sigma(x) = \sigma_1 + (\sigma_2-\sigma_1)\theta[x_3 - z(x_1,x_2)]. \quad (37)$$

Applying an analysis similar to the one above gives

$$\begin{aligned}
\partial_{z(x_1,x_2)}H_i(x_R,\omega) &= -(\sigma_2-\sigma_1)\varepsilon_{klj}\hat v_l G^{EK}_{ji}(x,x_R,\omega)\varepsilon_{kpq}\hat v_p E_q(x,\omega)\Big|_{(x_1,x_2,x_3=z)} \\
+[\hat\rho_2(\omega)-\hat\rho_1(\omega)]&\left[\hat\sigma(x,\omega)\hat v_k G^{EJ}_{ki}(x,x_R,\omega)\right][\hat\sigma(x,\omega)\hat v_p E_p(x,\omega)]\Big|_{(x_1,x_2,x_3=z)}, \quad (38)
\end{aligned}$$

where $\hat v_k$ is the unit normal to the surface at the point $x = (x_1, x_2, x_3 = z)$. It is a challenge to derive these equations working only in the space-time domain.

4. Reciprocity and optimization

Give me a (conjugate) gradient and I will invert the world
—Tarantola (ca. 1980)

Each iteration of wavefield inversion by Newton's method is equivalent to inverting the Born approximation[1] about the current model $m^{(0)}$. This is easily seen from the continuous version of (17) involving the Frechet derivative,

$$H_i(x_R,t) \simeq H_i^{(0)}(x_R,t) + \int_V \partial_{\sigma(x')}H_i(x_R,t)\delta\sigma(x')dx', \quad (39)$$

Substituting the expression for the Frechet derivative in this equation gives the Born (or distorted-wave Born) approximation for the magnetic field.

Newton's method is also closely related to a general least-squares approach to inversion, which seeks model parameters that minimize the (nonlinear) sum-of-squares,

$$L(m) = \sum_i [d_i - F_i(m)]^2\,. \quad (40)$$

[1]Since $m^{(0)}$ changes with each iteration, the background model becomes spatially inhomogeneous, and "distorted-wave Born approximation" is the more appropriate term. See, e.g., Taylor (1972).

The gradient of L involves the Jacobian matrix,

$$\begin{aligned}\frac{\partial L}{\partial m_j} &= -2\sum_i [d_i - F_i(m)]\,\frac{\partial F_i}{\partial m_j} \\ &= -2J_{ij}\delta d_i = -2J^T_{ji}\delta d_i,\end{aligned} \tag{41}$$

where J^T is the transpose of J. Setting the gradient to zero (the condition for a local minimum) gives the nonlinear equations,

$$\sum_i \frac{\partial F_i}{\partial m_j}(m^{(0)} + \delta m)\left[d_i - F_i(m^{(0)} + \delta m)\right] = 0, \quad j = 1, \ldots, M. \tag{42}$$

Newton's method applied to these gradient equations gives

$$\left(J^T_{ji}J_{ik} - H_{jk}\right)\delta m_k = J^T_{ji}\delta d_i, \tag{43}$$

where H_{jk} is the matrix ("Hessian"),

$$H_{jk} = \sum_i \frac{\partial^2 F_i}{\partial m_j \partial m_k}\delta d_i, \tag{44}$$

involving second partial derivatives of F. If the Hessian is dropped, equations (43) are just the normal equations for a least-squares solution of (18),

$$J^T_{ji}J_{ik}\delta m_k \simeq J^T_{ji}\delta d_i. \tag{45}$$

When these steps are iterated in the standard way, the algorithm is called the "Gauss-Newton" method of nonlinear least squares (Gill et al., 1981).

Neither Newton's method for (16) nor the Gauss-Newton method for (40) is practical for problems with many unknowns (thousands), as in high-resolution imaging. Often this is attributed to the difficulty of inverting the linear equations (45), whose dimension is the same as the number of unknowns. This is indeed a formidable task when the number of unknowns becomes large, but the number of calculations needed just to form these equations—i.e., to compute the partial derivatives—is larger. In the mid-1980s, however, a breakthrough occurred when it was recognized that reciprocity gives a fast way of computing the right-hand-side of (45), which is (the negative of) the gradient of L. This led to much research, continuing today, into gradient (steepest-descent) or conjugate gradient minimization of L. Tarantola (1984a, 1984b) was the first to propose and implement this approach; the application was inversion of acoustic (later elastic) wavefields in seismic exploration, which is truly a massive inverse problem involving millions of unknowns and billions of data.

Consider how this works for Maxwell's equations (5). Let the data be measurements of the (vector) magnetic field $H^{(d)}(x_R, t)$ as a function of time t at receiver locations x_R. A suitable functional to minimize is

$$\begin{aligned}L[\sigma(x), \epsilon(x), \mu(x)] &= \sum_{x_R}\int_{-\infty}^{\infty} |H^{(d)}(x_R, t) - H(x_R, t)|^2 dt, \\ &= \sum_{x_R}\int_{-\infty}^{\infty} \delta H_i(x_R, t)\delta H_i(x_R, t)dt,\end{aligned} \tag{46}$$

where $\delta H_i = (H_i^{(d)} - H_i)$ is the difference between the measured magnetic field and the magnetic field H_i computed in a model described by (continuous) parameters $\{\sigma(x), \epsilon(x), \mu(x)\}$. The quantities δH_i will be called "data residuals".

The gradient (Frechet derivative) of L with respect to $\sigma(x)$ is

$$\partial_{\sigma(x')} L = -2 \sum_{x_R} \int_{-\infty}^{\infty} \delta H_i(x_R, t) \partial_{\sigma(x')} H_i(x_R, t) dt, \tag{47}$$

(similar expressions apply for the gradients with respect to ϵ and μ). A final expression for the gradient follows from the formulas for the partial derivative derived above. It is instructive, however, to evaluate (47) directly using reciprocity. The integral is the cross-correlation (evaluated at zero lag time) of the data residuals and a partial derivative field, and should thus fit into a reciprocity theorem of correlation type (15). One of the states for the reciprocity theorem clearly must be the partial derivative field and its source. Substituting

$$\begin{aligned} H_i^b &= \partial_{\sigma(x')} H_i(x, t), \\ J_k^b &= E_k(x', t)\delta(x - x'), \\ K_j^b &= 0. \end{aligned}$$

into equation (15) gives

$$\int_V dx \int_{-\infty}^{\infty} K_i^a(x, t) \partial_{\sigma(x)} H_i(x, t) dt = -\int_{-\infty}^{\infty} E_k^a(x', t) E_k(x', t) dt. \tag{48}$$

To get the right cross-correlation on the left-hand-side, the source for state a must be a (point) magnetic dipole source at x_R whose vector amplitude is equal to the data residuals at all time. Let E_k^a be the field of this source,

$$\begin{aligned} K_i^a &= \delta H_i(x_R, t)\delta(x - x_R), \\ J_i^a &= 0, \\ E_k^a &= E_k^a(x, t) \text{ (the field of the source } K_i^a). \end{aligned} \tag{49}$$

Putting these states together gives

$$\int_{-\infty}^{\infty} \delta H_i(x_R, t) \partial_{\sigma(x)} H_i(x_R, t) dt = -\int_{-\infty}^{\infty} E_k^a(x', t) E_k(x', t) dt. \tag{50}$$

We still need to specify exactly how E_k^a is to be defined (and computed) so that other terms in the reciprocity theorem (15) vanish, leaving (50). When the constitutive parameters of state b (the physical state) have the form (4), the terms involving material properties vanish if the parameters of medium a (in which E_k^a propagates) are the time-reverse adjoints of b; i.e.,

$$\begin{aligned} \mu^a(x, t) &= \mu(x)\delta(-t) = \mu(x)\delta(t), \\ \hat{\epsilon}^a(x, t) &= \epsilon(x)\delta(-t) + \sigma(x)\theta(-t), \\ &= \epsilon(x)\delta(t) + \sigma(x)[1 - \theta(t)]. \end{aligned} \tag{51}$$

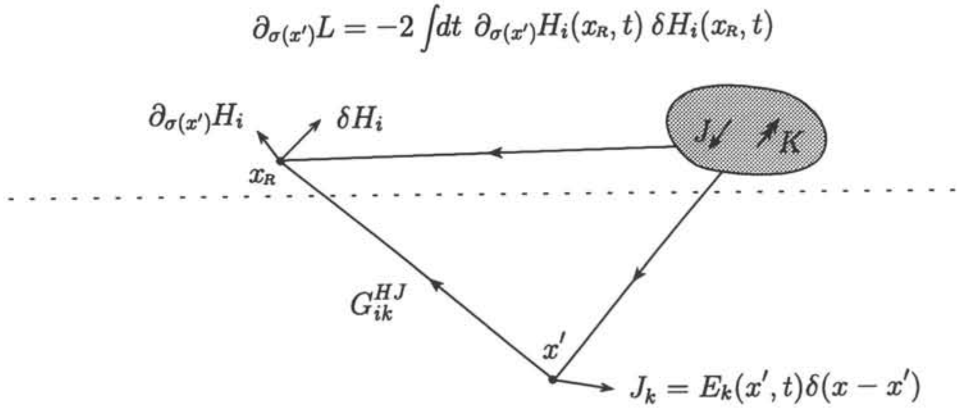

Figure 4. Physical picture in the direct formula for the gradient: The partial derivative magnetic field of Figure 3 propagates to a receiver position and interacts (via an inner product and correlation) with the magnetic field data residual.

The boundary term vanishes if the field in state a is anti-causally related to its sources (because state b is causally related to its sources; see De Hoop, 1995). Substituting the constitutive relations for state a into Maxwell's equations (1), we find that E_k^a is the (anti-causal) solution of the following equations,

$$\begin{aligned}\epsilon(x)\partial_t E_k^a - \sigma(x)E_k^a - \varepsilon_{kij}\partial_i H_j^a &= 0,\\ \varepsilon_{kij}\partial_i E_j^a + \mu(x)\partial_t H_k^a &= -\delta H_k(x_R,t)\delta(x-x_R).\end{aligned} \tag{52}$$

These equations are "adjoint" to Maxwell's equations. They differ from Maxwell's equations only in sign of the conductivity term. For positive conductivity, causal solutions of Maxwell's equation decay exponentially in (forward) time (because of skin effect), whereas solutions of equations (52) grow (exponentially) as time increases. This instability is unimportant, however, because the solution of the equations can easily by computed in reverse time (in a sense, these equations *must* to be computed in reverse time, because the anti-causal solution is needed!). To solve equations (52), start with (zero) final conditions on the field at some arbitrarily large time T (in principle, $T = \infty$) and step "backwards in time", $T \to (T - \delta t)$, e.g., with a FDTD time-stepping code. This reverse time-stepping is stable; in fact, the same modeling code that marches Maxwell's equations forward in time can be used to march the adjoint equations backwards in time (Wang et al., 1995).

4.1. Reciprocity and confusion

Equations (50) and (52) imply that the quantities needed to calculate the gradient of the "error" functional L can be obtained with two modeling runs: One to compute the fields in the current model $E_i(x',t)$ and $H_j(x',t)$, and a second to compute the adjoint fields E_i^a and H_j^a (in reverse time). The computations are (more or less) independent of the number of receiver positions: the sum over receivers in the error functional (46) carries through directly to a sum on the right-hand-side of (52). The same is true for the gradients with respect to μ and ϵ (easily derived from results given above). An open question—related to the global uniqueness of the inverse problem—is whether these gradients are always independent.

Equations (50) and (52) seem to have jumped at us from the mysteries of the reciprocity theorem of correlation type. Because they involve adjoint states and time reversal, strange tales are sometimes told about them—tales of fields traveling backwards in time (and of how to avoid the nightmare of instability), tales of fields "refocussing" perfectly on their (contrast) sources to produce delta-like resolution, even tales of fields violating reciprocity! Most of the mystery vanishes, however, when these formulas are understood in more direct fashion as a shortcut for computing a perfectly stable quantity—involving fields propagating forward in time—that would take ages to compute directly (for large models). To see this, substitute in formula (47) expression (30) for the derivative of the magnetic field with respect to conductivity to give an equivalent expression for the gradient:

$$\partial_{\sigma(x')}L = -2\sum_{x_R} \int_{-\infty}^{\infty} dt\, \delta H_i(x_R,t) \int_{-\infty}^{\infty} G_{ik}^{HJ}(x_R,x',t-t')E_k(x',t')dt'. \tag{53}$$

This equation has a straightforward interpretation (see Figure 4): The partial derivative of L with respect to the variation of conductivity at point x' is the time-correlation (at zero lag time) of two (data) fields: the (actual) data residual $\delta H_i(x_R,t)$ and the (fictitious) data at x_R generated by a point electric-current dipole source located at x' whose amplitude, direction, and time-dependence are that of the electric field at x' in the physical model.

All fields in equation (53) are causal, and the computation is as stable as Maxwell's equations. But computation of the gradient now requires a separate forward modeling run for each point x'. If the gradient is needed at thousands of points (as in imaging), this is impractical. When reciprocity is used, the full gradient appears at all points in just two forward modeling runs (this is still an amazing—if not wholly mysterious—result!).

Derivation of (50) (and 52) does not actually require a reciprocity theorem. It can be obtained from (53) by reversing the order of the time integration, reversing the direction of the time-integral, and using symmetry properties of the Green function (of course, these symmetries embody reciprocity). In detail, the steps are:

$$\begin{aligned}\partial_{\sigma(x')}L &= -2\sum_{x_R} \int_0^{\infty} dt\, \delta H_i(x_R,t) \int_{-\infty}^{\infty} G_{ik}^{HJ}(x_R,x',t-t')E_k(x',t')dt' \\ &= +2\sum_{x_R} \int_{-\infty}^{\infty} dt'\, E_k(x',t') \int_{t'}^{\infty} G_{ik}^{HJ}(x_R,x',t-t')\delta H_i(x_R,t)dt\end{aligned}$$

Table 2. Gradients of the sum-of-squares functional

Gradients

$$\partial_{\sigma(x')}L = -2\sum_{x_R}\int_{-\infty}^{\infty} dt'\, E_k(x',t')\int_{\infty}^{t'} \tilde{G}^{EK}_{ki}(x',x_R,t'-t)\delta H_i(x_R,t)dt$$

$$\partial_{\epsilon(x')}L = -2\sum_{x_R}\int_{-\infty}^{\infty} dt'\, \partial_t E_k(x',t')\int_{\infty}^{t'} \tilde{G}^{EK}_{ki}(x',x_R,t'-t)\delta H_i(x_R,t)dt$$

$$\partial_{\mu(x')}L = -2\sum_{x_R}\int_{-\infty}^{\infty} dt'\, \partial_t H_k(x',t')\int_{\infty}^{t'} \tilde{G}^{HK}_{ki}(x',x_R,t'-t)\delta H_i(x_R,t)dt$$

$$= -2\sum_{x_R}\int_{-\infty}^{\infty} dt'\, E_k(x',t')\int_{\infty}^{t'} \tilde{G}^{EK}_{ki}(x',x_R,t'-t)\delta H_i(x_R,t)dt. \tag{54}$$

The last step actually defines an (anti-causal) adjoint Green function $\tilde{G}^{EK}_{ki}$ with the property,[1]

$$\tilde{G}^{EK}_{ki}(x',x_R,t'-t) = -G^{HJ}_{ik}(x_R,x',t-t'). \tag{55}$$

$\tilde{G}^{EK}_{ki}$ is (naturally) the right Green function for the adjoint Maxwell's equations (52). Expressions for the other gradients are given in Table 2.

4.1.1. One good turn deserves another

The last derivation above hints at another formula for the gradient that can be obtained from a reciprocity theorem of convolution type (banishing anti-causal states). In the convolution theorem (11) (evaluated at zero time), use for state b the partial derivative field and its source:

$$-\int_V dx\int_{-\infty}^{\infty} \partial_{\sigma(x')}H^b_j(x,t)K^a_j(x,-t)dt = \int_{-\infty}^{\infty} E^a_i(x',-t)E_i(x',t)dt \tag{56}$$

If state a is

$$\begin{aligned} K^a_j &= \delta H_j(x_R,-t)\delta(x-x_R),\\ J^a_i &= 0,\\ E^a_i &= E^a_i(x,t) \text{ (the field of the source } K^a_j), \end{aligned} \tag{57}$$

[1]The convention here differs from others (see, e.g., Felsen and Marcuvitz, 1973; Wang et al., 1995) that include a spatial reversal ($x \to -x$) in the adjoint equations, leading to

$$\tilde{G}^{EK}_{ki}(x',x_R,t'-t) = G^{HJ}_{ik}(x_R,x',t-t').$$

The difference is just the sign of the source terms in the adjoint equations.

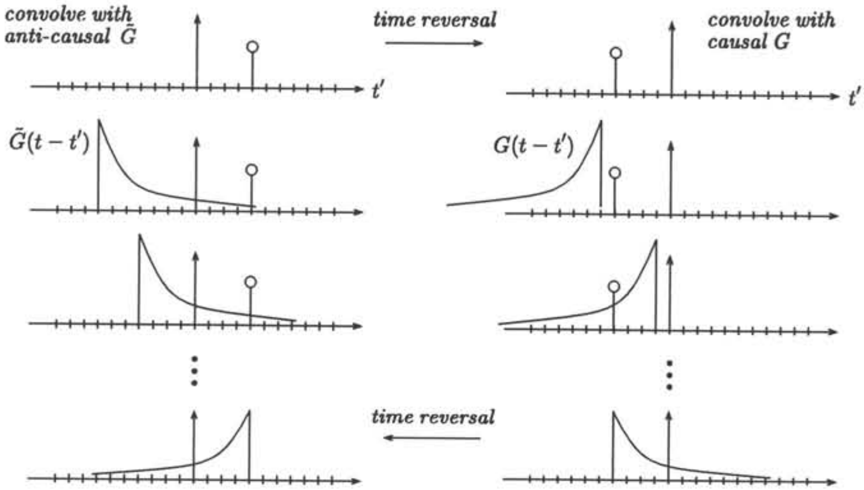

Figure 5. Time reversal of the source and causal propagation, followed by a time reversal of the field, is equivalent to "reverse-time" anti-causal propagation.

where E_i^a satisfies Maxwell's equations (1), equation (56) becomes

$$-\int_{-\infty}^{\infty} \partial_{\sigma(x')} H_j^b(x_R, t)\delta H_j(x_R, t)dt = \int_{-\infty}^{\infty} \overline{E_i^a}(x', t)E_i(x', t)dt. \tag{58}$$

The overbar (as before) indicates a time-reversal, $\overline{E_i^a}(x,t) = E_i^a(x,-t)$. Two reversals are applied here: First, the data residuals are reversed in time to give a source function for Maxwell's equations; second, the field produced by this source is itself reversed in time to give $\overline{E_i^a}$. Figure 5 shows how this result is equivalent to (54).

4.2. Reverse propagation and backpropagation

Equations (50) and (52) (or 54) for the gradient of L resemble the prescription for the seismic imaging method called "wave-equation migration", which was derived by Claerbout (1971) using physical arguments and analogies with optical holography. In migration, an image of acoustic reflectors in the earth is obtained from the cross-correlation of two fields: the incident field of the source and a (scattered) field downward continued ("backpropagated") from the receivers into the medium. This formalism has spawned a whole industry of (successful) methods for extrapolating wavefields and imaging seismic data in complex models (Berkhout, 1980). Tarantola (1984a) first pointed out the similarity between migration and wavefield inversion by the gradient method. Wang et al. (1995) showed how the gradient formalism carries over directly to diffusive electromagnetic imaging using Maxwell's equations without displacement currents.

In fact, the correspondence between gradient minimization of L and migration is not perfect. In seismic migration—at least in its original form—the field is backpropagated from the measurement surface (usually the earth's surface) as the boundary values of a wavefield, by solving an inverse boundary value problem or by using a Kirchhoff integral (Huygens principle) of the form,

$$\int_S dx \left(\tilde{G}\partial_n U - U\partial_n \tilde{G}\right), \tag{59}$$

where U are the data residuals, $\tilde{G}$ is an adjoint Green function, and ∂_n is a normal derivative to surface S. In the gradient formula, however, the residual field radiates in reverse time as a source distribution (not as boundary values). Recently, Zhdanov and his students at the University of Utah (Zhdanov et al., 1995; Zhadanov and Traynin, 1995) have completed the picture by showing how the formula for migration follows from a gradient method for a rigorous inverse problem. With measurements over a surface S, minimize the integrated power flow (Poynting vector) of the residual field through the surface (instead of minimizing the error functional L),

$$P[\sigma(x), \mu(x), \epsilon(x)] = \int_T dt \int_S dx_R\, \hat{v}_k \varepsilon_{kij} \delta E_i(x_R, t) \delta H_j(x_R, t), \tag{60}$$

where $\delta E_i = (E_i^{(d)} - E_i)$ and $\delta H_i^{(d)} = (H_i^{(d)} - H_i)$ are electric and magnetic field data residuals, and $\hat{v}_k$ is the unit normal to the surface (pointing away from the scattering region).

The gradient of P with respect to conductivity is

$$\partial_{\sigma(x')} P = -\int_T dt \int_S dx_R\, \hat{v}_k \varepsilon_{kij} \left[\delta E_i(x_R, t) \partial_{\sigma(x')} H_j(x_R, t) + \partial_{\sigma(x')} E_i(x_R, t) \delta H_j(x_R, t)\right]. \tag{61}$$

Substituting expressions for the derivatives and rearranging gives

$$\begin{aligned}\partial_{\sigma(x')} P = \int_{-\infty}^{\infty} dt' E_p(x', t') \int_T dt \int_S dx_R \Big[&\tilde{G}_{pj}^{EK}(x', x_R, t' - t) \varepsilon_{jki} \hat{v}_k \delta E_i(x_R, t) \\ &- \tilde{G}_{pi}^{EJ}(x', x_R, t' - t) \varepsilon_{ikj} \hat{v}_k \delta H_j(x_R, t)\Big].\end{aligned} \tag{62}$$

The inner integrals over the data coordinates t and x_R are a vector electromagnetic diffraction integral (De Hoop, 1995) analogous to the scalar integral (59).

5. Analysis and discussion

Efficient algorithms for gradient minimization have allowed an attack on truly large, nonlinear inverse problems for wavefields. Many variations of the method have been proposed, along with clever regularization schemes to control the nonlinear search and shape the final model (Van den Berg and Kleinman, 1995). The results obtained, though, have been (somewhat) disappointing. Gradient methods are painfully slow to converge near a minimum (and conjugate-gradient methods are not much better).

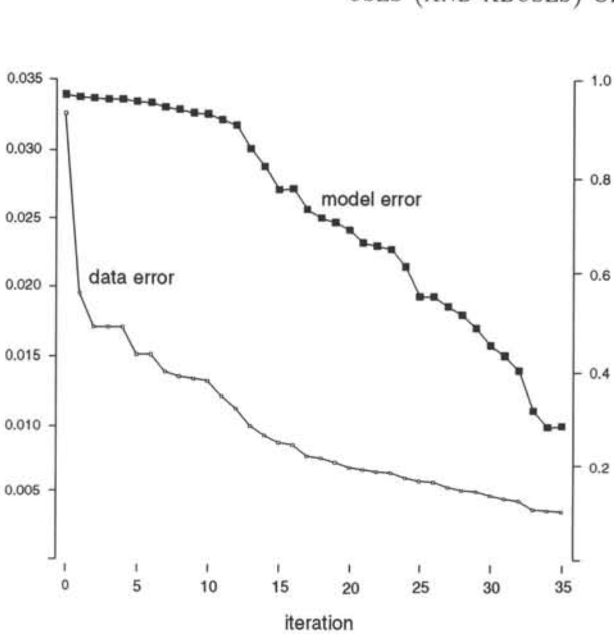

Figure 6. Typical convergence of gradient minimization (from Wang et al., 1995). After a fast initial reduction of the error, the gradient method creeps toward a minimum. Model error measures the size of a regularization term.

Figure 6 shows a typical convergence rate (from Wang et al., 1995). Fast calculation of the gradient tends to be offset by the number of gradient steps needed to reach a minimum. Moghaddam et al. (1991) showed that the gradient method and (an approximate version of) the Gauss-Newton method were actually competitive in the total number of operations needed to solve an inverse problem for moderate-sized models (a hundred or so unknowns). The extra computations needed to compute partial derivatives and solve the normal equations in the Gauss-Newton method were offset by the smaller number of steps it needed to converge (of course, for really large models, Gauss-Newton is prohibitive). This is well known in optimization theory: Newton's method converges quadratically near a minimum; a gradient method, linearly.

The difference between the Gauss-Newton method (iterative distorted-wave Born inversion) and the gradient method is the inverse of the normal equations:

$$\begin{aligned} \delta m_k^G &\sim J_{ki}^T \delta d_i \\ \delta m_k^{GN} &\sim (J^T J)_{kj}^+ J_{ji}^T \delta d_i, \end{aligned} \tag{63}$$

where $(J^T J)^+$ is the generalized inverse of the matrix

$$(J^T J)_{kj} = J_{kl}^T J_{lj}. \tag{64}$$

Although this matrix can not be computed easily for large models, the continuous operator to which it is related is (conceptually) a simple quantity, which can be inverted (approximately) when measurements are complete. This is a fruitful area for further research in applications of reciprocity to wavefield inversion.

We can illustrate these ideas in a simple case by considering the scalar (lossy wave) equation,

$$\left[\nabla^2 - \epsilon(x)\mu\partial_{tt}^2 - \sigma(x)\mu\partial_t\right] E(x,t) = -S(x,t), \tag{65}$$

where μ is constant, but ϵ and σ vary. The field E could be a component of the electric field in a (2D) TE-mode. The analysis is easier to follow in the frequency domain, with harmonic time-dependence $\exp(-i\omega t)$, where

$$\left[\nabla^2 + \omega^2\mu\epsilon(x) + i\omega\mu\sigma(x)\right] E(x,\omega) = -S(x,\omega). \tag{66}$$

Let E^b be a background state for (66), satisfying

$$\left[\nabla^2 + \omega^2\mu\epsilon^b(x) + i\omega\mu\sigma^b(x)\right] E^b(x,\omega) = -S(x,\omega), \tag{67}$$

and let $E^s = (E - E^b)$ be a scattered state, satisfying

$$\left[\nabla^2 + \omega^2\mu\epsilon^b(x) + i\omega\mu\sigma^b(x)\right] E^s(x,\omega) = -i\omega\mu\sigma^s(x)E(x,\omega), \tag{68}$$

where only σ varies from the background state: $\epsilon = \epsilon^b$ and $\sigma^s = (\sigma - \sigma^b)$ is the conductivity contrast.

The Green function for the background medium satisfies

$$\left[\nabla^2 + \omega^2\mu\epsilon^b(x) + i\omega\mu\sigma^b(x)\right] G(x,x',\omega) = -\delta(x-x'), \tag{69}$$

and is causal: $G(x,x',t) \equiv 0,\ t < 0$. The adjoint Green function $\tilde{G}$ satisfies

$$\left[\nabla^2 + \omega^2\mu\epsilon^b(x) - i\omega\mu\sigma^b(x)\right] \tilde{G}(x,x',\omega) = -\delta(x-x'), \tag{70}$$

and is anti-causal: $\tilde{G}(x,x',t) \equiv 0,\ t > 0$. The two Green functions are symmetric in their own spatial arguments and Hermitian-symmetric together,

$$\{G,\tilde{G}\}(x',x,\omega) = \{G,\tilde{G}\}(x,x',\omega), \quad \tilde{G}(x',x,\omega) = G^*(x,x',\omega), \tag{71}$$

where * indicates complex conjugate.

Let data be the scattered field measured on a surface S *surrounding the scattering region*, $E^{(d)} = E^s(x_R,\omega)$. Migration processes the scattered data by backpropagation,

$$E^I(x',\omega) = \oint_S dx_R \left[\partial_n\tilde{G}(x',x_R,\omega)E^s(x_R,\omega) - \tilde{G}(x',x_R,\omega)\partial_n E^s(x_R,\omega)\right], \tag{72}$$

creating an image field $E^I(x',\omega)$ (∂_n is the outward normal derivative on S). E^I is an intermediate quantity that needs to be operated on by an "imaging condition" (involving perhaps spatial operators and a sum over frequency) to create the final image. An expression relating E^I to the contrast σ^s is obtained by substituting in equation (72) the integral formula for E^s,

$$E^s(x_R,\omega) = \mu \int_V i\omega G(x_R, x, \omega)\sigma^s(x)E(x,\omega)dx. \tag{73}$$

The result is

$$E^I(x',\omega) = \mu \int_V i\omega Q(x', x, \omega)E(x,\omega)\sigma^s(x)dx, \tag{74}$$

where

$$Q(x',x,\omega) = \oint_S dx_R\Big[\partial_n \tilde{G}(x', x_R, \omega)G(x_R, x, \omega) - \tilde{G}(x', x_R, \omega)\partial_n G(x_R, x, \omega)\Big]. \tag{75}$$

One can show (using reciprocity or Green's theorem) that

$$\begin{aligned} Q(x',x,\omega) &= \tilde{G}(x,x',\omega) - G(x',x,\omega) + 2i\omega\mu\int_V \sigma^b(x'')\tilde{G}(x',x'',\omega)G(x,x'',\omega)dx'' \\ &= -G^I(x',x,\omega) + 2i\omega\mu\int_V \sigma^b(x'')G^*(x',x'',\omega)G(x'',x,\omega)dx'', \end{aligned} \tag{76}$$

where G^I is proportional to the imaginary part of the Green function,

$$G^I = (G - G^*) = 2i\, Im(G).$$

Equations (74) and (76) are general results for any background medium. Another general result is that

$$\frac{\mu\epsilon^b(x')}{2\pi}\int_{-\infty}^{\infty} d\omega\,(-i\omega)G^I(x',x,\omega) = \delta(x-x'). \tag{77}$$

Equation (77) suggests an imaging condition that actually gives an approximate inversion for $\sigma^s(x)$. Assume that the second term in (76) is negligible compared to the first (e.g., the background conductivity σ^b is small or 0), and consider

$$\frac{\epsilon^b(x')}{2\pi}\int_{-\infty}^{\infty} d\omega\,\frac{E^I(x',\omega)}{E^b(x',\omega)} = \frac{\mu\epsilon^b(x')}{2\pi}\int_V dx\int_{-\infty}^{\infty} d\omega\,(-i\omega)G^I(x',x,\omega)\frac{E(x,\omega)}{E^b(x',\omega)}\sigma^s(x) \ + \ error. \tag{78}$$

The total field in the integral of the right-hand-side is (of course) unknown, but we can write

$$\begin{aligned} E(x,\omega) &= E^b(x,\omega) + E^s(x,\omega) \\ &= \Big[E^b(x',\omega) + \partial_i E^b(x',\omega)(x_i - x_i') + \cdots\Big] + E^s(x,\omega) \end{aligned} \tag{79}$$

Substituting above and absorbing the derivatives of E^b and the scattered field into the error term gives

$$\begin{aligned} \frac{\epsilon^b(x')}{2\pi}\int_{-\infty}^{\infty} d\omega\,\frac{E^I(x',\omega)}{E^b(x',\omega)} &= \frac{\mu\epsilon^b(x')}{2\pi}\int_V dx\int_{-\infty}^{\infty} d\omega\,(-i\omega)G^I(x',x,\omega)\sigma^s(x) \ + \ error \\ &= \sigma^s(x') \ + \ error. \end{aligned} \tag{80}$$

The quantity E^I is essentially the gradient term that comes from minimizing a power-flow functional in the scattered field; the operator $Q(x', x, \omega)$ is a continuous form of the operator $(J^T J)$ from the Gauss-Newton method of nonlinear wavefield inversion. The operation (80) gives an approximate inverse (a parametrix) of the integral operator $Q(x', x, \omega)$. In fact, the gradient term for a power-flow functional of E^s is (essentially)

$$E^G(x', \omega) = E^{b*}(x', \omega) E^I(x', \omega) \tag{81}$$

and the corresponding approximate inverse is

$$\frac{\epsilon^b(x')}{2\pi} \int_{-\infty}^{\infty} d\omega \, \frac{E^G(x', \omega)}{|E^b(x', \omega)|^2}. \tag{82}$$

Implementing the approximate inverse requires little more work than computing the gradient. In slightly different form, these equations were first derived rigorously by Esmersoy (Esmersoy, 1985; see also, Esmersoy and Oristaglio, 1988) for acoustic imaging. But similar formulas, derived by physical arguments, appear in Claerbout (1976). Esmersoy (1985) also treats cases where measurements do not surround the scatterer (as they rarely do in geophysics!). It is not known whether this result is optimal, or how to estimate the error terms for general models. Moreover, simple formulas for the case when σ^b is large, or when both σ and ϵ vary, have not yet been derived.

The approach described here can naturally be motivated by considerations of reciprocity (De Hoop, 1995). And all of this can be done in the space-time domain with the full, first-order Maxwell's equations in dispersive, anisotropic media. (We leave this as an exercise for the inspirer!)

References

Berkhout, A.J., 1980, Seismic Migration: Imaging of Acoustic Energy by Wavefield Extrapolation, Elsevier, Amsterdam.

Blok, H., and M.C.S. Zeijlmans, M.C.S., 1987, Reciprocity and the formulation of inverse profiling problems, Radio Science, **22**, 1137-1147.

Claerbout, J.F., 1971, Toward a unified theory of reflector mapping, Geophysics, **36**, 467-481.

Claerbout, J.F., 1976, Fundamentals of Geophysical Data Processing McGraw-Hill, New York.

De Hoop, A.T., 1987, Time-domain reciprocity theorems for electromagnetic fields in dispersive media, Radio Science, **22**, 1171-1178.

De Hoop, A.T., 1995, Handbook of Radiation and Scattering of Waves, Academic Press Limited, London.

De Hoop, M.V., and A.T. de Hoop, 1995, Wavefield reciprocity and optimization in remote sensing, Scientific report, Schlumberger-Cambridge Research.

De Hoop, A.T., and H.J. Stam, 1988, Time-domain reciprocity theorems for elastodynamic wave fields in solids with relaxation and their application to inverse problems, Wave Motion, **10**, 479-489.

Esmersoy, C., 1985, The backpropagated field approach to multi-dimensional velocity inversion, Ph.D. thesis, Massachusetts Institute of Technology, USA

Esmersoy, C., and M.L. Oristaglio, 1988, Reverse-time wavefield extrapolation, imaging, and inversion, Geophysics, **53**, 920-931.

Felsen, L.B., and N. Marcuvitz, 1973, Radiation and Scattering of Waves, Prentice-Hall, Englewood Cliffs, New Jersey.

Gill, P.E., W. Murray and M.H. Wright, 1981, Practical Optimization, Academic Press Limited, London.

Hohmann, G.W., and A.P. Raiche, 1987, Inversion of controlled-source electromagnetic data, in: Electromagnetic Methods in Applied Geophysics, M.N. Nabighian (ed.), Society of Exploration Geophysicists.

Jupp, D.L.B., and K. Vozoff, 1977, Two-dimensional magnetotelluric inversion: Geophysical Journal of the Royal Astronomical Society, **50**, 333-352.

McGillivray, P.R., D.W. Oldenburg, R.G. Ellis, and T.M. Habashy, 1994, Calculation of sensitivities for the frequency-domain electromagnetic problem, Geophysical Journal International, **116**, 1-4.

Moghaddam, M., W.C. Chew and M.L. Oristaglio, 1991, A comparison of the Born iterative method and Tarantola's method for an electromagnetic time-domain inverse problem: International Journal of Systems and Technology, **3**, 318-333.

Oristaglio, M.L., and M.H. Worthington, 1980, Inversion of surface and borehole electromagnetic data for two-dimensional electrical conductivity models, Geophysical Prospecting, **28**, 633-657.

Rodi, W.L., 1976, A technique for improving the accuracy of finite element solutions for magnetotelluric data, Geophysical Journal of the Royal Astronomical Society, **44**, 483-506.

Tarantola, A., 1984a, Inversion of seismic reflection data in the acoustic approximation, Geophysics, **49**, 1259-1266.

Tarantola, A., 1984b, Linearized inversion of seismic reflection data, Geophysical Prospecting **32**, 998-1015.

Taylor, J.R., 1972, Scattering Theory, Wiley, New York.

Van den Berg, P.M., and R.E. Kleinman, 1995, An total variation enhanced modified gradient algorithm for profile reconstruction, Inverse problems, **11**, L5-L10.

Wang, T., M.L. Oristaglio, A. Tripp and G. Hohmann, 1994, Inversion of diffusive transient electromagnetic data by a conjugate gradient method, Radio Science, **29**, 1143-1156.

Zhdanov, M.S., and P. Traynin, 1996, Inversion versus migration in two-dimensional geoelectrical problems, CEMI 1995-1996 Final Report, 262-299.

Zhdanov, M.S., and O. Portniaguine, 1996, Time domain electromagnetic migration in the solution of inverse problems, CEMI 1995-1996 Final Report, 300-347.

Reciprocity, Radiation Conditions and Uniqueness

Ralph E. Kleinman and Thomas S. Angell

Center for the Mathematics of Waves, Department of Mathematical Sciences
University of Delaware, Newark, Delaware 19716, U.S.A.

Abstract

This year marks the 100th anniversary of two landmark papers, Lorentz's work on reciprocity and Sommerfeld's treatment of the half plane problem. These works provided the foundation for a century of progress in scattering and diffraction. It is well known that reciprocity and radiation conditions are intimately interconnected in establishing uniqueness for scattering by bounded obstacles in free space, an essential ingredient in showing that the mathematical model of scattering problems is well posed. In the present paper we present an alternate mathematical formulation which employs a different form of radiation condition and show that this new formulation is equivalent to the standard one, not only for scattering by objects in free space but also scattering by objects in semibounded domains such as a half space or a wave guide where boundary conditions must be imposed on the boundary of the domain as well as the scatterer.

1. Introduction

It is well known that the problem of scattering by a bounded obstacle (or obstacles) in free space is well posed provided the scattering surface satisfies certain smoothness conditions. That is, there exists a unique solution that is stable with respect to changes in the boundary data. Mathematically, the problem is to find a solution of the Helmholtz equation

$$(\nabla^2 + k^2)\, u(\boldsymbol{x}) \quad \text{for} \quad \boldsymbol{x} \in \boldsymbol{R}^n \backslash \bar{D}_i\,, \tag{1}$$

where $x = (x_1, x_2, \ldots x_n)$ denotes a position vector in $\boldsymbol{R}^n$, n is the dimension of the space, D_i denotes a bounded, simply connected domain (or a finite number of such domains) with boundary Γ and $\bar{D}_i = D_i \cup \Gamma$ denotes the closure of D_i. The surface Γ is assumed to be smooth enough to permit the use of the Gauss–Green theorems and we designate such surfaces as smooth. The field $u(\boldsymbol{x})$ is required to satisfy a boundary condition on Γ and in order to establish uniqueness an additional restriction is needed which usually is given in the form of the radiation condition

$$\frac{\partial u}{\partial r} - iku = o\left(\frac{1}{r^{\frac{n-1}{2}}}\right) \quad \text{as} \quad r = |\boldsymbol{x}| \to \infty\,. \tag{2}$$

The literature on the radiation condition (1) is vast and no attempt is made to give more than a few key references. In his original proof, Sommerfeld (1912), required, in addition to (2), a finiteness or boundedness condition

$$\lim_{r\to\infty} r^{\frac{n-1}{2}}\, u(\boldsymbol{x}) < \infty\,. \tag{3}$$

For free space scattering problems this additional condition was shown to be superfluous by, e.g., Magnus (1942), Rellich, (1943), Atkinson, (1949) and Wilcox, (1956). This superfluousness holds regardless of whether $\operatorname{Im} k = 0$ or $\operatorname{Im} k > 0$. However we will show subsequently that when $\operatorname{Im} k = 0$ a condition similar to (3) will prove useful in our reformulation. We remark that while many people have noted that the boundedness condition may be dispensed with if one imposes a radiation condition, it is also true that when $\operatorname{Im} k > 0$ the radiation condition may be disposed with if one imposes a boundedness condition. This is not true, however, when $\operatorname{Im} k = 0$.

The standard uniqueness proof for scattering in free space depends heavily on the fact if

$$\lim_{R\to\infty} \int\limits_{S_R} |u|^2 \, ds = 0\,, \tag{4}$$

where S_R is the surface of a ball of radius R, then $u(\boldsymbol{x}) = 0$ in $\mathbb{R}^n \backslash D_i$. This is a consequence of what is known in the western literature as Rellich's lemma (Rellich, 1943), although Vekua (1967), cites earlier references. Alternative forms of the radiation condition are discussed by Neittaanmäki and Roach (1987), and in open waveguides by Nosich (1994).

When the scatterer is contained in a waveguide, the situation is quite different. The field is decomposed into a finite number of propagating modes, each of which satisfies a condition of the form

$$\frac{\partial u_j}{\partial r} - ik_j u_j = O\left(\frac{1}{r^{\frac{n-1}{2}}}\right) \quad \text{as} \quad r \to \infty\,, \tag{5}$$

as well as infinite number of evanescent modes which decay exponentially as $r \to \infty$. The existence of evanescent modes means that there is no counterpart of the Vekua–Rellich lemma for wave guides hence the uniqueness proof cannot parallel that for scattering in free space.

A method for establishing field representations in the absence of a scatterer was outlined by Sveshnikov (1951), in which uniqueness is first established when $\operatorname{Im} k > 0$ and then invoking the principle of limiting absorption to obtain a solution when $\operatorname{Im} k = 0$. The decomposition into propagating and evanescent modes then follows as a consequence. However this argument is quite sophisticated, requiring some heavy machinery of analysis. A straightforward derivation for real k was curiously missing from the literature until very recently. Xu (1990) purports to give a uniqueness proof in which he requires the imposition of (5) on each propagating mode. A careful discussion of the uniqueness question was provided by Angell et al. (1996), where conditions are imposed on the field itself and do not require *a priori* knowledge of the propagating wave numbers, k_j.

In the present work we extend the results of Angell et al. (1996), and provide a general formulation of scattering problems involving an alternative to the radiation conditions (2) and (5). This new formulation covers a variety of physical settings including scattering in free space, a half space, and waveguides and uniqueness is discussed in each of these cases.

2. Mathematical formulation

Assume that the scatterer $\bar{D}_i$ is imbedded in a physical domain, D_e, which may be the entire space, $\mathbb{R}^n$, or an unbounded subset of $\mathbb{R}^n$. For example the physical scattering domain, D_e, may be the half space, $D_e = \{\boldsymbol{x}|x_n < 0\}$, or the (parallel plate) waveguide, $D_e = \{\boldsymbol{x}| -h < x_n < 0\}$.

The scattering problem involves the determination of the way in which the scatterer perturbs a primary field, $u_0(\boldsymbol{x})$, the field that would exist in the absence of the scatterer. When $D_e = \mathbb{R}^n$, the primary field is taken to be the incident field, $u^{inc}(\boldsymbol{x})$, which is often a plane wave or a point source. When D_e is a half space a boundary condition must be imposed on the plane $x_n = 0$ and $u_0(\boldsymbol{x})$ must satisfy this condition. For example, if $u^{inc}(\boldsymbol{x})$ is given and a Dirichlet boundary condition is imposed on $x_n = 0$, then $u_0(\boldsymbol{x}) = u^{inc}(\boldsymbol{x}) - u^{inc}(\boldsymbol{x}_i)$ where $\boldsymbol{x}_i = (x_1, x_2, \dots, -x_n)$, the image of $\boldsymbol{x}$ in the $x_n = 0$ plane. In the wave guide problem the specification of $u_0(\boldsymbol{x})$ may be more complicated, see e.g. Lambert and Lesselier (1995), for the Green's function in a wave guide.

In any and all cases, the starting point in the formulation of a scattering problem the specification of a primary field, $u_0(\boldsymbol{x})$, which satisfies the required boundary condition on the boundary of the physical domain, ∂D_e.

In what follows we present the new formulation in the simple case when Dirichlet conditions are imposed on both the boundary of the physical domain as well as the boundary of the scatterer but a similar formulation is available for Neumann or Robin boundary conditions as well as the case when different boundary conditions are imposed on the scatterer than those imposed in the boundary of the physical domain.

Our formulation of the scattering problem then consists of finding the scattered field, $u(\boldsymbol{x})$, such that for a given $u_0(\boldsymbol{x})$ and k real and positive,

$$(\nabla^2 + k^2)\, u(\boldsymbol{x}) = 0 \text{ for } \boldsymbol{x} \in D_e \backslash \bar{D}_i\,, \tag{6}$$

$$u(\boldsymbol{x}) = -u_0(\boldsymbol{x}) \text{ for } \boldsymbol{x} \in \Gamma \text{ and } \boldsymbol{x} \in \partial D_e\,, \tag{7}$$

$$\lim_{R\to\infty} \int_{S_R} |u|^2\, ds = c_0 < \infty\,, \tag{8}$$

and

$$\operatorname{Im} \int_S \bar{u}\, \frac{\partial u}{\partial n}\, ds = c_1 \geq 0\,, \tag{9}$$

where condition (9) is to hold on every smooth surface that divides D_e into two parts, one of which contains the scatterer Γ. Thus S may be any smooth closed surface in $\bar{D}_e$ that contains Γ in its interior or an open surface with boundary on ∂D_e (see Figure 1, left). As an example of the latter, when D_e is a waveguide, S could be a surface in D_e which connects the wave guide walls (see Figure 1, right). The surface S_R is now taken to be the boundary of the intersection of D_e and a domain parameterized by R which approaches $\mathbb{R}^n$ as $R \to \infty$, e.g. a ball of radius R or a cube of side R. Moreover equation (9) is required to hold for every component of any orthogonal decomposition of u on S. That is, if $u = u_1 + u_2$ and $\int_S u_1 \bar{u}_2\, ds = 0$, then

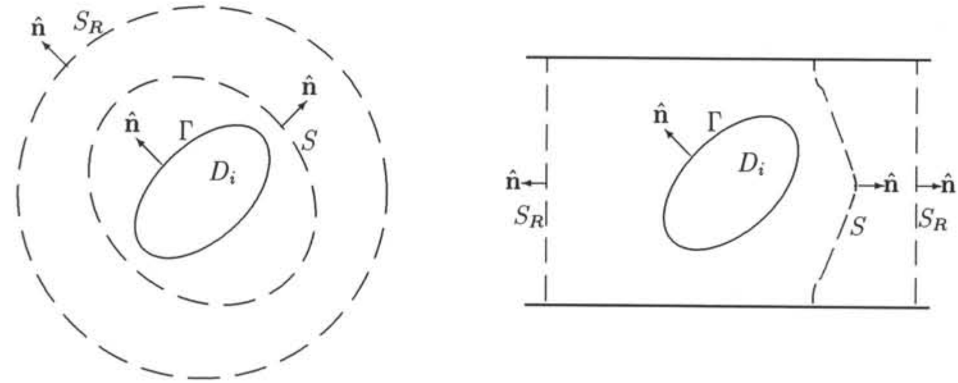

Figure 1. Free space scattering and wave guide scattering.

$$\operatorname{Im} \int_S \bar{u}_j \frac{\partial u_j}{\partial n} \, ds = c_j \geq 0 \,, \; j = 1, 2 \,. \tag{10}$$

The normal derivative, $\frac{\partial}{\partial n} = \hat{\mathbf{n}} \cdot \nabla$, is taken in the sense that $\hat{n}$ is directed into the portion of D_e which does not contain Γ.

Conditions (8)–(10) replace the radiation conditions in the usual formulation of scattering problems. Condition (8) is very similar to Sommerfeld's boundedness condition, (3), when $D_e = \mathbb{R}^n$. In our formulation we find it very useful to rehabilitate this condition since conditions (9) and (10) appear weaker than the standard radiation condition, although they do embody the physical principle that the flux of energy scattered by Γ through any surface containing Γ is non-negative. It should be noted that there is an implicit assumption of a suppressed time dependence of $e^{-i\omega t}$. If a harmonic time dependence $e^{i\omega t}$ were assumed, the inequality in (9) and (10) would be reversed. We now state the uniqueness theorem as follows:

If u satisfies conditions (6)–(10) *and $u_0 = 0$ then $u = 0$.*

The proof will be given for two special cases, when D_e is the entire space and when D_e is a half space. Moreover we delineate the difficulties associated with uniqueness when D_e is the interior of a wave guide. We will give the details in the case when $n = 2$ however the proofs when $n > 2$ are essentially the same except that series representations of solutions involve different eigenfunctions.

3. Free space

Here we show that the new formulation covers the well known case when $D_e = \mathbb{R}^2$. In this case the boundary condition (7) is imposed only on the scattering surface Γ. Then standard separation of variables techniques applied to (6) and (7) imply that outside the circle that circumscribes Γ, u has a uniformly convergent series representation

$$u(\boldsymbol{x}) = \sum_{n=-\infty}^{\infty} [a_n H_{|n|}^{(1)}(kr) + b_n\, H_{|n|}^{(2)}(kr)]\, e^{in\theta}\,. \tag{11}$$

Choosing S_R to be the circle of radius R, condition (8) implies that

$$\lim_{R\to\infty} 2\pi R \sum_{n=-\infty}^{\infty} \{|a_n H_{|n|}^{(1)}(kR) + b_n H_{|n|}^{(1)}(kR)|^2\} = c_0 < \infty \tag{12}$$

or

$$\lim_{R\to\infty} 2\pi R \sum_{n=-\infty}^{\infty} \{(|a_n|^2+|b_n|^2)|H_{|n|}^{(1)}(kR)|^2+a_n\bar{b}_n(H_{|n|}^{(1)}(kR))^2+\bar{a}_n b_n(\overline{H_{|n|}^{(1)}}(kR))^2\} = c_0<\infty \tag{13}$$

where we have used the fact that for real k

$$\overline{H_{|n|}^{(1)}}(kR) = H_{|n|}^{(2)}(kR)\,. \tag{14}$$

Introducing the asymptotic form of the Hankel functions

$$H_{|n|}^{(1)}(kR) = \sqrt{\frac{2}{\pi kR}}e^{ikR-i|n|\frac{\pi}{2}-i\frac{\pi}{4}} + O\left(\frac{1}{R^{3/2}}\right) \tag{15}$$

into equation (13) yields

$$\lim_{R\to\infty} \frac{4}{k} \sum_{n=-\infty}^{\infty} \{|a_n|^2+|b_n|^2+2|a_n||b_n|\, \cos(2ikR-|n|\pi-\frac{\pi}{2}+\arg a_n-\arg b_n)\} = c_0 < \infty\,. \tag{16}$$

In order for the limit to exist it must follow that

$$|a_n b_n| = 0\,. \tag{17}$$

Equation (17) is a consequence of the boundedness condition (8) and shows that either a_n or b_n vanishes. Now we turn to condition (10) to show that it is b_n that vanishes. On S_R all of the terms in (11) are orthogonal hence condition (10) implies that

$$\operatorname{Im} 2\pi R(\bar{a}_n \bar{H}_{|n|}^{(1)}(kR) + \bar{b}_n \bar{H}_{|n|}^{(2)}(kR))\, \frac{\partial}{\partial R}(a_n H_{|n|}^{(1)}(kR) + b_n H_{|n|}^{(2)}(kR)) = c_n \geq 0\,. \tag{18}$$

Employing the asymptotic term (15) we find

$$\begin{aligned}&\operatorname{Im} \frac{4}{k}(\bar{a}_n e^{-ikR+i|n|\frac{\pi}{2}+i\frac{\pi}{4}} + \bar{b}_n\, e^{ikR-i|n|\frac{\pi}{2}-i\frac{\pi}{4}})\,\cdot \\ &\frac{d}{dR}(a_n e^{ikR-i|n|\frac{\pi}{2}-i\frac{\pi}{4}} + b_n e^{-ikR+i|n|\frac{\pi}{2}+i\frac{\pi}{4}}) + o\left(\frac{1}{R}\right) = c_n \geq 0\end{aligned} \tag{19}$$

or, after straight forward simplification

$$4\{|a_n|^2 - |b_n|^2\} + O\left(\frac{1}{R}\right) = c_n \geq 0\,. \tag{20}$$

Either a_n or b_n is zero and the only choice for which (20) holds is $b_n = 0$. Hence outside a sphere circumscribing Γ

$$u(\boldsymbol{x}) = \sum_{n=-\infty}^{\infty} a_n H_{|n|}^{(1)}(kr)\, e^{in\theta}\,. \tag{21}$$

Then uniqueness follows almost immediately since if u satisfies a homogeneous boundary condition on Γ and, for real k, u and $\bar{u}$ satisfy the same Helmholtz equation in the domain exterior to Γ and interior to S_R

$$\begin{aligned} 0 &= \int_{\Gamma} \left(\bar{u}\frac{\partial u}{\partial n} - u\frac{\partial \bar{u}}{\partial n}\right)\, d\Gamma = \int_{S_R} \left(\bar{u}\frac{\partial u}{\partial n} - u\frac{\partial \bar{u}}{\partial n}\right)\, ds = 2i\,\mathrm{Im}\int_{S_R} \bar{u}\frac{\partial u}{\partial n}\, ds \\ &= 4\sum_{n=-\infty}^{\infty} |a_n|^2 + O\left(\frac{1}{R}\right)\,. \end{aligned} \tag{22}$$

Hence u vanishes outside the circumscribing sphere and, by analytic continuation, outside Γ.

4. The half space

In the case where the scatterer lies below the line $x_2 = 0$ on which a boundary condition is imposed, D_e is taken to be the lower half plane and ∂D_e is the line $x_2 = 0$. The homogeneous form of problem (6)–(10) requires that $u = 0$ on Γ and $u = 0$ on $x_2 = 0$. The surface S_R in this case is taken to be the semi–circle of radius $R, \pi \leq \theta \leq 2\pi$ together with the line $x_2 = 0$, $-R \leq x_1 \leq R$. Conditions (6) and (7) imply that outside any semicircle containing Γ and center at the origin,

$$u(\boldsymbol{x}) = \sum_{n=1}^{\infty} [a_n H_n^{(1)}(kr) + b_n H_n^{(2)}(kr)]\sin(n\theta)\,,\ \pi \leq \theta \leq 2\pi\,. \tag{23}$$

From this point the argument completely parallels the argument in the free space case and will not be repeated.

5. The wave guide

Now we consider the case when the scatterer is located in a parallel plate waveguide. The development that follows, based on the formulation (6)–(10) is similar to that developed in Angell et al. (1996). The physical domain D_e in this case consists of the layer $\{(x,y)| -\infty < x < \infty, -h < y < 0\}$ where for simplicity we use coordinates (x, y) rather than (x_1, x_2). The boundary of D_e consists of the lines, $y = 0$ and

$y = -h$. The homogeneous form of the boundary condition (7) is $u(\boldsymbol{x}) = 0$ for $\boldsymbol{x} \in \Gamma$ and $u(x, 0) = u(x, -h) = 0$. Without loss of generality we assume that the scatterer is contained in the rectangle, $-L \leq x \leq L$, $-h \leq y \leq 0$. Since Γ is bounded there is always such an L. Then for $|x| > L$, standard separation of variables techniques lead to the representation

$$\begin{aligned} u(x,y) &= \sum_{n=1}^{\infty} (a_n^+ \, e^{ik_n x} + b_n^+ \, e^{-ik_n x}) \, \sin(\frac{n\pi y}{h}), \quad x > L, \\ &= \sum_{n=1}^{\infty} (a_n^- \, e^{ik_n |x|} + b_n^- \, e^{-ik_n |x|}) \, \sin(\frac{n\pi y}{h}), \quad x < -L, \end{aligned} \tag{24}$$

where

$$k_n = \sqrt{k^2 - \frac{n^2 \pi^2}{h^2}}. \tag{25}$$

For any fixed real k there exists an N such that k_n is positive for $n \leq N$ and is pure imaginary for $n > N$ (k_{N+1} maybe zero for some values of k) in which case we write

$$k_n = i|k_n|. \tag{26}$$

We always use the positive square root. Then equation (24) may be rewritten as

$$\begin{aligned} u(x,y) &= \sum_{n=1}^{N} (a_n^+ \, e^{ik_n x} + b_n^+ \, e^{-ik_n x}) \, \sin(\frac{n\pi y}{h}) \\ &\qquad + \sum_{n=N+1}^{\infty} (a_n^+ \, e^{-|k_n| x} + b_n^+ \, e^{|k_n| x}) \, \sin(\frac{n\pi y}{h}), \quad x > L, \\ &= \sum_{n=1}^{N} (a_n^- \, e^{ik_n |x|} + b_n^- \, e^{-ik_n |x|}) \, \sin(\frac{n\pi y}{h}) \\ &\qquad + \sum_{n=N+1}^{\infty} (a_n^- \, e^{-|k_n x|} + b_n^- \, e^{|k_n x|}) \, \sin(\frac{n\pi y}{h}), \quad x < -L. \end{aligned} \tag{27}$$

In this waveguide case we choose the surface S_R to be the boundary of the rectangle $-R \leq x \leq R$, $-h \leq y \leq 0$ where R is taken larger than L. Then since $u = 0$ on $y = 0$ and $y = -h$ and the functions $\sin \frac{n\pi y}{h}$ satisfy the orthogonality condition

$$\int_{-h}^{0} \sin(\frac{n\pi y}{h}) \, \sin(\frac{m\pi y}{h}) \, dy = \frac{h}{2} \, \delta_{n,m}, \tag{28}$$

condition (8) becomes

$$\begin{aligned} &\lim_{R\to\infty} \frac{h}{2} \sum_{n=1}^{N} \{|a_n^+ \, e^{ik_n R} + b_n^+ \, e^{ik_n R}|^2 + |a_n^- \, e^{ik_n R} + b_n^- \, e^{-ik_n R}|^2\} \\ &\quad + \frac{h}{2} \sum_{n=N+1}^{\infty} \{|a_n^+ \, e^{-|k_n| R} + b_n^+ \, e^{|k_n| R}|^2 + |a_n \, e^{-|k_n| R} + b_n^- \, e^{|k_n| R}|^2\} = c_0 < \infty \\ = &\lim_{R\to\infty} \frac{h}{2} \sum_{n=1}^{N} \{|a_n^+|^2 + |b_n^+|^2 + 2|a_n^+ b_n^+| \cos(2k_n R + \arg\, a_n^+ - \arg\, b_n^+) \end{aligned}$$

$$
\begin{aligned}
&\qquad +|a_n^-|^2 + |b_n^-|^2 + 2\,|a_n^- b_n^-|\ \cos(2k_n R + \arg\, b_n^- - \arg\, a_n^-)\} \\
&+ \frac{h}{2} \sum_{n=N+1}^{\infty} \{|a_n^+|^2\, e^{-2|k_n|R} + |b_n^+|\, e^{2|k_n|R} + 2\,\mathrm{Re}\, a_n^+\, \bar{b}_n^+ \\
&\qquad +|a_n^-|^2\, e^{-2|k_n|R} + |b_n^-|^2\, e^{2|k_n|R} + 2\,\mathrm{Re}\, a_n^-\, \bar{b}_n^-\} = c_0 < \infty\,. \qquad (29)
\end{aligned}
$$

In order for the limit to exist it must be true that

$$
|a_n^+ b_n^+| = |a_n^- b_n^-| = 0\,, \quad n \le N\,, \tag{30}
$$

and

$$
b_n^+ = b_n^- = 0\,, \quad n > N\,. \tag{31}
$$

If $k_{N+1} = 0$ we may assume that (31) hold for $n = N+1$. Equation (31) implies that either a_n^+ or b_n^+ vanishes and either a_n^- or b_n^- vanishes for $n \le N$. To show that it is the b_n's which vanish, and thus obtain the representation in terms of propagating and evanescent modes, we will invoke condition (10), knowing now that the field has the representation

$$
\begin{aligned}
u(x,y) &= \sum_{n=1}^{N} (a_n^+\, e^{ik_n x} + b_n^+\, e^{-ik_n x})\ \sin(\frac{n\pi y}{h}) \\
&\qquad + \sum_{n=N+1}^{\infty} a_n^+\, e^{-|k_n|x}\ \sin(\frac{n\pi y}{h}), \quad x > L\,, \\
&= \sum_{n=1}^{N} (a_n^-\, e^{ik_n|x|} + b_n^-\, e^{-ik_n|x|})\ \sin(\frac{n\pi y}{h}) \qquad (32) \\
&\qquad + \sum_{n=N+1}^{\infty} a_n^-\, e^{-|k_n x|}\ \sin(\frac{n\pi y}{h}), \quad x < L\,,
\end{aligned}
$$

and either a_n^+ or b_n^+ vanishes and a_n^- or b_n^- vanishes for $n \le N$.

Turning to condition (10) we first choose S to be the line $x = R$, $-h \le y \le 0$. The scatterer is contained in the domain where $x < R$ and $\frac{\partial}{\partial n} = \frac{\partial}{\partial x}$ on S. Moreover each term in the series (32) is orthogonal to all the other terms on S. Hence on S, for $n \le N$ it follows that

$$
\begin{aligned}
\mathrm{Im} \int_S \bar{u}_n\, \frac{\partial u}{\partial n}\, ds &= \mathrm{Im}\, \frac{ik_n\, h}{2} (\bar{a}_n^+\, e^{-ik_n R} + \bar{b}_n^+\, e^{ik_n R})(a_n^+\, e^{ik_n R} - b_n^+\, e^{-ik_n R}) \\
&= \mathrm{Im}\, \frac{ik_n h}{2} \,[|a_n^+|^2 - |b_n^+|^2 + 2i|a_n^+\, b_n^+|\ \sin(2k_n R + \arg\, a_n^+ - \arg\, b_n^+)] \\
&= \frac{k_n h}{2}\, (|a_n^+|^2 - |b_n^+|^2) = c_n \ge 0\,. \qquad (33)
\end{aligned}
$$

Either a_n^+ or b_n^+ vanishes and the only choice for which the inequality (34) is satisfied is $b_n^+ = 0$.

A similar argument holds when S is chosen to be the line $x = -R$, $-h \le y \le 0$ where $\frac{\partial}{\partial n} = -\frac{\partial}{\partial x}$ which shows that $b_n^- = 0$ when $n \le N$. This shows that the new formulation (6)–(10) leads to the standard series representation of solutions

$$
\begin{aligned}
u(x,y) &= \sum_{n=1}^{N} a_n^+ \, e^{ik_n x} \, \sin(\frac{n\pi y}{h}) + \sum_{n=N+1}^{\infty} a_n^+ \, e^{-|k_n| x} \, \sin(\frac{n\pi y}{h}), \quad x > L\,, \\
&= \sum_{n=1}^{N} a_n^- \, e^{ik_n |x|} \, \sin(\frac{n\pi y}{h}) + \sum_{n=N+1}^{\infty} a_n^- \, e^{-|k_n x|} \, \sin(\frac{n\pi y}{h}), \quad x < -L\,. \quad (34)
\end{aligned}
$$

Note that the derivation of this representation was independent of the boundary condition on Γ and therefore is valid for both homogeneous and inhomogeneous boundary conditions. We now discuss the uniqueness question, that is, if $u = 0$ on Γ, does u vanish everywhere.

Let us denote by Ω_R, that portion of D_e exterior to Γ and interior to the rectangle, $-R \leq r \leq R$, $-h \leq y \leq 0$ where, as before, $R > L$ so that (34) holds. The boundary of Ω_R consists of the boundary of the rectangle as well as the scatterer Γ. The fact that k is real and u vanishes on Γ as well as ∂D_e enables us to deduce that

$$
\begin{aligned}
0 = \int_\Gamma \left(\bar{u} \, \frac{\partial u}{\partial n} - u \, \frac{\partial \bar{u}}{\partial n} \right) \, ds &= \int_{|x|=R} \left(\bar{u} \, \frac{\partial u}{\partial n} - u \, \frac{\partial \bar{u}}{\partial n} \right) \, ds \\
&= 2i \, \mathrm{Im} \int_{|x|=R} \bar{u} \, \frac{\partial u}{\partial n} \, ds\,, \quad (35)
\end{aligned}
$$

where Green's theorem has been used. Using the representation (34) and the same computation exhibited in (33) we find that

$$
0 = \frac{h}{2} \sum_{n=1}^{N} k_n (|a_n^+|^2 + |a_n^-|^2)\,. \quad (36)
$$

Therefore all of the propagating modes vanish. However, in contrast to the free space case where all of the modes are propagating and the Vekua–Rellich lemma enables us to conclude that u vanishes identically, the waveguide environment allows for the existence of exponentially decaying evanescent modes. That is, we have shown that if $u = 0$ on Γ then

$$
\begin{aligned}
u(x,y) &= \sum_{n=N+1}^{\infty} a_n^+ \, e^{-|k_n| x} \, \sin(\frac{n\pi y}{h}), \quad x > L\,, \\
&= \sum_{n=N+1}^{\infty} a_n^- \, e^{-|k_n x|} \, \sin(\frac{n\pi y}{h}), \quad x < -L\,. \quad (37)
\end{aligned}
$$

Recent results concerning trapped waves indicate that, in the present example, additional restrictions on Γ must be imposed in order to conclude that all of the coefficients $a_n^\pm$ vanish and that therefore u vanishes in $D_e \backslash \bar{D}_i$. This work is under way.

6. Conclusions

In this paper we have provided a new formulation of scattering problems in the frequency domain which features an alternative to the well known radiation condition.

This alternative condition embodies the boundedness condition of Sommerfeld as well as the physical requirement that energy scattered by an object radiate away from the object. It is demonstrated that the new formulation allows uniqueness to be established not only in the case of scattering in free space but also in situations where additional restrictions are placed on the physical domain. This new formulation is more general than previous formulations in the sense that the same conditions are imposed on the field regardless of the physical domain. Explicit uniqueness proofs are provided in two special cases, scattering in free space and scattering in a half space. The problems associated with uniqueness for scattering in a waveguide is illuminated.

Acknowledgment

Effort partially sponsored by the Air Force Office of Scientific Research, Air Force Material Command, USAF, under grant number F9620–96–1–0039. The U.S. Government is authorized to reproduce and distribute reprints for Governmental purposes notwithstanding any copyright notation thereon. Also supported by CNRS–NSF International Cooperation Grant #INT–9415493, and a NATO Collaborative Research Grant #CR6–940999.

References

Angell, T.S., R.E. Kleinman, C. Rozier and D. Lesselier, 1996, Uniqueness and complete families for an acoustic waveguide problem, submitted to Wave Motion.

Atkinson, F. V., 1949, On Sommerfelds "radiation condition", Philosophical Magazine, **40**, 645-651.

Lambert, M., and D. Lesselier, 1995, On the retrieval of the plane wave reflection coefficient of a seabed in shallow water, Acta Acustica **4**, 243-249.

Magnus, W., 1942, Über Eindentigkeitsfragen bei einer Randwertaufgabe, Jahresbericht der Deutschen Mathematiker-Vereinigung, **52**, 177-188.

Neittaanmäki, P., and G.F. Roach, 1987, Weighted Sobolev spaces and exterior problems for the Helmholtz equation, Proceedings of the Royal Society of London, **A410**, 373-383.

Nosich, A. I., 1994, Radiation conditions, limiting absorption principle, and general relations in open waveguide scattering, Journal of Electromagnetic Waves and Applications, **8**, 329-353.

Rellich, F., 1943, Über das asymptotische Verhalten der Lösungen von $\Delta u + \lambda u = 0$ in unendlichen Gebeeten, Jahresbericht der Deutschen Mathematiker-Vereinigung, **53**, 57-64.

Sommerfeld, A., 1912, Die greensche funktion der schwingungsgleichung, Jahresbericht der Deutschen Mathematiker-Vereinigung, **21**, 309-353.

Sveshnikov, A. G., 1951, Limiting absorption principle for a waveguide, Doklady Akademii Nauk SSSR, **80**, 391-344 (in Russian).

Vekua, 1967, New Methods for Solving Elliptic Equations, North Holland, Amsterdam.

Wilcox, C. H., 1956, A Generalization of Theorems of Rellich and Atkinson, Proceedings of the American Mathematical Society, **7**, 271–276.

Xu, Y., 1990, The propagating solutions and far–field patterns for acoustic harmonic waves in a finite depth ocean, Applicable Analysis, **35**, 129-151.

The algebraic merits of inverse scattering

Patrick M. Dewilde
Circuits and Systems Laboratory, DIMES
Delft University of Technology, P.O. Box 5031, 2600 GA Delft, the Netherlands

Abstract

Scattering and inverse scattering theory have had a long standing interaction with complex function theory. Important problems concerning the characterization of certain types of functions have found a scattering interpretation and, conversely, insight in scattering theory has lead to their solution. It turns out that the properties concerned are algebraic in nature and that the scattering methods lead to new algorithms in numerical linear algebra. The paper traces the main steps in the reasoning.

1. Introduction

My interactions with Aad de Hoop have not been so much on the concept of reciprocity, although I have had the occasion of using the theory in the context of modeling interconnects on an integrated circuits, they have been more concerned with the use of mathematics in engineering and especially the relation between algebra en scattering. Although there is quite a qualitative difference between scattering in 3D space as described in the recent but already classical Handbook which De Hoop (1995) has published and scattering theory as used by researchers in Network Theory or Signal Processing, I believe that an interaction between the two fields may be interesting and fruitful, especially if it focuses on fundamental mathematical properties.

The scattering paradigm used in this paper consists of the definition of a 'medium' which propagates 'waves'. The medium has a right and a left side, waves may be incident at either side, and due to interactions in the medium, there are reflected waves at both sides as well (see Figure 1).

We shall assume that the medium is linear, causal and 'lossless', i.e. interactions require a finite amount of nonnegative time and there is no generation or loss of energy in the medium. The wave quantities are functions of either discrete or continuous time (depending on the context), typically they will be represented by time dependent vectors denoted as $a(t)$, and their energy is measured by the square of a quadratic norm such as $\int \|a(t)\|^2 dt$ or $\sum \|a(t)\|^2$. Because of our interest in numerical linear algebra, only the simplest possible cases will be considered here, but the ideas have a power and generality that transcends them.

We start out with Schur's parameterization theory for functions which are analytic and contractive in an open domain of the complex plane (we take the unit disc as prime example), and its interpretation as a prototype inverse scattering problem. The 'algebraification' produces a new criterion for contractive matrices (or operators in general), and has important applications in estimation theory (Burg's maximum entropy estimation) and in model reduction theory.

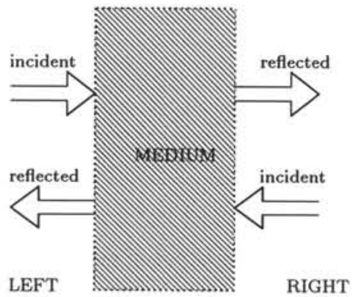

Figure 1. The scattering paradigm used in this paper.

The next section is concerned with the problem of constrained interpolation and its relation to scattering properties of a medium. Schur's theory turns out to be a special case of this rather more general approach, which can nicely be solved by exploitation of the state space properties of the scattering medium in its 'inverse scattering' form. In its algebraic version, the theory leads to the solution, in inverse scattering form, of the 'minimum sensitivity control problem' - a prime example of closed form solution for an optimization problem in linear differential games.

The third section considers the approximation of a transfer operator with one of minimal 'complexity' given a tolerable error norm. In complex function theory, this problem can be translated to an interpolation problem of a different kind than those treated in the previous section, but it leads also to an inverse scattering problem, but now of a partially anticausal medium. Also this problem can be made algebraic and its solution leads to a new algebraic result: a method to approximate a given matrix with one of lowest possible complexity, given a measure for tolerance (and, of course, a nice measure of complexity).

We conclude with pointing out some generalizations and connections.

2. Schur's parameterization

Schur's classical paper (Schur, 1917) on the parameterization of contractive functions which are analytic in the unit disc $\mathbf{D}$ of the complex plane $\mathbf{C}$ dates form 1917, but was unfortunately largely unknown in the applied mathematics community (except to complex analysts). As a result, its main ideas were rediscovered many times, e.g. in Circuit Theory (Darlington synthesis) and Estimation Theory (the many variations on Levinson's algorithm). Its interpretation as an inverse scattering method, and its 'algebraification' has lead to a flurry of modern methods for 'fast algorithms', for a recent account, see Kailath and Sayed (1995).

For the sake of an easy discussion (to be generalized soon), let us start out with a scalar function $S(z)$ which is analytic in $\mathbf{D} = \{z \in \mathbf{C} : |z| < 1\}$, the open unit disc of the complex plane (other domains can be conformally transformed to $\mathbf{D}$ without much harm). Let's concentrate on criteria to answer the question: when is $S(z)$ contractive, i.e. such that $\forall z \in \mathbf{D} : |S(z)| \leq 1$? We do not want (and are not able!) to test all points $z \in \mathbf{D}$. Schur's parameterization provides for a numerically feasible test. Let's call 'CS' the condition 'S is contractive in $\mathbf{D}$'.

Step 1: Define the 'reflection coefficient, $\rho_0 = S(0)$. A necessary condition for CS is $|\rho_0| \leq 1$. It splits in two cases:

- $|\rho_0| = 1$. Then S is necessarily a constant of modulus 1 by the maximum modulus theorem of complex analysis, and CS is (now trivially) satisfied.
- $|\rho_0| < 1$. Then define the new function, $S^{(1)} = \dfrac{S(z) - \rho_0}{z(1 - \bar{\rho}_0 S(z))}$.
  S will satisfy CS iff in addition to $|\rho_0| < 1$, $S^{(1)}$ satisfies CS.

It turns out that $S^{(1)}$ is 'simpler' than S. This leads to the recursion:

Step n: Define $\rho_{n-1} = S^{n-1}(0)$. A necessary condition for CS is certainly $|\rho_{n-1}| \leq 1$ (in addition to $\forall k < n-1 : |\rho_k| < 1$). Again the analysis splits in two cases:

- $|\rho_{n-1}| = 1$. Then S^{n-1} is necessarily a constant of modulus 1 if it satisfies CS.
- $|\rho_{n-1}| < 1$. Then define the new function, $S^{(n)} = \dfrac{S^{(n-1)}(z) - \rho_0}{z(1 - \bar{\rho}_0 S^{(n-1)}(z))}$,
  and CS will be satisfied in this case iff, in addition, $S^{(n)}(z)$ satisfies CS.

Proceed with the recursion!

The result is Schur's parameterization theorem:

Theorem 1 *A complex function $S(z)$ which is analytic in the open unit disc of the complex plane will be contractive iff its Schur parameterization produces either:*

- *an infinite series of reflection coefficients $\rho_0, \rho_1, \rho_2, \cdots$, which are all smaller than one in modulus, or*
- *a finite series of reflection coefficients $\rho_0, \rho_1, \cdots, \rho_n$, in which the last coefficient ρ_n has modulus one (the recursion then terminates implicitly with a constant modulus one function and $S(z)$ is unitary on the unit circle).*

Schur's test is indeed a very practical one. Not only does it reduce the CS problem to a recursion, even a finite version of that recursion produces useful approximations to S. The scattering interpretation provides more insight in the process.

2.1. A scattering interpretation of Schur's parameterization

The key is provided by a bilinearization of Schur's algorithm. Let us write:

$$S^{(n)}(z) = \frac{B^{(n)}}{A^{(n)}}, \tag{1}$$

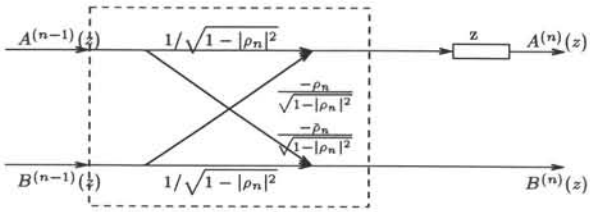

Figure 2. The 'inverse scattering' interpretation of Schur's algorithm.

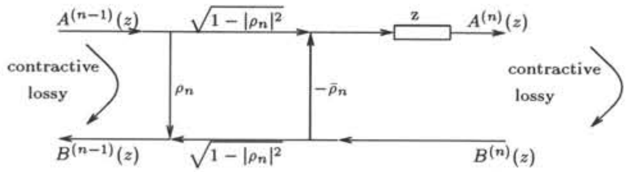

Figure 3. The lossless medium with its waves corresponding to the Schur situation.

then Schur's recursion can be linearized, using a strategic constant K_n, as follows:

$$\begin{aligned} A^{(n)}(z) &= K_n z[A^{(n-1)}(z) - \bar{\rho}_{n-1}B^{(n-1)}(z)], \\ B^{(n)}(z) &= K_n[B^{(n-1)}(z) - \rho_{n-1}A^{(n-1)}(z)]. \end{aligned} \tag{2}$$

A good choice for K_n is $K_n = \frac{1}{\sqrt{1-|\rho_n|^2}}$, this gives the following relation between the quantities:

$$[A^{(n)}(z)\ B^{(n)}(z)] = [A^{(n-1)}(z)\ B^{(n-1)}(z)] \begin{bmatrix} \frac{z}{\sqrt{1-|\rho_n|^2}} & -\frac{\rho_n}{\sqrt{1-\rho_n}} \\ -\frac{\bar{\rho}_n z}{\sqrt{1-|\rho_n|^2}} & \frac{1}{1-|\rho_n|^2} \end{bmatrix}. \tag{3}$$

The rightmost matrix, which we call $\theta_n(z)$ can now be interpreted as transferring a set of 'left waves' $A^{(n-1)}$, $B^{(n-1)}$ to a set of 'right waves' $A^{(n)}$, $B^{(n)}$ with conservation of energy. It is called a *chain scattering matrix*. The conservation is a consequence of the algebraic properties of θ_n, which is a cascade of a hyperbolic or J-unitary matrix for the signature matrix $J = [1 \dotplus -1]$ ($\dotplus$ indicates a sequence of diagonal entries), and a pure delay on the top line - see Figure 2. The waves $A^{(n-1)}$, $B^{(n)}$ are 'incident' (the first from the left, the second from the right environment), while $B^{(n-1)}$ and $A^{(n)}$ are reflected into the environment. Therefore, a correct, physical scattering picture, in which the physical directions of waves is respected and the medium behaves in a truly lossless way, is given in Figure 3.

2.2. Algebraification of Schur's algorithm

Suppose now that S is instead an $n \times n$ matrix. We wonder when S is a contraction, i.e. using $\tilde{\cdot}$ for Hermitian conjugation ($[\tilde{S}]_{ij} \doteq \bar{S}_{ji}$), when is $I - S\tilde{S} \geq 0$? A straight conversion of Schur's algorithm to an algebraic setting (Dewilde and Deprettere, 1988) is obtained when S is taken upper diagonal (the more general case follows immediately):

$$S = \begin{bmatrix} s_{11} & s_{12} & \cdots & s_{1n} \\ 0 & s_{22} & \cdots & s_{2n} \\ & & \ddots & \vdots \\ 0 & & & s_{nn} \end{bmatrix}. \tag{4}$$

Look now at the main diagonal:

$$S_0 = \begin{bmatrix} s_{11} & 0 & \cdots & 0 \\ 0 & s_{22} & \cdots & 0 \\ & & \ddots & \vdots \\ 0 & & & s_{nn} \end{bmatrix}. \tag{5}$$

S will be contractive iff $\forall i : |s_{ii}| \leq 1$. If one s_{ii} has modulus one, then the other elements in row and column i must be zero, and the problem can be deflated, else the s_{ii} are strictly less than 1 in modulus, $\|S_0\| < 1$ (for the usual Euclidean norm) and we should be able to execute a recursive Schur step on the matrix as before in the complex calculus case. What is the Schur step now? We need a little more sophistication, but it is well worth the effort since the formulas that we shall obtain are fairly generally and applicable in other contexts as well.

Consider the 'Halmos form' based on S_0:

$$H(S_0) = \begin{bmatrix} I & -S_0 \\ -\tilde{S}_0 & I \end{bmatrix} \begin{bmatrix} (I - S_0\tilde{S}_0)^{-\frac{1}{2}} & 0 \\ 0 & (I - \tilde{S}_0 S_0)^{-\frac{1}{2}} \end{bmatrix}. \tag{6}$$

A little calculation shows that $H(S_0)$ is indeed a generalized hyperbolic matrix (it is J-unitary for the signature $J = I_n \dot{+} - I_n$), and that the (generalized) Schur transformation needed on S now reads:

$$S^{(1)} = (I - S_0\tilde{S}_0)^{\frac{1}{2}}(I - S\tilde{S}_0)^{-1}(S - S_0)(I - \tilde{S}_0 S_0)^{-\frac{1}{2}}. \tag{7}$$

The main diagonal of $S^{(1)}$ is zero (it is still upper triangular!), and the next step can then be executed on the next upper diagonal (this effectively performs the 'shift'). This procedure is again recursive and leads to a complete parameterization of the original matrix in terms of diagonals, a recursive procedure to check the contractivity, and a corresponding Schur like theorem.

2.3. Interpolation and approximation

A slight modification of Schur's algorithm leads to the classical theory of maximum entropy interpolation, also known as 'Burg's theory' in geophysics (Burg, 1975). Assume that a covariance of a second order process is given: $c_0, c_1, c_2, \cdots$ corresponding to the spectral density function (with $i \doteq \sqrt{-1}$),

$$W(e^{i\theta}) = \sum_{k=-\infty}^{\infty} c_k e^{ik\theta}, \tag{8}$$

and define the corresponding 'Caratheodory function'

$$C(z) = c_0 + 2c_1 z + 2c_2 z^2 + \cdots = c_0 + 2\sum_{k=1}^{\infty} c_k z^k. \tag{9}$$

$C(z)$ is 'positive real' or PR in the unit disc of the complex plane, meaning that its real part is nonnegative there. A PR function can easily be turned into a contractive one by the Cayley transform:

$$S(z) = (C(z) - c_0)(C(z) + c_0)^{-1}. \tag{10}$$

Schur's algorithm can then be applied to $S(z)$ to obtain a test for PR-ness of $C(z)$. Keeping in line with our 'wave' philosophy, this can be streamlined as follows. We take as system of (left) waves $[(C(z)+c_0)\ (C(z)-c_0)]$ and start the Schur recursion (this time we can start with a delay, followed by a hyperbolic rotation because now $B^{(0)}(0) = C(0) - c_0 = 0$). After n such steps (with the hyperbolic rotation following rather than preceding) we obtain a polynomial matrix $\Theta_n(z)$ of degree n, for which

$$[(C(z)+c_0)\ (C(z)-c_0)]\Theta_n(z) = z^n[A^{(n)}(z)\ B^{(n)}(z)], \tag{11}$$

such that also $B^{(n)}(0) = 0$. $\Theta_n(z)$ has many remarkable properties. Its entries are closely related to a set of orthogonal polynomials on the unit circle of the complex plane with respect to a measure given by the spectral density. In fact, $\Theta_{22}(z) = \frac{p_n(z)+q_n(z)}{2}$ and $\Theta_{12}(z) = \frac{p_n(z)-q_n(z)}{2}$ where the $p_n(z)$'s are such polynomials and the $q_n(z)$'s are orthogonal w.r. to a conjugate spectrum. They all have their zeros strictly outside the closed unit disc, a fact which is due to the physical passivity (contractivity) of the corresponding scattering matrix. If $C_n \doteq \frac{q_n}{p_n}$, then it is PR also, and C shares with C_n the first $n+1$ coefficients c_k: $C(z) - C_n(z) = z^{n+1}F(z)$ for some $F(z)$ which is analytic in the open unit disc. It turns out that the spectral density corresponding to $C_n(z)$ is given by

$$W_n(e^{i\theta}) = \frac{1}{\overline{p_n(e^{i\theta})}p_n(e^{i\theta})}. \tag{12}$$

Since $p_n(z)$ is polynomial, $W_n(e^{i\theta})^{-1}$ is a pseudopolynomial of order n whose inverse W interpolates the $2n+1$ central entries of $W(e^{i\theta})$. It can be shown that, hence, W_n is the maximum entropy interpolating density of order n for W (see further).

Although these properties appear very specific for certain sets of polynomials and certain analytic functions, they are actually algebraic in nature, and they generalize nicely to matrices or more general operators. We briefly summarize the generalization for upper triangular matrices. Suppose that, originally, a symmetric or Hermitian matrix W had been given with diagonals $W_k : k = -(n+1)\cdots(n+1)$ - W could represent a covariance of a finite process if it is positive definite - and let C be the upper triangular matrix derived from W, with main diagonal C_0 and further:

$$C \doteq C_0 + 2\sum_{k=1}^{n} C_k. \tag{13}$$

W will be positive definite iff the upper triangular 'Schur'-matrix $S = (C - C_0)(C + C_0)^{-1}$ is contractive (again the Cayley transform!) Let us apply the algebraic (diagonal based) Schur algorithm on the 'wave' matrix $[C + C_0 \; C - C_0]$ (assuming no singularities, which will be the case when W is strictly positive definite). Suppose that we perform n Schur steps, and hence obtain a partial matrix Θ_n with just $n+1$ non-zero diagonals in each block-entry. Suppose that $\Theta_n(z)$ is a chain scattering matrix as obtained in the algebraic algorithm described above. Then we can define a matrix

$$C_n = ((\Theta_n)_{22} - (\Theta_n)_{12})((\Theta_n)_{22} + (\Theta_n)_{12})^{-1}. \tag{14}$$

It turns out that C_n has the property that $\frac{C_n + \tilde{C}_n}{2} \geq 0$ - the algebraic equivalent of PR. If we define, moreover, $T_{fn}(z) \doteq ((\Theta_n)_{22} + (\Theta_n)_{12})^{-1}$, then we find

$$W_n \doteq \frac{C_n + \tilde{C}_n}{2} = \tilde{T}_{fn} T_{fn}. \tag{15}$$

Just as before, C_n will coincide with C in its first $n+1$ diagonals, and $W - W_n$ will be zero in a central diagonal band of width $2n+1$. W_n is a 'maximum entropy' interpolant of W, because W_n^{-1} is zero outside the band which supports the interpolation, the characteristic maximum entropy feature. Indeed, the 'entropy' of a positive definite matrix W is given by $\ln \det W$, and if w_{ij} corresponds to a free entry (outside the band), then, with M_{ij} the minor corresponding to w_{ij}

$$\frac{\partial}{\partial w_{ij}} \ln \det W = \frac{M_{ij}}{\det W} = [W^{-1}]_{ji}, \tag{16}$$

which must hence be zero when the maximum entropy solution is reached.

The previous theory has found a host of important and interesting applications in spectral estimation theory (linear predictive coding and DPCM), in model reduction theory of chip interconnects (Dewilde, 1988), and in seismic signal processing.

3. Generalized interpolation

A cascaded scattering medium has many more interesting properties in store! Although some of them are not obvious in a physical situation, they can be made plausible through reference to one. In particular, we use the z-transform which refers to time-discrete systems consistently, yet imagine the properties in a continuous time setting. This will not lead to mistakes if each point made is proven separately on its own merits. Consider a lossless cascade with resonant cavities as shown in Figure 4.

Suppose that the cavities have complex resonating frequencies $z_1, z_2, \cdots, z_n$, now in the open unit disc (this stretches the imagination somewhat, but it can be motivated!) If $S_L(z)$ is the scattering matrix of a passive load on the left of the medium, and $S(z)$ describes the scattering at the input, then $S(z_i)$ is independent of S_L because the resonating sections do not allow for signal propagation, they produce 'transmission zeros' in the cascade! In addition $S(z)$ is a contractive function as soon as S_L is, irrespective of its precise value. Turning the reasoning around, we see that the solution

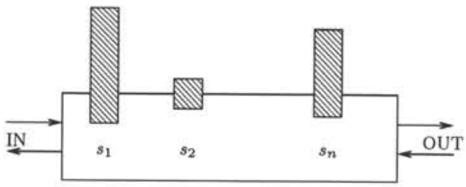

Figure 4. A lossless cascade with resonant cavities producing transmission zeros.

of a constrained interpolation problem could possibly be found by solving an inverse scattering problem. We show now how this comes about. Let the interpolation points be points in $\mathbf{D}$ - the unit disc of the complex plane, and assume that the desired interpolation values are given by a corresponding set $\{s_i : i = 1 \cdots n\}$. This is data given at the input of a (lossless) scattering medium which we are supposed to determine, and preferably a minimal one as well. Although a recursive algorithm in the taste of the Schur recursion given above is possible here, we follow a different route, which utilizes the state space description of the chain scattering matrix.

A state space description of any time discrete system with finite dimensional state sequence $\{x(t) : t \text{ integer}\}$, assuming $u(t), y(t), x(t)$ row vectors of possibly variable dimensions where the sequence $u(t)$ is the input of the system, $y(t)$ the output, is given by:

$$\begin{aligned} x(t+1) &= x(t)A(t) + u(t)B(t), \\ y(t) &= x(t)C(t) + u(t)D(t). \end{aligned} \tag{17}$$

When the system is time invariant, then the matrices A, B, C, D are constant and also the dimensions of each type of vectors - in particular, A is a square matrix. The description is said to be minimal if the dimension of $x(t)$ is minimal at each point in time. Even a minimal state description is not unique, a state transformation $\hat{x}(t) = x(t)R(t)$ with a non-singular transformation matrix $R(t)$ induces an equivalent state representation:

$$\begin{aligned} \hat{x}(t+1) &= \hat{x}(t)R^{-1}(t)A(t)R(t+1) + u(t)B(t)R(t+1), \\ y(t) &= \hat{x}(t)R^{-1}(t)C(t) + u(t)D(t). \end{aligned} \tag{18}$$

Suppose now that $A(t), B(t), C(t), D(t)$ is a minimal state space representation of a causal, lossless chain scattering matrix. What characterizes these matrices as such? The answer is given by the following proposition, which is valid under some technical assumptions on the stability of the transition matrices $A(t)$ - we skip details:

Proposition 2 *$A(t), B(t), C(t), D(t)$ will be a state space representation of a causal lossless chain scattering matrix if and only if there exists a state transformation $R(t)$ such that the transition matrix*

$$\begin{bmatrix} R^{-1}(t)A(t)R(t+1) & R^{-1}(t)C(t) \\ B(t)R(t+1) & D(t) \end{bmatrix} \tag{19}$$

is J-unitary for conformal signature matrices of the type $J = I_n \dot{+} I_p \dot{+} -I_q$ (in which n is the local state dimension, p the dimension of the incident wave and q the dimension of the reflected wave, all possibly time-varying).

Proposition 2 says that there exists a state space representation for the chain scattering matrix in which the value of the state space variable actually represents the energy balance - it would correspond to a physical, lossless realization.

Returning back to our interpolation problem, let's look first at the time invariant situation. It turns out that the interpolation data $\{z_i, s_i : i = 1 \cdots n\}$ determine the matrices A, B of some realization for the relevant chain scattering operator $\Theta(z)$. These are called the reachability matrices of the system because they control how its state is generated from the inputs. The next ingredient to solve the interpolation problem is given by

Proposition 3 *The chain scattering matrix $\Theta(z)$ will interpolate the given input data set, if it has a (minimal) state space representation for which the reachability operators are:*

$$A = \begin{bmatrix} z_1 & & & \\ & z_2 & & \\ & & \ddots & \\ & & & z_n \end{bmatrix}, \quad B = \begin{bmatrix} 1 & 1 & \cdots & 1 \\ s_1 & s_2 & \cdots & s_n \end{bmatrix}. \tag{20}$$

We have already two of the main ingredients for the solution of the interpolation problem, we need two more. An analysis of the J-unitarity condition for the state realization given by proposition 2 leads to the search for a state transformation matrix R for which

$$[\tilde{R}\tilde{A}\tilde{R}^{-1} \ \tilde{R}\tilde{B}] \begin{bmatrix} I_n & & \\ & I_p & \\ & & -I_q \end{bmatrix} \begin{bmatrix} R^{-1}AR \\ BR \end{bmatrix} = I. \tag{21}$$

Hence $\Lambda \doteq \tilde{R}^{-1}R^{-1}$ should be the solution of the so called Lyapunov-Stein equation

$$\tilde{A}\Lambda A + \tilde{B}JB = \Lambda. \tag{22}$$

For R to exist, it is necessary that Λ be positive definite.

A solution to (22) in the form of an infinite sum (assuming A stable, certainly a necessary condition) can be given:

$$\Lambda = \sum_{i=0}^{\infty} \tilde{A}^i \tilde{B} J B A^i. \tag{23}$$

In this relatively simple case, the summation produces a closed form, the celebrated Nevanlinna-Pick matrix:

$$\Lambda = \begin{bmatrix} \frac{1-|s_1|^2}{1-|z_1|^2} & \cdots & \frac{1-\bar{s}_1 s_n}{1-\bar{z}_1 z_n} \\ & \cdots & \\ \frac{1-\bar{s}_n s_1}{1-\bar{z}_n z_1} & \cdots & \frac{1-|s_n|^2}{1-|z_n|^2}. \end{bmatrix}. \tag{24}$$

Having found R, we must construct the relevant chain scattering matrix next. This problem reduces to a J-unitary completion of the J-isometric partial definition of the state space description for Θ given by

$$\begin{bmatrix} R^{-1}AR & \star \\ BR & \star \end{bmatrix}. \tag{25}$$

In the present (relatively simple) case, this can also be done in closed form, see e.g. Gohberg *et al.* (1990) for a recent account. In any event, if R exists, then the solution to the (strict) constrained interpolation problem exists as well. It is given in terms of a chain scattering operator $\Theta(z)$ loaded in a passive but otherwise general scattering operator $S_L(z)$. If we denote the corresponding input scattering function $S(z)$ by $\mathbf{T}_\Theta(S_L)$, then we obtain the Nevanlinna-Pick theorem

Theorem 4 *Given a set of n points $\{z_i : i = 1 \cdots n\}$ in the open unit disc $\mathbf{D}$ of the complex plane and a set of n complex values $\{s_i : i = 1 \cdots n\}$, then a (strictly) contractive analytic function $S(z)$ will exist iff the Nevanlinna-Pick matrix Λ given by (24) is (strictly) positive definite. All possible solutions are given in the strict case as $\mathbf{T}_\Theta(S_L)$ where Θ is a lossless chain scattering matrix with reachability matrices given by (20).*

(In the singular case solutions can be given as well, but they are more involved.)

The inverse scattering method just described generalizes to matrices and time-varying systems. This requires the introduction of the notion of a generalized shift. If we have a (non uniform) time sequence $x(k)$, we can still define the shift xZ : $(xZ)(k) \doteq x(k-1)$. If T is a (general bounded) causal operator (an upper triangular matrix e.g.) and D is a diagonal operator, then we shall say that T is (left-)divisible by D if we can write $T = (Z - D)T_1$ with T_1 also causal and bounded. The definition implies that the dimensions of Z and D are conformal with T and T_1 (quite some latitude is possible here). One should realize that Z does not commute with operators or matrices: $ZT \neq TZ$ unless T is a doubly infinite Töplitz matrix corresponding to a time invariant operator. In fact, we find here a kind of pseudo-commutativity which works just as well. Let Z^* be the adjoint (in this case also inverse) of Z, then $T^{(1)} \doteq ZTZ^*$ is like T but all elements shifted one notch down the diagonals in the south-east direction. We define more generally: $T^{(n)} \doteq Z^nTZ^{*n}$, in which n may be positive and negative. Let's furthermore introduce the projection operators: $\mathbf{P}$ maps a matrix or operator on its causal part (i.e. on its upper diagonals), $\mathbf{P}_0$ on its instantaneous part or main diagonal and $\mathbf{P}'$ on its strictly anticausal part (it is the complement of $\mathbf{P}$). One should be careful here with the notion of boundedness: if T is a bounded operator, then the upper part of T, $\mathbf{P}(T)$, is not necessarily bounded! But again, we shall not worry about technical 'details'.

The Nevanlinna-Pick problem described in the previous paragraphs generalizes immediately to the algebraic situation if one replaces the z_i by diagonals D_i, and the s_i by 'diagonal values' S_i, diagonals for which $S - S_i$ must be divisible by $Z - D_i$. The generalized state space description given by (17) can easily be brought in this formalism, and used to describe algebraic computations. We collect the system matrices

$A(n), B(n), \cdots$ in new diagonal matrices such as $A \doteq [\cdots \dot{+} A(-1) \dot{+} A(0) \dot{+} A(1) \cdots]$ i.e. A is a block matrix such that $A_{ij} = A(i)\delta_{ij}$ for the Kronecker delta δ_{ij}. The state equations 17 can then be written succinctly as:

$$\begin{array}{rcl} xZ^* & = & xA + uB, \\ y & = & xC + uD. \end{array} \tag{26}$$

and the resulting transfer operator or matrix is given by

$$T = D + BZ(I - AZ)^{-1}C \tag{27}$$

at least if meaning can be given to the inverse of $(I - AZ)$ - see further. The generalized interpolation problem will find a solution if there exists a lossless chain scattering operator with a state description having the reachability operators

$$A = \begin{bmatrix} D_1 & & & \\ & D_2 & & \\ & & \ddots & \\ & & & D_n \end{bmatrix}, \quad B = \begin{bmatrix} I & I & \cdots & I \\ S_1 & S_2 & \cdots & S_n \end{bmatrix}. \tag{28}$$

This will be the case when there exists a diagonal state transformation operator R and hence a positive definite solution to the generalized Lyapunov-Stein equation in the diagonal matrix $\Lambda = \tilde{R}^{-1}R^{-1}$:

$$\tilde{A}\Lambda A + \tilde{B}JB = \Lambda^{(-1)}. \tag{29}$$

The following remarks are in order here:

- The Lyapunov-Stein equation now involves a diagonal shift, because of the non-commutativity of the shift operator Z.
- The signature operator J must be adapted to the 'time-varying' situation. It tallies incident and reflected waves per time point: $J \doteq [\cdots \dot{+} I_{p(-1)} \dot{+} - I_{q(-1)} \dot{+} I_{p(0)} \dot{+} - I_{q(0)} \dot{+} I_{p(1)} \dot{+} - I_{q(1)} \dot{+} \cdots]$.
- Special attention must be devoted to the stability properties of the diagonal operator A. In the time invariant case A is stable when all its eigenvalues are in the open unit disc of the complex plane, guaranteeing that $\lim_{k\to\infty} A^k = 0$. Here we must require that $\lim_{k\to\infty}(ZA)^k = 0$. The quantity $\ell_A \doteq \lim_{k\to\infty} \|(ZA)^k\|^{\frac{1}{k}}$ is known as the 'spectral radius' of ZA, and stability (again a necessary condition) is ensured when $\ell_A < 1$. (This condition is much less stringent than $\|A\| < I!$). We have $(ZA)^k = Z^k A^{(k-1)} \cdots A^{(1)}A$. Let us define $A^{\{k\}} \doteq A^{(k-1)} \cdots A^{(1)}A$, then $\|(ZA)^k\| = \|A^{\{k\}}\|$ and $\ell_A = \lim_{k\to\infty} \|A^{\{k\}}\|^{\frac{1}{k}}$. When $\ell_A < 1$, then there exists a bounded inverse to $(I - AZ)$ given by the Neumann series:

$$(I - AZ)^{-1} = I + \sum_{k=1}^{\infty}(AZ)^k. \tag{30}$$

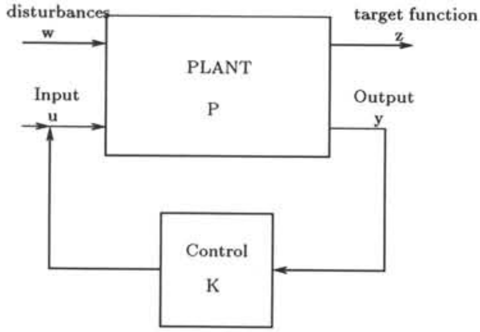

Figure 5. Minimal sensitivity control: the situation.

Again, (29) can be solved as an infinite sum, assuming stability of A:

$$\Lambda = \left[\sum_{k=0}^{\infty} \tilde{A}^{\{k\}}\tilde{B}JBA^{\{k\}}\right]^{(1)}. \tag{31}$$

The solution to the (strict) constrained interpolation problem will exist iff Λ is a strictly positive definite operator, in which case all possible solutions are again given in terms of a lossless chain scattering matrix terminated in a causal contractive load S_L: $S = \mathbf{T}_\Theta(S_L)$ where Θ is obtained through J-unitary completion of

$$\begin{bmatrix} R^{-1}AR^{(-1)} & \star \\ BR^{(-1)} & \star \end{bmatrix}. \tag{32}$$

3.1. Minimal sensitivity control

Perhaps the best application of the previous interpolation theory is to minimal sensitivity control. We give a brief introduction to this subject emphasizing the connection with scattering theory - we refer the interested reader to the extensive literature. Figure 5 describes the situation.

Suppose that we are given a 'plant' which interacts with its environment via four signals or data streams: u is a vector of the available inputs for control, vector w represents all external disturbances (noise e.g.) which have an effect at some point in the system, y are the available (measurable) output streams, and z are quantities on which we wish to minimize disturbances. Our goal will be to design a controller acting on the inputs u and using data from y in such a way that (a) the resulting closed loop plant is stable, and (b) the sensitivity operator mapping disturbances from w to z is minimized. (This problem is known as the 'four block minimum sensitivity problem' - because of the split between the control and sensitivity input/output's. Needless to say some inputs or outputs may coincide). We assume that both plant and control are described by linear operators. In general the plant is not necessarily stable, and some of the operators may be incomplete etc... the theory for this problem is quite

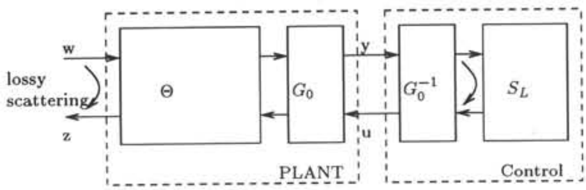

Figure 6. The chain formulation for the sensitivity problem.

involved! As a first simplification, we set as our goal to constrain the sensitivity function in norm, which we can as well normalize to 1. So we request that the sensitivity operator which maps w to $z = wS$ has $\|S\| \leq 1$. This problem was first formulated by Zames (1981). It was solved in Doyle *et al.* (1989) using more or less a brute force technique, solutions in terms of chain scattering operators appeared around 1988 by a number of authors, following the tracks originally laid out in Ball and Helton (1983). The trick is to convert the plant operator $P : [w, u] \to [z, y]$ to a chain operator: $G : [w, z] \to [y, u]$, see Figure 6.

Suppose now that we are able to factor the chain operator G as $G = \Theta G_0$, in which Θ is a lossless chain scattering matrix and G_0 is a stable causal operator such that also G_0^{-1} is also stable and causal (such operators are called 'outer' or 'minimal phase'). Then S will automatically be causal and contractive (and hence stable) if $K = G_0^{-1} S_L$ for any causal, contractive (i.e. passive) load S_L. Hence, the factorization $G = \Theta G_0$ of G in a lossless chain scattering matrix and a minimal phase factor solves the sensitivity problem! It turns out that this factorization is in fact equivalent to a constrained interpolation problem of a somewhat more involved kind than described above. Indeed, G and Θ must share 'transmission zeros' in the cascade displayed in Figure 6. However, the factorization puts requirements on G *and* on G^{-1} which both may have unstable parts. This then produces a so-called double-sided constrained interpolation problem which goes beyond the present discussion.

4. Minimal complexity approximations

A final, rather general algebraic problem for which we can give a solution in at least one important setting using inverse scattering theory is the problem of approximating a given matrix or operator with one of the lowest possible computational complexity, given an acceptable tolerance. Let us first introduce two classical instances, one algebraic and the other analytic. Suppose that T is a matrix close to singular. One can wonder: given an adequate norm $\|\cdot\|$ and a tolerable measure $\epsilon > 0$ for the error, does there exists an approximate matrix T_a of minimal possible rank, such that $\|T - T_a\| < \epsilon$? The answer in the case of the very strong Frobenius norm (valid for the Euclidean norm as well) is attributed to Jacobi and was found in the course of the previous century: perform a singular value decomposition (SVD) of T, discard all singular values $\sigma_k < \epsilon$ and write:

$$T_a = \sum_{k=1}^{\ell} \sigma_k u_k \tilde{v}_k. \tag{33}$$

in which the $\{u_k, v_k\}$ are the singular vectors (or Schmidt pairs) corresponding to the significant singular values σ_k. The computational complexity of the vector-matrix product xT_a is of the order $n * \ell$ instead of n^2, which may be a very sizable reduction if $\ell \ll n$. More importantly, the singular vectors often have a physical meaning (e.g. the 'signal space' in signal detection applications), for that reason the SVD has become a major workhorse for signal processing engineers. However, the method only works when T is indeed close to singular, and its effective rank ℓ is very low indeed. But what if T is intrinsically non-singular? Can we still find nice minimal complexity approximants?

A second classical complexity reduction method is known as the 'Hankel norm approximation' of a transfer function. Suppose that $T(z)$ is a given, causal and stable rational transfer matrix (it is analytic in the open unit disc, say), and suppose that its Smith-MacMillan degree is n ($T(z)$ then has a state space representation with state space of minimal dimension n as well). Given an ϵ, can we find an approximating (causal and stable) transfer matrix T_a such that $\|T - T_a\| < \epsilon$ for some meaningful norm and T_a has minimal state space complexity (Smith-MacMillan degree)? An attractive closed form answer to this problem is known for the so called 'Hankel norm'. Let us assume $T(z)$ strictly causal, then $T(z) = t_1 z + t_2 z^2 + \cdots$ and the Hankel norm is given by the norm of the operator

$$H_T = \begin{bmatrix} t_1 & t_2 & t_3 & \cdots \\ t_2 & t_3 & t_4 & \cdots \\ t_3 & t_4 & \cdots & \cdots \\ \cdots & \cdots & \cdots & \cdots \end{bmatrix}. \tag{34}$$

H_T is the operator which, for any time point, maps (strictly) past inputs to future outputs. It can be defined for any kind of dynamical system and its norm is relatively easy to compute. It turns out that the Hankel norm is stronger than the quadratic norm, but weaker that the supremum norm on the unit circle, which is too strong for approximation purposes anyway, since rational transfer functions are not dense in the set of stable and causal transfer functions for that norm. Analysis leads again to a classical interpolation problem, but one of quite a different type from the previous section, namely one known as of the 'Schur-Takagi' type (Adamjan *et al.*, 1971). It can be solved, once again, using inverse scattering techniques, now, however, with a different type of chain scattering matrices. These do conserve energy but they are unphysical in the sense that the corresponding scattering operator is not causal, corresponding to partial propagation of waves running backward in time. We show the construction directly in the algebraic domain (Dewilde and Van der Veen, 1993).

We start out with a 'high order' representation of the operator T to be approximated, i.e. a very close approximant to T which uses a finite data set with as much data as needed and which has a state space representation given by three diagonal operators $\{A, B, C\}$, in which A is a stable diagonal operator and which is such that $\{A, C\}$ is isometric, i.e. such that $\tilde{A}A + \tilde{C}C = I$ (this can always and easily be achieved, even for infinite dimensional operators, by using a series expansion in the diagonals of T up to any desired order - for convenience we identify T with this representation). Next, we determine diagonal matrices B_u and D_u which complete the isometric $\{A, C\}$ so that

$$\begin{bmatrix} A & C \\ B_u & D_u \end{bmatrix} \tag{35}$$

is unitary. Let U be the corresponding (causal and unitary) operator, and define

$$\Delta^* \doteq TU^*. \tag{36}$$

It turns out that Δ is again causal and bounded (by the definition of U). Let a tolerance matrix ϵ be given as well (this time it may be a diagonal matrix with varying entries). Consider now the reachability matrix:

$$\begin{bmatrix} A \\ B_u \\ \epsilon^{-1}B \end{bmatrix}, \tag{37}$$

and suppose that Θ is a J-unitary chain scattering matrix which has a state representation with this reachability matrix. The various definitions insure that

$$U^*\Theta_{12} - T^*\epsilon^{-1}\Theta_{22} \doteq -\beta \tag{38}$$

is bounded and causal. If we define $T' \doteq \epsilon\Theta_{22}^{-*}\beta'^*$ and $S = \Theta_{12}\Theta_{22}^{-1}$ then S is a contractive but not necessarily causal input scattering matrix, and we find that

$$T - T' = \epsilon S^* U. \tag{39}$$

A further analysis shows the following:
(a) Θ will exist if the solution of the Lyapunov-Stein equation,

$$\Lambda^{(-1)} = \tilde{A}\Lambda A + \tilde{B}\epsilon^2 B, \tag{40}$$

is such that $\Lambda \doteq I - M$ is boundedly invertible (the solution M will always exist, but, if Λ is not invertible, we will have hit a 'singular case' which can be fixed e.g. by adapting ϵ.)
(b) Θ is a causal J-unitary chain scattering matrix, but it does not satisfy the losslessness constraint. That would only be the case if Λ were positive definite. At each time point k, a non singular Λ will have $\sigma_+(k)$ positive and $\sigma_-(k)$ negative eigenvalues.
(c) Since $\|S\| < 1$ and $\|U\| = 1$ we have that $\|\epsilon^{-1}(T - T')\| < 1$. But T' is not causal. It we take the causal part of T' for T_a, $T_a \doteq \mathbf{P}(T')$, then the celebrated Nehari theorem states that $\|\epsilon^{-1}(T - T_a)\|_H < 1$, i.e. T_a approximates T better than ϵ in Hankel norm.
(d) Finally, T_a has minimal state complexity. In fact, its local state complexity is given by $\sigma_-(k)$ and it can be shown that this is indeed minimal.

We see that, once more, a powerful technique from analysis can be turned into an algebraic method which provides a solution to an old approximation problem, and the solution is found using the inverse scattering paradigm.

5. Final discussion

One may wonder why inverse scattering proves to be such a powerful mathematical method. We have hinted at some partial answers already. The inherent physical constraints due to losslessness, or more generally J-unitarity provide part of the answer. In addition, cascading gives algebraic constraints on the input function which translate as interpolation properties. The combination of the two allows us to solve constrained optimization problems, and these are not easy to solve in the first place. But there is undoubtedly more below the surface.

References

Adamjan, V.M., D.Z. Arov and M.G. Krein, 1971, Analytic properties of schmidt pairs for a hankel operator and the schur-takagi problem, USSR Sbornik, **15**, 31-73.

Ball, J.A., and J.W. Helton, 1983, A beurling-lax theorem for the lie group u(m,n) which contains most classical interpolation theory, Journal of Operator Theory, **9**, 107-142.

Burg, J.P., 1975, Maximum entropy spectral analysis, Ph.D. Thesis, Stanford University.

De Hoop, A.T., 1995, Handbook of Radiation and Scattering of Waves, Academic Press Lmited, London.

Dewilde, P.M., 1988, New algebraic methods for modelling large-scale integrated circuits., International Journal of Circuit Theory and Applications, **16**, 473-503.

Dewilde, P.M., and E.F. Deprettere, 1988, The generalized schur algorithm: approximation and hierarchy, Operator Theory: Advances and Applications, **16**, 437-503.

Dewilde, P.M., and A.J. van der Veen, 1993, On the Hankel-norm approximation of upper-triangular operators and matrices, Integral Equations and Operator Theory, **17**, 1-45.

Gohberg, E., J.A. Ball and L. Rodman, 1990, Interpolation of Rational Matrix Functions, Operator Theory: Advances and Applications, **45**, Birkhäuser Verlag, Basel.

Doyle, J.C., K. Glover, P.P. Khargonekar, and B.C. Francis, 1989, State space solutions to standard $\langle_2$ and $\langle_\infty$ control problems, IEEE Transactions on Automatic Control, **AC-34**, 831-846.

Kailath, T., and A.H. Sayed, 1995, Displacement structure: Theory and applications. SIAM Review, **37**, 297-386.

Schur, I., 1917, Ueber potenzreihen, die im innern des einheitskreises beschränkt sind, Journal für die Reine und Angewandte Mathematik, **147**, 205-232, English translation: Operator Theory: Advances and Applications, **18**, 31-59, Birkhäuser Verlag, Basel,1986.

Zames, G., 1981, Feedback and optimal sensitivity: Model reference transformations, multiplicative seminorms, and approximate inverses, IEEE Transactions on Automatic Control, **AC-26**, 301-320.

Wavefield Reciprocity and Local Optimization in Remote Sensing

Maarten V. de Hoop
Center for Wave Phenomena
Colorado School of Mines, Golden CO 80401, U.S.A.

Abstract

A general local optimization approach to imaging/inversion in remote sensing is presented. The approach is based on the time-domain reciprocity theorems of the time-convolution and the time-correlation types that apply to wavefields in linear, time-invariant configurations. The wavefields satisfy a system of linear, first-order, partial differential equations in space-time of a general class to which acoustic waves in fluids, elastic waves in solids and electromagnetic waves belong. An optimization procedure is developed that leads to a guaranteed decrease in the mismatch of the measured field in a chosen domain of observation. Special attention is paid to the asymptotic behavior of the scheme, the analysis leading to an integration with the Generalized Radon Transform approach to linearized multi-parameter inversion.

1. Introduction

In this paper, we discuss the wave-theoretical framework of local optimization approaches to the inverse scattering problem in remote sensing. In the discussion, we cover the issues of matching observed data in the least squares (weak) sense with simulations, of adjoint scattering operators and states, of preconditioning and of integration with asymptotic analysis. The fundamental reciprocity theorems of the time-convolution and time-correlation types (De Hoop, 1988) form the basis of our analysis; medium perturbations are introduced through the contrast-source formulation; a local Born approximation is employed to generate a series expansion for the actual reconstruction.

An important aspect of taking the reciprocity relation of the time-correlation type as a point of departure is that it induces a proper norm in the function space of the pertaining wavefields and thus leads, via the iterative minimization according to a chosen criterion, to a 'minimum-norm' gradient technique with a guaranteed decreasing error in the data fit (Lions, 1968; Tarantola and Valette, 1982). Special attention is paid to how the different wave types contribute. Within the framework of reciprocity, there is still some freedom in the choice of norm. This choice allows for a statistical reformulation of the inverse problem.

The fundamental aspects of the optimization method are discussed here and the results are integrated with the imaging conditions of migration/inversion, both the ones based on the Generalized Radon Transform (see Miller *et al.*, 1987, and Esmersoy and Oristaglio, 1988), and the ones based on full-wave theory (see Claerbout, 1971, and Berkhout, 1982), by means of preconditioning. Sophisticated preconditioning can be designed with the aid of linearized inversion.

2. The basic equations

2.1. The hyperbolic system of equations

Let the *field matrix* $F_P = F_P(\boldsymbol{x}, t)$ of the wave motion be composed of the components of the two wavefield quantities whose inner product represents the area density of power flow (Poynting vector). Then, F_P satisfies a system of linear, first-order, partial differential equations of the general form

$$(\mathcal{D}_{IP} + M_{IP}\partial_t)\, F_P = Q_I\,, \quad \mathcal{D}_{IP} = \mathcal{D}_{IP}(\nabla)\,,\ M_{IP} = M_{IP}(\boldsymbol{x})\,, \tag{1}$$

where uppercase Latin subscripts are used to denote the pertaining matrix elements and the summation convention for repeated subscripts applies. In Equation (1), $\mathcal{D}_{IP}$ is a symmetric, block off-diagonal *spatial differentiation operator matrix*, M_{IP} is the *medium matrix* that is representative for the properties of the (arbitrarily inhomogeneous, anisotropic) media and $Q_I = Q_I(\boldsymbol{x}, t)$ is the *volume source density matrix* that is representative for the action of the volume sources that generate the wavefield. Also, surface sources will be included in the discussion. The corresponding *surface source density matrix* is denoted by

$$q_I = [\mathcal{N}_{IP}F_P]^{+}_{-} = \mathcal{N}_{IP}F_P|^{+} + \mathcal{N}_{IP}F_P|^{-}\,, \tag{2}$$

where $[\cdot]^{+}_{-}$ denotes the jump across the support of the surface source distributions and $\mathcal{N}_{IP}$ is the *unit normal operator* that arises from $\mathcal{N}_{IP} = \mathcal{D}_{IP}(\boldsymbol{n})$, where $\boldsymbol{n}$ is, on each of the two faces of the surface, the unit vector along the normal oriented away from the domain that surrounds that surface,

The medium parameters are assumed to be piecewise continuous. Across a surface of discontinuity in medium properties, the parameters may jump by finite amounts. On the assumption that the interface is passive and that the wavefield quantities must remain bounded on either side of the interface, the wavefield must satisfy the boundary condition of the continuity type

$$\mathcal{N}_{IP}F_P \quad \text{is continuous across source-free interface}\,. \tag{3}$$

In view of the linearity of the wave motion, the principle of superposition ensures that the wavefield F_P that is generated by the volume source distribution Q_I and the surface source distributions q_I can be written as the superposition of point-source contributions through the use of a *Green's tensor*. The latter is a solution of the system of differential equations

$$(\mathcal{D}_{IP} + M_{IP}\partial_t)\, G_{PI'} = \delta^{+}_{II'}\delta_{\boldsymbol{x}'}\delta_{t'}\,, \tag{4}$$

where $\delta_{.}(.)$ is the Dirac distribution. In view of the time invariance of the medium, the Green's tensor depends on t and t' only through the difference $t - t'$.

2.2. The reciprocity concatenation matrices

In the reciprocity theorems to be discussed in Section 3, two diagonal matrices δ^-_{QI} and δ^+_{QI} occur that concatenate out of the wavefields pertaining to two admissible states their interaction. For acoustic waves in fluids the diagonal matrix δ^-_{QI} is given by diag$[1,-1,-1,-1]$, and for elastic waves in solids and electromagnetic waves by diag$[1,1,1,-1,-1,-1,-1,-1,-1,-1,-1,-1]$. The diagonal matrix δ^+_{QI} is just the unit matrix: $\delta^+_{QI}=1$ for $Q=I$, $\delta^+_{QI}=0$ for $Q\neq I$.

For the reciprocity theorem of the *time-convolution* type to hold, a necessary and sufficient condition proves to be

$$\delta^-_{QI}\mathcal{D}_{IP} = -\delta^-_{PJ}\mathcal{D}_{JQ} \; . \tag{5}$$

This condition requires that the block-diagonal part of $\mathcal{D}_{IP}$ is anti-symmetric and that its block off-diagonal part is symmetric.

For the reciprocity theorem of the *time-correlation* type to hold, a necessary and sufficient condition proves to be

$$\delta^+_{QI}\mathcal{D}_{IP} = \delta^+_{PJ}\mathcal{D}_{JQ} \; . \tag{6}$$

This condition requires that $\mathcal{D}_{IP}$ is symmetric. The two conditions are independent, but if they are satisfied simultaneously, $\mathcal{D}_{IP}$ is a symmetric, block off-diagonal matrix operator. It is noted that the medium matrix M_{IP} is not subjected to any restriction of this kind.

2.3. Asymptotic ray theory: eikonal and transport equations

To understand the singular behavior of the wave solution of system (1) we employ the standard asymptotic expansion for the field matrix,

$$F_P(\boldsymbol{x},t) = \sum_{\text{modes,paths}} \sum_{n=0}^{\infty} F_P^{(n)}(\boldsymbol{x})\, f_n(t-\tau(\boldsymbol{x})) \; , \tag{7}$$

where τ is the travel time along a characteristic, assuming there is single source signature the derivative of which coincides with f_0 and that generates the field, and

$$(f_n)' = f_{n-1} \; , \quad n = 1,2,\cdots \; . \tag{8}$$

For notational convenience, set $F_P^{(n)} \equiv 0$ for $n<0$. Substituting the asymptotic expansion into (1) away from any source distributions yields

$$\mathcal{D}_{IP}(\nabla)\, F_P^{(n-1)} + [\mathcal{D}_{IP}(\boldsymbol{\gamma}) + M_{IP}(\boldsymbol{x})]\, F_P^{(n)} = 0 \; , \quad n = 0,1,\cdots \; , \tag{9}$$

where

$$\boldsymbol{\gamma} = \nabla\tau \tag{10}$$

is the so-called *slowness vector*. Collecting the zero-order terms, yields the Christoffel equation

$$[\mathcal{D}_{IP}(\boldsymbol{\gamma}) + M_{IP}(\boldsymbol{x})]\, F_P^{(0)} = 0 \; . \tag{11}$$

The zero-order field constituent can be written in the form

$$F_P^{(0)} = A^{(0)}\,\Xi_P\,, \tag{12}$$

where $A^{(0)}$ is a scalar amplitude. Substituting (12) into (11) leads to the eigenvalue equation

$$[\mathcal{D}_{IP}(\boldsymbol{\gamma}) + M_{IP}(\boldsymbol{x})]\,\Xi_P = 0\,, \quad \Xi_P = \Xi_P(\boldsymbol{x},\boldsymbol{\gamma})\,. \tag{13}$$

Non-trivial solutions to (13) must satisfy

$$\det[\mathcal{D}_{IP}(\boldsymbol{\gamma}) + M_{IP}(\boldsymbol{x})] = 0\,, \tag{14}$$

which equation is equivalent to the *eikonal* equation. Collecting the first-order terms from (9) and contracting the result with $F_I^{(0)}$, leads in view of (11) to

$$F_I^{(0)}(\mathcal{D}_{IP}(\nabla)\,F_P^{(0)}) = 0\,. \tag{15}$$

Using the symmetry of $\mathcal{D}$, cf. (6), and imposing that the medium matrix is symmetric as well, this equation can be rewritten as a conservation law,

$$\tfrac{1}{2}\partial_p[F_I^{(0)}\mathcal{D}_{IP}(\boldsymbol{i}_p)\,F_P^{(0)}] = 0\,. \tag{16}$$

In here, we identify the vectorial quantity, $\mathrm{P}_p = \frac{1}{2}F_Q\mathcal{D}_{QP}(\boldsymbol{i}_p)\,F_P$, which, in the energy balance, appears to be the Poynting vector. Equation (16) is equivalent to the *transport* equation.

3. The reciprocity theorems

Let C_t denote time convolution and R_t denote time correlation. In the wavefield reciprocity theorems certain *interaction quantities* are considered between two states in a subdomain D of $\mathbb{R}^3$. Each of the two states has its own medium and its own volume source distribution. Let the superscripts Y and Z indicate the two states.

The reciprocity theorem of the time-convolution type can be formulated as

$$\begin{aligned}
&\int_D \left[\delta^-_{QI}\,\mathsf{C}_t(Q_I^Y, F_Q^Z) - \delta^-_{PJ}\,\mathsf{C}_t(F_P^Y, Q_J^Z)\right]\,\mathrm{d}V(\boldsymbol{x}) \\
&\quad = \int_{\partial D}\delta^-_{QI}\mathcal{N}_{IP}\,\mathsf{C}_t(F_P^Y, F_Q^Z)\,\mathrm{d}A(\boldsymbol{x}) + \int_S \delta^-_{QI}\,[\mathcal{N}_{IP}\,\mathsf{C}_t(F_P^Y, F_Q^Z)]^+_-\,\mathrm{d}A(\boldsymbol{x}) \\
&\quad + \int_D(\delta^-_{QI}M^Y_{IP} - \delta^-_{PJ}M^Z_{JQ})\,\partial_t\mathsf{C}_t(F_P^Y, F_Q^Z)\,\mathrm{d}V(\boldsymbol{x})\,,
\end{aligned} \tag{17}$$

while the reciprocity theorem of the time-correlation type follows as

$$\begin{aligned}
&\int_D \left[\delta^+_{QI}\,\mathsf{R}_t(Q_I^Y, F_Q^Z) + \delta^+_{PJ}\,\mathsf{R}_t(F_P^Y, Q_J^Z)\right]\,\mathrm{d}V(\boldsymbol{x}) \\
&\quad = \int_{\partial D}\delta^+_{QI}\mathcal{N}_{IP}\,\mathsf{R}_t(F_P^Y, F_Q^Z)\,\mathrm{d}A(\boldsymbol{x}) + \int_S \delta^+_{QI}\,[\mathcal{N}_{IP}\,\mathsf{R}_t(F_P^Y, F_Q^Z)]^+_-\,\mathrm{d}A(\boldsymbol{x}) \\
&\quad + \int_D(\delta^+_{QI}M^Y_{IP} - \delta^+_{PJ}M^Z_{JQ})\,\partial_t\mathsf{R}_t(F_P^Y, F_Q^Z)\,\mathrm{d}V(\boldsymbol{x})\,.
\end{aligned} \tag{18}$$

3.1. Wavefield extrapolation

In the reconstruction process, certain wavefield extrapolation formulas are needed to relate the different wavefields at arbitrary positions and times of observation to their respective volume or (actual or equivalent) surface source distributions. In these wavefield extrapolation formulas the causal Green's tensor for an unbounded domain occurs. The wavefield extrapolation formulas follow from the global reciprocity theorems given in (17) and (18) by identifying State Y with the actual wavefield state (for which no superscript will be used) and State Z with a Green's state that corresponds to a point-source excited causal wavefield defined in the entire $\mathbb{R}^3$. Then,

$$\chi_D(\boldsymbol{x}')\, F_P(\boldsymbol{x}',t) = \int_D \mathsf{C}_t(Q_I(\boldsymbol{x},.), G_{PI}(\boldsymbol{x}',\boldsymbol{x},.))\,\mathrm{d}V(\boldsymbol{x})$$
$$- \int_{\partial D} \mathcal{N}_{IP'}\, \mathsf{C}_t(F_{P'}(\boldsymbol{x},.), G_{PI}(\boldsymbol{x}',\boldsymbol{x},.))\,\mathrm{d}A(\boldsymbol{x}) - \int_S \mathsf{C}_t(q_I(\boldsymbol{x},.), G_{PI}(\boldsymbol{x}',\boldsymbol{x},.))\,\mathrm{d}A(\boldsymbol{x})$$
$$\text{for} \quad \boldsymbol{x}' \in \mathbb{R}^3 . \tag{19}$$

Equation (19) is the wavefield extrapolation formula of the time-convolution type. The wavefield extrapolation formula of the time-correlation type has exactly the same structure.

4. Contrast-source formulation and Born approximation

The first step towards constructing a solution of the inverse problem consists of applying an embedding procedure and introducing a contrast-source formulation. Subsequently, a linearization procedure, known as the Born approximation, is applied to the corresponding volume density of contrast source.

4.1. Embedding and contrast-source procedures

In the actual configuration, to be 'sensed', a target region of bounded support D_{con} is present where the constitutive properties of the medium differ by a certain amount from the ones of a known *embedding*. In the case of *time-lapse* experiments, the embedding corresponds to the initial state. The embedding occupies the entire $\mathbb{R}^3$ and its Green's tensor is assumed to be known. Known volume or surface sources of fixed strengths and fixed bounded supports D_{src} and S_{src}, respectively, generate an interrogating wavefield. The difference between the values of this wavefield when generated in the embedding and the ones in the actual configuration are indicative for the presence of D_{con}. This difference wavefield is observed in a domain D_{obs} or on a surface S_{obs}, both of bounded support. The observations last a finite time interval $[0,T]$. In general, the intersection of D_{con} and either D_{obs} or S_{obs} is empty; this neednot be the case for either D_{src} and S_{src} on one hand and D_{obs} and S_{obs} on the other hand.

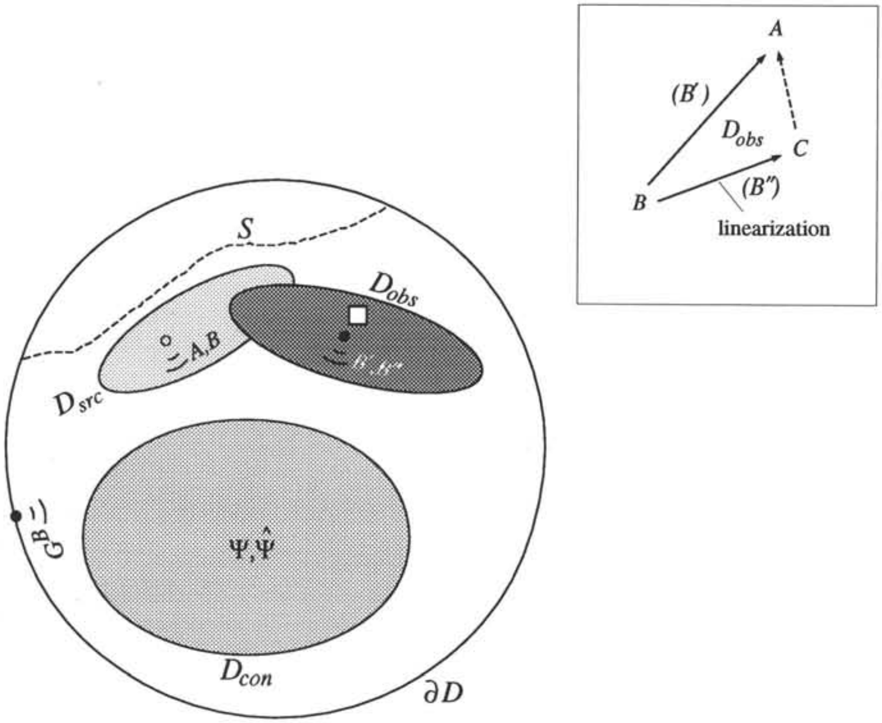

Figure 1. The configuration and the optimization states.

The wavefield state in the actual configuration will be denoted by the superscript A, the wavefield state in the embedding by the superscript B. Since $Q_I^A = Q_I^B$ and $q_I^A = q_I^B$, the difference $F_P^A - F_P^B$ between the wavefields F_P^A and F_P^B then satisfies the system of equations

$$(\mathcal{D}_{IP} + M_{IP}^B \partial_t)(F_P^A - F_P^B) = Q_I^{A,B} \, , \tag{20}$$

where

$$Q_I^{A,B} = -\mathcal{C}_{IP}^{A,B} \, \partial_t F_P^A \, , \quad \mathcal{C}_{IP}^{A,B} = (M_{IP}^A - M_{IP}^B) \, \chi_{D_{con}} \, , \tag{21}$$

is the volume source density of the *contrast sources*, whose support is D_{con}, while $F_P^A - F_P^B$ is continuous across S_{src}.

4.2. The (first-order) Born approximation

In the Born approximation, the unknown wavefield F_P^A in the right-hand side of (21) is replaced by its known zero-order approximation F_P^B for $\boldsymbol{x} \in D_{con}$. With this, we have

$$-Q_I^{A,B} = \mathcal{C}_{IP}^{A,B} \, \partial_t F_P^A \simeq \mathcal{C}_{IP}^{A,B} \, \partial_t F_P^B \, . \tag{22}$$

Note that the Born approximation only involves the volume contrast source density and that it does not affect the field in the chosen background medium of State B (that may be arbitrarily inhomogeneous and anisotropic). The use of the Born-approximated volume density of contrast source is also known as the *linearization procedure* in remote sensing. Considering the linearization as a variation, we may parametrize the medium M with parameters $\boldsymbol{\delta}$ that relate to particular properties of the medium. Then (summation over repeated Greek subscripts)

$$\mathcal{C}_{IP}^{A,B} \simeq \left.\frac{\partial(M_{IP})}{\partial(\boldsymbol{\delta}_\mu)}\right|_{\boldsymbol{\delta}^B} [\boldsymbol{\delta}^A - \boldsymbol{\delta}^B]_\mu \,. \tag{23}$$

4.3. Linearized wavefield extrapolation

The difference wavefield $F_P^A - F_P^B$ is expressible in terms of the volume density of its contrast source through the wavefield extrapolation formula of the time convolution type. Application of (19), with $\boldsymbol{x}$ and $\boldsymbol{x}'$ interchanged, to (20) and the entire $\mathbb{R}^3$ yields

$$(F_P^A - F_P^B)(\boldsymbol{x},.) = \int_{D_{con}} \mathsf{C}_t(Q_I^{A,B}(\boldsymbol{x}',.), G_{PI}^B(\boldsymbol{x},\boldsymbol{x}',.))\,\mathrm{d}V(\boldsymbol{x}') \,. \tag{24}$$

For the later use of this representation in its linearized version, it is notationally advantageous to consider it as an operator acting on the medium contrast. Correspondingly, we introduce the local kernel $\mathcal{E}_{PIP'}^B$ as

$$\mathcal{E}_{PIP'}^B(\boldsymbol{x},\boldsymbol{x}',.) = \partial_t \mathsf{C}_t(F_{P'}^B(\boldsymbol{x}',.), G_{PI}^B(\boldsymbol{x},\boldsymbol{x}',.)) \quad \text{on} \quad \mathbb{R}^3 \times D_{con} \,, \tag{25}$$

which entails

$$(F_P^A - F_P^B)(\boldsymbol{x},.) \simeq -\int_{D_{con}} \mathcal{E}_{PIP'}^B(\boldsymbol{x},\boldsymbol{x}',.)\,\mathcal{C}_{IP'}^{A,B}(\boldsymbol{x}')\,\mathrm{d}V(\boldsymbol{x}') \,, \tag{26}$$

and the global operator

$$\boldsymbol{L}_{PIP'}^B \;:\; \mathcal{C}_{IP'}^{A,B} \to (F_P^A - F_P^B)$$

(note the sign) through $F_P^A - F_P^B = \boldsymbol{L}_{PIP'}^B(\mathcal{C}_{IP'}^{A,B})$. The operator $\boldsymbol{L}^B$ can be interpreted as the Fréchet derivative of F^A with respect to M^A at M^B.

The *adjoint* of $\boldsymbol{L}^B$ with respect to the standard inner product in $L^2(\mathbb{R}^4)$ (over $D_{obs} \times \mathbb{R}$) follows from the linearized reciprocity theorem (18) with anti-causal State Z, taken at zero correlation time shift,

$$\int_{D_{obs}} \delta_{PJ}^+ \,\mathsf{R}_t(\boldsymbol{L}_{PIP'}^B[\mathcal{C}_{IP'}^{A,B}], Q_J^Z)(\boldsymbol{x},0)\,\mathrm{d}V(\boldsymbol{x}) \simeq \int_{D_{con}} \delta_{QI}^+ \,\mathcal{C}_{IP}^{A,B}\,(\boldsymbol{L}^B)_{PQJ}^T[Q_J^Z]\,\mathrm{d}V(\boldsymbol{x}) \tag{27}$$

with

$$(\boldsymbol{L}^B)_{PQJ}^T[Q_J^Z](\boldsymbol{x}) = \partial_t \mathsf{R}_t(F_P^B, F_Q^Z)(\boldsymbol{x},0) \,. \tag{28}$$

In case the State Z is chosen to be causal, a boundary contribution to the adjoint occurs. Consider the boundary integral of (18), substitute (26) and interchange the order of integration,

$$\begin{aligned}\int_{\partial D} \delta^+_{QJ}\mathcal{N}_{JP}(\boldsymbol{x})\, \mathsf{R}_t(\boldsymbol{L}^B_{PIP'}[\mathcal{C}^{A,B}_{IP'}], F^Z_Q)(\boldsymbol{x},0)\,\mathrm{d}A(\boldsymbol{x}) = \\ -\int_{D_{con}}\int_{\partial D} \delta^+_{QJ}\mathcal{N}_{JP}(\boldsymbol{x})\,\mathsf{R}_t(\mathcal{E}^B_{PIP'}(\boldsymbol{x},\boldsymbol{x}',.), F^Z_Q(\boldsymbol{x},.))(0)\,\mathrm{d}A(\boldsymbol{x})\,\mathcal{C}^{A,B}_{IP'}(\boldsymbol{x}')\,\mathrm{d}V(\boldsymbol{x}')\,.\end{aligned} \tag{29}$$

Thus, the *complete* adjoint of $\boldsymbol{L}^B$ can be written as

$$\begin{aligned}(\boldsymbol{L}^B)^T_{PQJ}[Q^Z_J](\boldsymbol{x}) = \partial_t\mathsf{R}_t(F^B_P, F^Z_Q)(\boldsymbol{x},0) \\ -\int_{\partial D}\mathcal{N}_{IP'}(\boldsymbol{x}')\,\mathsf{R}_t(\mathcal{E}^B_{P'QP}(\boldsymbol{x}',\boldsymbol{x},.), F^Z_I(\boldsymbol{x}',.))(0)\,\mathrm{d}A(\boldsymbol{x}')\,.\end{aligned} \tag{30}$$

4.4. Linearized wavefield extrapolation in the geometrical ray approximation

In this subsection, we complement the previous analysis with an analysis of the singular behavior of the linearized wavefield extrapolator and its adjoint. To this end, we will constrain ourselves to a point source of fixed type I', i.e.,

$$Q^B_J = \delta^+_{JI'}\delta_{\boldsymbol{s}}(\boldsymbol{x})\delta_0(t)\,,$$

indicating the source location by $\boldsymbol{s}$. Let the point of observation be $\boldsymbol{x} = \boldsymbol{r}$. Then, in $\mathcal{E}^B_{PIP'}$, using reciprocity we have

$$F^B_{P'}(\boldsymbol{x}',.) = G^B_{P'I'}(\boldsymbol{x}',\boldsymbol{s},.)\,,\quad G^B_{PI}(\boldsymbol{x},\boldsymbol{x}',.) = G^B_{IP}(\boldsymbol{x}',\boldsymbol{r},.)\,. \tag{31}$$

To show whether certain quantities relate to the first ($\boldsymbol{s}$) or the second ($\boldsymbol{r}$) field in the equation above, we employ $\tilde{\ }$'s for the first and $\hat{\ }$'s for the second. We will omit the superscript B for both fields. While applying the geometrical ray approximation, we will separate the contributions from the different modes and paths, and consider these independently. Thus, in the geometrical ray approximation (25) becomes

$$\mathcal{E}^B_{PIP'}(\boldsymbol{r},\boldsymbol{x}',.) \simeq \tilde{\Xi}_{I'}(\boldsymbol{s})\hat{\Xi}_P(\boldsymbol{r})\tilde{\Xi}_{P'}(\boldsymbol{x}')\hat{\Xi}_I(\boldsymbol{x}')\,\tilde{A}^{(0)}(\boldsymbol{x}')\hat{A}^{(0)}(\boldsymbol{x}')\,\partial^3_t\delta(t-\tilde{\tau}(\boldsymbol{x}')-\hat{\tau}(\boldsymbol{x}'))\,. \tag{32}$$

The integral over D_{con} in (26) reduces to an integral over the *isochron*

$$\{\boldsymbol{x}' \in D_{con} \mid \tilde{\tau}(\boldsymbol{x}') + \hat{\tau}(\boldsymbol{x}') = t\}\,, \tag{33}$$

and thus obtains the structure of a Generalized Radon Transform. The properties of this particular transform have been discussed in detail by Rakesh (1988).

To analyze the adjoint extrapolation operator, let Q^Z_J be represented by

$$Q^Z_J(\boldsymbol{x},t) = \int \delta^+_{JP'}\delta_{\boldsymbol{r}}(\boldsymbol{x})\,Q^Z_{P'}(\boldsymbol{r},t)\,\mathrm{d}\boldsymbol{r}\,.$$

Then (28) leads to

$$(\boldsymbol{L}^B)^T_{PQJ}[Q^Z_J](\boldsymbol{x}) = -\int \mathsf{R}_t(G^B_{I'P}(\boldsymbol{s},\boldsymbol{x},.), \mathsf{C}_t(G^B_{JQ}(\boldsymbol{r},\boldsymbol{x},.), \partial_t Q^Z_J(\boldsymbol{r},.)))(0)\,\mathrm{d}\boldsymbol{r}\,. \tag{34}$$

In the geometrical ray approximation the right-hand side becomes

$$(\boldsymbol{L}^B)^T_{PQJ}[Q^Z_J](\boldsymbol{x}) \simeq \tag{35}$$
$$\int \tilde{\Xi}_{I'}(\boldsymbol{s})\hat{\Xi}_J(\boldsymbol{r})\tilde{\Xi}_P(\boldsymbol{x})\hat{\Xi}_Q(\boldsymbol{x})\,\tilde{A}^{(0)}(\boldsymbol{x})\hat{A}^{(0)}(\boldsymbol{x})\,\partial_t^3 Q^Z_J(\boldsymbol{r},\tilde{\tau}(\boldsymbol{x})+\hat{\tau}(\boldsymbol{x}))\,\mathrm{d}\boldsymbol{r}\ ,$$

which is an integration over the *diffraction set*

$$\{(\boldsymbol{r},t) \in D_{obs} \times [0,T] \mid t = \tilde{\tau}(\boldsymbol{x}) + \hat{\tau}(\boldsymbol{x})\}\ , \tag{36}$$

and has in fact the structure of the dual Generalized Radon Transform. Beylkin (1985) introduced this dual to derive the inverse Generalized Radon Transform. For the geometrical ray approximations of the wavefield extrapolator and its adjoint in State B, we will employ the shorthand notation $\boldsymbol{L}^\infty_{PIP'}$ and $(\boldsymbol{L}^\infty)^T_{PQJ}$, respectively.

5. The local optimization approach to inversion

The local optimization approach to inversion starts with selecting a suitable error criterion that quantifies the 'misfit' $\epsilon^{A,B}$ between the wavefields in the States A and B as far as they are observed in the observational domain D_{obs}. Let the measuring process be described by the linear operation $W_{MP}(\sigma)$, defined on D_{obs} for all t, and parametrized by σ. A choice of misfit that suits our purpose is provided by

$$\epsilon^{A,B}(\sigma) = \int_{D_{obs}}\int_{t\in\mathbb{R}}[W_{MP}(\sigma)(F^A_P - F^B_P)]\,\delta^+_{MN}\,[W_{NQ}(\sigma)(F^A_Q - F^B_Q)]\,\mathrm{d}V(\boldsymbol{x})\,\mathrm{d}t\ . \tag{37}$$

The operator $W_{MP}(\sigma)$ may reveal the *statistical* variations in the measurements. Obviously, $\epsilon^{A,B} > 0$ when $F^B_P \not\equiv F^A_P$ for $\boldsymbol{x} \in D_{obs}$. The expression for $\epsilon^{A,B}$ can be regarded as a time correlation at zero time shift. Introducing, under appropriate conditions, the adjoint W^T of the operator W with respect to the real inner product on $L^2(D_{obs} \times \mathbb{R})$, the misfit can be written in the form

$$\epsilon^{A,B}(\sigma) = \int_{D_{obs}} \delta^+_{PJ}\,\mathsf{R}_t((F^A_P - F^B_P),(W^TW)_{JQ}(\sigma)(F^A_Q - F^B_Q))(\boldsymbol{x},0)\,\mathrm{d}V(\boldsymbol{x})\ . \tag{38}$$

Note that W^TW is self-adjoint and positive, and can really be considered as a single operator or pre-processor. In view of the reciprocity relations to apply, it should satisfy the criterion that $(W^TW)_{JQ}(\sigma)(F^A_Q - F^B_Q)$ defines an equivalent source distribution, in a configuration with the medium parameters of State B.

5.1. The optimization condition

The aim of the optimization approach is to construct a State C with a medium matrix M^C_{IP} that deviates from M^B_{IP} only in the domain D_{con}, has an accompanying causal wavefield F^C_P that is generated by the same sources as in the States A and B, i.e., $Q^C_I = Q^B_I = Q^A_I$ and $q^C_I = q^B_I = q^A_I$, and that has the property that the mismatch between the States A and C is less than the mismatch between the States A and B. Now, with $F_P^A - F_P^B = (F_P^A - F_P^C) + (F_P^C - F_P^B)$, (37) can be rewritten as

$$\epsilon^{A,B} = \epsilon^{A,C} + 2\int_{D_{obs}}\int_{t\in\mathbb{R}} \delta_{JN}^{+}\,(F_P^C - F_P^B)\,(W^TW)_{JQ}(F_Q^A - F_Q^C)\,\mathrm{d}V(\boldsymbol{x})\,\mathrm{d}t + \epsilon^{B,C}. \quad (39)$$

We assume that $F_P^C \not\equiv F_P^B$ for $\boldsymbol{x} \in D_{obs}$ i.e. the contrast volume source density associated with the medium update $\mathcal{C}_{IP}^{C,B}$ in D_{con} is assumed not to lead to a vanishing difference field in D_{obs}. Then, $\epsilon^{B,C} > 0$. As a consequence of (39), the condition $\epsilon^{A,C} < \epsilon^{A,B}$ is met by requiring that

$$\int_{D_{obs}}\int_{t\in\mathbb{R}} \delta_{PJ}^{+}\,(F_P^C - F_P^B)\,(W^TW)_{JQ}(F_Q^A - F_Q^C)\,\mathrm{d}V(\boldsymbol{x})\,\mathrm{d}t = 0\ , \quad (40)$$

which is the *optimization condition.* To rewrite it in a form in which the difference between data and simulation $F_Q^A - F_Q^B$ occurs, we substitute

$$F_Q^A - F_Q^C = (F_Q^A - F_Q^B) - (F_Q^C - F_Q^B)\ ,$$

and obtain

$$\begin{aligned}&\int_{D_{obs}}\int_{t\in\mathbb{R}} \delta_{PJ}^{+}\,(F_P^C - F_P^B)\,(W^TW)_{JQ}(F_Q^A - F_Q^B)\,\mathrm{d}V(\boldsymbol{x})\,\mathrm{d}t \\ &= \int_{D_{obs}}\int_{t\in\mathbb{R}} \delta_{PJ}^{+}\,(F_P^C - F_P^B)\,(W^TW)_{JQ}(F_Q^C - F_Q^B)\,\mathrm{d}V(\boldsymbol{x})\,\mathrm{d}t\ .\end{aligned} \quad (41)$$

Note that the right-hand side of this equation is positive, thus the left-hand side has to be positive as well. From it we have to determine $\mathcal{C}_{IP}^{C,B}$ with its support D_{con}. To relate the difference field in D_{obs} to its contrast sources in D_{con} yet to be determined, the reciprocity relation of the time correlation type is applied, first, to the left-hand side. To this end, we consider the quantity $F_P^B - F_P^C$ as a wavefield and the quantity $Q_J^{B'} = (W^TW)_{JQ}(F_Q^A - F_Q^B)$ as the (known) volume source density with D_{obs} as its support, of a computational State B' with associated (causal or anti-causal) wavefield $F_P^{B'}$ in the medium with the known medium matrix

$$M_{PQ}^{B'} = M_{QP}^{B}\ .$$

Then, application of (18) to the domain interior to a closed surface ∂D that completely surrounds both D_{obs} and D_{con}, i.e., $D_{obs} \cup D_{con} \subset D$, yields

$$\begin{aligned}&\int_{D_{obs}}\int_{t\in\mathbb{R}} \delta_{PJ}^{+}\,(F_P^C - F_P^B)\,(W^TW)_{JQ}(F_Q^A - F_Q^B)\,\mathrm{d}V(\boldsymbol{x})\,\mathrm{d}t \\ &= \int_{D_{obs}} \delta_{PJ}^{+}\,\mathsf{R}_t(F_P^C - F_P^B, (W^TW)_{JQ}(F_Q^A - F_Q^B))(\boldsymbol{x},0)\,\mathrm{d}V(\boldsymbol{x}) \\ &= \int_{D_{con}} \delta_{QI}^{+}\,\mathsf{R}_t(\partial_t F_P^C, F_Q^{B'})(\boldsymbol{x},0)\,\mathcal{C}_{IP}^{C,B}(\boldsymbol{x})\,\mathrm{d}V(\boldsymbol{x}) \\ &\qquad + \int_{\partial D} \delta_{QI}^{+}\,\mathcal{N}_{IP}\,\mathsf{R}_t(F_P^C - F_P^B, F_Q^{B'})(\boldsymbol{x},0)\,\mathrm{d}A(\boldsymbol{x})\ .\end{aligned} \quad (42)$$

Carrying out a similar procedure to the right-hand side of (41), involves the introduction of a computational State B'' with volume source density $Q_J^{B''} = (W^T W)_{JQ}(F_Q^C - F_Q^B)$ and medium matrix

$$M_{PQ}^{B''} = M_{PQ}^{B'} .$$

In the latter derivation, replace $(F_Q^A - F_Q^B)$ by $(F_Q^C - F_Q^B)$ and $F_Q^{B'}$ by $F_Q^{B''}$. Substituting the result and (42) into (41), the optimization condition takes the form

$$\mathcal{P} = \mathcal{Q} , \tag{43}$$

in which

$$\begin{aligned}\mathcal{P} &= \int_{D_{con}} \delta_{QI}^{+} \, \mathsf{R}_t(\partial_t F_P^C, F_Q^{B'})(\boldsymbol{x},0)\, \mathcal{C}_{IP}^{C,B}(\boldsymbol{x})\, \mathrm{d}V(\boldsymbol{x}) \\ &\quad + \int_{\partial D} \delta_{QI}^{+} \, \mathcal{N}_{IP}\, \mathsf{R}_t(F_P^C - F_P^B, F_Q^{B'})(\boldsymbol{x},0)\, \mathrm{d}A(\boldsymbol{x}) , \\ \mathcal{Q} &= \int_{D_{con}} \delta_{QI}^{+} \, \mathsf{R}_t(\partial_t F_P^C, F_Q^{B''})(\boldsymbol{x},0)\, \mathcal{C}_{IP}^{C,B}(\boldsymbol{x})\, \mathrm{d}V(\boldsymbol{x}) \\ &\quad + \int_{\partial D} \delta_{QI}^{+} \, \mathcal{N}_{IP}\, \mathsf{R}_t(F_P^C - F_P^B, F_Q^{B''})(\boldsymbol{x},0)\, \mathrm{d}A(\boldsymbol{x}) = \epsilon^{C,B} .\end{aligned} \tag{44}$$

In these expressions, the wavefield $F_P^C - F_P^B$ satisfies the equation (cf. (20))

$$(\mathcal{D}_{IP} + M_{IP}^B \partial_t)\,(F_P^C - F_P^B) = Q_I^{C,B} ,$$

where (cf. (21))

$$Q_I^{C,B} = -\mathcal{C}_{IP}^{C,B}\, \partial_t F_P^C .$$

So far, no approximations have been made. However, since $\mathcal{C}_{IP}^{C,B}$ is yet to be determined, we are inclined to avoid the evaluation of F^C. To this end, we *locally linearize* the expressions above in the contrast sources. This means that

- in the volume integrals F_P^C is replaced by F_P^B, cf. (22),
- in the surface integrals $F_P^C - F_P^B$ is replaced by $\boldsymbol{L}_{PIP'}^B[\mathcal{C}_{IP'}^{C,B}]$, cf. (26),
- the source distribution $Q_J^{B''}$ is replaced by $(W^T W)_{JQ} \boldsymbol{L}_{QIP'}^B[\mathcal{C}_{IP'}^{C,B}]$, cf. (26).

We denote the linearized versions of $\mathcal{P}$ and $\mathcal{Q}$ by $\mathcal{P}_{lin}$ and $\mathcal{Q}_{lin}$, respectively.

For the wavefield extrapolation in states B' and B'' we have the choice between a causal and an anti-causal one. For the anti-causal extrapolation the integral over ∂D in $\mathcal{P}$ and $\mathcal{Q}$ vanishes.

5.2. Imaging and the improvement condition

Into the boundary integrals occurring in the expressions for $\mathcal{P}_{lin}$ and $\mathcal{Q}_{lin}$ we will now substitute (26). As in the derivation of (30) we will interchange the integrations over ∂D and over D_{con}. Then

$$\mathcal{P}_{lin} = \int_{D_{con}} \delta_{QI}^{+}\, \Psi_{PQ}^{B'}(\boldsymbol{x})\, \mathcal{C}_{IP}^{C,B}(\boldsymbol{x})\, \mathrm{d}V(\boldsymbol{x}) \tag{45}$$

with

$$\Psi^{B'}_{PQ}(\boldsymbol{x}) = \partial_t \mathsf{R}_t(F^B_P, F^{B'}_Q)(\boldsymbol{x}, 0) \\ - \int_{\partial D} \mathcal{N}_{I'P'}(\boldsymbol{x}')\, \mathsf{R}_t(\mathcal{E}^B_{P'QP}(\boldsymbol{x}', \boldsymbol{x}, .), F^{B'}_{I'}(\boldsymbol{x}', .))(0)\, \mathrm{d}A(\boldsymbol{x}') \; . \tag{46}$$

In this expression we identify two kernels,

$$\mathcal{I}^{B,B'}_{PQ}(\boldsymbol{x}) = \partial_t \mathsf{R}_t(F^B_P, F^{B'}_Q)(\boldsymbol{x}, 0) \quad \text{on} \quad D_{con} \tag{47}$$

and

$$\mathcal{B}^{B,B'}_{PQ}(\boldsymbol{x}, \boldsymbol{x}') = \mathcal{N}_{I'P'}(\boldsymbol{x})\, \mathsf{R}_t(\mathcal{E}^B_{P'QP}(\boldsymbol{x}', \boldsymbol{x}, .), F^{B'}_{I'}(\boldsymbol{x}, .))(0) \quad \text{on} \quad D_{con} \times \partial D \; . \tag{48}$$

A likewise procedure applied to $\mathcal{Q}_{lin}$ leads to the introduction of $\Psi^{B''}_{PQ}(\boldsymbol{x})$. Unlike $\Psi^{B'}_{PQ}(\boldsymbol{x})$, the matrix $\Psi^{B''}_{PQ}(\boldsymbol{x})$ depends on the medium update $\mathcal{C}^{C,B}_{IP}$ through the volume source density of State B''. The presence of concatenation matrix δ^{+}_{QI} in (45) amounts to taking the *trace* of the integrand. The kernel $\mathcal{I}^{B,B'}$ can be considered as a L^2-inner product with respect to time evaluated at each point in D_{con}. It is also noticed that this kernel is a function of the actual source and receiver locations associated with our single experiment.

To construct an approximate solution, the unknown matrix function $\mathcal{C}^{C,B}$ is now written as

$$\mathcal{C}^{C,B}_{IP}(\boldsymbol{x}) = \alpha\, \Phi_{IP}(\boldsymbol{x}) \; , \tag{49}$$

where $\alpha = \alpha(\sigma)$ is an expansion coefficient and Φ is an expansion function belonging to the same space as $\mathcal{C}^{C,B}$ (i.e., it is supposed to have the same structure and have its support in D_{con}). In applications, Φ is referred to as the *image* matrix. In accordance with the local linearization and (49), we replace State B'' by a State $\widehat{B}$ with

$$Q^{B''}_J = \alpha\, Q^{\widehat{B}}_J \;\; \text{hence} \;\; F^{B''}_Q = \alpha\, F^{\widehat{B}}_Q \; , \tag{50}$$

where $F^{\widehat{B}}$ is the wavefield extrapolated away from $Q^{\widehat{B}}$. On the basis of expansion (49), we introduce $\widehat{\mathcal{P}}$ and $\widehat{\mathcal{Q}}$ as

$$\mathcal{P}_{lin} = \alpha\, \widehat{\mathcal{P}} \quad \text{and} \quad \mathcal{Q}_{lin} = \alpha^2\, \widehat{\mathcal{Q}} \; . \tag{51}$$

Then solving condition (43) amounts to

$$\alpha = \widehat{\mathcal{P}} / \widehat{\mathcal{Q}} \; . \tag{52}$$

With State $\widehat{B}$ is associated a matrix function $\Psi^{\widehat{B}}(\boldsymbol{x})$ defined through (46). Thus we find

$$\widehat{\mathcal{P}} = \int_{D_{con}} \delta^{+}_{QI}\, \Psi^{B'}_{PQ}(\boldsymbol{x}) \Phi_{IP}(\boldsymbol{x})\, \mathrm{d}V(\boldsymbol{x}) \; , \tag{53}$$

$$\widehat{\mathcal{Q}} = \int_{D_{con}} \delta^{+}_{QI}\, \Psi^{\widehat{B}}_{PQ}(\boldsymbol{x}) \Phi_{IP}(\boldsymbol{x})\, \mathrm{d}V(\boldsymbol{x}) \; . \tag{54}$$

To achieve anything at all, viz., $\alpha \neq 0$, the *improvement condition* $\widehat{\mathcal{P}} \neq 0$, must be satisfied. (Note, however, that this condition does not guarantee convergence of the procedure.) To achieve positive definiteness of the entire domain integral, as in the gradient method, we choose

$$\Phi_{IP}(\boldsymbol{x}) = \left[\delta^+_{QI}\, \Psi^{B'}_{PQ}(\boldsymbol{x}) + \eta\, \phi_{IP}\right] \chi_{D_{con}}(\boldsymbol{x}) \; ; \tag{55}$$

η is a scalar quantity, and the matrix ϕ_{IP} is constant and equal to

$$\phi_{IP} = \frac{1}{|D_{con}|} \int_{D_{con}} \delta^+_{QI}\, \Psi^{B'}_{PQ}(\boldsymbol{x})\, \mathrm{d}V(\boldsymbol{x}) \, , \tag{56}$$

the volume average of $\Psi^{B'}_{PI}$. The improvement condition requires that

$$\eta \neq - \frac{\dfrac{1}{|D_{con}|} \displaystyle\int_{D_{con}} \left(\delta^+_{QI}\, \Psi^{B'}_{PQ}(\boldsymbol{x})\right)^2 \mathrm{d}V(\boldsymbol{x})}{\left(\dfrac{1}{|D_{con}|} \displaystyle\int_{D_{con}} \delta^+_{QI}\, \Psi^{B'}_{PQ}(\boldsymbol{x})\, \mathrm{d}V(\boldsymbol{x})\right)^2} \tag{57}$$

(summed over I's and P's). If either $\widehat{\mathcal{P}}$ or $\widehat{\mathcal{Q}}$ becomes zero, the scheme fails unless we are, for $\widehat{\mathcal{P}} = 0$, at the exact solution already.

5.3. Operator formalism

We reconsider the expressions for $\Psi^{B'}_{PQ}$, $\Psi^{B''}_{PQ}$ and $\Psi^{\widehat{B}}_{PQ}$ and write them in terms of the operator $\boldsymbol{L}^B$ introduced in Section 4. Using (30), we find that

$$\Psi^{B'}_{PQ} = (\boldsymbol{L}^B)^T_{PQJ}[(W^T W)_{JQ'}(F^A_{Q'} - F^B_{Q'})] \, , \tag{58}$$

while, in conjunction with (26), we have

$$\Psi^{B''}_{PQ} = (\boldsymbol{L}^B)^T_{PQJ}[(W^T W)_{JQ'} \boldsymbol{L}^B_{Q'IP'}[\mathcal{C}^{C,B}_{IP'}]] \, , \tag{59}$$

and

$$\Psi^{\widehat{B}}_{PQ} = (\boldsymbol{L}^B)^T_{PQJ}[(W^T W)_{JQ'} \boldsymbol{L}^B_{Q'IP'}[\Phi_{IP'}]] \, . \tag{60}$$

The operator formalism is convenient to expose the connection of the proposed iterative inversion procedure with imaging and direct, weak, linearized inversion procedures. The main thing to note is that according to (35) in the geometrical ray approximation $\Psi^{B'}_{PQ}$ is the outcome of a 'weighted diffraction stack', which is represented in wave-theoretical form by (34). In this context $\boldsymbol{x} \in D_{con}$ is referred to as the (geometrical) image or the (wave) focal point, respectively.

6. The method of preconditioning

6.1. Weak, linearized inversion

In the steepest-descent-type iterative inversion scheme of Section 5, where $-\Phi_{IP'}$ is the 'gradient', the improvement condition led to medium update,

$$\Phi_{IP'} = \Psi^{B'}_{P'I} \, , \quad \mathcal{C}^{C,B}_{IP'} = \alpha\, \Phi_{IP'} = \alpha\, \Psi^{B'}_{P'I} \quad \text{with} \quad \alpha = \widehat{\mathcal{P}}/\widehat{\mathcal{Q}} \, . \tag{61}$$

Here, α is just a multiplicative factor, which through σ may vary with the image point. In the direct weak, linearized inversion scheme on the other hand, we would have to solve the matrix integral equation

$$\Psi_{PQ}^{B''} = \Psi_{PQ}^{B'} \quad \text{with} \quad \Psi_{PQ}^{B''} = (\boldsymbol{L}^B)^T_{PQJ}[(W^TW)_{JQ'}\boldsymbol{L}^B_{Q'IP'}[\mathcal{C}^{A,B}_{IP'}]] \,, \tag{62}$$

in accordance with (59). Under certain constraints, $(\boldsymbol{L}^B)^T_{PQJ}$ $(W^TW)_{JQ'}\boldsymbol{L}^B_{Q'IP'}$ is a pseudo-differential operator and its *parametrix* exists. Let us denote this parametrix by $\boldsymbol{\alpha}^B_{IP'PQ}$, then the medium contrast follows as

$$\mathcal{C}^{A,B}_{IP'} = \boldsymbol{\alpha}^B_{IP'PQ}[\Psi^{B'}_{PQ}] \,. \tag{63}$$

Substituting (58) into this expression leads to a direct inversion formula, with operator $\boldsymbol{\alpha}^B_{IP'PQ}$ $(\boldsymbol{L}^B)^T_{PQJ}$. In the geometrical ray approximation, this operator constitutes the inverse Generalized Radon Transform, which we will denote as $\boldsymbol{\alpha}^{\infty}_{IP'PQ}$ $(\boldsymbol{L}^{\infty})^T_{PQJ}$.

6.2. Preconditioning and image enhancing

In the method of preconditioning one introduces a linear operator, $\boldsymbol{U}^B_{IP'J}$ say, such that the composition

$$\boldsymbol{L}^B_{PIP'}\boldsymbol{U}^B_{IP'J} \quad \text{is close to the identity.} \tag{64}$$

The essence of preconditioning is to improve the expansion function. The original choice of expansion function, $\Phi_{IP'} = \Psi^{B'}_{P'I}$, is replaced by

$$\Phi_{PQ} = \boldsymbol{U}^B_{QPJ}[(W^TW)_{JQ'}(F^A_{Q'} - F^B_{Q'})] \,, \tag{65}$$

compare (55) and (58). With this modification, the expressions for $\widehat{\mathcal{P}}$ and $\widehat{\mathcal{Q}}$, (53)-(54), remain unchanged. The condition (64) allows the improvement condition that $\widehat{\mathcal{P}} \neq 0$ to hold simultaneously.

We can rewrite the procedure just described upon representing the medium update by

$$\mathcal{C}^{C,B}_{IP'} = \boldsymbol{U}^B_{IP'J}[H^{C,B}_J] \,. \tag{66}$$

Here, $H^{C,B}_J$ should be interpreted as a fictitious volume source density. Expanding this source density according to

$$H^{C,B}_J(\boldsymbol{x},t) = \alpha\, \Phi^H_J(\boldsymbol{x},t) \,, \tag{67}$$

leads to the relationship

$$\Phi_{PQ} = \boldsymbol{U}^B_{QPJ}[\Phi^H_J] \,. \tag{68}$$

This equation is then substituted into the expressions for $\widehat{\mathcal{P}}$ and $\widehat{\mathcal{Q}}$. In $\widehat{\mathcal{Q}}$ with (60) we thus have

$$\Psi^{\widehat{B}}_{PQ} = (\boldsymbol{L}^B)^T_{PQJ}[(W^TW)_{JQ'}\boldsymbol{L}^B_{Q'IP'}[\boldsymbol{U}^B_{IP'J'}[\Phi^H_{J'}]]] \,. \tag{69}$$

The improvement condition is now satisfied if

$$\Phi^H_{J'} = (W^TW)_{J'Q'}(F^A_{Q'} - F^B_{Q'}) \,. \tag{70}$$

In choosing a preconditioner, one aims to achieve that the relative (amplitude) variations in the image matrix are more representative for the actual medium perturbation than the original image matrix. We say that the image is enhanced.

6.3. Examples of preconditioners

We will discuss two particular preconditioners; both can either be based on the geometrical ray approximation or be based on the leading-order terms of the generalized Bremmer coupling series. The idea is to let the preconditioner resemble the linearized inversion operator given by (63) and hence modify the expansion function to a multi-parameter-like matrix of images.

In the framework of the geometrical ray approximation, we are thus led to the choice,

$$\boldsymbol{U}^{B}_{IP'J} = \boldsymbol{\alpha}^{\infty}_{IP'PQ}\,(\boldsymbol{L}^{\infty})^{T}_{PQJ}\,, \tag{71}$$

the Generalized Radon Transform inversion. This preconditioner can be replaced by a composition of a corrector and the adjoint operator leading to the original expansion function,

$$\boldsymbol{U}^{B}_{IP'J} = \boldsymbol{\alpha}^{\infty}_{IP'PQ}\,(\boldsymbol{L}^{B})^{T}_{PQJ}\,, \tag{72}$$

cf. (55) and (58). Esmersoy and Oristaglio (1988) and Esmersoy and Miller (1989) implicitly found $\boldsymbol{\alpha}^{\infty}_{IP'PQ}$ for such a preconditioner in the case of acoustic waves in two dimensions. Typically, $\boldsymbol{\alpha}^{\infty}_{IP'PQ}$ consists of an obliquity correction – which requires ray tracing to be carried out in the medium of State B to define a directional derivative along the rays associated with the field of State B', and applying it – and an amplitude correction. Sevink (1996) exploited this class of preconditioners further.

If the preconditioner allows the structure dual to the one in (72), viz.,

$$\boldsymbol{U}^{B}_{IP'J} = (\boldsymbol{L}^{B})^{T}_{IP'J'}\,V_{J'J}\,, \tag{73}$$

the corrector, $V_{J'J}$, can be absorbed in $(W^TW)_{JQ'}$ which brings the preconditioning into the data or observational domain.

7. Conclusions

We have used reciprocity to derive an optimization procedure for inverse scattering. The optimization approach has been widely used in applications. It is a reasonable approach, in particular, when the acquisition geometry with which the remote sensing is carried out is sparse, the regime where a direct inverse approach breaks down. Also, optimization schemes are attractive when a priori information is available and should be taken into account. In our paper we have critically reviewed the optimization formulation of the inverse problem and derived some refinements as well.

The iterative scheme we have proposed is of the preconditioned steepest-descent type. More sophisticated iterative schemes can be derived in a manner similar to the one discussed here. The formalism accounts for the leading non-linearity consistently with reciprocity. The resulting iterative scheme yields a series solution to the (non-linear) inverse scattering problem in case the starting value for the medium in the initial computational state is not too far from the one for the actual state. For this condition to hold, the smoothly varying component in the actual medium properties should be determined prior by other techniques.

The rôle of the higher-order terms in the series or iterative solution of the inverse problem, is to compensate or 'deconvolve' for incomplete acquisition geometries and for some non-linearities such as those associated with 'interbed multiples' (for a discussion on the latter in a one-dimensional system, see Snieder, 1990). These terms can improve the resolution of the final result. It is conjectured that the scale of variation of the medium should be gradually increased at each iteration by a proper adjustment of the expansion functions. The latter adjustment can be accomplished by a multi-resolution analysis.

Iterative schemes can also mimic layer stripping, a procedure arising naturally in the invariant-imbedding approach to nonlinear inversion (Weston, 1992). In our formulation, we have allowed for operators that can slide time windows over the observations in accordance with pre-evaluated arrival times associated with waves scattered from image points at increasing depths: the result of a previous window is used as the initial computational medium for the subsequent window.

References

De Hoop, A.T., 1988, Time-domain reciprocity theorems for acoustic wave fields in fluids with relaxation, Journal of the Acoustical Society of America, **84**, 1877-1882.

Lions, J.L., 1968, Contrôle optimal de systèmes gouvernés par des équations aux dérivées partielles, Dunod-Gauthier Villars, Paris.

Tarantola, A., and B. Valette, 1982, Generalized nonlinear inverse problems solved using the least-squares criterion, Revue of Geophysics and Space Physics, **20**, 219-232.

Miller, D., M. Oristaglio and G. Beylkin, 1987, A new slant on seismic imaging: migration and integral geometry, Geophysics, **52**, 943-964.

Esmersoy, C., and M. Oristaglio, 1988, Reverse-time wave-field extrapolation, imaging, and inversion, Geophysics, **53**, 920-931.

Claerbout, J.F., 1971, Toward a unified theory of reflector mapping, Geophysics **36**, 467-481.

Berkhout, A.J., 1982, Seismic Migration, Developments in Solid Earth Geophysics 14A, Elsevier, Amsterdam.

Rakesh, 1988, A linearised inverse problem for the wave equation, Communications in Partial Differential Equations, **13**, 573-601.

Beylkin, G., 1985, Imaging of discontinuities in the inverse scattering problem by inversion of the causal generalized Radon transform, Journal of the Mathematical Physics **26**, 99-108.

Esmersoy, C., and D. Miller, 1989, "Backprojection versus backpropagation in multidimensional linearized inversion, Geophysics **54**, 921-926.

Sevink, G.J.A., 1996, Asymptotic Seismic Inversion, Ph.D. Thesis, Delft University of Technology, Delft.

Snieder, R., 1990, A perturbative analysis of nonlinear inversion, Geophysical Journal International **101**, 545-556.

Weston, V.H., 1992, Invariant imbedding and wave splitting in $\mathbb{R}^3$: II. The Green function approach to inverse scattering, Inverse Problems, **8**, 919-947.

Susceptibility Analysis of an Open-Wire Signalling System

Dirk Quak
Laboratory of Electromagnetic Research, Faculty of Electrical Engineering
Delft University of Technology, P.O. Box 5031, 2600 GA Delft, the Netherlands

Abstract

The susceptibility of an open-wire signalling system, used to control operational devices, to electromagnetic disturbances is analyzed with the aid of Lorentz's reciprocity theorem. Voltages in the terminations of the system induced by a transient disturbance, e.g., lightning, are determined and numerical results are presented.

1. Introduction

In a number of technical applications, open-wire systems are used to control operational devices, equipment or systems, e.g., open-wire signalling systems in the automatic guidance of unmanned vehicles and loop-signalling systems in highway traffic control. These open systems are susceptible to electromagnetic disturbances that can cause a disruption of the proper operation of relevant control systems. The influence of the terminations of the open-wire signalling lines on the character and magnitude of the induced disturbing voltages will be analyzed. These disturbing voltages in open-wire signalling systems might occur at container terminals where container transportation from quay cranes to storage locations is fully remote controlled. Since in a particular practical case the lightning stroke induced fields cause the most frequent disruption in the normal operation, we investigate in particular this source of electromagnetic interference. As the most elementary constituent of a more extended open-wire signalling system we consider the case where two wires are present above a groundplane.

The system is modeled as a transmission-line system consisting of conducting wires over a perfectly conducting plane. The signalling wires are conducting wires located parallel to the earth and hence, the proximity of the groundwater level completes the model of a transmission-line system. In the analysis it is assumed that the operation of the transmission-line system can be adequately described in terms of its dominant modes, i.e., its quasi-TEM modes. Our analysis is carried out in the time Laplace-transform domain (s-domain). The reciprocity theorem for electromagnetic fields due to H.A. Lorentz is used as a tool for the susceptibility analysis of the configuration. This theorem expresses the interaction of two non-identical electromagnetic states in a configuration (De Hoop, 1995). By a suitable choice of these two states, the susceptibility of the system to incident radiation is analyzed. Now, one state is chosen to be the actual electromagnetic field in the configuration. The total field is made up of an incident field and a scattered field. The other state is an auxiliary state and is chosen as the state which consists of a traveling quasi-TEM mode on the

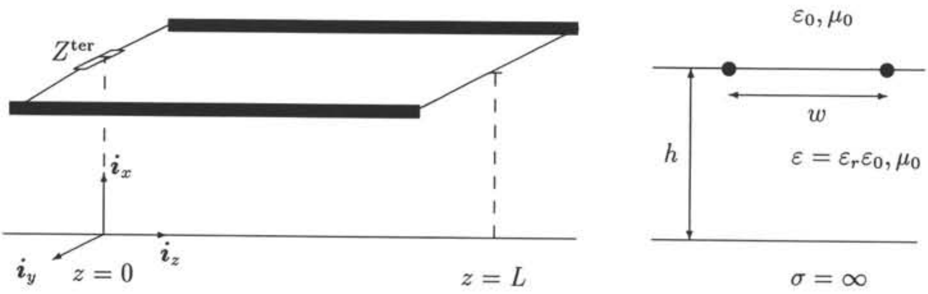

(a) (b)

Figure 1. Configuration consisting of three homogeneous layers with two parallel wires in an interface, (a) closed loop in the plane $z = h$, (b) cross-sectional view.

transmission-line system that is terminated in the same way as the line in the actual situation. The excitation of this auxiliary field is executed by a current source of unit strength at the position where the voltage is required. The resulting interaction integral over the domain of the bounded source of the disturbance yields the value of the required voltage. To obtain values of this quantity in time-domain the s-domain quantity is written as a convolution integral of two time-domain quantities, one being the lightning return stroke and the other one the time-domain electric-field strength in the auxiliary state. This approach (Quak and Wiemans, 1989) is somewhat complementary to the usual literature on the subject of coupling of electromagnetic fields to transmission-line systems, where transmission-line equations with distributed induced current and voltage sources are derived and applied (Taylor *et al.*, 1965, Paul, 1976, Kami and Sato, 1985).

2. Description of the configuration

The configuration under consideration consists of a pair of parallel wires at the transition of a vacuum half-space and a layer of finite thickness. The presence of groundwater below this layer is accounted for by assuming the presence of a perfectly conducting plane. Hence, we have a configuration of which the medium properties vary in a single direction of space only. The position in space is denoted as $\boldsymbol{x} = x\boldsymbol{i}_x + y\boldsymbol{i}_y + z\boldsymbol{i}_z$. Partial differentiation with respect to x, y and z will be denoted by the operators ∂_x, ∂_y and ∂_z, respectively, and the nabla-operator by $\boldsymbol{\nabla} = \boldsymbol{i}_x\partial_x + \boldsymbol{i}_y\partial_y + \boldsymbol{i}_z\partial_z$. The direction in which the medium properties vary is chosen to be the x-direction, the vector $\boldsymbol{i}_x$ points vertically upwards. The layer of finite thickness ($0 < x < h$) is modeled as a dielectric with relative permittivity ε_r. The conductivity of this layer is assumed to be negligible with respect to the conductivity in the half-space $x < 0$. The parallel wires are located in the plane $x = h$ and the z-direction is chosen parallel to these wires (Figure 1). The length of the wires is L. The distance w between the two wires and the height h of the layer are small compared to the wavelength of the incident radiation, which is a prerequisite for the quasi-TEM mode operation. It is evident that the radius of the wires is so small that the field quantities of the incident radiation does not vary significantly over the cross-sections of the wires, so the incident field on the wires may be replaced, if necessary, by its values at the center lines of the wires. The normal operation of this system is in the differential mode. In this operation the electronics of the control equipment are coupled to the conducting wires at $z = 0$, while at $z = L$ the wires are mutually connected by a short-circuit. The normal operation of this system may be disturbed by an external disturbance, such as lightning. This external disturbance is modeled as an electromagnetic pulse that is perpendicular to the groundplane. For interference from external disturbances the common-mode operation of this system presents the most serious difficulties.

3. The Lorentz reciprocity theorem

As the point of departure for our analysis we use the Laplace-transformed electromagnetic field equations

$$-\nabla\times\hat{\boldsymbol{H}} + \hat{\eta}\hat{\boldsymbol{E}} = -\hat{\boldsymbol{J}}^{\mathrm{e}}, \tag{1}$$

$$\nabla\times\hat{\boldsymbol{E}} + \hat{\zeta}\hat{\boldsymbol{H}} = -\hat{\boldsymbol{K}}^{\mathrm{e}}. \tag{2}$$

In these equations $\hat{\eta} = \sigma + s\varepsilon$ is the medium's transverse admittance per length and $\hat{\zeta} = s\mu$ the medium's longitudinal impedance per length with σ its conductivity, ε its permittivity and μ its permeability. The Lorentz reciprocity theorem interrelates the electromagnetic fields in two "States" that can occur in one and the same domain in space. In our application, one state will be the *transmitting state*, to be denoted by the superscript T, the other will be the *receiving state*, to be denoted by the superscript R. Typically, the transmitting state serves to analyze the *emission properties* of a device, while the receiving state serves to analyze its *susceptibility* or *immunity properties*.

Let $\mathcal{D}$ be a bounded domain in space in which the two electromagnetic states occur and denote by $\partial\mathcal{D}$ the boundary surface of $\mathcal{D}$ with unit vector $\boldsymbol{\nu}$ along its normal oriented away from $\mathcal{D}$. Denote by $\{\hat{\boldsymbol{E}}^T, \hat{\boldsymbol{H}}^T\} = \{\hat{\boldsymbol{E}}^T, \hat{\boldsymbol{H}}^T\}(\boldsymbol{x}, s)$ the complex frequency domain electromagnetic field in the transmitting state and by $\{\hat{\boldsymbol{J}}^{\mathrm{e};T}, \hat{\boldsymbol{K}}^{\mathrm{e};T}\} = \{\hat{\boldsymbol{J}}^{\mathrm{e};T}, \hat{\boldsymbol{K}}^{\mathrm{e};T}\}(\boldsymbol{x}, s)$ its volume source densities. Further, denote by $\{\hat{\boldsymbol{E}}^R, \hat{\boldsymbol{H}}^R\} = \{\hat{\boldsymbol{E}}^R, \hat{\boldsymbol{H}}^R\}(\boldsymbol{x}, s)$ the complex frequency domain electromagnetic field in the receiving state and by $\{\hat{\boldsymbol{J}}^{\mathrm{e};R}, \hat{\boldsymbol{K}}^{\mathrm{e};R}\} = \{\hat{\boldsymbol{J}}^{\mathrm{e};R}, \hat{\boldsymbol{K}}^{\mathrm{e};R}\}(\boldsymbol{x}, s)$ its volume source densities. Then, Lorentz's reciprocity theorem states that

$$\begin{aligned}&\int_{\boldsymbol{x}\in\partial\mathcal{D}} \boldsymbol{\nu}\cdot(\hat{\boldsymbol{E}}^T\times\hat{\boldsymbol{H}}^R - \hat{\boldsymbol{E}}^R\times\hat{\boldsymbol{H}}^T)\,\mathrm{d}A \\ &= \int_{\boldsymbol{x}\in\mathcal{D}} [-\hat{\boldsymbol{E}}^T\cdot\hat{\boldsymbol{J}}^{\mathrm{e};R} - \hat{\boldsymbol{H}}^R\cdot\hat{\boldsymbol{K}}^{\mathrm{e};T} + \hat{\boldsymbol{E}}^R\cdot\hat{\boldsymbol{J}}^{\mathrm{e};T} + \hat{\boldsymbol{H}}^T\cdot\hat{\boldsymbol{K}}^{\mathrm{e};R}]\,\mathrm{d}V,\end{aligned} \tag{3}$$

provided that the (isotropic) media in the two states are the same. In case $\partial\mathcal{D}$ encloses all sources, the surface integral over $\partial\mathcal{D}$ is an invariant and equals the value over the "sphere at infinity", which can be shown to give a vanishing contribution in view of the causality of the fields in both the transmitting and the receiving state.

An important case is the one when $\partial\mathcal{D}$ is the boundary surface of the termination of an N-port circuit device, in the interior of which the quasi-static approximation of an electric field can be employed (Kirchhoff circuit). In this approximation,

$$\hat{\boldsymbol{E}}^T \simeq -\boldsymbol{\nabla}\hat{\phi}^T \quad \text{and} \quad \hat{\boldsymbol{E}}^R \simeq -\boldsymbol{\nabla}\hat{\phi}^R, \tag{4}$$

where $\hat{\phi}^T = \hat{\phi}^T(\boldsymbol{x}, s)$ and $\hat{\phi}^R = \hat{\phi}^R(\boldsymbol{x}, s)$ are the electric scalar potentials in the transmitting and the receiving situations, respectively. In the neighborhood of the termination standardly a reference point is chosen where $\hat{\phi}^T$ and $\hat{\phi}^R$ have the value zero. The polarities of the voltages and the orientations of the electric currents in the transmitting state and in the receiving state have to be chosen to make them unique.

The first step in the susceptibility analysis of a device, equipment or system consists of extracting out of it a passive Kirchhoff circuit that is situated in the bounded domain $\mathcal{D}$ inside some closed surface $\partial\mathcal{D}$. Across the closed surface the Kirchhoff circuit is connected to the remaining part of the system by N conducting wires that can carry electric conduction currents and on which the voltages with respect to some reference point in the neighborhood of the closed surface are defined.

In the *transmitting situation*, the remaining configuration outside the closed surface is considered as an N-port system that is accessible at its ports. Let $\{\hat{V}_1^T, ..., \hat{V}_N^T\}$ be the values of the voltages at the ports and $\{\hat{I}_1^T, ..., \hat{I}_N^T\}$ the electric currents fed at the ports in the remaining configuration. With the standard convention that the polarities of the voltages and the orientation of the electric currents are chosen such that the electromagnetic power flow is oriented into the system, the relation between the voltages and the electric currents can, in view of the linearity of the system, be expressed either as

$$\hat{V}_n^T = \sum_{m=1}^{N} \hat{Z}_{n,m}^T \hat{I}_m^T \quad \text{for } n = 1, ..., N, \tag{5}$$

where $\hat{Z}_{n,m}^T$ is the *input impedance* of the remaining configuration, or as

$$\hat{I}_n^T = \sum_{m=1}^{N} \hat{Y}_{n,m}^T \hat{V}_m^T \quad \text{for } n = 1, ..., N, \tag{6}$$

where $\hat{Y}_{n,m}^T$ is the *input admittance* of the remaining configuration.

In the *receiving situation*, the passive Kirchhoff circuit is considered as a load that is, at its N accessible ports, connected to the activating part of an equivalent voltage-source (Thévenin) circuit or an activating part of an equivalent electric-current source (Norton) circuit. The relationship between the voltages $\{\hat{V}_1^R, ..., \hat{V}_N^R\}$ and the electric currents $\{\hat{I}_1^R, ..., \hat{I}_N^R\}$ fed into the circuit is, in view of the linearity of the circuit and adhering to the convention that the polarities of the voltages and the orientation of the electric currents are chosen such that the electromagnetic power flow is oriented into the circuit, then given by either

$$\hat{V}_m^R = \sum_{n=1}^{N} \hat{Z}_{m,n}^{\mathrm{L}} \hat{I}_n^R \quad \text{for } m = 1, ..., N, \tag{7}$$

where $Z^{\mathrm{L}}_{m,n}$ is the *load impedance* of the Kirchhoff circuit or by

$$\hat{I}^R_m = \sum_{n=1}^{N} \hat{Y}^{\mathrm{L}}_{m,n} \hat{V}^R_n \quad \text{for } m = 1, ..., N, \tag{8}$$

where $Y^{\mathrm{L}}_{m,n}$ is the *load admittance* of the Kirchhoff circuit.

With these preliminaries the Lorentz reciprocity theorem is applied to the domain $\mathcal{D}$. At the (conducting) terminals of the N-port, $\hat{\phi}^T$ and $\hat{\phi}^R$ then take on the values $\{\hat{V}^T_1, ..., \hat{V}^T_N\}$ and $\{\hat{V}^R_1, ..., \hat{V}^R_N\}$. Let, further, $\{\hat{I}^T_1, ..., \hat{I}^T_N\}$ and $\{\hat{I}^R_1, ..., \hat{I}^R_N\}$ be the total electric currents (conduction current + displacement current) as defined above, then

$$\int_{\boldsymbol{x}\in\partial\mathcal{D}} \boldsymbol{\nu}\cdot(\hat{\boldsymbol{E}}^T \times \hat{\boldsymbol{H}}^R - \hat{\boldsymbol{E}}^R \times \hat{\boldsymbol{H}}^T)\,\mathrm{d}A = \sum_{n=1}^{N}(-\hat{V}^T_n \hat{I}^R_n - \hat{V}^R_n \hat{I}^T_n). \tag{9}$$

Equation (9) provides the link between the Maxwell field description in terms of the electric and magnetic field strengths and the Kirchhoff circuit description in terms of the voltages and the electric currents. Note, however, that the latter is only applicable in the quasi-static approximation where (4) holds, whereas the former is generally applicable.

4. Analysis of multiconductor transmission lines

4.1. General N-channel system

In the present section we present some elements of the analysis of low-frequency electromagnetic interference phenomena along multi-conductor transmission lines. Here, "low-frequency" means that the cross-sectional extent of the guiding structure is small compared to the wavelength of the pertaining field; the extent in the longitudinal direction is not subject to such a restriction.

Let a system of $N+1$ labeled conductors ($N \geq 1$) be parallel to the z-axis of a chosen orthogonal, Cartesian reference frame. The conductor with label (0) is used as a reference conductor for defining the voltages of the remaining N conductors in a particular cross-section of the system. In any section of the transmission-line system, its behavior is governed by the coupled system of differential equations

$$\partial_z[\hat{V}] + [\hat{Z}][\hat{I}] = 0, \tag{10}$$
$$\partial_z[\hat{I}] + [\hat{Y}][\hat{V}] = 0, \tag{11}$$

where we use brackets tot denote matrices or arrays ($[\hat{V}]$ and $[\hat{I}]$ are $N \times 1$ matrices, while $[\hat{Z}]$ and $[\hat{Y}]$ are $N \times N$ matrices). In Equations (10) and (11), z is the coordinate along the line (m), $\hat{V}_p$ is the voltage of the p-th conductor (V), $\hat{I}_q$ is the electric current along the q-th conductor (A), $\hat{Z}_{m,p} = R_{m,p} + sL_{m,p}$ is the longitudinal impedance between the m-th and the p-th conductor per length of the system (Ω/m), and $\hat{Y}_{n,q} = G_{n,q} + sC_{n,q}$ is the transverse admittance between the n-th and the q-th conductor per length of the system (S/m). The matrices $[R], [L], [G]$ and $[C]$ are the per unit length resistance, inductance, conductance and capacitance matrices, respectively. The sequences of voltages $[\hat{V}]$ and electric currents $[\hat{I}]$ are uniquely determined by specifying how a particular section of the transmission line is (either actively, or passively) terminated.

4.2. Characteristic impedance matrix

The actual voltages and electric currents in the transmission line system that arise from given excitations in the presence of known terminations at the near and far ends and that are, for our specific case, influenced by the interfering externally induced source voltages and electric currents can conveniently be expressed in terms of the modal voltages and modal electric currents. These voltages and electric currents satisfy a system of linear differential equations with constant coefficients and zero right-hand sides.

Consider now a transmission-line section that occupies the domain in between the cross-sections $z = 0$ and $z = L$. In general, the electric voltages and electric currents along the multiconductor transmission line consist of a superposition of modes traveling in the direction of increasing z that can be conceived as to be generated at the cross-section $z = 0$ and whose propagation factors are written as $\exp(-\hat{\gamma}^{[\mu]}z)$ and modes traveling in the direction of decreasing z that can be conceived as to be generated at the cross-section $z = L$ and whose propagation factors are written as $\exp[-\hat{\gamma}^{[\mu]}(L - z)]$. Hence, with this we can write the desired general solution as

$$[\hat{V}(z)] = \sum_{\mu=1}^{N}[\hat{v}^{[\mu]}]\{\hat{A}^{[\mu]}\exp(-\hat{\gamma}^{[\mu]}z) + \hat{B}^{[\mu]}\exp[-\hat{\gamma}^{[\mu]}(L - z)]\}, \tag{12}$$

$$[\hat{I}(z)] = [\hat{Z}]^{-1}\sum_{\mu=1}^{N}[\hat{v}^{[\mu]}]\{\hat{\gamma}^{[\mu]}\hat{A}^{[\mu]}\exp(-\hat{\gamma}^{[\mu]}z) - \hat{\gamma}^{[\mu]}\hat{B}^{[\mu]}\exp[-\hat{\gamma}^{[\mu]}(L - z)]\}, \tag{13}$$

in which $\hat{\gamma}^{[\mu]}$ denotes the propagation coefficient of the μ-th mode, $[\hat{v}^{[\mu]}]$ its properly normalized, modal voltage and $[\hat{i}^{[\mu]}]$ the corresponding normalized modal electric current. If the desired direction of signal transmission is from the (actively excited) cross-section $z = 0$ to the (passively terminated) cross-section $z = L$, the system of modes traveling in the direction of increasing z is the desired one and the system of modes traveling in the direction of decreasing z is unwanted. The presence of the latter is due to reflection at the passive end. Such a reflection can be avoided by properly selecting the terminating network (reflectionless termination). This may be achieved by terminating the transmission line with its *characteristic impedance* network. The characteristics of this network are such that a system of modes traveling in the direction of increasing z does not discern any difference between a line of infinite length ($L \to \infty$) and a line of finite length terminated by this network. Denoting the $N \times N$ impedance matrix of this network by $[\hat{Z}^{c}]$ the relation

$$[\hat{V}(L)] = [\hat{Z}^{c}][\hat{I}(L)] \tag{14}$$

has to hold at $z = L$. Substituting the expressions for $[\hat{V}]$ and $[\hat{I}]$ as presented in (12) and (13) and taking into account the absence of the reflected waves, we obtain

$$\sum_{\mu=1}^{N}[\hat{v}^{[\mu]}]\{\hat{A}^{[\mu]}\exp(-\hat{\gamma}^{[\mu]}L)\} = [\hat{Z}^{c}][\hat{Z}]^{-1}\sum_{\mu=1}^{N}[\hat{v}^{[\mu]}]\{\hat{\gamma}^{[\mu]}\hat{A}^{[\mu]}\exp(-\hat{\gamma}^{[\mu]}L)\}, \tag{15}$$

which has to hold for any set of mode amplitudes $\hat{A}^{[\mu]}$ $(\mu = 1, ..., N)$. In order to rewrite (15) in matrix notation we introduce the $N \times N$ matrix $[\hat{v}_M]$, in which the μ-th column $(\mu = 1, ..., N)$ represents the normalized modal voltage $[\hat{v}^{[\mu]}]$ and the $N \times N$ matrix $[\hat{\gamma}_M]$, which is a diagonal matrix with $\hat{\gamma}^{[\mu]}$ $(\mu = 1, ..., N)$ as elements. The products of the modal amplitude $\hat{A}^{[\mu]}$ with the factor $\exp(-\hat{\gamma}^{[\mu]}L)$ are arranged as an $N \times 1$ matrix $[\hat{A}^{[\mu]}\exp(-\hat{\gamma}^{[\mu]}L)]$. With these notations (15) can be rewritten as

$$\Big[[\hat{v}_M] - [\hat{Z}^{c}][\hat{Z}]^{-1}[\hat{v}_M]\,[\hat{\gamma}_M]\Big][\hat{A}^{[\mu]}\exp(-\hat{\gamma}^{[\mu]}L)] = 0 \tag{16}$$

which has to hold for arbitrary values of $\hat{A}^{[\mu]}$ $(\mu = 1, ..., N)$. Hence, we obtain

$$[\hat{Z}^{c}] = [\hat{v}_M][\hat{\gamma}_M]^{-1}[\hat{v}_M]^{-1}[\hat{Z}]. \tag{17}$$

In case the dielectric in which the conductors are situated is homogeneous, it can be shown (Weeks, 1972), that the velocity of propagation of the modes is the same for each mode. The matrix $[\hat{\gamma}_M]$ reduces to the product of the $N \times N$ unit matrix and a scalar quantity $\hat{\gamma}$, which is determined by the medium properties and the complex frequency s. Equation (17) reduces in this case to

$$[\hat{Z}^{c}] = \hat{\gamma}^{-1}[\hat{Z}]. \tag{18}$$

For the special case of a homogeneous lossless dielectric and perfect conductors the relation

$$\hat{\gamma} = s(\varepsilon\mu)^{1/2} = s/c \tag{19}$$

holds (Weeks, 1972), where c is the velocity of propagation along the transmission line. The characteristic impedance matrix reduces in this case to

$$[Z^{c}] = c[L]. \tag{20}$$

4.3. Symmetric system of two transmission lines – Common-mode and differential-mode operation

If a system of two transmission lines (i.e., three conductors) has a *plane of symmetry*, such that the conductors with labels (1) and (2) and the reference conductor with label (0) have this plane of symmetry in common, it is advantageous to decompose the two voltages $\hat{V}_1$ and $\hat{V}_2$ and the two electric currents $\hat{I}_1$ and $\hat{I}_2$ into a *common-mode* part according to

$$\hat{V}^{\mathrm{cm}} = \tfrac{1}{2}(\hat{V}_1 + \hat{V}_2), \qquad \hat{I}^{\mathrm{cm}} = \tfrac{1}{2}(\hat{I}_1 + \hat{I}_2), \tag{21}$$

and a *differential-mode* part according to

$$\hat{V}^{\mathrm{dm}} = \tfrac{1}{2}(\hat{V}_1 - \hat{V}_2), \qquad \hat{I}^{\mathrm{dm}} = \tfrac{1}{2}(\hat{I}_1 - \hat{I}_2). \tag{22}$$

These modes satisfy the equations

$$\partial_z \hat{V}^{\mathrm{cm}} + (\hat{Z}_{1,1} + \hat{Z}_{1,2})\hat{I}^{\mathrm{cm}} = 0, \tag{23}$$
$$\partial_z \hat{I}^{\mathrm{cm}} + (\hat{Y}_{1,1} + \hat{Y}_{1,2})\hat{V}^{\mathrm{cm}} = 0, \tag{24}$$

and

$$\partial_z \hat{V}^{\mathrm{dm}} + (\hat{Z}_{1,1} - \hat{Z}_{1,2})\hat{I}^{\mathrm{dm}} = 0, \tag{25}$$
$$\partial_z \hat{I}^{\mathrm{dm}} + (\hat{Y}_{1,1} - \hat{Y}_{1,2})\hat{V}^{\mathrm{dm}} = 0, \tag{26}$$

respectively. The decomposition into common-mode and differential-mode parts has both conceptual and computational advantages. For example, the propagation coefficients of the common mode follows from (23) and (24) as

$$\hat{\gamma}^{\mathrm{cm}} = [(\hat{Z}_{1,1} + \hat{Z}_{1,2})(\hat{Y}_{1,1} + \hat{Y}_{1,2})]^{1/2} \quad \text{with } \mathrm{Re}(\hat{\gamma}^{\mathrm{cm}}) > 0 \text{ for } \mathrm{Re}(s) > 0, \tag{27}$$

and the propagation coefficient of the differential mode from Equation (25) and (26) as

$$\hat{\gamma}^{\mathrm{dm}} = [(\hat{Z}_{1,1} - \hat{Z}_{1,2})(\hat{Y}_{1,1} - \hat{Y}_{1,2})]^{1/2} \quad \text{with } \mathrm{Re}(\hat{\gamma}^{\mathrm{dm}}) > 0 \text{ for } \mathrm{Re}(s) > 0. \tag{28}$$

For the common and the differential mode propagating in the direction of increasing z, the relations

$$\hat{V}^{\mathrm{cm}} = (\hat{\gamma}^{\mathrm{cm}})^{-1}(\hat{Z}_{1,1} + \hat{Z}_{1,2})\hat{I}^{\mathrm{cm}} = \hat{Z}^{\mathrm{c;cm}}\hat{I}^{\mathrm{cm}}, \tag{29}$$
$$\hat{V}^{\mathrm{dm}} = (\hat{\gamma}^{\mathrm{dm}})^{-1}(\hat{Z}_{1,1} - \hat{Z}_{1,2})\hat{I}^{\mathrm{dm}} = \hat{Z}^{\mathrm{c;dm}}\hat{I}^{\mathrm{dm}}, \tag{30}$$

hold, respectively, in which $\hat{Z}^{\mathrm{c;cm}}$ and $\hat{Z}^{\mathrm{c;dm}}$ are scalar quantities. In case of a lossless dielectric and perfect conductors this reduces to

$$Z^{\mathrm{c;cm}} = \left(\frac{L_{1,1} + L_{1,2}}{C_{1,1} + C_{1,2}}\right)^{1/2}, \qquad Z^{\mathrm{c;dm}} = \left(\frac{L_{1,1} - L_{1,2}}{C_{1,1} - C_{1,2}}\right)^{1/2}. \tag{31}$$

From (29) and (30) it follows immediately, by adding and subtracting, that

$$[\hat{Z}^{\mathrm{c}}] = \tfrac{1}{2}\begin{bmatrix} \hat{Z}^{\mathrm{c;cm}} + \hat{Z}^{\mathrm{c;dm}} & \hat{Z}^{\mathrm{c;cm}} - \hat{Z}^{\mathrm{c;dm}} \\ \hat{Z}^{\mathrm{c;cm}} - \hat{Z}^{\mathrm{c;dm}} & \hat{Z}^{\mathrm{c;cm}} + \hat{Z}^{\mathrm{c;dm}} \end{bmatrix} \tag{32}$$

and

$$[\hat{Y}^{\mathrm{c}}] = [\hat{Z}^{\mathrm{c}}]^{-1} = \tfrac{1}{2}\begin{bmatrix} 1/\hat{Z}^{\mathrm{c;cm}} + 1/\hat{Z}^{\mathrm{c;dm}} & 1/\hat{Z}^{\mathrm{c;cm}} - 1/\hat{Z}^{\mathrm{c;dm}} \\ 1/\hat{Z}^{\mathrm{c;cm}} - 1/\hat{Z}^{\mathrm{c;dm}} & 1/\hat{Z}^{\mathrm{c;cm}} + 1/\hat{Z}^{\mathrm{c;dm}} \end{bmatrix}. \tag{33}$$

The termination of this symmetric system of two transmission lines in combination with the perfectly conducting plane in such a way that no reflection occurs, can either be effected by a T-network or by a Π-network. The network elements of the T-network follow directly from the characteristic impedance matrix $[\hat{Z}^{\mathrm{c}}]$ and the network elements of the Π-network from the characteristic admittance matrix $[\hat{Y}^{\mathrm{c}}]$. In the Π-network the impedances between each conductor and the groundplane equal $\hat{Z}^{\mathrm{c;cm}}$, while the mutual impedance equals $2\hat{Z}^{\mathrm{c;cm}}\hat{Z}^{\mathrm{c;dm}}/(\hat{Z}^{\mathrm{c;cm}} - \hat{Z}^{\mathrm{c;dm}})$. These impedances terminate the common mode as well as the differential mode characteristically. The common mode, however, is terminated characteristically by the equal impedances $\hat{Z}^{\mathrm{c;cm}}$ between the conductors and the groundplane independent of the value of the mutual impedance. Similarly, characteristic termination of the differential mode can be achieved by a balanced network with an impedance seen between the two conductors with the ground open of $2\hat{Z}^{\mathrm{c;dm}}$ (Marx, 1973).

5. Application of Lorentz's reciprocity theorem to the configuration

As outlined in the Introduction the aim of this study is to determine the influence of an electromagnetic disturbance on the input quantities of control equipment that uses an open-wire system for its functional operation. In this section we consider as source of the electromagnetic disturbance a lightning stroke, that results from a negative cloud-to-ground discharge and that is directed perpendicular to the surface of the earth. The location and the nature of the stroke are known. The reciprocity theorem is applied to the half-space $z > 0$. The passive Kirchhoff circuit that is extracted out of the system encompasses the termination networks that terminate the transmission-line system. In the transmitting state ("T" state) we apply an excitation at one of the ports by an electric current source of unit strength (the lightning stroke is absent in the "T" state). In the receiving state ("R" state) the disturbing source consists of the lightning stroke. Application of (3) and of (9) yields

$$\hat{V}_i^R = -\int_{\mathcal{D}^R} \hat{\boldsymbol{E}}^T \cdot \hat{\boldsymbol{J}}^R \mathrm{d}V \qquad (i = 1, ..., 4), \tag{34}$$

in which $\hat{V}_i^R$ is the voltage that occurs at port i $(1 = 1, ..., 4)$, due to the lightning stroke, and $\mathcal{D}^R$ denotes the domain in which the lightning stroke is present. The lightning stroke itself is described by the volume current density $\hat{\boldsymbol{J}}^R$. In (34) $\hat{\boldsymbol{E}}^T$ denotes the electric field strength in the domain $\mathcal{D}^R$ due to the unit strength electric current source at port i. In the application of Lorentz's reciprocity theorem, that results in (34), the contribution of the dielectric displacement current in the layer with dielectric constant $\varepsilon = \varepsilon_r\varepsilon_0$ to the electric field strength in the domain of the lightning stroke is neglected. In both states, the "T" state as well as the "R" state, the transmission-line system is terminated by the same passive network. The difference between the "T" state and the "R" state of the system is that in the "T" state at one port the electric current source of unit strength is present, which in the "R" state is replaced by an open port. Effectively the complete system can be seen from this perspective as a one-port system, from which it immediately follows that the summation in (9) over the ports reduces to a contribution of a single port only as is expressed in (34). In the literature several models are presented for the return stroke current. In a recent paper (Nucci *et al.*,1990) a comparison of these models is presented. In our analysis the modified transmission-line model is chosen, by which the functional form of the electric current density in the lightning channel reads

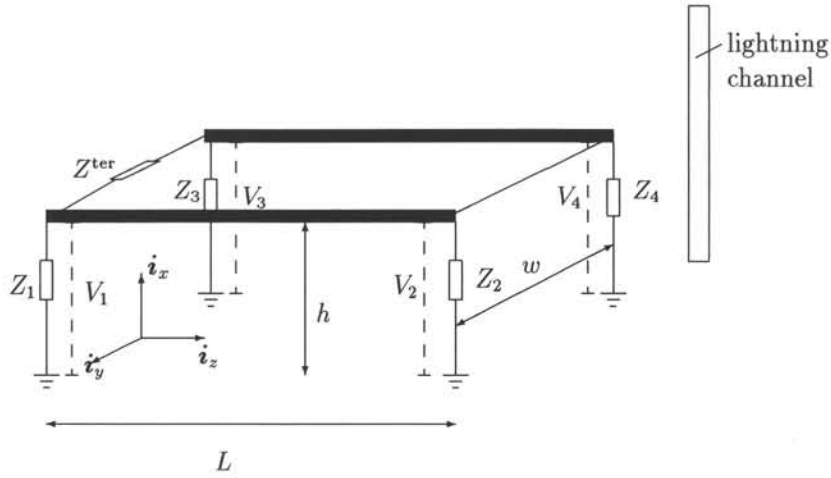

Figure 2. Actual configuration with terminations and lightning channel.

$$\boldsymbol{J}^R(\boldsymbol{x}, t) = \exp(-x/\lambda) i_{cb}(t - x/v)\delta(y - y_{ch})\delta(z - z_{ch})\boldsymbol{i}_x, \tag{35}$$

in which λ is a decay constant to take into account the removal of the leader charge from the channel, v is the velocity of the return stroke wavefront, $\{x, y_{ch}, z_{ch}\}$ denotes the center line of the lightning channel and $i_{cb}(t)$ denotes the channel-base current. It is assumed that the lightning stroke is perpendicular to the surface of the earth. This implies (cf. (34)) that only the x-component of the electric field strength due to the action of the electric current source of unit strength in the "T" state is required. The electric field strength follows from the standard source-type integral representations for electromagnetic fields generated by known sources. The source domain has to be decomposed in the domain occupied by the transmission lines and the domain occupied by the terminations. In the transmission-line part the quasi-TEM modes (common mode and differential mode) are present, propagating in the direction of increasing and of decreasing z. The amplitude coefficients of this modal decomposition are provided by the matrix analysis associated with the theory outlined in Section 4. The electric currents in the network elements constituting the load impedances are taken to be constant along the relevant network branches. These currents follow from the conditions that hold at the terminations of the transmission-line sections and that are determined by the load impedances of the terminating network. Substitution of the expressions for $\hat{\boldsymbol{J}}^R(\boldsymbol{x}, s)$ and $\hat{\boldsymbol{E}}^T(\boldsymbol{x}, s)$ results in a multidimensional integral over the lightning channel and the transmission-line system with its terminations. The integrand of this integral is in the s-domain the product of the pulse shape, exponential functions representing time delays resulting from finite propagation velocities in vacuum, along the transmission line and the lightning channel, and an amplitude decay factor. In the time-domain these exponential functions translate into a delay of the pulse and we obtain for $V^R(t)$ a multidimensional integral of the time delayed

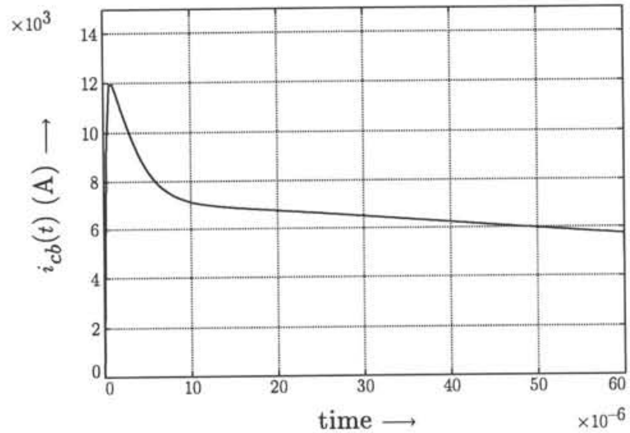

Figure 3. Pulse shape of the channel-base current $i_{cb}(t)$.

pulseshape itself and the time delayed differentiated pulse shape.

6. Numerical results

In this section we present some numerical results pertaining to a configuration as depicted in Figure 2. In this figures the transmission-line section of length L in the plane $x = h$ is sketched. The section is terminated in the cross-sectional plane $z = 0$ by a Π-network, in which the impedance between the two wires is denoted by Z^{ter} and the impedances between the wires and the groundplane by Z_1 and Z_3. In the cross-sectional plane $z = L$ the wires of the transmission line are mutually connected by a short-circuit and by the impedances Z_2 and Z_4 to the groundplane. In our calculations the dielectric layer of thickness h is accounted for in the following way. For the electric current distribution on the transmission-line system in the "T" state, it was assumed that this electric-current distribution could be approximated by the electric current distribution on a transmission-line system with the same spatial dimensions, but with a homogeneous dielectric. The velocities of propagation of the modes on such a transmission-line system are the same. At a container terminal site the time required to traverse a signalling loop was measured and from this quantity an effective dielectric constant for the homogeneous dielectric was determined. Its value was fixed at $\varepsilon_r = 18$. For the determination of the electric field strength in the "T" state at the location of the lightning channel, it was assumed that the effect of the dielectric-displacement current in the layer could be neglected. Hence, the electric-field strength due to an electric-current distribution on the transmission-line system in a vacuum half-space was assumed. The pulse shape for the channel-base current of the lightning stroke is the same as the one considered by Nucci *et al.* (1993). It consists of the sum of two functions of the type

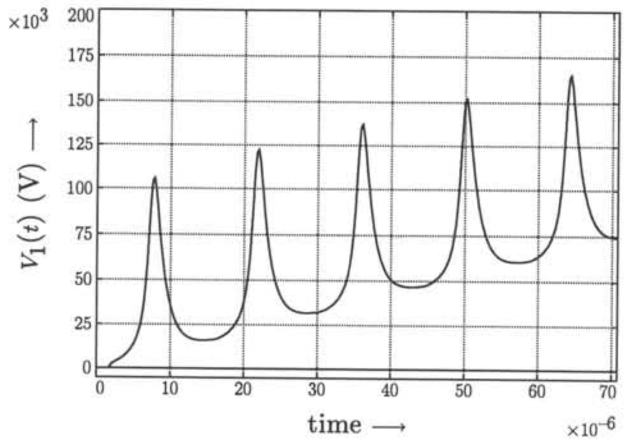

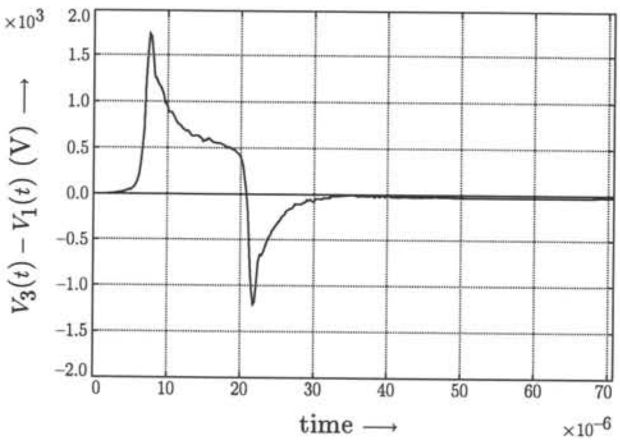

Figure 4. Port voltage $V_1(t)$ and differential-mode voltage $V_3(t) - V_1(t)$ for the transmission-line system in the absence of port impedances Z_1, Z_2, Z_3 and Z_4.

$$i_{cb}(t) = \frac{I_0(t/\tau_1)^n}{\eta[1 + (t/\tau_1)^n]} \exp(-t/\tau_2) \tag{36}$$

where

$$\eta = \exp[-(\tau_1/\tau_2)(n\tau_2/\tau_1)^{(1/n)}]. \tag{37}$$

In the first function we take $I_0 = 10.7$ kA, $\tau_1 = 0.25$ μs, $\tau_2 = 2.5$ μs and $n = 2$, while in the second function we take $I_0 = 6.5$ kA, $\tau_1 = 2.1$ μs, $\tau_2 = 230$ μs and $n = 2$. The pertaining pulse shape is depicted in Figure 3.

The signalling-wire system under consideration is of length $L = 1000$ m, the height h of the wires above the perfectly conducting plane (groundwater level) is 4 m and the mutual separation w of the wires is 8 m. The wire radius was fixed at 0.7 mm (cross-sectional area of the wire is 1.5 mm^2). The channel-base (the striking point

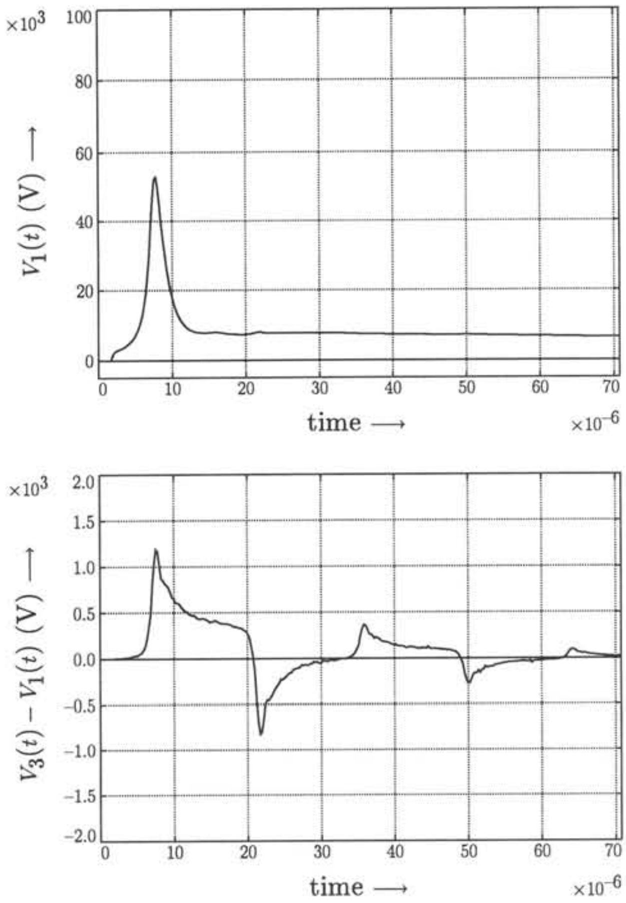

Figure 5. Port voltage $V_1(t)$ and differential-mode voltage $V_3(t) - V_1(t)$ for the transmission-line system in the presence of impedances $Z_1 = Z_2 = Z_3 = Z_4 = Z^{c;cm}$.

of the stroke) is equidistant from the transmission-line terminations, its coordinates are $x = 0$ m, $y = -50$ m, $z = 500$ m. For the channel height a value of 2 km is assumed, while the return-stroke velocity in the lightning channel is fixed at $1.3 \cdot 10^8$ m/s and the decay constant λ at 1.7 km. The transmission-line system is terminated in the cross-sectional plane $z = 0$ by the impedance Z^{ter} and in the plane $z = L$ by a short-circuit. For the magnitude of the impedance Z^{ter} the value $2Z^{c;dm}$ was chosen, since this presents a characteristic termination for the differential-mode when the transmission-line system is not grounded. In Figure 4 the voltages V_1 and $(V_3 - V_1)$ are presented in absence of the impedances Z_1, Z_2, Z_3 and Z_4 (cf. Figure 2). In Figure 5 the same voltages are presented in the presence of the impedances $Z_1 = Z_2 = Z_3 = Z_4 = Z^{c;cm}$. These impedances constitute a characteristic termination for the common mode, which is visible in the port voltage of Figure 5 by the absence of reflected pulses. With the assumed spatial dimensions of the transmission-line system and the effective dielectric constant $\varepsilon_r = 18$ the characteristic mode impedances are $Z^{c;cm} = 137\ \Omega$ and $Z^{c;dm} = 127\ \Omega$.

7. Conclusions

From Figures 4 - 5 it is evident that for a system as specified in Section 6 the time to traverse the signalling loop is not negligible. The application of transmission-line theory to account for delays and reflection of pulses on the line is necessary. The difference in termination of the transmission line results in a reduction of the magnitude of the occurring voltages at the line ends. An open-wire system like this is of course protected by surge arrestors. In the results presented above the presence of these surge arrestors and the action in case of surpassing the voltage threshold is not accounted for. The presence of the impedances Z_1, Z_2, Z_3 and Z_4, each equal to the characteristic impedance $Z^{c;cm}$ (cf. Figure 2), makes that the magnitude of disturbing voltages due to lightning in open-wire signalling systems is reduced. This reduction increases the possibility of normal operation of the open-wire signalling system without breakdown of the surge arrestors.

References

De Hoop, A.T., 1995, Handbook of Radiation and Scattering of Waves, Academic Press Limited, London.

Kami, Y., and R. Sato, 1985, Circuit-concept approach to externally excited transmission lines, IEEE Transactions on Electromagnetic Compatibility, **EMC-27**, 177-183.

Marx, K.D., 1973, Propagation modes, equivalent circuits, and characteristic terminations for multiconductor transmission lines with inhomogeneous dielectrics, IEEE Transactions on Microwave Theory and Techniques, **MTT-21**, 450-457.

Nucci, C.A., G. Diendorfer, M.A. Uman, F. Rachidi, M.V. Ianoz and C. Mazzetti, 1990, Lightning return stroke current models with specified channel-base currents: a review and comparison, Journal of Geophysical Research, **95**, 395-408.

Nucci, C.A., F. Rachidi, M.V. Ianoz and C. Mazzetti, 1993, Lightning-induced voltages on overhead lines, IEEE Transactions on Electromagnetic Compatibility, **EMC-35**, 75-86.

Paul, C.R., 1976, Frequency response of multi-conductor transmission lines illuminated by an electromagnetic field, IEEE Transactions on Electromagnetic Compatibility, **EMC-18**, 183-190.

Quak, D., and R. Wiemans, 1989, Analysis of the susceptibility of a two-wire transmission line to electromagnetic radiation, Proceedings of the 1989 International Symposium on Electromagnetic Compatibility, EMC'89, Nagoya, Japan, September 8-10, 469-474.

Taylor, C.D., R.S. Satterwhite and C.W. Harrison Jr., 1965, The response of a terminated two-wire transmission line excited by a non-uniform electromagnetic field, IEEE Transactions on Antennas and Propagation, **AP-13**, 987-989.

Weeks, W.T., 1972, Multiconductor transmission-line theory in the TEM approximation, IBM Journal on Research and Development, **16**, 604-611.

Reciprocity and the Finite-Element Modeling of Electromagnetic Wavefields

Gerrit Mur

Laboratory of Electromagnetic Research, Faculty of Electrical Engineering, Delft University of Technology, P.O. Box 5031, 2600 GA Delft, the Netherlands

Abstract

Because of their usual representation in integral form, reciprocity theorems are usually seen as tools to generate global field relations such as integral equations or integral representations and general properties of radiating structures such as antennas. In our contribution we will show that reciprocity relations can also be employed to generate useful equations that are of a much more local nature. In particular we will discuss the application of an electromagnetic reciprocity theorem to the finite-element modeling of three-dimensional electromagnetic wavefields. For simplicity we will confine our discussion to the finite-element modeling of the s-domain (time Laplace-transform domain) electromagnetic field equations using the pertinent s-domain convolution type reciprocity relation.

1. Introduction

In the present contribution we shall discuss a reciprocity-based finite element method for computing three-dimensional s-domain electromagnetic fields. A reciprocity based finite element method can be seen as an attractive alternative to existing methods that are usually based either on variational methods, in which finding the stationary point of a functional yields the solutions, see Rayleigh (1870) and Ritz (1909), or on weighted residuals, where the residual error is minimized in some sense, see Finlayson (1972). For a general discussion of the finite element method the reader is referred to Zienkiewicz and Taylor (1989) or Dhatt and Touzot (1984).

In our analysis we shall assume the three-dimensional space $\mathcal{D}$ to be subdivided into a collection of NT tetrahedra $\mathcal{T}(\mathrm{IT})$; $\mathrm{IT} = 1, \ldots, \mathrm{NT}$, (tetrahedra are simplices in 3-D, see Naber, 1980) that together span $\mathcal{D}$. We further assume that this subdivision is such that the vertices of the tetrahedra coincide with possible interfaces $\mathcal{I}$ between different media that may be present, see Figure 1. In case the outer boundary $\partial\mathcal{D}$ of $\mathcal{D}$ as well as the interfaces $\mathcal{I}$ in it are polyhedra this subdivision can be exact, it has to be approximate otherwise.

2. The field equations and boundary conditions

Substituting the constitutive equations into the s-domain electromagnetic field equations we obtain, in each subdomain where the constitutive parameters vary continuously with position,

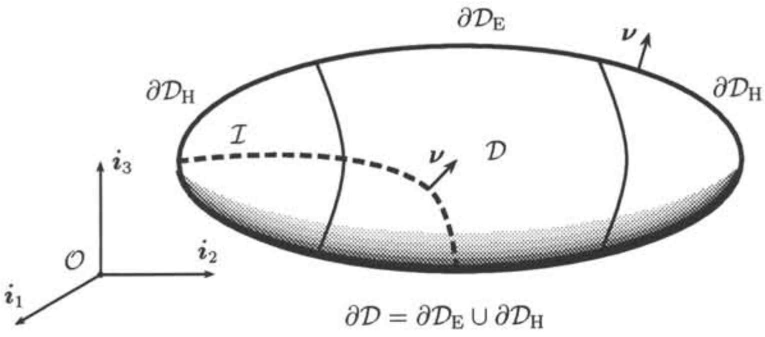

Figure 1. The domain of computation $\mathcal{D}$.

$$\hat{\boldsymbol{\eta}} \cdot \hat{\boldsymbol{E}} - \boldsymbol{\nabla} \times \hat{\boldsymbol{H}} = -\hat{\boldsymbol{J}}^{\mathrm{imp}}, \tag{1}$$

$$\hat{\boldsymbol{\zeta}} \cdot \hat{\boldsymbol{H}} + \boldsymbol{\nabla} \times \hat{\boldsymbol{E}} = -\hat{\boldsymbol{K}}^{\mathrm{imp}}, \tag{2}$$

in which

$$\hat{\boldsymbol{\eta}} = \boldsymbol{\sigma} + s\boldsymbol{\varepsilon}, \tag{3}$$

$$\hat{\boldsymbol{\zeta}} = s\boldsymbol{\mu}, \tag{4}$$

and where $\hat{\boldsymbol{J}}^{\mathrm{imp}}$ and $\hat{\boldsymbol{K}}^{\mathrm{imp}}$ are imposed volume source distributions of electric and magnetic current that are known throughout the domain of computation and where $\boldsymbol{\varepsilon}$, $\boldsymbol{\sigma}$ and $\boldsymbol{\mu}$ are known tensorial constitutive parameters. The field equations are supplemented by boundary conditions

$$\boldsymbol{\nu} \times \hat{\boldsymbol{E}} = \boldsymbol{\nu} \times \hat{\boldsymbol{E}}^{\mathrm{ext}} \text{ on } \partial\mathcal{D}_{\mathrm{E}}, \tag{5}$$

$$\boldsymbol{\nu} \times \hat{\boldsymbol{H}} = \boldsymbol{\nu} \times \hat{\boldsymbol{H}}^{\mathrm{ext}} \text{ on } \partial\mathcal{D}_{\mathrm{H}}, \tag{6}$$

where $\boldsymbol{\nu}$ is the unit vector directed outward along the normal to the outer boundary $\partial\mathcal{D} = \partial\mathcal{D}_{\mathrm{E}} \cup \partial\mathcal{D}_{\mathrm{H}}$ (with $\partial\mathcal{D}_{\mathrm{E}} \cap \partial\mathcal{D}_{\mathrm{H}} = \emptyset$) of the domain of computation $\mathcal{D}$ and where the vector functions $\boldsymbol{\nu} \times \hat{\boldsymbol{E}}^{\mathrm{ext}}$ and $\boldsymbol{\nu} \times \hat{\boldsymbol{H}}^{\mathrm{ext}}$ are known along the relevant parts $\partial\mathcal{D}_{\mathrm{E}}$ and $\partial\mathcal{D}_{\mathrm{H}}$ of the outer boundary, respectively. For $\Re(s) > 0$, the equations (1) - (6) define an s-domain electromagnetic field problem with a unique solution.

3. The compatibility relations

According to Love (1959) compatibility relations are properties of a field that are direct consequences of the field equations and that must be satisfied to allow those equations to have a solution. Consequently, for the solution of the electromagnetic field equations to exist it should satisfy the electromagnetic compatibility relations. An analysis of Maxwell's equations reveals that three different types of electromagnetic compatibility relations can be distinguished.

3.1. Domain type compatibility relations

Taking the divergence of (1) and (2) it follows that in each subdomain where the constitutive parameters vary continuously with position the electromagnetic field should satisfy the conditions

$$\boldsymbol{\nabla} \cdot \hat{\boldsymbol{\eta}} \cdot \hat{\boldsymbol{E}} = -\boldsymbol{\nabla} \cdot \hat{\boldsymbol{J}}^{\mathrm{imp}}, \tag{7}$$

$$\boldsymbol{\nabla} \cdot \hat{\boldsymbol{\zeta}} \cdot \hat{\boldsymbol{H}} = -\boldsymbol{\nabla} \cdot \hat{\boldsymbol{K}}^{\mathrm{imp}}. \tag{8}$$

3.2. Interface type compatibility relations

At the interfaces $\mathcal{I}$ between adjacent subdomains with different constitutive parameters the above, divergence-type, compatibility relations reduce to the following conditions on the normal component of the electric and the magnetic flux density across an interface

$$\boldsymbol{\nu} \cdot (\hat{\boldsymbol{\eta}} \cdot \hat{\boldsymbol{E}} + \hat{\boldsymbol{J}}^{\mathrm{imp}}) = \text{continuous on } \mathcal{I}, \tag{9}$$

$$\boldsymbol{\nu} \cdot (\hat{\boldsymbol{\zeta}} \cdot \hat{\boldsymbol{H}} + \hat{\boldsymbol{K}}^{\mathrm{imp}}) = \text{continuous on } \mathcal{I}, \tag{10}$$

where $\boldsymbol{\nu}$ is the unit vector along the normal to the interface $\mathcal{I}$.

3.3. Outer boundary type compatibility relations

At the outer boundary the conditions on the normal component of the flux through an interface reduce to

$$\boldsymbol{\nu} \cdot \hat{\boldsymbol{\eta}} \cdot \hat{\boldsymbol{E}} = +\boldsymbol{\nu} \cdot (\boldsymbol{\nabla} \times \hat{\boldsymbol{H}}^{\mathrm{ext}} - \hat{\boldsymbol{J}}^{\mathrm{imp}}) \text{ on } \partial\mathcal{D}_{\mathrm{H}}, \tag{11}$$

$$\boldsymbol{\nu} \cdot \hat{\boldsymbol{\zeta}} \cdot \hat{\boldsymbol{H}} = -\boldsymbol{\nu} \cdot (\boldsymbol{\nabla} \times \hat{\boldsymbol{E}}^{\mathrm{ext}} + \hat{\boldsymbol{K}}^{\mathrm{imp}}) \text{ on } \partial\mathcal{D}_{\mathrm{E}}, \tag{12}$$

where $\boldsymbol{\nu}$ is the unit vector along the normal to the outer boundary $\partial\mathcal{D}$.

Note that the electromagnetic compatibility relations are all of the divergence type, either specifying volume or surface conditions. For more general discussions of the importance of the electromagnetic compatibility relations in finite-element methods for electromagnetics the reader is referred to Mur (1994a) for general time-domain electromagnetic fields and to Lager and Mur (1994) for static and stationary electric and magnetic fields.

4. The field expansion

For the computation of the electric and the magnetic field strengths we use the expansions

$$[\hat{\boldsymbol{E}}](\boldsymbol{x},s) = \sum_{\mathrm{I^E}=1}^{\mathrm{N^E}} \hat{E}(\mathrm{I^E},s)\boldsymbol{W}^{\mathrm{E}}(\mathrm{I^E},\boldsymbol{x}) \text{ for } \boldsymbol{x} \in \mathcal{D}, \tag{13}$$

where $\{\boldsymbol{W}^{\mathrm{E}}(\mathrm{I^E},\boldsymbol{x});\ \mathrm{I^E}=1,...,\mathrm{N^E}\}$ is the sequence of the expansion functions for the electric field strength and $\{\hat{E}(\mathrm{I^E},s);\ \mathrm{I^E}=1,...,\mathrm{N^E}\}$ is the sequence of its expansion coefficients, and

$$[\hat{\boldsymbol{H}}](\boldsymbol{x},s) = \sum_{\mathrm{I^H}=1}^{\mathrm{N^H}} \hat{H}(\mathrm{I^H},s)\boldsymbol{W}^{\mathrm{H}}(\mathrm{I^H},\boldsymbol{x}) \text{ for } \boldsymbol{x} \in \mathcal{D}, \tag{14}$$

where $\{\boldsymbol{W}^{\mathrm{H}}(\mathrm{I^H},\boldsymbol{x});\ \mathrm{I^H}=1,...,\mathrm{N^H}\}$ is the sequence of the expansion functions for the magnetic field strength and $\{\hat{H}(\mathrm{I^H},s);\ \mathrm{I^H}=1,...,\mathrm{N^H}\}$ is the sequence of its expansion coefficients. The supports of the expansion functions are their simplicial stars that are denoted by

$$\mathcal{S}^{\mathrm{E}}(\mathrm{I^E}) = \text{ simplicial star of } \boldsymbol{W}^{\mathrm{E}}(\mathrm{I^E},\boldsymbol{x}) \text{ with } \mathrm{I^E}=1,...,\mathrm{N^E}, \tag{15}$$

and

$$\mathcal{S}^{\mathrm{H}}(\mathrm{I^H}) = \text{ simplicial star of } \boldsymbol{W}^{\mathrm{H}}(\mathrm{I^H},\boldsymbol{x}) \text{ with } \mathrm{I^H}=1,...,\mathrm{N^H}, \tag{16}$$

respectively.

In each tetrahedron out of which a particular simplicial star is composed, the (local) expansion functions are taken to be polynomial interpolation functions of the nodal, edge or face type. For a discussion of the relative merits of these and some other types of expansion functions as regards accuracy and efficiency the reader is referred to Mur (1994b).

5. The reciprocity theorem

Piecewise polynomial expansions for the electric and the magnetic field strengths cannot pointwise exactly satisfy the electromagnetic field equations (1) and (2). Hence, the relevant expansions can only serve to construct a solution to the electromagnetic field problem in some approximative manner. The finite-element method provides such a scheme by typically replacing the condition of pointwise satisfaction of the equations by the (weaker) condition that some weighted form of the equations, over the domain of computation, is satisfied exactly ("the method of weighted residuals"). In this respect, a weighted form of the electromagnetic field equations could serve our purpose. In the present contribution, however, we have the opportunity to choose the Lorentz reciprocity relation as an alternative, and possibly very attractive, point of departure. The finite-element modeling of time Laplace-transform domain electromagnetic field problems will therefore be based upon the s-domain (convolution-type) reciprocity relation, which for the domain $\mathcal{D}$ of computation, with boundary surface $\partial\mathcal{D}$, is

$$\begin{aligned}\int_{\boldsymbol{x}\in\partial\mathcal{D}} \boldsymbol{\nu}\cdot\left[\hat{\boldsymbol{E}}^{\mathrm{A}}\times\hat{\boldsymbol{H}}^{\mathrm{B}}-\hat{\boldsymbol{E}}^{\mathrm{B}}\times\hat{\boldsymbol{H}}^{\mathrm{A}}\right]\mathrm{d}A \\ =\int_{\boldsymbol{x}\in\mathcal{D}}(\hat{\boldsymbol{H}}^{\mathrm{A}}\cdot(\hat{\boldsymbol{\zeta}}^{\mathrm{B}}-\hat{\boldsymbol{\zeta}}^{\mathrm{A;T}})\cdot\hat{\boldsymbol{H}}^{\mathrm{B}}-\hat{\boldsymbol{E}}^{\mathrm{A}}\cdot(\hat{\boldsymbol{\eta}}^{\mathrm{B}}-\hat{\boldsymbol{\eta}}^{\mathrm{A;T}})\cdot\hat{\boldsymbol{E}}^{\mathrm{B}})\mathrm{d}V \\ +\int_{\boldsymbol{x}\in\mathcal{D}}(\hat{\boldsymbol{J}}^{\mathrm{imp;A}}\cdot\hat{\boldsymbol{E}}^{\mathrm{B}}-\hat{\boldsymbol{K}}^{\mathrm{imp;A}}\cdot\hat{\boldsymbol{H}}^{\mathrm{B}}-\hat{\boldsymbol{J}}^{\mathrm{imp;B}}\cdot\hat{\boldsymbol{E}}^{\mathrm{A}}+\hat{\boldsymbol{K}}^{\mathrm{imp;B}}\cdot\hat{\boldsymbol{H}}^{\mathrm{A}})\mathrm{d}V.\end{aligned} \tag{17}$$

In this reciprocity theorem, State A is identified with the selected global expansions pertaining to both the electric and the magnetic field strength, while State B is successively identified with specimens out of an appropriate sequence of computational states.

To establish a relationship between the expansion coefficients of the electric and the magnetic field strengths at adjacent locations, we select for the successive computational states specimens of the constructed global expansion functions such that the equations pertaining to State B

$$\hat{\boldsymbol{\eta}}^{\mathrm{B}}\cdot\hat{\boldsymbol{E}}^{\mathrm{B}}-\boldsymbol{\nabla}\times\hat{\boldsymbol{H}}^{\mathrm{B}}=-\hat{\boldsymbol{J}}^{\mathrm{imp;B}}, \tag{18}$$

$$\hat{\boldsymbol{\zeta}}^{\mathrm{B}}\cdot\hat{\boldsymbol{H}}^{\mathrm{B}}+\boldsymbol{\nabla}\times\hat{\boldsymbol{E}}^{\mathrm{B}}=-\hat{\boldsymbol{K}}^{\mathrm{imp;B}}, \tag{19}$$

are exactly satisfied.

From the physical point of view it is obvious that two different types of computational states can be distinguished, viz. the electric and the magnetic state, they will be discussed separately.

5.1. Electric computational states

The electric computational states are taken as:

$$\hat{\boldsymbol{E}}^{\mathrm{B}}=\boldsymbol{W}^{\mathrm{E}}(\mathrm{J}^{\mathrm{E}},\boldsymbol{x}),\ \text{for } \mathrm{J}^{\mathrm{E}} = 1,...,\mathrm{N}^{\mathrm{E}},\qquad \hat{\boldsymbol{H}}^{\mathrm{B}}=\boldsymbol{0},\qquad \hat{\boldsymbol{\eta}}^{\mathrm{B}}=\boldsymbol{0}, \tag{20}$$

with the consequence that

$$\hat{\boldsymbol{J}}^{\mathrm{imp;B}}=\boldsymbol{0},\qquad \hat{\boldsymbol{K}}^{\mathrm{imp;B}}=-\boldsymbol{\nabla}\times\boldsymbol{W}^{\mathrm{E}}(\mathrm{J}^{\mathrm{E}},\boldsymbol{x}),\ \text{for } \mathrm{J}^{\mathrm{E}} = 1,...,\mathrm{N}^{\mathrm{E}}. \tag{21}$$

Substitution of (13) - (14) and (20) - (21) in (17) leads to

$$\begin{aligned}\sum_{\mathrm{I}^{\mathrm{H}}=1}^{\mathrm{N}^{\mathrm{H}}}\hat{H}(\mathrm{I}^{\mathrm{H}},s)\int_{\boldsymbol{x}\in\partial\mathcal{D}\cap\mathcal{S}^{\mathrm{E}}(\mathrm{J}^{\mathrm{E}})\cap\mathcal{S}^{\mathrm{H}}(\mathrm{I}^{\mathrm{H}})}\boldsymbol{\nu}\cdot(\boldsymbol{W}^{\mathrm{H}}(\mathrm{I}^{\mathrm{H}},\boldsymbol{x})\times\boldsymbol{W}^{\mathrm{E}}(\mathrm{J}^{\mathrm{E}},\boldsymbol{x}))\mathrm{d}A \\ =\sum_{\mathrm{I}^{\mathrm{E}}=1}^{\mathrm{N}^{\mathrm{E}}}\hat{E}(\mathrm{I}^{\mathrm{E}},s)\int_{\boldsymbol{x}\in\mathcal{S}^{\mathrm{E}}(\mathrm{I}^{\mathrm{E}})}\boldsymbol{W}^{\mathrm{E}}(\mathrm{J}^{\mathrm{E}},\boldsymbol{x})\cdot\hat{\boldsymbol{\eta}}(\boldsymbol{x},s)\cdot\boldsymbol{W}^{\mathrm{E}}(\mathrm{I}^{\mathrm{E}},\boldsymbol{x})\mathrm{d}V \\ +\int_{\boldsymbol{x}\in\mathcal{S}^{\mathrm{E}}(\mathrm{J}^{\mathrm{E}})}\boldsymbol{W}^{\mathrm{E}}(\mathrm{J}^{\mathrm{E}},\boldsymbol{x})\cdot\hat{\boldsymbol{J}}^{\mathrm{imp}}(\boldsymbol{x},s)\mathrm{d}V \\ -\sum_{\mathrm{I}^{\mathrm{H}}=1}^{\mathrm{N}^{\mathrm{H}}}\hat{H}(\mathrm{I}^{\mathrm{H}},s)\int_{\boldsymbol{x}\in\mathcal{S}^{\mathrm{E}}(\mathrm{J}^{\mathrm{E}})\cap\mathcal{S}^{\mathrm{H}}(\mathrm{I}^{\mathrm{H}})}(\boldsymbol{\nabla}\times\boldsymbol{W}^{\mathrm{E}}(\mathrm{J}^{\mathrm{E}},\boldsymbol{x}))\cdot\boldsymbol{W}^{\mathrm{H}}(\mathrm{I}^{\mathrm{H}},\boldsymbol{x})\mathrm{d}V, \\ \text{for } \mathrm{J}^{\mathrm{E}} = 1,...,\mathrm{N}^{\mathrm{E}},\end{aligned} \tag{22}$$

where we have dropped the superscript A to simplify the notation.

5.2. Magnetic computational states

The magnetic computational states are taken as:

$$\hat{\boldsymbol{E}}^{\mathrm{B}} = \mathbf{0}, \qquad \hat{\boldsymbol{H}}^{\mathrm{B}} = \boldsymbol{W}^{\mathrm{H}}(\mathrm{J}^{\mathrm{H}}, \boldsymbol{x}), \text{ for } \mathrm{J}^{\mathrm{H}} = 1, ..., \mathrm{N}^{\mathrm{H}}, \qquad \hat{\boldsymbol{\zeta}}^{\mathrm{B}} = \mathbf{0}, \tag{23}$$

with the consequence that

$$\hat{\boldsymbol{K}}^{\mathrm{imp;B}} = \mathbf{0}, \qquad \hat{\boldsymbol{J}}^{\mathrm{imp;B}} = \boldsymbol{\nabla} \times \boldsymbol{W}^{\mathrm{H}}(\mathrm{J}^{\mathrm{H}}, \boldsymbol{x}), \text{ for } \mathrm{J}^{\mathrm{H}} = 1, ..., \mathrm{N}^{\mathrm{H}}. \tag{24}$$

Substitution of (13) - (14) and (23) - (24) in (17) and dropping the superscript A leads to

$$\begin{aligned}
&\sum_{\mathrm{I}^{\mathrm{E}}=1}^{\mathrm{N}^{\mathrm{E}}} \hat{E}(\mathrm{I}^{\mathrm{E}}, s) \int_{\boldsymbol{x} \in \partial\mathcal{D} \cap \mathcal{S}^{\mathrm{E}}(\mathrm{I}^{\mathrm{E}}) \cap \mathcal{S}^{\mathrm{H}}(\mathrm{J}^{\mathrm{H}})} \boldsymbol{\nu} \cdot (\boldsymbol{W}^{\mathrm{E}}(\mathrm{I}^{\mathrm{E}}, \boldsymbol{x}) \times \boldsymbol{W}^{\mathrm{H}}(\mathrm{J}^{\mathrm{H}}, \boldsymbol{x})) \mathrm{d}A \\
&= - \sum_{\mathrm{I}^{\mathrm{H}}=1}^{\mathrm{N}^{\mathrm{H}}} \hat{H}(\mathrm{I}^{\mathrm{H}}) \int_{\boldsymbol{x} \in \mathcal{S}^{\mathrm{H}}(\mathrm{I}^{\mathrm{H}}) \cap \mathcal{S}^{\mathrm{H}}(\mathrm{J}^{\mathrm{H}})} \boldsymbol{W}^{\mathrm{H}}(\mathrm{J}^{\mathrm{H}}, \boldsymbol{x}) \cdot \hat{\boldsymbol{\zeta}}(\boldsymbol{x}, s) \cdot \boldsymbol{W}^{\mathrm{H}}(\mathrm{I}^{\mathrm{H}}, \boldsymbol{x}) \mathrm{d}V \\
&\qquad - \int_{\boldsymbol{x} \in \mathcal{S}^{\mathrm{E}}(\mathrm{J}^{\mathrm{E}})} \boldsymbol{W}^{\mathrm{H}}(\mathrm{J}^{\mathrm{H}}, \boldsymbol{x}) \cdot \hat{\boldsymbol{K}}^{\mathrm{imp}}(\boldsymbol{x}, s) \mathrm{d}V \\
&- \sum_{\mathrm{I}^{\mathrm{E}}=1}^{\mathrm{N}^{\mathrm{E}}} \hat{E}(\mathrm{I}^{\mathrm{E}}, s) \int_{\boldsymbol{x} \in \mathcal{S}^{\mathrm{E}}(\mathrm{I}^{\mathrm{E}}) \cap \mathcal{S}^{\mathrm{H}}(\mathrm{J}^{\mathrm{H}})} (\boldsymbol{\nabla} \times \boldsymbol{W}^{\mathrm{H}}(\mathrm{J}^{\mathrm{H}}, \boldsymbol{x})) \cdot \boldsymbol{W}^{\mathrm{E}}(\mathrm{I}^{\mathrm{E}}, \boldsymbol{x}) \mathrm{d}V, \\
&\qquad\qquad \text{for } \mathrm{J}^{\mathrm{H}} = 1, ..., \mathrm{N}^{\mathrm{H}}.
\end{aligned} \tag{25}$$

5.3. The system of equations

Equations (22) and (25) constitute a system of N^{E} and N^{H} simultaneous, linear, algebraic relations in the sequences $\{\hat{E}(\mathrm{I}^{\mathrm{E}});\ \mathrm{I}^{\mathrm{E}} = 1, ..., \mathrm{N}^{\mathrm{E}}\}$ and $\{\hat{H}(\mathrm{I}^{\mathrm{E}});\ \mathrm{I}^{\mathrm{H}} = 1, ..., \mathrm{N}^{\mathrm{H}}\}$ of expansion coefficients. The terms on the right-hand sides that arise from the source distributions are known. The terms on the left-hand side that arise from parts of $\partial\mathcal{D}$ at which explicit boundary conditions are prescribed, are known; the other terms are unknown.

For the terms in the expansions of the electric and/or magnetic field that are known explicitly because of the explicit boundary conditions (5) and (6), the corresponding computational states should be left out in (22) and (25). To apply standard routines from numerical linear algebra, the resulting system should be organized such that all unknowns occur at the left-hand side and all knowns at the right-hand side. Because of using polynomial expansion functions and assuming the constitutive parameters to be polynomials in the spatial coordinates, all integrals occurring in (22) and (25) are elementary. The above equations yield a square system of linear algebraic equations.

6. Implementation of the compatibility relations

The system of linear algebraic equations resulting from the above straightforward application of reciprocity turns out to be singular, or at least ill conditioned, for many practical applications. The way to overcome this difficulty is to include the compatibility relations into the formulation. When using a variational technique or weighted residuals the compatibility conditions are usually implemented by making them a part of the variational expression of the weighting procedure. Sometimes it is also possible to impose the conditions directly in the same way as explicit boundary conditions are imposed. Examples of the implementation of compatibility relations were presented by Mur (1993) and by Lager and Mur (1996). In a context of weighted residuals the actual method of implementation was discussed extensively by Lager (1996).

The reciprocity theorem does, however, not allow for an extension so as to allow the inclusion of the compatibility relations in the reciprocity relations themselves. Consequently, because of the necessity to include the compatibility relations into a reciprocity based finite-element formulation of the electromagnetic field equations, one has to add the linear algebraic equations representing these relations to the system of algebraic equations resulting directly from reciprocity. Each of the equations (7) - (12) yields linear algebraic equations that can be added to the existing square system mentioned above. This can be done in two ways. In the first method the additional equations are added to the existing set of equations because of which the resulting set of equations will become overdetermined. In the second method the additional equation are used to replace existing equations that are of no use in the configuration. This method is discussed extensively by Lager (1996). In both cases the resulting system of equations can be solved by using either direct or iterative techniques.

Recently the idea of including the electromagnetic compatibility relations in a finite element formulation of electromagnetic field problems was adopted in a discussion of structured, reciprocity based, computational methods for electromagnetic wavefield computation presented by De Hoop (1996).

7. Conclusions

For the time-harmonic case, where $s = j\omega$, Mur and De Hoop (1985) presented a method using weighted residuals. By selecting the same expansion functions, choosing the sets of computational states to be identical to these sets of expansion functions and ignoring the compatibility relations one obtains a system of linear algebraic equations identical to the one obtained by Mur and De Hoop. A limitation of that method turned out to be that it can be used for "high frequency" problems only. For "low frequency" problems the results tend to deteriorate. The reason for this is that, although the field equations are solved accurately, the compatibility relations are not modeled accurately, and indeed the errors found in the solution tended to be in the divergence of the solution, the field equations being solved relatively accurately. This stresses the importance of making the divergence properties (compatibility relations) a part of the (reciprocity-based) finite-element formulation.

Acknowledgement

The research presented in this contribution has been financially supported through a Research Grant from the Stichting Fund for Science, Technology and Research (a companion organization of the Schlumberger Foundation in the U.S.A.). This support is gratefully acknowledged.

References

De Hoop, A.T., 1996, Electromagnetic wavefield computation - a structured approach based on reciprocity, Proceedings of 25th URSI General Assembly, Lille, France, Report Et/EM 1996-23, Laboratory of Electromagnetic Research, Delft, the Netherlands.

Dhatt, G., and G. Touzot, 1984, The Finite Element Method Displayed, John Wiley & sons, Chichester.

Finlayson, B.A., 1972, The Method of Weighted Residuals and Variational Principles, Academic press.

Lager, I.E., 1996, Finite element modelling of static and stationary electric and magnetic fields, Ph.D. Thesis, Delft University of Technology, the Netherlands.

Lager, I.E., and G. Mur, 1994, Compatibility relations for time-domain and static electromagnetic field problems, ACES Journal, **9**, 25-29.

Lager, I.E., and G. Mur, 1996, The finite-element modeling of static and stationary electric and magnetic fields, IEEE Transactions on Magnetics, **MAG-32**, 631-634.

Love, A.E.H., 1959, A Treatise on the Mathematical Theory of Elasticity, Cambridge University Press, London.

Mur, G., 1993, The finite-element modeling of three-dimensional electromagnetic fields using edge and nodal elements, IEEE Transactions on Antennas and Propagation, **AP-41**, 948-953.

Mur, G., 1994a, Compatibility relations and the finite-element formulation of electromagnetic field problems, IEEE Transactions on Magnetics, **MAG-30**, 2972-2975.

Mur, G., 1994b, Edge elements, their advantages and their disadvantages, IEEE Transactions on Magnetics, **MAG-30**, 3552-3557.

Mur, G., and A.T. de Hoop, 1985, A finite-element method for computing three-dimensional electromagnetic fields in inhomogeneous media: IEEE Transactions on Magnetics, **MAG-21**, 2188-2191.

Naber, L., 1980, Topological Methods in Euclidean space: Cambridge University Press.

Ritz, W., 1909, Über eine neue Methode zur Lösung gewissen Variationsprobleme der mathematischen Physik, J. Reine angew. Math., **135**, 1-61.

Strutt, J.W., (Lord Rayleigh), 1870, On the theory of resonance, Trans. Roy. Soc., London, **A161**, 77-118.

Zienkiewicz, O. C. and R. L. Taylor, 1989, The Finite Element Method, Vol. 1, McGraw-Hill Book Company.

Profile Inversion by Error Reduction in the Source Type Integral Equations

Peter M. van den Berg and **Kasper F.I. Haak**
Laboratory of Electromagnetic Research, Faculty of Electrical Engineering
Centre for Technical Geoscience, Delft University of Technology
P.O. Box 5031, 2600 GA Delft, the Netherlands

Abstract

A simultaneous reconstruction of the permittivity and electrical conductivity of a bounded object from scattered electromagnetic field data is discussed. The inverse scattering problem is considered as an inverse source problem. The inverse source problem is solved with a conjugate gradient iterative method, in which, in each iteration, the updated contrast sources are simply enforced to satisfy a local constitutive source/field relation. The method is very simple, computationally very cheap and leads to surprisingly good reconstruction results.

1. Introduction

The configuration in an electromagnetic inverse scattering problem generally consists of a background medium with known electromagnetic properties, occupying the entire $\mathbb{R}^3$ (the embedding medium), in which in principle, the radiation from given electromagnetic sources can be calculated. In the embedding, an either known or guessed, bounded domain $\mathbb{D}^S$ (the object domain) is present in which the medium properties show an unknown contrast with the ones of the embedding. The contrasting domain is irradiated by an incident electromagnetic field that is generated by sources in some subdomain $\mathbb{D}^i$ of $\mathbb{R}^3$ and that propagates in the embedding. In some bounded domain $\mathbb{D}^\Omega$ (the data domain) of $\mathbb{R}^3$, and exterior to $\mathbb{D}^S$, the scattered electromagnetic field is accessible to measurement.

The objective is to reconstruct the medium parameters (or their contrasts with the ones of the embedding) from a set of measured values of the electric field and/or the magnetic field in $\mathbb{D}^S$. The scattered wavefield is, by its nature, causally related to the contrast sources by which it is generated. Therefore De Hoop (e.g., Handbook on Radiation of Scattering of Waves, 1995) has suggested very often that the easiest way to address the inverse scattering problem is to consider it as an inverse source problem with the contrast volume source densities as the fundamental unknowns. The scattered field follows from these contrast sources through a source type of integral representation. Once the contrast volume source distributions have been determined, the scattered wave field is calculated in the object domain $\mathbb{D}^S$ and since the incident wavefield and the medium parameters of the embedding are known, the parameters of the embedding follow from the local constitutive relation between the contrast sources and the field values. In principle, this procedure solves the nonlinear scattering problem by direct linear methods, without assuming that the contrast in medium parameters is small. However, a straightforward implementation leads to good results for small values of the contrast in the medium parameters only. This method is also used to obtain a useful starting value for the modified gradient method (Kleinman and Van den Berg, 1994). A full inversion is defeated by the non-uniqueness of the inverse source problem that must be solved first to obtain the contrast sources from the measured field data. The inverse source problem is non-unique because of nonradiating sources that generate a zero electromagnetic field in the data domain $\mathbb{D}^{\Omega}$. This observation is also made by De Hoop, see Habashy *et al.* (1993), where this method is called the naive STIE (source type integral equation) method. If the contrast sources include any non-radiating constituents, then the data contain no information about these currents, and it is therefore impossible, without other information about the physics of the pertaining problem, to reconstruct the contrast sources. This non-uniqueness of the contrast sources is to be removed by invoking the remaining conditions to be satisfied. In the latter, the conditions that the reconstructed contrast-in-medium parameters must be independent of the incident wavefield plays a crucial role. Habashy *et al.* (1993) have modified this naive STIE method to incorporate this feature. In fact, with the STIE method the data are inverted only once for the radiating sources. A subsequent iterative procedure determines the non-radiating sources, which is based upon the generation of "invisible" basis functions.

Within the scope of this symposium in honour of Adrianus T. de Hoop it is the occasion to return to the main idea of the naive STIE method. As already said in the Preface of this book, he is able to simplify difficult problems and the objective of the present paper is to investigate whether his original ideas of the STIE method can be used to simplify the difficult inverse scattering problem. We show that a naive conjugate gradient iterative method may be used to invert the linear inverse source problem, however, in each iteration, the updated contrast sources are replaced by sources that satisfy the remaining physics. This introduces the nonlinearity of the inverse scattering problem, but this non-linearity can be handled by employing Polak-Ribière conjugate gradient directions. We show that the reconstruction of the non-radiation sources is superfluous and that we are now able to reconstruct objects, with moderate contrasts in medium parameters, from multiple source receiver measurements at a single frequency. The method is very simple and is computationally very efficient.

2. The source type integral equations

We formulate the problem in the temporal Laplace-transform domain with complex parameter s. The position in space is denoted by the position vector $\boldsymbol{x}$. We assume that only sources of the electric type are present. From Lorentz' reciprocity theorem the source type integral representation for the electric field strength $\hat{\boldsymbol{E}}^{s}$ immediately follows as

$$\hat{\boldsymbol{E}}^{s}(\boldsymbol{x}',s) = \int_{\boldsymbol{x}\in\mathbb{D}^{s}} \hat{\mathrm{G}}(\boldsymbol{x}',\boldsymbol{x},s)\cdot\hat{\boldsymbol{J}}^{s}(\boldsymbol{x},s)\mathrm{dv}\,, \quad \text{for } \boldsymbol{x}'\in\boldsymbol{R}^{3}\,, \tag{1}$$

where $\hat{\boldsymbol{J}}^s$ is the volume density of electric current in the source domain $\mathbb{D}^S$ and $\hat{\mathbf{G}}$ is the electric-field Green tensor. This Green tensor is the electric field strength at $\boldsymbol{x}'$ radiated by an electric-current point source at $\boldsymbol{x}$ in the isotropic embedding medium with with permittivity $\hat{\varepsilon}(\boldsymbol{x}, s)$, electric conductivity $\hat{\sigma}(\boldsymbol{x}, s)$ and permeability $\hat{\mu}(\boldsymbol{x}, s)$.

In the scattering problem, in $\mathbb{D}^S$ an isotropic object is present with permittivity $\hat{\varepsilon}^s(\boldsymbol{x}, s)$, electric conductivity $\hat{\sigma}^s(\boldsymbol{x}, s)$ and permeability $\hat{\mu}(\boldsymbol{x}, s)$. Then, this object is characterized by a contrast source distribution in $\mathbb{D}^S$, viz.,

$$\hat{\boldsymbol{J}}^s = [\hat{\sigma}^s - \hat{\sigma} + s(\hat{\varepsilon}^s - \hat{\varepsilon})]\, \hat{\boldsymbol{E}}\,, \tag{2}$$

$$= \hat{C}\, \hat{\boldsymbol{E}}\,, \tag{3}$$

where $\hat{\boldsymbol{E}}$ is the total electric field in $\mathbb{D}^S$ given by

$$\hat{\boldsymbol{E}} = \hat{\boldsymbol{E}}^i + \hat{\boldsymbol{E}}^s\,, \tag{4}$$

and $\hat{\boldsymbol{E}}^i$ denotes the incident electric field. The contrast quantity $\hat{C} = \hat{C}(\boldsymbol{x}, s)$ is representative for the presence of the scattering object.

In an inverse scattering problem both the field $\hat{\boldsymbol{E}}$ and the contrast $\hat{C}$ are unknown. These unknowns are not independent but are related to each other by the so-called object equation. This equation follows by requiring consistency in $\mathbb{D}^S$. From (1) and (4) we arrive at

$$\hat{\boldsymbol{E}}(\boldsymbol{x}', s) = \hat{\boldsymbol{E}}^i(\boldsymbol{x}', s) + \int_{\boldsymbol{x}\in\mathbb{D}^S} \hat{\mathbf{G}}(\boldsymbol{x}', \boldsymbol{x}, s) \cdot \hat{\boldsymbol{J}}^s(\boldsymbol{x}, s)\mathrm{dv}\,, \quad \text{for } \boldsymbol{x}' \in \mathbb{D}^S\,, \tag{5}$$

while $\hat{\boldsymbol{J}}^s = \hat{C}\, \hat{\boldsymbol{E}}$. If the scattered field is measured on Ω, which includes measurement error, noise and any other signal contamination, then (1) will in general not be satisfied if the data replace the scattered field values $\hat{\boldsymbol{E}}^s(\boldsymbol{x}', s)$. When $\hat{\boldsymbol{E}}^s$ is replaced by the data we call (1) the data equation. In fact we use this data equation to define the discrepancy between the measured data and the predicted scattered field corresponding to $\hat{C}$ and $\hat{\boldsymbol{E}}$ in $\mathbb{D}^S$.

In order to discuss our solution of the inverse scattering problem we write our equations in an operator form and we denote the electric field strength by the symbol u and the source strength by w and we omit the hats. We assume that the object is irradiated successively by a number of known incident fields $u_j^i(\boldsymbol{x})$, $j = 1, \cdots, J$. For each incident field, the total field will be denoted by $u_j(\boldsymbol{x})$, the measured scattered field data are denoted by $f_j(\boldsymbol{x})$ and the electric current source strength by $w_j(\boldsymbol{x})$. Then, the data equation of (1) is written as

$$(G^\Omega w_j)(\boldsymbol{x}) = f_j(\boldsymbol{x})\,, \quad \boldsymbol{x} \in \mathbb{D}^\Omega\,, \quad j = 1, \cdots, J\,, \tag{6}$$

while the object equation of (4) is written as

$$u_j(\boldsymbol{x}) = u_j^i(\boldsymbol{x}) + (G^S w_j)(\boldsymbol{x})\,, \quad \boldsymbol{x} \in \mathbb{D}^S\,, \quad j = 1, \cdots, J\,, \tag{7}$$

with the local source/field relation

$$w_j(\boldsymbol{x}) = C(\boldsymbol{x}) u_j(\boldsymbol{x})\,, \quad j = 1, \cdots, J\,. \tag{8}$$

The inverse scattering problem consists of determining the contrast $C(\boldsymbol{x}) \in U_{ad}$ from a knowledge of the incident fields u_j^i in $\mathbb{D}^S$ and the data f_j in $\mathbb{D}^\Omega$. The space of admissible function U_{ad} should incorporate any a priori information about the contrast. With (6) – (8) our inverse scattering problem will be cast as an optimization problem. In fact, we use the data equation (6) to define the discrepancy between the measured data and the predicted scattered field corresponding to C, u_j and w_j in $\mathbb{D}^S$, while the object equation (7) and the local source/field relation (8) are constraints that have to be satisfied as well. In order to have a measure of the discrepancy in the data equation we define an inner product $\langle \cdot, \cdot \rangle_{\mathbb{D}^\Omega}$ and norm $\| \cdot \|_{\mathbb{D}^\Omega}$ in $L^2(\mathbb{D}^\Omega)$. The basic idea for solving the inverse problem is the iterative reconstruction of sequences $w_{j,n}$, which converges to minimizers of the functional

$$F(w_j) = \frac{\sum_{j=1}^J \|\rho_j\|^2_{\mathbb{D}^\Omega}}{\sum_{j=1}^J \|f_j\|^2_{\mathbb{D}^\Omega}}, \tag{9}$$

where

$$\rho_j(\boldsymbol{x}) = f_j(\boldsymbol{x}) - (G^\Omega w_j)(\boldsymbol{x}) \tag{10}$$

is the residual error in the data equation, while (7) and (8) are necessary constraints.

3. The naive STIE method

We first note that the data equation (6) is a linear equation for w_j. Hence a standard conjugate gradient iterative scheme can be employed as an iterative scheme to solve the data equation for each j. However, we rather want to minimize $F(w_j)$ of (9) and this is achieved by the following conjugate gradient scheme:

$$w_{j,0} = 0, \quad \rho_{j,0} = f_j, \tag{11}$$

$$w_{j,n} = w_{j,n-1} + \alpha_n v_{j,n}, \quad v_{j,n} = g_{j,n} + \gamma_n v_{j,n-1}. \tag{12}$$

Here, $g_{j,n}$ is the gradient of F with respect to changes in w_j and is given by

$$g_{j,n} = G^{\Omega^\star} \rho_{j,n-1}, \quad \rho_{j,n-1} = f_j - G^\Omega w_{j,n-1}, \tag{13}$$

where $G^{\Omega^\star}$ denotes the operator adjoint to G^Ω. The real-valued constants α_n and γ_n are given by

$$\alpha_n = \frac{\sum_{j=1}^J \langle \rho_{j,n-1}, G^\Omega v_{j,n} \rangle_{\mathbb{D}^\Omega}}{\sum_{j=1}^J \|G^\Omega v_{j,n}\|^2_{\mathbb{D}^\Omega}}, \quad \gamma_n = \frac{\sum_{j=1}^J \|g_{j,n}\|^2_{\mathbb{D}^\Omega}}{\sum_{j=1}^J \|g_{j,n-1}\|^2_{\mathbb{D}^\Omega}}. \tag{14}$$

It is obvious that the convergent solution of this scheme may be written as a solution of the symmetrized equation, $G^\Omega G^{\Omega^\star} h_j = f_j$, where $w_j = w_j^{min}$ is related to h_j through $w_j^{min} = G^{\Omega^\star} h_j$. It can be shown that this is the minimum norm solution of the data equation (6) (see Habashy *et al.*, 1995), i.e.,

$$\|w_j\|_{\mathbb{D}^S} \geq \|w_j^{min}\|_{\mathbb{D}^S}, \tag{15}$$

where we have defined an inner product $\langle\cdot,\cdot\rangle_{\mathbb{D}^S}$ and norm $\|\cdot\|_{\mathbb{D}^S}$ in $L^2(\mathbb{D}^S)$. In our notation the proof is as follows. The difference with another particular solution is defined as $w_j^\Delta = w_j - w_j^{min}$. Then $G^\Omega w_j^\Delta = 0$ for $\boldsymbol{x} \in \mathbb{D}^\Omega$, and $\langle w_j^{min}, w_j^\Delta\rangle_{\mathbb{D}^S} = \langle G^{\Omega\star} h_j, w_j^\Delta\rangle_{\mathbb{D}^S} = \langle h_j, G^\Omega w_j^\Delta\rangle_{\mathbb{D}^\Omega} = 0$, which shows that w_j^Δ is orthogonal to w_j^{min}. Hence, $\|w_j\|^2_{\mathbb{D}^S} = \|w_j^{min}\|^2_{\mathbb{D}^S} + \|w_j^\Delta\|^2_{\mathbb{D}^S}$ and w_j^{min} is indeed the particular solution with the smallest norm.

Let we now assume that we have carried out N iterations and that $w_{j,N}$ represents the contrast sources approximately. Then, the field inside $\mathbb{D}^S$ follows from (7) as

$$u_{j,N} = u_j^i + G^S w_{j,N}\,. \tag{16}$$

With $u_{j,n}$ and $w_{j,N}$, the approximate contrast follows from

$$C_N(\boldsymbol{x}) = \begin{matrix}\arg\min\\ C(\boldsymbol{x}) \in U_{ad}\end{matrix} \left(\sum_{j=1}^{J} |w_{j,N}(\boldsymbol{x}) - C(\boldsymbol{x})u_{j,N}(\boldsymbol{x})|^2\right) \tag{17}$$

leading to

$$C_N(\boldsymbol{x}) = \frac{\sum_{j=1}^{J} w_{j,N}(\boldsymbol{x})\overline{u}_{j,N}(\boldsymbol{x})}{\sum_{j=1}^{J} |u_{j,N}(\boldsymbol{x})|^2}\,, \tag{18}$$

where the overbar denotes complex conjugate.

3.1. Positivity

When we are working in the temporal Fourier domain with $s = j\omega$ and we have the a priori information that the contrast may be written as

$$C(\boldsymbol{x}, j\omega) = \sigma^s(\boldsymbol{x}) - \sigma(\boldsymbol{x}) + j\omega[\varepsilon^s(\boldsymbol{x}) - \varepsilon(\boldsymbol{x})]\,, \tag{19}$$

where σ^s and ε^s are real non-negative quantities, we take this a priori information into account by using a slightly modified analysis of Habashy *et al.* (1994) and Kleinman and Van den Berg (1995), we obtain the following approximations

$$\sigma_N^s(\boldsymbol{x}) = \left(\frac{\sum_{j=1}^{J}\left(\mathrm{Re}\left\{[w_{j,N}(\boldsymbol{x}) + \sigma(\boldsymbol{x})u_{j,N}(\boldsymbol{x})]\dfrac{\overline{u}_{j,N}(\boldsymbol{x})}{|u_{j,N}(\boldsymbol{x})|}\right\}\right)^2}{\sum_{j=1}^{J}|u_{j,N}(\boldsymbol{x})|^2}\right)^{\frac{1}{2}} \tag{20}$$

and

$$\varepsilon_N^s(\boldsymbol{x}) = \frac{1}{\omega}\left(\frac{\sum_{j=1}^{J}\left(\mathrm{Im}\left\{[w_{j,N}(\boldsymbol{x}) + j\omega\varepsilon(\boldsymbol{x})u_{j,N}(\boldsymbol{x})]\dfrac{\overline{u}_{j,N}(\boldsymbol{x})}{|u_{j,N}(\boldsymbol{x})|}\right\}\right)^2}{\sum_{j=1}^{J}|u_{j,N}(\boldsymbol{x})|^2}\right)^{\frac{1}{2}}\,. \tag{21}$$

3.2. Error check

Once we have computed C_N we may update the contrast sources $w_{j,N+1}$ using the relation

$$w_{j,N+1} = C_N u_{j,N} \,. \tag{22}$$

After substitution of this modified contrast source in our cost functional,

$$F(w_{j,N+1}) = \frac{\sum_{j=1}^{J} \|\rho_{j,N+1}\|^2_{\mathbb{D}^\Omega}}{\sum_{j=1}^{J} \|f_j\|^2_{\mathbb{D}^\Omega}} \,, \tag{23}$$

with residual error

$$\rho_{j,N+1} = f_j - G^\Omega w_{j,N+1} \,, \tag{24}$$

the value of this cost function should be small enough. From a number of numerical experiments we have observed that this is only true for small values of the contrast and/or low frequencies. Only under these circumstances an adequate profile inversion is arrived at.

3.3. A numerical example

We illustrate the behaviour of the naive STIE method with a numerical example of the scattering by a two-dimensional object that consists of concentric square cylinders, an inner cylinder, d by d, with contrast $\chi = 0.6+2.0i$, surrounded by an outer cylinder, $2d$ by $2d$, with contrast $\chi = 0.3+0.4i$, as shown in Figure 1a. Synthetic "measured" data were found by numerical solution of the forward problem as described in Kleinman and Van den Berg (1993). The measurement surface S was chosen to be a circle of radius $3d$ containing the test domain D which was a square, $3d$ by $3d$. Twenty nine stations ($J = 29$) were located uniformly on the surface S with each station serving successively as a line source and all stations acting as receivers. The test domain was discretized into 29×29 subsquares. We take $\lambda = 3d$ and $\lambda = d$, where λ is the

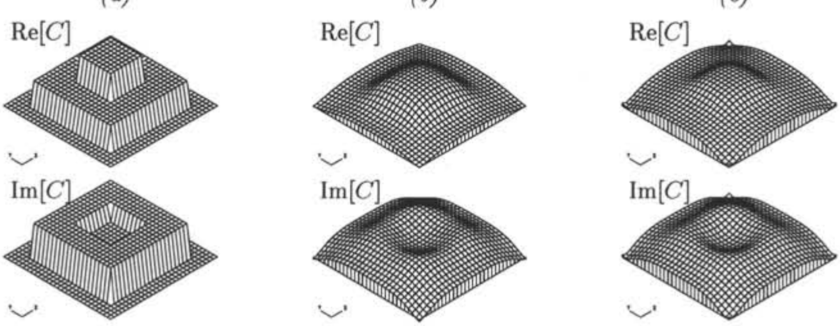

Figure 1. The original profile *(a)* and the reconstructed profiles after 32 iterations using the naive STIE method (test domain = $\lambda \times \lambda$) without positivity *(b)* and with positivity *(c)*.

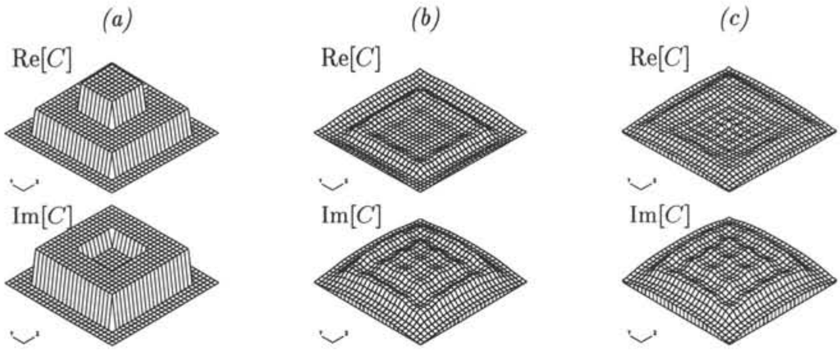

Figure 2. The original profile *(a)* and the reconstructed profiles after 32 iterations using the naive STIE method (test domain $= 3\lambda \times 3\lambda$) without positivity *(b)* and with positivity *(c)*.

wavelength in the background (exterior) medium. Once the square root of the error measure $F_n = F(w_{j,n})$ is less than 10^{-4}, the iteration is terminated and the contrast is determined either without positivity requirements, by using (18), or with positivity requirements, by using (20) and (21). The reconstructions are shown in Figure 1, for $\lambda = 3d$ and in Figure 2, for $\lambda = d$. Further, the square root of the error measure $F = F(w_{j,n})$ is plotted in Figure 3. After determination of the contrast, the final error of (23) is computed. Note the large jump in this error quantity. This jump increases with smaller wavelengths. We also have observed that this jump increases for higher contrasts and no good reconstruction is achieved. From this we conclude that the naive STIE method works well for small objects (large wavelengths) and small contrasts. But for these large wavelengths the resolution of the reconstructed profile is not very high. The conclusion is that, for profile reconstruction beyond the Born approximation, the naive STIE method is not very useful.

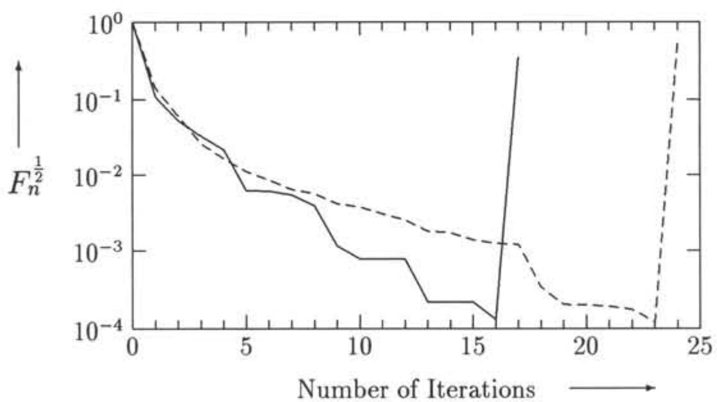

Figure 3. Error $F_n^{\frac{1}{2}}$ as a function of the number of iterations, for $\lambda = 3d$ (solid line) and for $\lambda = d$ (dashed line).

4. Error reduction in the STIE method

In order to make the previous inversion algorithm operative for larger contrasts and/or higher frequencies, we modify the algorithm in such a way that after each iteration the contrast sources $w_{j,n}$ are replaced by $w_{j,n} = C_n u_{j,n}$. We then arrive the following modified conjugate gradient STIE scheme:

$$w_{j,0} = 0\,, \quad \rho_{j,0} = f_j\,, \tag{25}$$

and then we compose an intermediate update

$$w'_{j,n} = w_{j,n-1} + \alpha'_n v_{j,n}\,, \quad v_{j,n} = g_{j,n} + \gamma'_n v_{j,n-1}\,. \tag{26}$$

Here, $g_{j,n}$ is the gradient of F with respect to changes in w_j and is given by

$$g_{j,n} = G^{\Omega\star} \rho_{j,n-1}\,, \quad \rho_{j,n-1} = f_j - G^S w_{j,n-1}\,. \tag{27}$$

The complex-valued constants α'_n and γ'_n are given by

$$\alpha'_n = \frac{\sum_{j=1}^{J} \langle \rho_{j,n-1}, G^{\Omega} v_{j,n} \rangle_{\mathbb{D}^\Omega}}{\sum_{j=1}^{J} \|G^{\Omega} v_{j,n}\|^2_{\mathbb{D}^\Omega}}\,, \quad \gamma'_n = \frac{\sum_{j=1}^{J} \langle g_{j,n}, g_{j,n} - g_{j,n-1} \rangle_{\mathbb{D}^\Omega}}{\sum_{j=1}^{J} \|g_{j,n-1}\|^2_{\mathbb{D}^\Omega}}\,. \tag{28}$$

In each iteration, the field inside $\mathbb{D}^S$ follows from (7) as

$$u_{j,n} = u_j^i + G^S w'_{j,n}\,. \tag{29}$$

With $u_{j,n}$ and $w'_{j,n}$, the approximate contrast follows from

$$C_n = \begin{matrix} \arg\min \\ C \in U_{ad} \end{matrix} \left(\sum_{j=1}^{J} \|w'_{j,n} - C\, u_{j,n}\|^2 \right) \tag{30}$$

leading to

$$C_n = \frac{\sum_{j=1}^{J} w'_{j,n} \overline{u}_{j,n}}{\sum_{j=1}^{J} |u_{j,n}|^2}\,. \tag{31}$$

Alternatively, with the a priori information of positivity, the expressions of (20) – (21) can be used, with N replaced by n. Finally, the new update for the contrast source is obtained as

$$w_{j,n} = C_n u_{j,n}\,. \tag{32}$$

Note that the real-valued constant α_n has been replaced by a complex-valued α'_n. Further note that the real-valued γ_n in the Fletcher-Reeves directions (Brodlie, 1997) of (12) has been replaced by a complex-valued γ'_n in the so-called Polak-Ribière directions (Brodlie, 1977) of (26). For the linear problem of the previous section, the orthogonality of the gradients leads to $\langle g_{j,n}, g_{j,n-1} \rangle = 0$, so that the Fletcher-Reeves directions and the Polak-Ribière directions coincide. But in each iteration of our new scheme we have modified the updated contrast sources in a non-linear way and this non-linearity destroys the orthogonality properties present in a linear conjugate gradient scheme. Once the scheme loses it effectiveness due to the fact that the gradients $g_{j,n}$ and $g_{j,n-1}$ are not very different anymore, one has to restart the scheme. However, when this is the case, we have $\gamma'_n \approx 0$ and the Polak-Ribière directions become approximately the gradient directions $g_{j,n}$, and the updating is restarted automatically.

4.1. A numerical example

We consider the example of Subsection 3.3. We now apply the iterative scheme developed in this section. We consider the single frequency case ($s = j\omega$) such that $\lambda = 3d$. In Figure 4 (without imposing positivity) and Figure 5 (imposing positivity), the reconstruction results are shown after 16, 32 and 64 iterations, respectively. We observe that the results are much better than the ones of the naive STIE method and the imposition of positivity constraints leads to a slightly improved reconstruction. In Figure 6, we present the square root of error measure F_n as a function of the number of iterations, specifically we have plotted the value of $F(w'_{j,n})$ and $F(w_{j,n})$, successively. The jump $F(w_{j,n}) - F(w'_{j,n})$ at each iteration does not change substantially. This jump is related to the residul error that remains after minimization of the error in the local source/field relation.

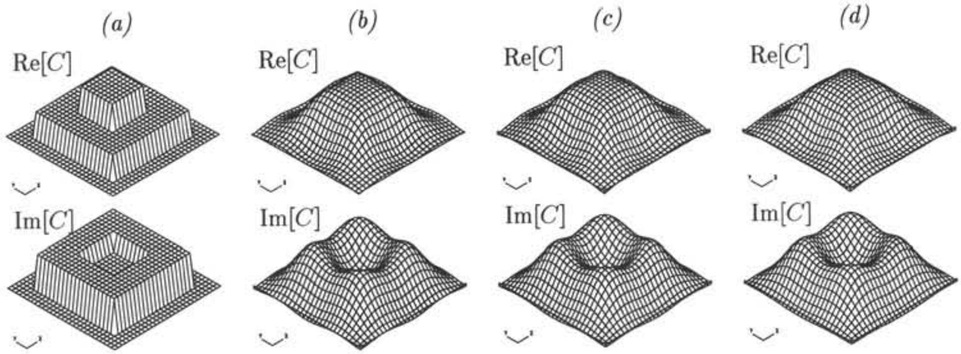

Figure 4. The original profile *(a)* and the reconstructed profiles after *(b)* 16 iterations, *(c)* 32 iterations and *(d)* 64 iterations; without positivity (test domain = $\lambda \times \lambda$).

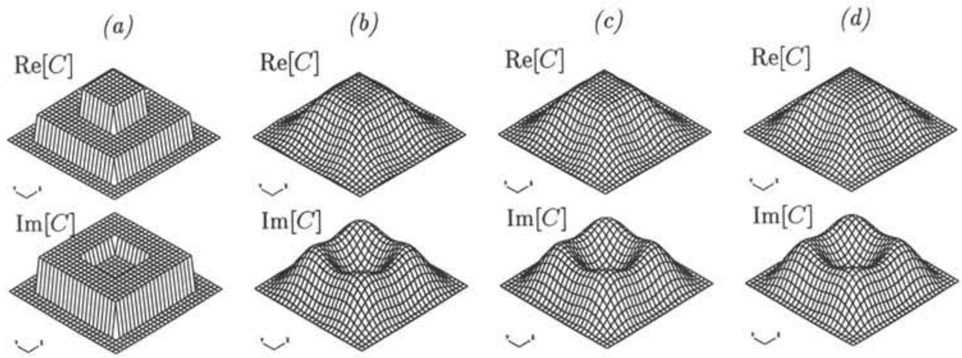

Figure 5. The original profile *(a)* and the reconstructed profiles after *(b)* 16 iterations, *(c)* 32 iterations and *(d)* 64 iterations; with positivity (test domain = $\lambda \times \lambda$).

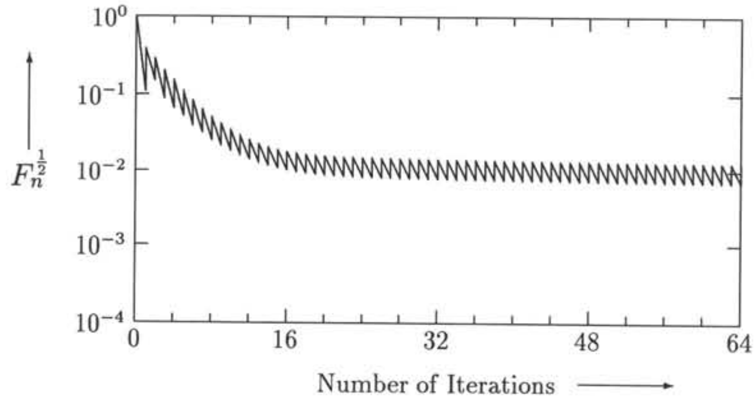

Figure 6. Error $F_n^{\frac{1}{2}}$ as a function of the number of iterations, for $\lambda = 3d$.

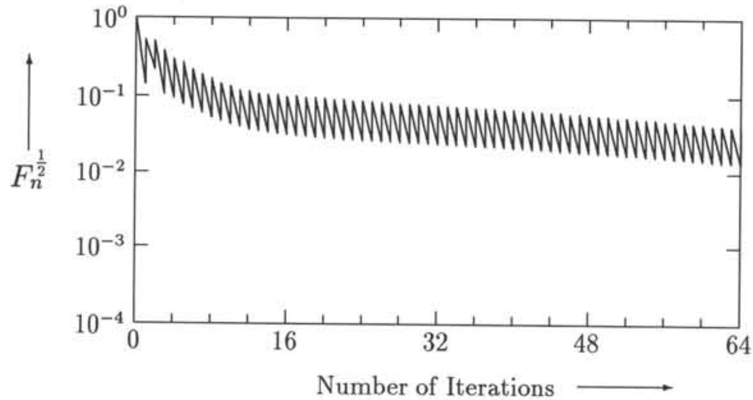

Figure 7. Error $F_n^{\frac{1}{2}}$ as a function of the number of iterations, for $\lambda = d$.

As next step we decrease the wavelength such that $\lambda = d$. Then, the error measures are presented in Figure 7. We now observe that the jumps $F(w_{j,n}) - F(w'_{j,n})$ are increased. However, the reconstruction results are improved significantly, as can be seen in Figure 8 (without imposition of positivity) and in Figure 9 (with imposition of positivity constraints). Already after 16 iterations a reasonable result is achieved. When we compare these results using the modified gradient method (Kleinman and Van den Berg, 1993), we observe that the results after 64 iterations (with positivity constraint) of Figure 9 are even better than the results obtained after 128 iterations with the modified gradient method. In this respect it is mentioned that the computation time of one iteration is less than a tenth of the one of the modified gradient method, and the computer memory needed in the present method is a third of the memory needed for the modified gradient method. In fact, the computation time of one iteration is less than the computation time of one iteration needed to solve the forward problem with a conjugate gradient method.

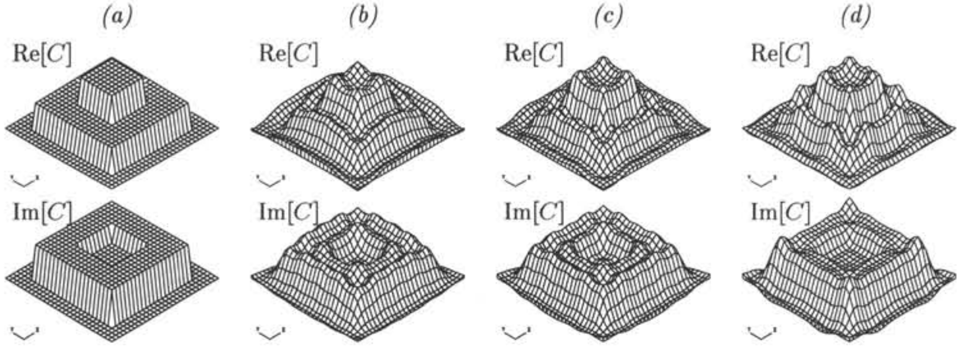

Figure 8. The original profile *(a)* and the reconstructed profiles after *(b)* 16 iterations, *(c)* 32 iterations and *(d)* 64 iterations; without positivity (test domain $= 3\lambda \times 3\lambda$).

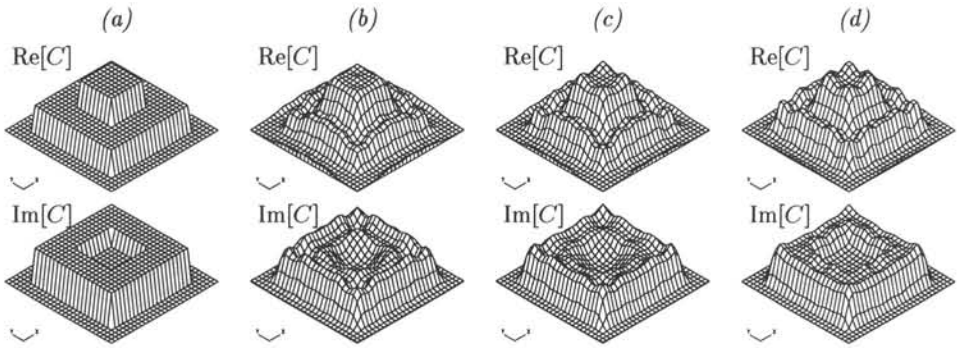

Figure 9. The original profile *(a)* and the reconstructed profiles after *(b)* 16 iterations, *(c)* 32 iterations and *(d)* 64 iterations; with positivity (test domain $= 3\lambda \times 3\lambda$).

We have further decreased the wavelength and we have also increased the material contrast. We have observed that the jumps $F(w_{j,n}) - F(w'_{j,n})$ in the error curves increase and that at some point no convergence is achieved. Even the scheme does not start properly, but jumps back and forth between two high values of the error measure. Roughly speaking we have observed that the method produces good reconstruction results when $kD < 4\pi$, where $k = 2\pi/\lambda$ is the wavenumber and D is the sidelength of our square test domain. This is less than the limit we have observed with the original modified gradient method, where Kleinman and Van den Berg (1993) have detected good reconstruction results when $kD < 6\pi$. At the other hand we have observed that we may increase the upper limit of reconstruction, by starting with the modified gradient method and performing a few iterations. This leads to some contrast profile and some approximate fields; subsequently we determine the approximate contrast sources by a simple multiplication. These contrast sources are taken as initial estimate for $w_{j,0}$ and we then run the present STIE scheme.

5. Conclusions

We have developed a new inversion scheme based on the source type of integral equations. The scheme excels in its simplicity and it yields surprisingly good reconstruction results. In any case the proposed method is a competitive candidate for the replacement of inversion and improvement of inversion schemes based on the first Born approximation approximation and/or backpropagation. In view of small amount of necessary computer time and computer memory a full three-dimensional implementation is feasible on the present-day computers (workstations).

Extension of the method to multi-frequency inversion (time-domain inversion) is straightforward; in each iteration, the data equation has to be minimized for each particular frequency (or time) and subsequently we require consistency in the local source/field relation for all source locations and frequencies (or time instants through a convolution). The dispersive behaviour (relaxation in time) of the material quantities should be known. After minimization of the error in the source/field relation, for all source locations and frequencies (time instants), we arrived at an approximate contrast and we can determine an update for the contrast sources.

Finally, it is noted that we can enhance the reconstruction by adding a penalty term to the source/field relations that takes into account some a priori information with respect to the contrast profile. A nonlinear constraint that minimizes the total variation of the contrast profile in the $L^1(\mathbb{D}^S)$-norm seems to be a good candidate (Van den Berg and Kleinman, 1995). It sharps the edges of the contrast profile significantly and in addition it diminishes the sensitivity to noisy data.

References

Brodlie, K.W., 1977, Unconstrained minimization, in The State of Art in Numerical Analysis, edited by D.A.H. Jacobs, Academic Press, New York, 255-257.

De Hoop, A.T., 1995, Handbook of Radiation and Scattering of Waves, Academic Press Limited, London.

Habashy, T.M, M.L.Oristaglio and A.T. de Hoop, 1994, Simultaneous nonlinear reconstruction of two-dimensional permittivity and conductivity, Radio Science, **29**, 1101–1118.

Kleinman, R.E., and P.M. van den Berg, 1993 An extended range modified gradient technique for profile inversion, Radio Science, **28**, 877-884.

Kleinman, R.E., and P.M. van den Berg, 1994, Two-dimensional location and shape reconstruction, Radio Science, **29**, 1157–1169.

Press, W.H., B.P. Flannery, S.A. Teukolsky and W.T. Vetterling, 1986, Numerical Recipes, The art of Scientific Computing, Cambridge Unversity Press, New York, 305–306.

Van den Berg, P.M., and R.E. Kleinman, 1995, A total variation enhanced modified gradient algorithm for profile reconstruction, Inverse Problems, **11**, L5-L10.

4D Geophysical Monitoring as an Application of the Reciprocity Theorem

Jacob T. Fokkema and **Peter M. van den Berg**
Centre for Technical Geoscience,
Delft University of Technology, Delft, the Netherlands

Abstract

4D Geophysical monitoring is gaining interest to characterize changes in the subsurface. These changes are important in the understanding of dynamic geological processes such as, e.g., the effect of gas and oil extraction and the in-situ stress changes. In order to quantify the differences in measurements we propose a method based on the reciprocity formulation. We arrive at a representation of the difference measurements in terms of the change of medium parameters in the factual contrast domain. This formulation leads to a method to handle prestack 4D imaging and using a (distorted) Born approximation a way to perform a linearized inversion.

1. Introduction

Seismic imaging is concerned with the use of sound waves to delineate contrast in the medium parameters. Then following the standard analysis this contrast is associated with changes in the geological structure of the subsurface. The oil industry has successfully used this technique to delineate oil and gas fields. In the same spirit induced changes in the subsurface geology can also be detected if they can be related to a change in the medium parameters. However this is only true if the time rate of change is happening on a time scale which is much larger than the experiment time of a standard seismic survey. The seismic activity associated with this type of diagnosis is known as 4D seismics or time-lapse seismics. In the spring of 1996, the chairman and chief executive of Schlumberger, Mr. E. Baird, announced that the productivity of existing oil fields could be boosted from a recovery rate of 35% to a recovery rate of 50%. In this context, Mr. Baird (Corzine, 1996) was hinting at an application of the 4D seismic technology by stating that the key to achieve such gain would be a more accurate seismic image with the ability to monitor in real time the fluid movements within the oil reservoirs. The idea of monitoring this kind of changes originates from Nur *et al.* (1984) who observed significant changes in the compressional wave speed in cores saturated with heavy oil as a function of the ambient temperature. From this observation he conjectured that seismic techniques could be used to monitor the thermal effect of injected steam to enhance the oil recovery of a reservoir. Today we can confirm that Nur's conjecture is a viable option in reservoir management (Lumley, 1995, and Lee, 1996). Not only thermal effects on wave propagation can be monitored. Cruts *et al.* (1995) showed that induced stress in reservoir rock changes the anisotropy of rock parameters. This study is important for the gas-producing fields in the Northern part of the Netherlands. The hydrostatic pressure drop in the reservoir due to gas production induces the subsidence and triggers small earth quakes. In this case 4D seismics could be used to forecast the stress-build up in the medium and its geological consequences.

Up to this point the results of the 4D experiment have been employed to produce a difference dataset from the survey at the start and the one after a certain time span (see for example Lumley, 1995). Then from this difference conclusions are drawn with respect to the medium change. In this paper we show how this difference is related to the restricted area where the changes occur using the reciprocity theorem. Moreover this formulation allows us to connect the two observations in an algorithmic fashion which makes it possible to handle 4D prestack imaging and to formulate an inversion approach based on the (distorted) Born approximation, or on a more sophisticated nonlinear inversion scheme.

2. Application of the field reciprocity theorem

In all reciprocity theorems two field states are distinguished. These states can be completely different, although they share the same spatial domain ($\mathbb{D}$) of application and they are related via an interaction quantity. The boundary surface of $\mathbb{D}$ is denoted by $\partial\mathbb{D}$ with the normal vector ν_k (see Figure 1). This reciprocity theorem is known (De Hoop, 1995) as Rayleigh's theorem for acoustic waves in fluids, Betti's theorem for elastic waves, and Lorentz' theorem for electromagnetic waves. All these theorems can be written in generic form

$$\begin{aligned}\int_{\boldsymbol{x}\in\partial\mathbb{D}} &[\text{Interaction of the Field states}]_k\,\nu_k\,\mathrm{dA}\\ &= \int_{\boldsymbol{x}\in\mathbb{D}}[\text{Interaction of the Field and Material states}]\,\mathrm{dV}\\ &\qquad + \int_{\boldsymbol{x}\in\mathbb{D}}[\text{Interaction of the Field and Source states}]\,\mathrm{dV}\,, \qquad (1)\end{aligned}$$

where $\boldsymbol{x}$ denotes the position vector in space.

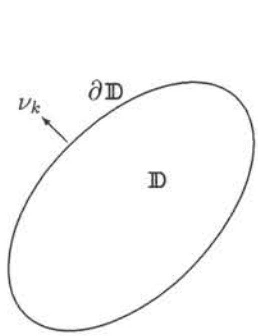

Figure 1. Configuration for the application of the reciprocity theorem.

Table 1. Acoustic states

	State A	State B
Field state	pressure, particle velocity	pressure, particle velocity
Material state	mass density, compressibility	mass density, compressibility
Source state	volume density of injection rate volume density of volume force	volume density of injection rate volume density of volume force

In order to keep the notation as lucid as possible, we restrict ourselves to the acoustic isotropic wavefield problem with the fundamental first-order equations in the Laplace-transformed domain with s as Laplace parameter,

$$\partial_k \hat{p} + s\rho \hat{v}_k = \hat{f}_k \,, \tag{2}$$

$$\partial_k \hat{v}_k + s\kappa \hat{p} = \hat{q} \,, \tag{3}$$

where $\hat{p} = \hat{p}(\boldsymbol{x}, s)$ is the pressure, $\hat{v}_k = \hat{v}_k(\boldsymbol{x}, s)$ is the particle velocity, $\rho = \rho(\boldsymbol{x})$ is the mass density, $\kappa = \kappa(\boldsymbol{x})$ is the compressibility, $\hat{f}_k = \hat{f}_k(\boldsymbol{x}, s)$ is the volume density of volume force, and $\hat{q} = \hat{q}(\boldsymbol{x}, s)$ is the volume density of injection rate. Using these states (see Table 1) in the generic form of (1) leads to (Fokkema and Van den Berg, 1993)

$$\begin{aligned}\int_{\boldsymbol{x}\in\partial\mathbb{D}} & (\hat{p}^A \hat{v}_k^B - \hat{p}^B \hat{v}_k^A)\nu_k \mathrm{dA} \\ &= \int_{\boldsymbol{x}\in\mathbb{D}} [s(\rho^B - \rho^A)\hat{v}_k^A \hat{v}_k^B - s(\kappa^B - \kappa^A)\hat{p}^A \hat{p}^B]\mathrm{dV} \\ &\quad + \int_{\boldsymbol{x}\in\mathbb{D}} (\hat{f}_k^A \hat{v}_k^B + \hat{q}^B \hat{p}^A - \hat{f}_k^B \hat{v}_k^A - \hat{q}^A \hat{p}^B)\mathrm{dV} \,. \end{aligned} \tag{4}$$

It is noted that Lord Rayleigh (1894) denotes this theorem as Helmholtz' theorem. The first integral on the right-hand side of (4) vanishes in case the material states are the same. Under these conditions, the interaction between the two states is only related to the source distributions in the two states. If, in addition, these source distributions vanish in some domain, the relevant interactions are zero in that domain.

The particular choice of the two states is dictated by the application. Some of them are well-known. In most cases, only the source states differ. In this context, we mention the direct-source problem (forward modeling), wavefield decomposition, deghosting and the inverse-source problem. In other cases, also the material states differ. As examples we mention the direct- and inverse-scattering problems (formulation through contrast sources). In these applications, one state represents the actual situation, while the other is a judiciously chosen auxiliary (computational) state. The power of the reciprocity theorem is well illustrated in the removal of surface-related wave phenomena in marine seismics (Fokkema and Van den Berg, 1993). In the latter case the two states are the actual state and a desired state. Another possibility is to cope with two actual states, for example transmitter-receiver reciprocity. This situation is often denoted as physical reciprocity and is connected with the common view of reciprocity. This application is characterized by the difference in the source states.

The present problem of 4D geophysical monitoring is also formulated through the reciprocity theorem, in which again two actual states occur, however now the material states differ. The change of the material state has occurred after that some time has elapsed.

3. Non-interacting 4D geophysical monitoring

To distinguish between the two time instants of observation we use the superscript $^{(1)}$ to denote the acoustic quantities at the first time, $t = t_1$, while we use the superscript $^{(2)}$ to denote the quantities at the second time $t = t_2 > t_1$. We assume that the sources that generate the acoustic wavefield do not change. For the simplicity of the discussion, we further assume that there is no contrast in the mass density. Then, the two acoustic wavefields satisfy

$$\partial_k \hat{p}^{(1,2)} + s\rho \hat{v}_k^{(1,2)} = \hat{f}_k \,, \tag{5}$$

$$\partial_k \hat{v}_k^{(1,2)} + s\kappa^{(1,2)} \hat{p}^{(1,2)} = \hat{q} \,. \tag{6}$$

We further define a Green's (computational) state. This is the acoustic wavefield from a point source of volume injection in an embedding medium with mass density ρ and compressibility κ and satisfies

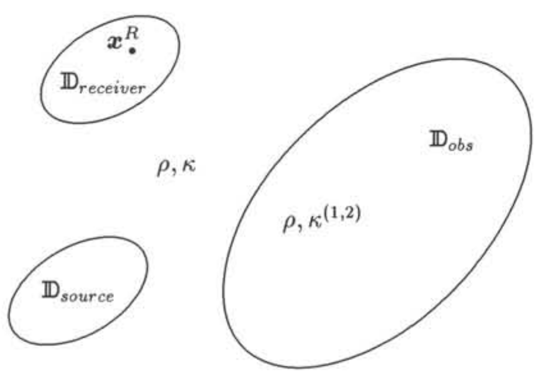

Figure 2. The observation, the source and receiver domains.

Table 2. States in the reciprocity theorem

	State A (actual state)	State B (volume-injection Green's state)
Field state	$\{\hat{p}^{(1,2)}, \hat{v}_k^{(1,2)}\}(\boldsymbol{x}, s)$	$\{\hat{p}^q, \hat{v}_k^q\}(\boldsymbol{x}\vert\boldsymbol{x}^R, s)$
Material state	$\{\rho, \kappa^{(1,2)}\}(\boldsymbol{x})$	$\{\rho, \kappa\}(\boldsymbol{x})$
Source state	$\{\hat{q}, \hat{f}_k\}(\boldsymbol{x}, s)$	$\{\hat{q}^B(s)\delta(\boldsymbol{x}-\boldsymbol{x}^R), 0\}$
Domain $\mathbb{R}^3$ (see Figure 2)		

$$\partial_k \hat{p}^q + s\rho \hat{v}_k^q = 0\,, \tag{7}$$

$$\partial_k \hat{v}_k^q + s\kappa \hat{p}^q = \hat{q}^B \delta(\boldsymbol{x}-\boldsymbol{x}^R)\,, \tag{8}$$

where $\delta(\boldsymbol{x}-\boldsymbol{x}^R)$ denotes the three-dimensional spatial Dirac distribution operative at the receiver point with position vector $\boldsymbol{x}^R$, while $\hat{q}^B$ is an arbitrary constant only depending on s.

We apply the reciprocity theorem of (4). To this end, State A is taken to be either the actual state at $t = t_1$ or $t = t_2$, while State B is taken to be the Green's state (cf. Table 2). The theorem is is applied to the domain interior to the sphere S_Δ with radius Δ and center at the origin of the chosen coordinate system; Δ is so large that S_Δ completely surrounds $\mathbb{D}_{source}$, $\mathbb{D}_{receiver}$ and $\mathbb{D}_{obs}$ (see Figure 2). In view of the causality condition the integral over S_Δ vanishes. Hence, we have

$$\begin{aligned} 0 = &-\int_{\boldsymbol{x}\in\mathbb{D}_{obs}} s(\kappa-\kappa^{(1,2)})\hat{p}^{(1,2)}\hat{p}^q \mathrm{dV} \\ &+\int_{\boldsymbol{x}\in\mathbb{D}_{source}} (\hat{f}_k \hat{v}_k^q - \hat{q}\hat{p}^q)\mathrm{dV} + \int_{\boldsymbol{x}\in\mathbb{D}_{receiver}} \hat{q}^B \delta(\boldsymbol{x}-\boldsymbol{x}^R)\hat{p}^{(1,2)}\mathrm{dV}\,. \end{aligned} \tag{9}$$

The right-hand side of this equation learns that at the time instants t_1 and t_2 the total wavefield (the third term) is related to the scattered wavefield due to the contrast with respect to the embedding (the first term) and the incident wavefield (the second term) which is the same for both instants. Then subtracting the result for time t_1 from the result for t_2 we end up with

$$\hat{q}^B[\hat{p}^{(2)}(\boldsymbol{x}^R, s) - \hat{p}^{(1)}(\boldsymbol{x}^R, s)] = -\int_{\boldsymbol{x}\in\mathbb{D}_{obs}} [s(\kappa^{(2)}-\kappa)\hat{p}^{(2)}\hat{p}^q - s(\kappa^{(1)}-\kappa)\hat{p}^{(1)}\hat{p}^q]\mathrm{dV}\,. \tag{10}$$

Note that in the left-hand side of (10) the measured difference in the acoustic pressure occurs. A similar expression for the differences in the particle velocities is arrived at by taking a volume-force Green's state. We do not elaborate on this, because it does not contribute to the present discussion on 4D technology.

3.1. Distorted Born approximation

When we assume that the changes in the material properties during the time interval $[t_1, t_2]$ are small, we may assume that

$$\hat{p}^{(2)}(\boldsymbol{x}, s) = \hat{p}^{(1)}(\boldsymbol{x}, s), \quad \text{when } \boldsymbol{x} \in \mathbb{D}_{obs} . \tag{11}$$

This has the consequence that (10) simplifies to

$$\hat{q}^B[\hat{p}^{(2)}(\boldsymbol{x}^R, s) - \hat{p}^{(1)}(\boldsymbol{x}^R, s)] = -\int_{\boldsymbol{x}\in\mathbb{D}_{2-1}} s(\kappa^{(2)} - \kappa^{(1)})\hat{p}^{(1)}(\boldsymbol{x}, s)\hat{p}^q(\boldsymbol{x}|\boldsymbol{x}^R, s)]\mathrm{dV} . \tag{12}$$

We observe that due this choice the domain integral on the right-hand side of (12) has reduced to the domain of the factual change in contrast, D_{2-1} (see Figure 3). Although it seems from (12) that the Born approximation has only been made in the domain D_{2-1}, it is stressed that the approximation is made over the larger domain D_{obs}. This limits the validity of (12) seriously. The validity of the approximation depends on the choice of the embedding through $\hat{p}^q$, which seems arbitrary. This suggests that there exists an optimal choice for the embedding, which will be the subject of the next section.

4. Interacting monitoring

In order to eliminate the ambiguity of the embedding we now follow a different approach in which we make optimal use of the power of the reciprocity theorem. In a reciprocity theorem two states interact. Since the embedding is the same at the two

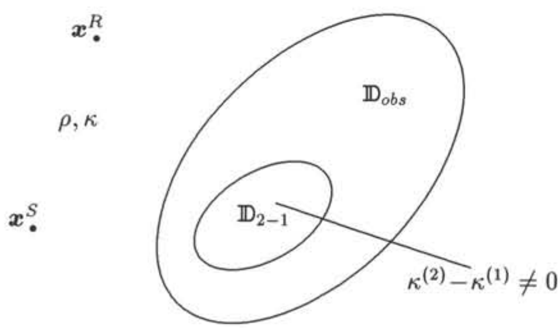

Figure 3. The domain of factual change in contrast.

Table 3. States in the reciprocity theorem

	State A (actual state at $t = t_1$)	State B (actual state at $t = t_2$)
Field state	$\{\hat{p}^{(1)}, \hat{v}_k^{(1)}\}(\boldsymbol{x}\|\boldsymbol{x}^S, s)$	$\{\hat{p}^{(2)}, \hat{v}_k^{(2)}\}(\boldsymbol{x}\|\boldsymbol{x}^R, s)$
Material state	$\{\rho, \kappa^{(1)}\}(\boldsymbol{x})$	$\{\rho, \kappa^{(2)}\}(\boldsymbol{x})$
Source state	$\{\hat{q}^{(1)}(s)\delta(\boldsymbol{x}-\boldsymbol{x}^S), 0\}$	$\{\hat{q}^{(2)}(s)\delta(\boldsymbol{x}-\boldsymbol{x}^R), 0\}$
Domain $\mathbb{R}^3$ (see Figure 3)		

time instants we choose the actual wavefields as the interacting quantities. To this end, State A is associated with the actual wavefield at $t = t_1$ and State B is associated with the actual wavefield at $t = t_2$ (see Table 3). In order to simplify the analysis we only consider point sources of the volume-injection type. The source of State A, situation (1), is taken at $\boldsymbol{x} = \boldsymbol{x}^S$, while the source of State B, situation (2), is taken at $\boldsymbol{x} = \boldsymbol{x}^R$. Then, the reciprocity theorem (4) is applied to the domain interior to the sphere S_Δ with radius Δ and center at the origin of the chosen coordinate system; Δ is so large that S_Δ completely surrounds $\boldsymbol{x}^S$, $\boldsymbol{x}^R$ and $\mathbb{D}_{obs}$ (see Figure 3). In view of the causality condition the integral over S_Δ vanishes. Hence, we have

$$
\begin{aligned}
0 = &-\int_{\boldsymbol{x}\in\mathbb{D}_{2-1}} s(\kappa^{(2)}-\kappa^{(1)})\hat{p}^{(1)}\hat{p}^{(2)}\mathrm{dV} \\
&+\int_{\boldsymbol{x}\in\mathbb{R}^3}[\hat{q}^{(2)}\delta(\boldsymbol{x}-\boldsymbol{x}^R)\hat{p}^{(1)}(\boldsymbol{x}|\boldsymbol{x}^S, s) - \hat{q}^{(1)}\delta(\boldsymbol{x}-\boldsymbol{x}^S)\hat{p}^{(2)}(\boldsymbol{x}|\boldsymbol{x}^R, s)]\mathrm{dV}\,. \quad (13)
\end{aligned}
$$

Next we use physical reciprocity. This reciprocity is obtained from the theorem (4) by interacting the actual wavefields at $t = t_2$ from a source at $\boldsymbol{x} = \boldsymbol{x}^S$ (State A) and at $\boldsymbol{x} = \boldsymbol{x}^R$ (State B). The result is simply given as

$$
\hat{p}^{(2)}(\boldsymbol{x}^S|\boldsymbol{x}^R, s) = \hat{p}^{(2)}(\boldsymbol{x}^R|\boldsymbol{x}^S, s)\,. \quad (14)
$$

Using this physical reciprocity, we obtain

$$
\begin{aligned}
&\hat{q}^{(1)}\hat{p}^{(2)}(\boldsymbol{x}^R|\boldsymbol{x}^S, s) - \hat{q}^{(2)}\hat{p}^{(1)}(\boldsymbol{x}^R|\boldsymbol{x}^S, s) \\
&\qquad = -\int_{\boldsymbol{x}\in\mathbb{D}_{2-1}} s(\kappa^{(2)}-\kappa^{(1)})\hat{p}^{(1)}(\boldsymbol{x}|\boldsymbol{x}^S, s)\hat{p}^{(2)}(\boldsymbol{x}|\boldsymbol{x}^R, s)]\mathrm{dV}\,. \quad (15)
\end{aligned}
$$

Note that in the left-hand side of (15) the measured difference in the acoustic pressure occurs. Equation (15) is an exact representation of the difference wavefield. When we compare this result with the approximation of (12) we conclude that apparently the optimal choice of the embedding has been achieved. Hence, the representation of (12) is not a viable option. Further, (15) suggests how to handle prestack 4D imaging. In prestack 3D imaging as advocated by Berkhout (1982), the upgoing measured wavefield is depropagated to a chosen depth level. Then this result is correlated with the downgoing source wavefield at the same depth level to obtain the reflection operator in the one-way sense. Extrapolating this procedure to the 4D case, it means that the measured wavefield at $t = t_2$ is depropagated to the domain D_{2-1}, while the upgoing wavefield at $t = t_1$ is converted to a downgoing wavefield. Then, correlation of the the two wavefields in D_{2-1} leads to an image of the factual change in contrast between the two time instants. Note that this method needs an identical full seismic acquisition at the two time instants. Since the domain D_{2-1} of factual change in contrast is small compared to the intended coverage of the seismic acquisition as well as the factual changes in contrast are small, at $t = t_2$, we can suffice with such an acquisition technique that covers only the domain of interest, viz., the domain D_{2-1}. This means that the second acquisition focuses on D_{2-1}. Another advantage of the small changes in parameters is that we may employ a simpler linearized inversion method based on the Born approximation.

4.1. Born approximation

As before we assume that the changes in the material properties during the time interval $[t_1, t_2]$ are small, consequently we may assume that

$$\hat{p}^{(2)}(\boldsymbol{x}|\boldsymbol{x}^R, s) = \hat{p}^{(1)}(\boldsymbol{x}|\boldsymbol{x}^R, s), \quad \text{when } \boldsymbol{x} \in \mathbb{D}_{2-1}\,, \tag{16}$$

if $\hat{q}^{(1,2)} = \hat{q}$. Note that in this case unlike the situation in (11) the assumption has to be valid *only* in the domain of factual changing of the contrast, viz. in D_{2-1}. This has the consequence that (15) simplifies to

$$\hat{q}[\hat{p}^{(2)}(\boldsymbol{x}^R|\boldsymbol{x}^S, s) - \hat{p}^{(1)}(\boldsymbol{x}^R|\boldsymbol{x}^S, s)] = -\int_{\boldsymbol{x}\in\mathbb{D}_{2-1}} s(\kappa^{(2)} - \kappa^{(1)})\hat{p}^{(1)}(\boldsymbol{x}|\boldsymbol{x}^S, s)\hat{p}^{(1)}(\boldsymbol{x}|\boldsymbol{x}^R, s)\mathrm{dV}. \tag{17}$$

When the wavefields in D_{2-1} at $t = t_1$ are determined, an optimization scheme determines the change of the material parameters and its supporting domain D_{2-1} from the difference measurements. We observe that (17) is a linear equation for the factual change in parameters. In fact, this procedure constitutes the linearized form of the inversion problem.

4.2. Nonlinear inversion

In case the Born approximation cannot be made, we have to fall back on a nonlinear inversion scheme. The modified gradient method (Kleinman and Van den Berg, 1992) is a candidate, since it has given definite evidence of its effectiveness of profile reconstruction from experimental data (Van den Berg *et al.*, 1995). In this method we distinguish between a data equation and an object equation. Although we can carry out the following analysis for the general case of different source wavelets, for simplicity we restrict ourselves to the case of equal sources, i.e, $\hat{q}^{(1,2)} = \hat{q}$. The data equation is given by, cf. (15),

$$\hat{q}[\hat{p}^{(2)}(\boldsymbol{x}^R|\boldsymbol{x}^S,s)-\hat{p}^{(1)}(\boldsymbol{x}^R|\boldsymbol{x}^S,s)] = -\int_{\boldsymbol{x}\in\mathbb{D}_{2-1}} s(\kappa^{(2)}-\kappa^{(1)})\hat{p}^{(1)}(\boldsymbol{x}|\boldsymbol{x}^S,s)\hat{p}^{(2)}(\boldsymbol{x}|\boldsymbol{x}^R,s)\mathrm{dV}, \tag{18}$$

when $\boldsymbol{x}^R$ is chosen in the domain of observation. The left-hand side of (18) represents the known measured data. To make the nonlinear inversion scheme operational we require consistency inside the domain D_{2-1}. To this end we move the source point $\boldsymbol{x}^S$ inside this domain and rename this point as $\boldsymbol{x}'$. Then, using physical reciprocity again, this object equation is given by

$$\hat{q}\hat{p}^{(1)}(\boldsymbol{x}'|\boldsymbol{x}^R,s) = \hat{q}\hat{p}^{(2)}(\boldsymbol{x}'|\boldsymbol{x}^R,s) + \int_{\boldsymbol{x}\in\mathbb{D}_{2-1}} s(\kappa^{(2)}-\kappa^{(1)})\hat{p}^{(1)}(\boldsymbol{x}|\boldsymbol{x}',s)\hat{p}^{(2)}(\boldsymbol{x}|\boldsymbol{x}^R,s)\mathrm{dV}\,, \tag{19}$$

The left-hand side of (19) represents the known wavefield in the initial state with source position at $\boldsymbol{x} = \boldsymbol{x}^R$. The data equation and object equation represent two systems of equations from which the unknown wavefield $\hat{p}^{(2)}(\boldsymbol{x}|\boldsymbol{x}^R)$, $\boldsymbol{x} \in D_{2-1}$, and the factual change $\kappa^{(2)}-\kappa^{(1)}$ in $\mathcal{D}_{2-1}$ are determined simultaneously with the modified gradient method.

At this point it is worth to investigate the conditions under which the object equation can be solved using a Neumann-series solution, with the Born approximation as the first term, as a possible extension of De Hoop's proof (De Hoop, 1991) that, for the special case of a homogeneous embedding and limited contrast, the Neumann iterative solution of the integral equation converges for all real and positive values of s independent of the size of the contrasting domain. If this is the case, one can use the simple update directions used in over-relaxation methods, i.e, in each iteration the update direction for the wavefield is simply taken to be the residual error of (19).

5. Conclusions

In this paper we have argued that the reciprocity theorem can serve as an important instrument to study the interaction of different wavefield states that can occur in the same domain of space. In this respect we have followed our learned teacher Professor Adrianus T. de Hoop who has shown that in the electromagnetic, elastodynamic and acoustic case this approach leads to a valuable tool for the solution of wavefield problems.

In this paper we have focused on the use of the theorem in time-lapse problems, where the objectives are to monitor the change of medium parameters in time. We have simplified the discussion by restricting ourselves to the acoustic case. We have shown that starting from the reciprocity theorem an operational expression can be obtained for the difference in the measurements at the two time instants in terms of the difference in medium parameters and wavefields in the factual domain of change.

In our formulation we have shown that the determination of the difference in medium parameters leads to a nonlinear problem, assuming that we know the parameters and the wavefield in the initial state. If the change in medium parameters is small we can rely on the Born approximation in the domain of factual change. In this way we have linearized the inversion problem. When we want to make this Born approximation it is necessary that the measurements at the two time instants are exactly carried out in the same fashion.

When the Born approximation cannot be made we have to fall back on the nonlinear relations. In that case the data equation has to be supplemented with the object equation in order to guarantee consistency of the solution in the factual domain of contrast.

Finally we remark that the validity of the consequences of our 4D formulation, although formulated for the acoustic case, are equally valid for the electromagnetic and elastodynamic case.

References

Cruts, H.M.A., J. Groenenboom, A.J.W. Duijndam and J.T. Fokkema, 1995, Experimental verification of stress-induced anisotropy, Expanded Abstracts of Society of Exploration Geophysicists, 65th Annual Meeting, Houston, 894-897.

Berkhout, A.J., 1982, Seismic Migration: Imaging of Acoustic Energy by Wave Field Extrapolation. A. Theoretical Aspects, Elsevier, Amsterdam , 351 pp.

Corzine, R., 1996, New technology 'to bring boost in oil production', Financial Times, London, April 9.

De Hoop, A.T., 1991, Convergence criterion for the time-domain iterative Born approximation to scattering by an inhomogeneous, dispersive object, Journal of the Optical Society of America, **A8**, 1256-1260.

De Hoop, A.T., 1995, Handbook of Radiation and Scattering of Waves, Academic Press Limited, London.

Fokkema, J.T., and P.M. van den Berg, 1993, Seismic Applications of Acoustic Reciprocity, Elsevier, Amsterdam, 350 pp.

Kleinman, R.E., and P.M. van den Berg, 1992, A modified gradient method for two-dimensional problems in tomography, Journal of Computational and Applied Mathematics, **42**, 17-35.

Lee, D.S., 1996, Integrated seismic study for thermal monitoring, Journal of Seismic Exploration, **5**, 5-18.

Lord Rayleigh (J.W. Strutt), 1894, Theory of Sound, Macmillan, London; Dover, New York, 1945, vol. II, 145-147.

Lumley, D.E., 4D seismic monitoring of an active steamflood, 1995, Expanded Abstracts of Society of Exploration Geophysicists, 65th Annual Meeting, Houston, 203-206.

Nur, A., C. Tosaya and D. V-Thanh, 1984, Seismic monitoring of thermal enhanced oil recovery processes, Expanded Abstracts of Soc. of Expl. Geophysicists, 65th Annual Meeting, Washington DC, 118-121.

Van den Berg, P.M., M.G.Coté and R.E. Kleinman, 1995, "Blind" shape reconstruction from experimental data, IEEE Transactions on Antennas and Propagation, **43**, 1389-1396.

The Principle Role of Common Focus Point Gathers in Seismic Imaging

A.J. Berkhout

Laboratory of Seismic and Acoustics, Faculty of Applied Physics
Centre for Technical Geoscience, Delft University of Technology
P.O. Box 5046, 2600 GA Delft, the Netherlands

Abstract

The common focus point (CFP) gather is introduced and it is shown that this gather plays a key role in the imaging process of primary and multiple reflection energy.

1. Introduction

State-of-the-art seismic imaging technology assumes measurements of *primary* wavefields (P_0) for the extraction of subsurface reflection information (R^+). This means that in current imaging algorithms the relationship between the downgoing primary source wavefields (S^+) and the upgoing primary reflected wavefields (P_0^-) are estimated at each subsurface gridpoint (Figure 1a).

However, if measurements of the *multiple* wavefields are available as well (by applying a primary-multiple decomposition algorithm prior to imaging), new and independent reflection information can be obtained. If we consider multiple wavefields (M^-) for the extraction of reflection information, then the incident wave field for each reflector consists of the *total* (primaries + multiples) wavefield (P). We will distinguish two different situations for the multiple situation:

- The incident wavefield is *downgoing* (P^+) and the extracted reflection information is thus R^+ information;
- The incident wavefield is *upgoing* (P^-) and the extracted reflection information is thus R^- information.

In this paper we will consider both situations and we will compare them with the familiar primary case. Here we will present the problem from a *gridpoint* point of view, which makes the formulation consistent with the double focusing formulation (Berkhout, 1996; Berkhout and Verschuur, 1996).

2. Aiming for $\mathbf{R}^+$ with primary wavefields

The model for primary reflections at the acquisition surface z_0, being caused by the interference of downgoing source wavefields with inhomogeneities at depth level ($z_m = z_m^-$), is given by

$$\mathbf{\Delta P}_0(z_0) = \mathbf{D}^-(z_0)[\mathbf{W}^-(z_0, z_m)\mathbf{R}^+(z_m)\mathbf{W}^+(z_m, z_0)]\mathbf{S}^+(z_0) \tag{1}$$

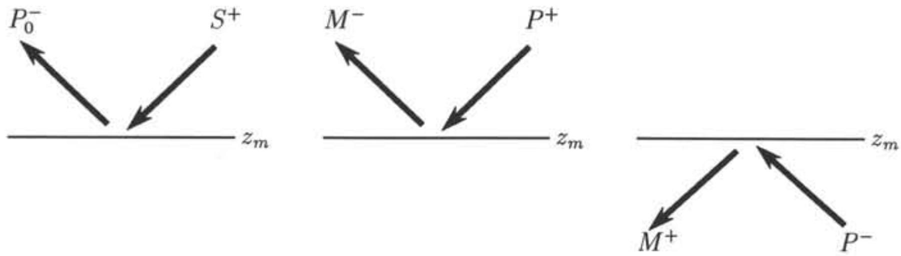

(a) $P_0^- = R^+S^+$ *(b)* $M^- = R^+P^+$ *(c)* $M^+ = R^-P^-$

Figure 1. Reflection information in primary (a) and multiple wavefields (b,c).

or

$$\mathbf{\Delta P}_0^-(z_0) = \mathbf{W}^-(z_0, z_m)\mathbf{R}^+(z_m)\mathbf{S}^+(z_m, z_0), \tag{2}$$

where

$$\mathbf{S}^+(z_m, z_0) = \mathbf{W}^+(z_m, z_0)\mathbf{S}^+(z_0). \tag{3}$$

First, let us consider the expression for all *downgoing* wavefields that are incident to gridpoint $(\vec{x}_j, z_m)$:

$$\vec{S}_j^+(z_m, z_0) = \vec{W}_j^+(z_m, z_0)\mathbf{S}^+(z_0), \tag{4}$$

where $\vec{W}_j^+(z_m, z_0)$ defines a row vector that represents the j^{th} row of propagation matrix $\mathbf{W}^+(z_m, z_0)$. Note that expression (4) formulates forward wavefield extrapolation from *all* individual source positions at the surface to *one* gridpoint position in the subsurface.

Next, let us also consider the expression for all *upgoing* primary wave fields that are emerging from the same gridpoint $(\vec{x}_j, z_m)$:

$$\Delta\vec{P}_j^-(z_m, z_0) = \vec{F}_j^-(z_m, z_0)\mathbf{\Delta P}_0(z_0), \tag{5}$$

where the vector $\vec{F}_j^-(z_m, z_0)$ represents the j^{th} row of the inverse of $\mathbf{D}^-(z_0)\mathbf{W}^-(z_0, z_m)$. In practice we generally choose for this inverse a scaled version of $[\mathbf{W}^-]^H$. Note that expression (5) formulates inverse wavefield extrapolation from *all* source-related detector positions at the surface to one gridpoint position in the subsurface. Hence, the row vector $\vec{F}_j^-(z_m, z_0)$ is the detector-related focusing operator for gridpoint $(\vec{x}_j, z_m)$ and $\Delta\vec{P}_j^-(z_m, z_0)$ is the focus point response in Common Focus Point (CFP) gather $\vec{P}_j^-(z_m, z_0)$.

The incident wavefield vector $\vec{S}_j^+$ and the reflected wavefield vector $\Delta\vec{P}_j^-$ are related via the gridpoint-oriented reflection coefficient matrix (Figure 2):

$$\Delta\vec{P}_j^-(z_m, z_0) = \tilde{\mathbf{R}}_j^+(z_m)\vec{S}_j^+(z_m, z_0), \tag{6}$$

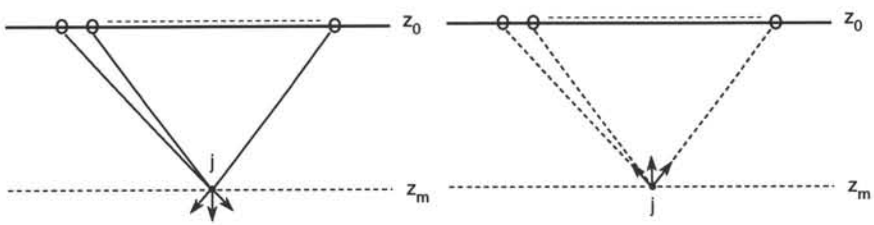

(a) $S_j^+(z_m, z_0)$ *(b)* $\Delta P_j^-(z_m, z_0)$

Figure 2. The incident wavefields (a) and the reflected wavefields (b) at the subsurface gridpoint $(\vec{x}_j, z_m)$.

$\tilde{\mathbf{R}}_j^+(z_m)$ being a diagonal matrix that contains the angle-dependent reflection coefficient of gridpoint $(\vec{x}_j, z_m)$. Under practical conditions the reflection coefficients need be estimated by minimizing the difference between the "measured" CFP gather and the modeled gridpoint response:

$$\vec{P}_j^-(z_m, z_0) - \tilde{\mathbf{R}}_j^+(z_m)\vec{S}_j^+(z_m, z_0) \;=\; minimum. \tag{7}$$

3. Aiming for $\mathbf{R}^+$ with multiple wavefields

The model for multiple reflections at acquisition surface z_0, being generated by the interference of *downgoing* total wavefields with inhomogeneities at depth level z_m ($z_m = z_m^-$), is given by

$$\mathbf{\Delta M}(z_0) = \mathbf{D}^-(z_0)[\mathbf{W}^-(z_0, z_m)\mathbf{R}^+(z_m)\mathbf{W}^+(z_m, z_0)]\mathbf{P}^+(z_0) \tag{8}$$

or

$$\mathbf{\Delta M}^-(z_0) = \mathbf{W}^-(z_0, z_m)\mathbf{R}^+(z_m)\mathbf{P}^+(z_m, z_0), \tag{9}$$

where

$$\mathbf{P}^+(z_m, z_0) = \mathbf{W}^+(z_m, z_0)\mathbf{P}^+(z_0). \tag{10}$$

First, let us consider for this situation (see Figure 1b) the expression for all downgoing total wavefields that are incident to gridpoint $(\vec{x}_j, z_m)$:

$$\vec{P}_j^+(z_m, z_0) = \vec{W}_j^+(z_m, z_0)\mathbf{P}^+(z_0), \tag{11}$$

where

$$\mathbf{P}^+(z_0) = \mathbf{R}^-(z_0)\mathbf{P}^-(z_0). \tag{12}$$

Next, let us also consider the expression for all *upgoing* wave fields that are emerging from gridpoint $(\vec{x}_j, z_m)$:

$$\Delta\vec{M}_j^-(z_m, z_0) = \vec{F}_j^-(z_m, z_0)\mathbf{\Delta M}(z_0). \tag{13}$$

Note that, similar to (5), expression (13) formulates focusing in detection, the focus point being $(\vec{x}_j, z_m)$.

Now, the incident wavefield vector $\vec{P}_j^+$ and the reflected wavefield vector $\vec{M}_j^-$ are related according to

$$\Delta\vec{M}_j^-(z_m, z_0) = \tilde{\mathbf{R}}_j^+(z_m)\vec{P}_j^+(z_m, z_0). \tag{14}$$

Under practical conditions the reflection coefficients need be estimated by minimizing the difference between the two "measured" CFP gathers:

$$\vec{M}_j^-(z_m, z_0) - \tilde{\mathbf{R}}_j^+(z_m)\vec{P}_j^+(z_m, z_0) = \ minimum. \tag{15}$$

4. Aiming for $\mathbf{R}^-$ with multiple wavefields

The model for multiple reflections at acquisition surface z_0, being generated by the interference of *upgoing* total wavefields with inhomogeneities at depth level z_m ($z_m = z_m^+$), is given by

$$\mathbf{\Delta M}(z_0) = \mathbf{D}^-(z_0)[\mathbf{X}_0(z_0, z_m)\mathbf{R}^-(z_m)\mathbf{F}^-(z_m, z_0)]\mathbf{P}(z_0) \tag{16}$$

or

$$\mathbf{\Delta M}^-(z_0) = \mathbf{X}_0(z_0, z_m)\mathbf{R}^-(z_m)\mathbf{P}^-(z_m, z_0), \tag{17}$$

where $\mathbf{P}$ represents the total wavefield and

$$\mathbf{P}^-(z_m, z_0) = \mathbf{F}^-(z_m, z_0)\mathbf{P}(z_0). \tag{18}$$

First, let us consider for this situation (see Figure 1c) the expression for all *upgoing* total wavefields that are incident to gridpoint $(\vec{x}_j, z_m)$:

$$\vec{P}_j^-(z_m, z_0) = \vec{F}_j^-(z_m, z_0)\mathbf{P}(z_0). \tag{19}$$

Next, let us also consider the expression for all *downgoing* wavefields that are emerging from gridpoint $(\vec{x}_j, z_m)$:

$$\Delta\vec{M}_j^+(z_m, z_0) = \vec{F}_j(z_m, z_0)\mathbf{\Delta M}(z_0), \tag{20}$$

where row vector $\vec{F}_j(z_m, z_0)$ represents the j^{th} row of the inverse of $\mathbf{D}^-(z_0)\mathbf{X}_0(z_0, z_m)$. In practice we choose for this inverse a scaled version of $[\mathbf{X}_0]^H$.

The incident wavefield vector $\vec{P}_j^-$ and the reflected wavefield vector $\Delta\vec{M}_j^+$ are related according to

$$\Delta\vec{M}_j^+(z_m, z_0) = \tilde{\mathbf{R}}_j^-(z_m)\vec{P}_j^-(z_m, z_0). \tag{21}$$

Under practical conditions the reflection coefficients need be estimated by minimizing the difference between the two CFP gathers:

$$\vec{M}_j^+(z_m, z_0) - \tilde{\mathbf{R}}_j^-(z_m)\vec{P}_j^+(z_m, z_0) = \ minimum. \tag{22}$$

5. Conclusions

- Seismic imaging has been formulated for both primaries and multiples. In both formulations CFP gathers play a central role.

- For *primaries* the forward model is given by

$$\mathbf{P}_0(z_0) = \mathbf{D}^-(z_0) \sum_m \mathbf{W}^-(z_0, z_m)\mathbf{R}^+(z_m)\mathbf{S}^+(z_m, z_0), \tag{23}$$

  where $\mathbf{S}^+$ represents the downgoing source wavefield. The related imaging equation for gridpoint $(\vec{x}_j, z_m)$ is given by

$$\vec{P}_j^-(z_m, z_0) - \tilde{\mathbf{R}}_j^+(z_m)\vec{S}_j^+(z_m, z_0) = \ minimum. \tag{24}$$

- - For *multiples* the forward model with respect to *downward* illumination is given by

$$\mathbf{M}(z_0) = \mathbf{D}^-(z_0) \sum_m \mathbf{W}^-(z_0, z_m)\mathbf{R}^+(z_m)\mathbf{P}^+(z_m, z_0), \tag{25}$$

    where $\mathbf{P}^+$ represents the downgoing total wavefield. The related imaging equation for gridpoint $(\vec{x}_j, z_m)$ is given by

$$\vec{M}_j^-(z_m, z_0) - \tilde{\mathbf{R}}_j^+(z_m)\vec{P}_j^+(z_m, z_0) = minimum. \tag{26}$$

  - For *multiples* the forward model with respect to *upward* illumination is given by

$$\mathbf{M}(z_0) = \mathbf{D}^-(z_0) \sum_m \mathbf{X}_0(z_0, z_m)\mathbf{R}^-(z_m)\mathbf{P}^-(z_m, z_0), \tag{27}$$

    where $\mathbf{P}^-$ represents the upgoing total wavefield. The related imaging equation for gridpoint $(\vec{x}_j, z_m)$ is given by

$$\vec{M}_j^+(z_m, z_0) - \tilde{\mathbf{R}}_j^-(z_m)\vec{P}_j^-(z_m, z_0) = minimum. \tag{28}$$

    For $m = 0$ expression (27) addresses the surface-related multiples. For $m > 0$ expression (28) addresses the interbed multiples.

References

Berkhout, A.J., 1996, Pushing the limits of seismic imaging part I: migration in terms of dynamic focusing, accepted for publication in Geophysics.

Berkhout, A.J., and Verschuur, D.J., 1996, Estimation of multiple scattering by iterative inversion part I: theoretical aspects, accepted for publication in Geophysics.

Scientific Life and Work of Adrianus T. de Hoop from 1950 to 1996 and beyond

Hans Blok

Laboratory of Electromagnetic Research, Faculty of Electrical Engineering Delft University of Technology, P.O. Box 5031, 2600 GA Delft, the Netherlands

Abstract

For more than forty years Professor Dr. Adrianus T. de Hoop has been actively involved in teaching and research in electromagnetic, acoustic and elastodynamic fields and waves, and in applied mathematics. That lifetime of scientific activities brought him recognition as an excellent teacher, an eminent applied mathematician and a renowned expert on wave propagation. In this contribution, his outstanding contributions to teaching and wave-field science and the contributions of his research students are discussed within the framework of his views on scientific engineering.

1. Introduction

On December 31, 1996, Dr. Adrianus T. de Hoop will officially retire as Professor of Electromagnetic Theory and Applied Mathematics at Delft University of Technology. By then, he will have been actively involved in teaching and research in electromagnetic, acoustic and elastodynamic fields and waves, and in applied mathematics, for more than forty years. A lifetime of teaching and research brought him recognition as an excellent teacher with a distinct style, an eminent applied mathematician and an internationally renowned expert on scattering and wave propagation. Although we do not expect his official retirement to end his involvement in science, his friends, colleagues, and former students have taken the opportunity of this occasion to organize this symposium on Wavefields and Reciprocity in his honour. In this contribution, it is my task to give a personal view of the scientific life and work of Adrian as perceived by me as his co-worker of the first hour and as one of his twenty-two (Ph.D.) research students. Rather than trying to present a scientific biography - the main points of which can be found in the preface of the symposium proceedings - I will focus on how his philosophy of scientific engineering becomes visible in his own work and that of his students. From the start of the Laboratory of Electromagnetic Research in 1964, Adrian had already developed a clear idea of what teaching and research at a university should be. One of the tasks he took upon himself and his new group was to create a scientific atmosphere from which eventually a "school" in electromagnetics and wavefield engineering would emerge. Closely connected to this, and not less important, was to raise a scientific offspring, so that in due time his ideas and philosophy about research and teaching could be transferred to the next generation. How well he succeeded in this goal, now that time has come, and what the impact of his work on the science of wavefields in the widest sense is might become clear from the way he supervised his twenty-two (Ph.D.) research students. His teaching and commitment inspired all the students with whom he came into contact, leaving a distinct scientific mark on them. Even on many students now supervised by his own former students, this mark is noticeable.

In this contribution, I will try to make visible this scientific mark, what the influence of Professor De Hoop was on the scientific development of his students. I will elaborate on the impact his work had on wavefield engineering. I will do this by placing some of his key papers and the thesis works of his students into the perspective of his views on the basic aspects of scientific engineering. There is no better way to express these views than the way he himself did in his acceptance lecture when awarded the Gold Research Medal ("Speurwerkprijs") of the Royal Institution of Engineers in The Netherlands in 1989 for his contributions to seismic wave theory. In the typical De Hoop's style he had condensed these aspects into three key words: "What?", "How?" and "Why?". In the scientific process, human curiosity leads to the keyword "What". Then the process of learning begins, which eventually leads to knowledge. The subsequent process of mastering knowledge leads on to the question "How?" and after that to understanding. Many engineers may now be tempted to say "That's it!". We can solve our specific engineering problem. In science and scientific engineering there is, however, one more step in the process to be pursued: that of philosophizing. Here the concept of understanding is supplied with an essential element, that of intuition, and an equally essential concept (though it is more difficult to grasp) that best can be called the quest for beauty. Philosophizing eventually leads to the final keyword "Why". This last part of the scientific process leads to insight, i.e. putting to oneself the question: "Could it structurally have been otherwise?"

This philosophy of scientific research - presented here in simplified form - did not come overnight to Professor De Hoop in his life with science. In his later research papers and his opus magnum, the 1995 Handbook of Radiation and Scattering of Waves (De Hoop, 1995), the various elements of this philosophy become more visible. However, it is amazing to see how, particularly the element of the quest for beauty becomes transparent in his early work; his discovery of the fascinating, elegant and widely used Cagniard-De Hoop technique conceived in his Ph.D. thesis in 1958 (De Hoop, 1958), and in his famous paper in 1960 (De Hoop, 1960).

Forty years of teaching and research have resulted in an impressive list of papers. Apart from that, there are many papers published by students and co-workers with whom he shared his knowledge. Only when he believed that his contribution covered a substantial part of the paper, he did act as co-author of that paper. Throughout his career, Professor De Hoop became famous among wave propagation experts from many fields: electromagnetics, acoustics and seismology. A few topics in particular in which he has made profound contributions I would like to mention here. As has been touched upon already, the Cagniard-De Hoop technique, his work on reciprocity theory, his fundamental contributions to computational techniques and his current area of research: the integration of the theories of wave propagation and diffusion. In the next section, I elaborate a little more on this. In all these years, while teaching and performing his research, Adrian de Hoop has supervised a succession of research students whose research topics have been well chosen for their applicability and educational and scientific values. In Section 3, I discuss briefly the main aspects of the thesis topics of his 22 Ph.D. students, and I will attempt to place them in the context of Adrian's contributions and his views on scientific engineering.

2. Contributions to science and engineering

Rather than attempting to discuss Professor De Hoop's entire contribution to wavefield science, I select a few main items characterized by keywords that are familiar to everybody who knows his work.

2.1. Cagniard-De Hoop technique

As mentioned in the Introduction, in 1960, De Hoop published his famous paper in which he first showed that a transform introduced by the French geophysicist Cagniard in 1939 could be modified into a practical tool for solving seismic (acoustic pulse) problems in a halfspace. Today, the Cagniard-De Hoop method is still the benchmark for the computation of wavefields in layered structures. At first, the technique was of interest only to the seismology community. The method, however, has shown amazing versatility: De Hoop extended the method to treat both elastic and electromagnetic waves in layered structures, and it is now equally important in these disciplines. More recently, colleagues and students under his guidance have used the method to treat problems of diffusion (electromagnetic waves in conductive media (De Hoop and Oristaglio, 1988)) and to compute the first accurate results for elastic (Van der Hijden, thesis 1987) and electromagnetic fields (Combee, thesis 1991) in layered, anisotropic media. Earlier attempts by myself to extend the Cagniard-De Hoop technique to continuously layered media (in my attempts, an Epstein profile) failed, but in 1990 (De Hoop, 1990a) and 1991 (Verweij and De Hoop, 1990) the extension from discrete layering to continuous layered media was made, an extension which some experts had claimed was impossible.

2.2. Reciprocity theorems

The interest and expertise of Professor De Hoop in reciprocity relations go back to 1959 (De Hoop, 1959). Since then, he has continued to exploit and extend the reciprocity relations to various areas where fields and waves are applied. He is noted for the way he has put emphasis on reciprocity as one of the most fundamental properties of fields and waves. For instance, he has established reciprocity as a unifying principle in inverse scattering problems (e.g. De Hoop and Stam, 1988). In his Handbook of Radiation and Scattering of Waves (De Hoop, 1995) he shows how the direct source problem, the inverse source problem, and the inverse scattering problem can be formulated in a natural manner with reciprocity as the point of departure. The unified approach to formulate wave and field problems can be detected in all the published work of his Ph.D. and M.Sc. students.

2.3. Computational methods

One of the objectives of the new Laboratory of Electromagnetic Research around 1964 was to make a contribution in the then entirely new area of computational modelling of wave and field problems. It was a time when emphasis on analytical and asymptotic techniques was still strong. The computer facilities at the university were very limited. The computer system, Telefunken TR4, at that time had memory space of 180 kB, its computational power 0.15 Mips. The IBM 360/65 installed a year later was ten times as fast.

Since then, Professor De Hoop and co-workers have made fundamental and substantial contributions to computational methods in wavefield engineering. Again, the reciprocity theorem is taken as a unifying point of departure leading to a structured approach to constructing computational schemes for evaluating the unknown field. In a recent invited paper presented at the 25th U.R.S.I. General Assembly, held in Lille, France, 28 August-5 September 1996, Electromagnetic wavefield computation - a structured approach based on reciprocity, (Internal Report Laboratory of Electromagnetic Research Et/EM 1996-23) he brought together many of his ideas developed over the years in a comprehensive approach. In this approach, the computational handling of a field problem often starts from a "weak" formulation, where the pointwise, or "strong", satisfaction of the equality signs in the equations is replaced by requirements on the equality of certain integrated, or "weighted", versions of the field equations. Such weighted versions can be considered to be special cases of the global reciprocity theorem that applies to two different admissible field "states" that are defined in one and the same domain in configuration space. Conceptually, a computational scheme for evaluating the field is then taken to describe the interaction between (a discretized version of) the actual field state and a suitably chosen "computational state". The latter is representative of the method at hand (for example, the finite-element method and its related method of weighted residuals, the integral-equation method, the domain-integration method. In this beautiful comprehensive paper, all key issues, according to De Hoop, that occur in a scientific process are present. De Hoop and his co-workers have introduced new types of finite elements that have yielded increased accuracy with reduced computation. They have also recognized that expanding the field quantities in terms of comparitively simple functions, the requirements of interface boundary conditions and compatibility boundary conditions, has to be replaced by a minimization of a necessary and sufficient error criterion.

2.4. Integration of wave propagation and diffusion

Professor De Hoop's recent area of research is the integration of the theories of wave propagation and diffusion, which govern the behaviour of seismic and electromagnetic fields in the earth. His particular emphasis is on common ways of approaching seismic and electromagnetic inverse problems through similarities in the underlying differential equations - the wave and diffusion equations - when viewed as the limits of the lossy wave equation (De Hoop, 1993). This work may lead to new ways of combining seismic and electromagnetic measurements to yield better images of the earth structure.

2.5. The Laboratory of Electromagnetic Research

Professor De Hoop can be considered as the founding father of the programme of activities in electromagnetic research as it has evolved since the Laboratory of Electromagnetic Research was founded in 1964. Today, the research activities of the laboratory involve fundamental research in electromagnetic fields and waves, and acoustic/elastodynamic fields and waves. Numerical and analytical techniques are the tools with which the electromagnetic or acoustic/elastodynamic properties of appropriate model configurations are analyzed, the latter being selected on the ground of their present-day or future technical or technological importance. In this respect, we can mention ground-penetrating radar, the combination of seismic and electromagnetic measurements to obtain images of the earth's structure, nondestructive eddy-current inspection of cracks and corrosion, induction logging, magnetic recording-head problem, electromagnetic compatibility, electromagnetic prospecting, guided-wave and integrated optics, laser amplifiers, hyperthermic oncology, acoustic transducers, cross-borehole tomography. Just a few of the applications that can be found in the 1995 Annual Review of Research of the Laboratory. In the first Annual Review of Research in 1977, the programme involved research and teaching in quantum electronics. For a number of years, quantum mechanical aspects of electromagnetic fields were part of the programme, this under supervision of Professor Dr. W. van Haeringen. The scientific leadership of Professor De Hoop as a consistent factor for all the years of its existence has brought the Laboratory in Delft to the stature of one of the leading groups in Europe. The 1995 Quality Assessment of Research in Electrical Engineering of the Association of Universities in The Netherlands (VSNU) by an international panel has shown that the programme of the Laboratory of Electromagnetic Research is at the international forefront. This with the following assessments: quality and productivity as excellent, relevance as good and viability as satisfactory, and with the comments:

> *The Group carries out very high quality research on innovative topics in Wavefield Modelling and Inverse Scattering, both for electromagnetics and acoustics. The scientific output is high in both publications and Ph.D.'s and enjoys world-wide recognition in the field. Thanks to a strong emphasis on interdisciplinary collaboration, notably in the Centre for Technical Geoscience, application-specific software has been developed, which has been successfully applied in many areas of industrial relevance. This has ensured a flow of external funding supporting the further work.*

The Laboratory of Electromagnetic Research is embedded in the Faculty of Electrical Engineering. Consequently, many of its research topics are associated with electrical engineering problems. Since 1982, Professor De Hoop has been involved in

Schlumberger-Doll Research, Ridgefield, Connecticut, U.S.A., and somewhat later he also became involved in Schlumberger Cambridge Research, Cambridge, U.K.. He and I became Visiting Scientists on a regular basis at one of those research laboratories, resulting in an increase in the research activities in geophysical prospecting. This is now a major part of the laboratory participation in the Delft research school, Centre for Technical Geoscience (CTG), in particular, it contributes to the discipline of imaging and wavefield inversion. A substantial activity of the Centre is the organization and implementation of four-year scientific programs to train Ph.D. students to become independent researchers.

Impossible as it is to discuss a lifetime of teaching and research in a few pages, I have tried to convey an idea of the impact Professor De Hoop's own scientific work has made on wavefield science and engineering. In the next section, I discuss briefly the main aspects of the research of his 22 Ph.D. students.

3. Supervised Ph.D. Research

Prior to the start of the Laboratory of Electromagnetic Research, Professor De Hoop was involved in the supervision of two research projects, each leading towards a Ph.D. thesis. The very first of his students was:

Alex de Bruijn, who received his M.Sc. Degree in engineering physics, and a doctorate in technical sciences in 1967, both from the Delft University of Technology. From 1967 to 1970, he was a postdoctoral fellow in building physics at the National Research Council of Ottawa, Canada. From 1970 to 1985, he was a senior scientist working on hydro-acoustic aspects of ship propeller cavitation, flow-induced noise and acoustic fluid-structure interaction at TNO-TPD in Delft. In 1985, he became group leader "Short-range sonar" Section at SACLANT Undersea Research Centre (NATO). From 1990 on he has been an independent scientific consultant in the fields of engineering acoustics, vibration control and underwater sound. The title of his thesis is: *Calculation of the edge effect of sound-absorbing structures* (1967). Thesis supervisors were Professors A.T. de Hoop and C.W. Kosten (Acoustics). Measurements of the sound absorption coefficient of sound-absorbing materials in reverberation chambers showed that they are dependent upon the dimensions of the test samples. The cause of this effect can be attributed to the sound diffraction phenomena in the vicinity of the edges of a sample, which result in additional sound absorption. To verify and validate the influence of these edge effects, the diffraction of a plane sound wave by (a) a straight edge of an acoustically hard half-plane and an absorbing half-plane, (b) by a sound-absorbing strip in a large rigid plane and (c) by a sound-absorbing, periodically uneven surface of rectangular profile, was investigated. The first problem was solved using the Wiener-Hopf technique. In that period of time, Professor De Hoop was investigating the potential possibilities of this technique to solve a variety of relevant problems, which resulted in a beautiful course on Wiener-Hopf methods for applied mathematicians. In the two other problems, Alex de Bruijn expanded the scattered field in a spectrum of plane waves and into waveguide modes in the rectangular grooves, respectively, subsequently, applying the appropriate boundary conditions. Even with the restricted computer facilities at that time, a proper understanding of the edge effects resulted from it.

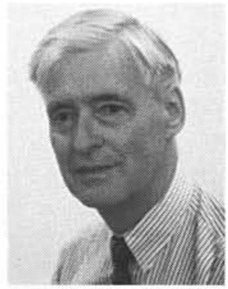

Hans J. Frankena, was born in Haarlem, the Netherlands and received his M.Sc. (1956) and Ph.D. (1967) degrees in electrical engineering from the Delft University of Technology. His initial research, as a research assistant at the group for electromagnetic theory of the Department of Electrical Engineering of that university, was devoted to electromagnetic wave propagation, especially in waveguides for microwaves. In 1965, he became a lecturer in that department. After his appointment in 1970 as a full professor in optics at the Department of Applied Physics of the same university, he conducted research in holography, especially holographic interferometry, laser technology, nonlinear optics and thin film optics. More recently, his attention has also been directed to integrated optics. From 1971 to 1979, he was the President of the Netherlands' Optics Committee; from 1975 to 1981, a board member of the Netherlands' Physical Society; from 1977 till 1979, the President of the European Optical Committee; and in the period 1978 to 1987, the Secretary-General of the International Commission for Optics. In 1987, he was elected Fellow of the Optical Society of America and received the President's Award of SPIE. The title of his thesis is: *Scattering of electromagnetic waves by a class of waveguide discontinuities* (1967, cum laude). In microwave engineering at that time, much attention was focused on microwave (and millimetre wave) antenna systems. In these systems, waveguide configurations were used as antenna feeds. In these configurations, bends and other discontinuities occur. This is the subject under investigation in the thesis of Hans Frankena. He analyzed filled rectangular and circular waveguides, waveguide discontinuities, and scattering by sheets in waveguides, scattering by angled bends in rectangular waveguides and symmetric Y-junctions. In the latter class of problems, the solution approach is certainly nontrivial as far as the completeness of field representations in the corner regions between homogeneous waveguide sections are concerned. The results of this thesis are very relevant to the design of today's wideband antenna systems for, e.g., ground-penetrating radars.

The sixties are remembered as a time of spectacular developments in quantum electronics. With the advent of microwave and optical masers, and the various types of lasers, sources of coherent light waves became available that made new applications in applied and nonlinear optics possible. These developments brought with them the possibility of communication at optical frequencies, which, if feasible, would revolutionize communication practice. The era of optical communications had arrived. Nobody could then have foreseen how successful the development would be. Optical communication was and still is an interdisciplinary activity in which applied physicists, electromagnetic modellers, communication engineers play important roles. In electromagnetics, it opened up a new field of research, optical wavefield engineering, or optical electromagnetics. It is no wonder that the first two research projects in the Laboratory of Electromagnetic Research, which had by then been founded, were in this new field.

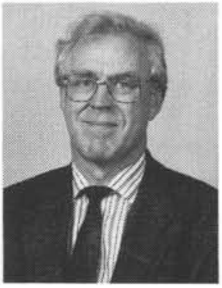

Hans Blok was born in Rotterdam, the Netherlands, on April 14, 1935. He received his degree in electrical engineering from the Polytechnic School, Rotterdam in 1956. He then received his B.Sc. and M.Sc. in electrical engineering and his Ph.D. in technical sciences, all from the Delft University of Technology, in 1961, 1963 and 1970, respectively. Since 1968, he has been a member of the scientific staff of the Laboratory of Electromagnetic Research at the Delft University of Technology. During these years, he has carried out research and lectured in the areas of signal processing, wave propagation, and scattering problems. During the academic year 1970-1971, he was a Royal Society Research Fellow in the Department of Electronics of the University of Southampton, U.K., where he was involved in experimental and theoretical research on lasers and nonlinear optics. In 1972, he was appointed associate professor at the Delft University of Technology, and in 1980 he was named professor. From 1980 to 1982, he was Dean of the Faculty of Electrical Engineering. During the academic year 1983-1984 he was a Visiting Scientist at Schlumberger-Doll Research (SDR), Ridgefield, Connecticut. Since then, he has been back there in the summertime on a regular basis. At SDR he was and is involved in electromagnetic prospecting problems. At present, his research interest is guided wave optics and inverse scattering problems with applications in nondestructive testing. The title of his thesis is: *Diffraction theory of open resonators* (1970, cum laude). Open resonators are an essential part in optically active devices such as a laser. In a laser there is an optically active medium, usually between the mirrors of an open resonator of the Fabry-Pérot type. The open resonator is the physical structure that confines electromagnetic energy to a small region in space where the interaction between matter and the electromagnetic field takes place. The theoretical analysis of open resonators at the time was dominated by Fox and Li's classical paper in 1961, providing an intuitive and physically satisfying explanation. In their theory, a mode in an open resonator is defined as a time-harmonic scalar wave which, being launched from a certain part of a system of reflectors, reproduces itself up to a constant factor after having completed a cycle of reflections in the system. This approach is entirely heuristic. It is based on a formally inconsistent analysis of a model of the resonator, which, though similar, is mathematically entirely different. In his thesis the classical theory of cavity resonators was chosen as point of departure. In this approach, a mode of the open resonator is defined as a non-trivial solution of the source-free electromagnetic field equations, satisfying the proper boundary conditions at the boundaries of the resonator system. As this states an eigenvalue problem, the non-trivial field distributed exists only at a sequence of complex frequencies, the characteristic frequencies corresponding with the free oscillations of the resonant structure. These free oscillations are similar to the ones later used in the singularity expansion method. After justifying a scalar formulation, the resulting treatment of the exact boundary value problem leads to a system of inhomogeneous (differential) integral equations of the first kind. In the range of optical frequencies, this system is very difficult to solve numerically. Therefore, an approximate method, in particular the modified Kirchhoff approximation was used which led to a system of simultaneous integral equations of the second kind. These equations were solved numerically by the method of moments, which was rather new at the time. This exciting research project became successful, because it combined physical insight and a rigorous mathematical approach. The second project in optical electromagnetics was the thesis work of Peter van den Berg.

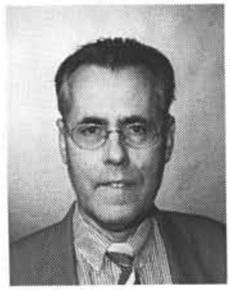

Peter M. van den Berg was born in Rotterdam, the Netherlands on November 11, 1943. He received his degree in electrical engineering from the Polytechnic School, Rotterdam in 1964, his B.Sc. and M.Sc. in electrical engineering and his Ph.D. in technical sciences, all from the Delft University of Technology, in 1966, 1968 and 1971, respectively. From 1967 to 1968, he was employed as a research engineer by the Dutch Patent Office. Since 1968, he has been a member of the scientific staff of the Laboratory of Electromagnetic Research at the Delft University of Technology. During these years he carried out research and taught in the area of wave propagation and scattering problems. During the academic year 1973-1974, he was a Visiting Lecturer at the Department of Mathematics, University of Dundee, Scotland, financially supported by the Dutch Niels Stensen Stichting. During a three-month period in 1980-1981, he was a Visiting Professor at the Institute of Theoretical Physics, Goteborg, Sweden. He was appointed full professor at the Delft University of Technology in 1981. During the summer breaks of the last years, he is a Visiting Scientist at Shell Research, Rijswijk. At present, his research interest is the efficient computation of field problems using iterative techniques based on error minimization, both for the forward scattering problem and the inverse scattering problem, as well as the use of wave phenomena in seismic data processing. The title of his thesis is: *Rigorous diffraction theory of optical reflection and transmission gratings* (1971). At the time, high quality optical diffraction gratings became available in large quantities. This resulted in a new interest in the solution of the two theoretical problems connected with the diffraction of light by gratings, viz. the problem of spectral image formation and the calculation of the power distribution amongst the different spectral orders. The scattering problem deals with plane-wave scattering by a perfectly reflecting periodic boundary and/or a dielectric medium of which one boundary is periodic. To solve these problems, a Green function formulation has been employed. The relevant Green functions have been chosen such that integral representations are obtained, in which only the contributions from the remaining unknown functions on a single period of the grating occur. This has been achieved by requiring that the Green function consists of waves which travel away from a plane "parallel" to the grating, while in the direction parallel to the grating it possesses a phase variation exactly opposite to that of the incident wave.

Subsequently, the remaining unknown wave functions on a single period of the grating have been determined with the aid of integral equations. The numerical solution of these integral equations has been achieved by applying the method of moments. The unknown functions have been expanded in terms of a sequence of functions defined on the interval of integration. Through use of this method, the integral equations have been replaced by a system of linear equations. Van den Berg has tried out various numerical strategies in the actual implementation. Thus, not only physical insight in the grating problem was obtained, but also experience and expertise in solving integral equations. Expertise that became useful in the next Ph.D. project.

Gerrit de Jong was born in St. Annaparochie, Friesland, the Netherlands, in September 1941. He received his degree in electrical engineering from the Polytechnical School of Leeuwarden in 1964. After military service in the Royal Air Force, he received his M.Sc. in electrical engineering in 1969 and his Ph.D. in technical sciences in 1973, both from the Delft University of Technology. From 1969 to 1973, he was a member of the scientific staff of the Laboratory of Electromagnetics Research in Delft. In 1973, he joined the Faculty of Geodetic Engineering where he, as an associate professor, became involved in the science of precise determination of positions on sea or land for offshore, navigational and land-surveying activities. Through his strong interest in aeronautics, he also played an important role in the avionics activities of the university. Today, he is a consultant in avionic and aeronautical problems. The title of his thesis is: *Generation of acoustic waves in piezo-electric devices* (1973). The strong interest in piezo-electric devices in several engineering areas at that time was the reason to start research in this field. He investigated the integral equation formulation of scattering or diffraction problems associated with the generation of acoustic waves in piezo-electric devices. Integral equations are obtained from suitable integral representations for the wave function, which in turn follow from a suitable reciprocity relation. This reciprocity relation is derived from the basic equations of piezo-electricity and can be considered as a fundamental theorem from which many properties of piezo-electric waves and devices can be derived. The configurations to be investigated were: the transmitting transducer, the receiving transducer and the piezo-electric delay line. Also, the generation of Bleustein-Gulyaev waves along a metallized piezo-electric halfspace and the phenomenon of energy trapping in piezo-electric devices were investigated. What was new to us in this project was the combining of mechanical quantities in integral representations and reciprocity theorems for the mechanical displacement and the electric potential in a piezo-electric medium. The results of this thesis boosted later research on ZnO transducers in the Sensor Laboratory of our faculty.

Tan Tik Hing was born in Semarang, Indonesia, on December 17, 1945. He received his M.Sc. in electrical engineering and Ph.D. in technical sciences, both from the Delft University of Technology in 1973 and 1975, respectively. In 1975, he joined Shell Research (KSEPL) in Rijswijk, the Netherlands, where he became involved in seismic research. He is currently on assignment from Shell International Exploration

and Production B.V. to the Geophysics Department of Shell Offshore Incorporated in New Orleans, Louisiana, U.S.A. The title of his thesis is: *Diffraction theory for time-harmonic elastic waves* (1975). With the experience of having solved several (scalar) electromagnetic and acoustic scattering problems in the laboratory, attention now focused on the scattering of elastic waves. Growing interest in geophysical problems led to two new research projects, the one we are now discussing here and one dealing with the diffraction of elastic SH-surface waves. The entire machinery of formulating and solving electromagnetic scattering problems has now been applied to the scattering of elastic waves by transparent obstacles. The result was a neat, compact thesis in which the formulation and numerical solution of the diffraction of time-harmonic elastic waves by cylindrical obstacles, plane, rigid strips and plane cracks of finite width have been fully covered. Partly overlapping, was a project where the diffraction of elastic surface waves was investigated.

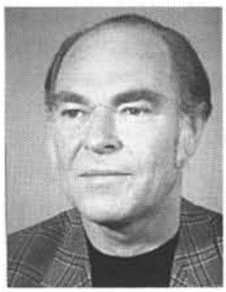

Fred L. Neerhoff was born in Den Helder, the Netherlands, on November 17, 1943, and received his M.Sc. in electrical engineering and his Ph.D., both from the Delft University of Technology in 1971 and 1977, respectively. Right after his Ph.D. thesis, Fred Neerhoff spent a year as a Research Associate at Northwestern University, Department of Civil Engineering, Illinois, U.S.A. After his return to the Laboratory of Electromagnetic Research in Delft, he continued to work on elastodynamic diffraction problems and taught a course in electromagnetics and vector analysis. In the meantime, he studied psychology at the State University of Leiden and also became a political labour activist for a couple of years. In 1984, he switched to the Laboratory of Network Theory, where he presently is an associate professor. There, he became heavily involved in teaching basic circuit theory. In the past years, he developed a new circuit theory curriculum, where nonlinearities are an integral part of a systematical and fundamental approach. His present research interests are in nonlinear dynamical system theory, especially in nonlinear dynamics of electronic circuits. The title of his thesis is: *Diffraction of elastic SH-surface waves* (1977). In this project, the integral equation approach for analyzing the diffraction of elastic surface waves by discontinuities in semi-infinite media or slabs has been successfully applied. The diffraction problems involve the scattering of Rayleigh or Love waves by inclusions or cracks, while the semi-infinite elastic medium may be uniform or horizontally layered. The Green functions in the formulation of the integral equations are represented as Fourier inversion integrals. All difficulties that are encountered in the numerical evaluation, e.g. the occurrence of (surface-wave) poles in the integrand of the Fourier integrals, etc. have been investigated. When dealing with the Love-wave diffraction by a crack, the elements of the scattering matrix of the crack, the radiation characteristics in the far-field region as well as the surface-to-bulk power conversion have been computed.

In the years following this project several papers with extensions and generalizations of this diffraction problem have been published. Parallel to the systematic use of integral equations of the Fredholm type in wavefield problems, research has been initiated on alternatives for the computation of electromagnetic fields in inhomogeneous media.

Gerrit Mur was born in Breukelen, the Netherlands, on February 16, 1942. He received his degree in electrical engineering from the Polytechnic School, Utrecht in 1963, his B.Sc. in electrical engineering in 1968, his M.Sc. in electrical engineering in 1970 and his Ph.D. in technical sciences in 1978, all from the Delft University of Technology. In 1963, he was employed as a teacher at the Polytechnic School in Utrecht. From 1968 to 1970, he was employed as a research student at the Laboratory of Electromagnetic Research, Faculty of Electrical Engineering, Delft University of Technology. Since 1970, he has been a member of the scientific staff of this Laboratory, currently he is an Associate Professor. During the academic year 1979-1980 he held a twelve-month fellowship in the European Science Exchange Program at the Department of Electrical and Electronic Engineering, University of Nottingham, Nottingham, U.K. His main research interests are the development of numerical methods for computing electromagnetic fields in complicated configurations containing inhomogeneous media. The title of his thesis is: *Computation of electromagnetic fields in homogeneous media: scattering and guiding properties* (1978). In this thesis, two alternatives to the standard integral equation method have been described. The first alternative also starts with a formulation of the field problem in terms of a Fredholm integral equation. Rather than being solved directly, this integral equation has been transformed into a related system of coupled Volterra integral equations of the second kind. The system has then been solved by a direct numerical quadrature. The major part of the thesis deals with a second alternative, which avoids the use of integral equations and starts from the electromagnetic-field equations, transforming them into a system of coupled first-order ordinary differential equations, by introducing a certain direction of propagation of the waves and an appropriate transverse modal expansion of the fields. The latter system can then be solved using standard techniques. The system of equations thus obtained, however, turns out to be numerically unstable and it has therefore been transformed into a stable system through a specific transformation scheme. The resulting approach has subsequently been applied to the scattering by inhomogeneities in closed waveguides with a rectangular cross-section, scattering by cylindrical objects in free space and to the problem of guided electromagnetic fields in open waveguiding structures located in free space.

The research for the next project was not carried out in our laboratory but in the Physical Laboratory of TNO in The Hague, the Netherlands, however, under supervision of Professor De Hoop and Professor L. Krul of the Microwave Laboratory of our faculty.

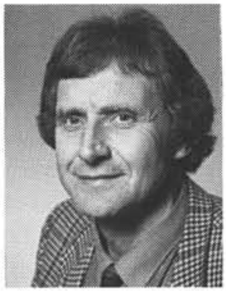

Helmut J. van Schaik was born in Woerden, the Netherlands, on August 6, 1943. After graduating from the HBS-B (Dutch General Secondary School) in Woerden, he received further education at the Rotterdam Polytechnic School, Department of Electrical Engineering. He graduated in 1963. After fulfilling his military service, he studied at the Delft University of Technology from 1965 and obtained his M.Sc. in electrical engineering in 1972. From 1972 to 1979, he was a member of the graduate staff at the Department of Microwaves of the TNO Physical Laboratory in The Hague. Here, he carried out research in the field of electromagnetic field problems. His main interests were the problems connected with phased-array antennas. The findings of this research led to the writing of a doctoral dissertation. At the moment, he fills the position of senior lecturer of mathematics at the Polytechnical Faculty of HR&O in Rotterdam. The title of his thesis is: *Theory and performance of a space-fed planar, phased-array antenna with 849 iris-loaded rectangular-waveguide elements and external matching sheet* (1979). An explicit phased-array antenna problem was at the basis of this research project. In the design of this antenna system for radar applications, many questions were open. In this thesis a theory to determine the influence of a matching sheet in front of the antenna on its performance has been developed. With respect to the coupling effects of individual radiators, the antenna is considered as an infinite grating, that is uniformly illuminated by the incident field. Further, the electromagnetic field in the far-field region of the antenna has been determined. Also, a method to transform the wave emitted by the feeding horn into one with a plane equiphase surface has been presented. Numerical and experimental results have been compared. As far as the computational effort is concerned, the matching procedure outlined in the thesis is superior to the at the time existing procedures.

In the next thesis we are back to a geophysical problem, viz. an extension of Van den Berg's work on gratings and Neerhoff's work on a single protrusion or indentation in an elastic surface to scattering by a periodic interface between two elastic media.

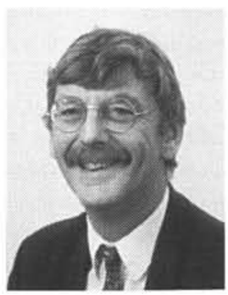

Jacob T. Fokkema was born in Leeuwarden, Friesland, the Netherlands on January 21, 1948. He obtained his electrical engineering degree from the Polytechnic School, Leeuwarden in 1969. After military service he received his M.Sc. in electrical engineering in 1976 and his Ph.D. in 1979, both at the Delft University of Technology. In 1979, he joined the scientific staff of the Laboratory of Network Theory in Delft. From 1980 to 1981, he was a postdoctorate fellow at the Integrated Systems Laboratory at Stanford University, California, U.S.A. In 1982 he became a scientific staff member of the Section Applied Geophysics of the Faculty of Mining and Petroleum Engineering in Delft. From 1987 to 1988, he was a Visiting Professor at the Federal University of Bahia, Institute of Geosciences and Physics, Salvador, Bahia, Brazil. Since 1993, he is a professor of Applied Geophysics of the Faculty of Mining and Petroleum Engineering, Delft University of Technology. The title of his thesis is: *Reflection and transmission of time-harmonic elastic waves by the periodic interface between two elastic media* (1979). This thesis deals with the scattering of elastic waves by the interface between two solids, being cylindrical in one direction and periodic in another direction. In particular, the behaviour of vertically polarized elastic waves have been analyzed. The horizontal polarized shear wave behaves similar to electromagnetic waves in this configuration. That problem has been extensively investigated by Van den Berg in his thesis. In the present problem too, the integral-equation method proved to be an effective tool. Excitingly new in this thesis was the discussion of the problem where the wave motion generated by a time-harmonic, buried line source acting in the interior of a semi-infinite elastic solid with a stress-free, period boundary. The approach discussed in the thesis applied satisfactorily to periodic profiles of arbitrary shape and dimensions. The thesis research was co-supervised by Dr. P.M. van den Berg. In the course of the analysis, Van den Berg and Fokkema have reinvestigated the applicability of the Rayleigh hypothesis, leading to three exciting research papers on that topic.

As can be seen from the Preface to this proceedings, in 1976-1977, Professor De Hoop was on leave of absence at the Philips Research Laboratories Eindhoven, where he performed research on magnetic recording theory. One of the projects he supervised at Philips was an analysis of three-dimensional magnetic fields in recording head configurations. The research worker at Philips was Alfred van Herk. Back in Delft, Professor De Hoop continued his interest in magnetic recording, leading to a very nice set of lecture notes on magnetic recording theory and another Ph.D. project. But, first, we discuss Van Herk's thesis.

Alfred van Herk was born in Rotterdam, the Netherlands in 1945. He received his M.Sc. in electrical engineering at the Delft University of Technology in 1967. From 1969 to 1986, he worked on magnetic recording, first at Twente University of Technology, the Netherlands, and after 1974, at Philips Research Laboratories, Eindhoven, the Netherlands and other Philips divisions. When in 1979, Professor De Hoop spent a sabbatical year at the Philips Research Laboratories to do research work on magnetic recording theory, Van Herk used this opportunity to write his Ph.D. thesis, again under Professor De Hoop's supervision. His career continued in the predevelopment of videorecorders (advanced recording heads and tapes) and in application development for magnetic tapes. In both functions he continued to develop many international contacts in the research and industrial world of magnetic recording. In 1987, Van Herk became responsible for the Professional Recording Group of Philips Industrial Electronics Division. This group developed and successfully put on the market the first high density voice recorder using multi-track, thin-film heads. This technology enabled 24 hours uninterrupted recording of 64 voice channels on one half-inch tape cassette. At present, Van Herk is general manager of Philips Industrial Electronics Services, the internal business and facility services company of the IE Division. IE

Services was created some years ago during the turnaround of the division in order to facilitate the change process of many staff departments into customer-oriented and value-adding service groups. The title of his thesis is: *Three-dimensional analysis of magnetic fields in recording head-configurations* (1980). Magnetic recording techniques are of widespread use for storing information of various kinds: sound, picture, computer data and measurement data. Of all the information stored at present, probably the largest part is stored with this technique and in many laboratories a continuing search for improvement of the performance of the recording systems is going on; in particular, the research is aimed at an increase of the storage capacity. One of the important parameters governing this storage capacity is the width of the tracks that are recorded on the magnetic medium. A drastic reduction of the track width and of the distance between adjacent track leads to difficulties. In this thesis, some of the relevant problems have been investigated, especially the ones that are connected with the side-fringing fields of magnetic heads, i.e. the fields whose influence reaches beyond the track width of the head. Analytical solutions of the side-fringing fields of an idealized head has been presented and compared with measurements. A magnetic-field surface-integral equation method has been introduced to compute the three-dimensional magnetic field of arbitrary magnetic heads, with magnetic and/or electric shields.

In the main stream of the research program in the laboratory attention was growing for time-domain scattering.

Gerard C. Herman was born in Rotterdam on April 4, 1954. In 1978, he received the M.Sc. in electrical engineering and in 1981, his Ph.D. in technical sciences, both at the Delft University of Technology. In 1982, he joined Shell Research in Rijswijk (KSEPL), the Netherlands, where he was involved in research in the area of forward and inverse wave propagation, seismic imaging and data processing. Since 1989, he is an associate professor in the Faculty of Applied Mathematics in Delft, working on problems in the area of forward and inverse scattering. The title of his thesis is: *Scattering of transient acoustic waves in fluids and solids* (1981, cum laude). This thesis (co-supervised by Dr. P.M. van den Berg) was especially devoted to the direct time-domain analysis and its implementation in the problem of the scattering of acoustic waves in fluids and solids. The main tool in the analysis is a time-domain integral-equation formulation, which has been derived from suitable source representations for acoustic field quantities. Frequency-domain results followed by Fourier inversion are used to check on the time-domain results. For general inhomogeneous obstacles embedded in a homogeneous, isotropic medium, domain-integral equations have been derived. For homogeneous obstacles also boundary-integral equations were considered. The integral equations have been discretized in space and time. One approach, the "marching-on-time-method" showed to lead to numerical instabilities. To overcome this problem two iterative methods have been discussed that do not suffer from these instabilities. One, that is not restricted in its applicability, is based upon the minimization of an integrated square error and looked very promising for further applications.

The theory of elastodynamic waves finds a wide range of applications. In the field of exploration geophysics, elastodynamic waves serve as a standard diagnostical tool used to probe the subsurface structure of the earth in the search of fossile energy resources. In the non-destructive evaluation of materials and mechanical structures, the scattering of elastodynamic waves by interior defects (such as inclusions or cracks) provides the opportunity to detect these defects by means of measurements carried out at the surface of the structure. In many cases, the theoretically obtained results for certain model (canonical) configurations serve as a guidance when interpreting experimentally acquired data in the more complicated situations met in practice. To serve this purpose, the relative importance of the different parameters that govern the behaviour of a certain model configuration should show up as clearly as possible in the results that apply to this model configuration. In the next thesis, two canonical problems have been considered: the propagation of elastodynamic waves in a stratified medium and the scattering of elastodynamic waves by a semi-infinite plane screen.

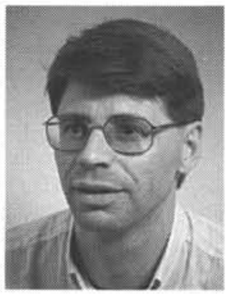

René du Cloux was born in Rijswijk, the Netherlands on January 8, 1958. He received his M.Sc. in electrical engineering from the Delft University of Technology, in 1982. From 1982 to 1986, he was a research assistant in the Laboratory of Electromagnetic Research and the Geophysics Group, Delft University of Technology. Under guidance of Professor De Hoop and Professor Grootendorst his work resulted in his Ph.D. Since 1986, he has been a research scientist at Philips Research Laboratories, Eindhoven, the Netherlands. As a member of the EMC Group and Applied Mathematics Group he was concerned with the development of tools for electromagnetics simulation: in particular, printed-circuit-board simulation and electromagnetic-compatibility analysis. These simulation tools are currently being introduced in the Philips system-design flow. Currently, he is a member of the VSLI Design Automation and Test Group, where he is concerned with the behavioural modelling of analogue and mixed digital-analogue electronic systems. The emphasis of this work is on the introduction of useful abstractions of analogue electronics, such that the complexity of the design of mixed analogue-digital systems can be controlled. The title of the thesis is: *Symmetry properties of elastodynamic wave fields and their application to space-time scattering theory* (1986, cum laude). The thesis supervisors were Professor A.W. Grootendorst of the Faculty of Applied Mathematics and Professor A.T. de Hoop. In the thesis, group theory has been used to analyze the symmetry considerations in elastodynamic scattering problems. The wave propagation in stratified media has been formulated in terms of the scattering-matrix theory. In that formatism, also the scattering operator of a semi-infinite screen has been introduced. The elastodynamic diffraction by a semi-infinite screen has been solved using the Cagniard-De Hoop technique.

Another research project in the area of exploration geophysics was carried out at Schlumberger-Doll Research, Ridgefield, Connecticut, U.S.A.

Jos H.M.T. van der Hijden is Business Development Director of KPN Kabel B.V. since February 1995. He is responsible for acquiring and running Cable TV networks in several European countries. Before that, he was Marketing Director of the Business Unit Mobile Communications Services of PTT Telecom, responsible for the marketing of mobile telephony and paging. Prior to this, he headed the strategy department of the Business Unit International Telecommunications. From 1989 to 1992, he was an associate with McKinsey & Company in Amsterdam, where he served clients both locally and abroad in various industries. In 1988, he graduated (MBA) with distinction from INSEAD, Fontainebleau, France. From 1981 to 1988, he worked at Schlumberger in New York, where his main responsibilities were in the development and commercialization of data interpretation services for clients in the petroleum industry. In 1987, he received his Ph.D. from the Delft University of Technology, based on a dissertation written while employed by Schlumberger. He graduated (M.Sc. in electrical engineering) from the Delft University of Technology in 1981. The title of his Ph.D. thesis is: *Propagation of transient elastic waves in stratified anisotropic media* (1987, cum laude). At the time he started his research, there was increasing evidence that in the interpretation of seismic data the influence of anisotropy had to be taken into account, especially when shear-wave data interpretation was aimed at. With this application in mind, a method to compute the seismic waves, that are generated by an impulsive source in a stratified anisotropic medium became the topic of his thesis. The problem has been solved by applying the Cagniard-De Hoop method. The general approach to the problem is similar as in the previous thesis we discussed, but becomes considerably more complicated due to the anisotropic nature of the elastic media. In particular, the computation of the Cagniard-De Hoop contours in anisotropic media required a careful analysis due to the presence of cusps in slowness and wave curves for the various relevant wave types. As a new element in this thesis can be mentioned the introduction of the concept of generalized rays, making it possible to write the total wave motion as the superposition of generalized ray constituents. This approach facilitated the interpretation of the results.

Also, the next research project was performed outside the Laboratory of Electromagnetic Research, though it involved one of its former students.

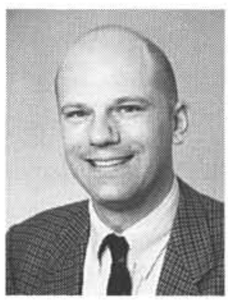

Raphic M. van der Weiden received both his M.Sc. (1983) in electrical engineering, under supervision of Professor A.T. de Hoop, and his Ph.D. (1988) in technical sciences from the Delft University of Technology. He joined Shell Research, Rijswijk, the Netherlands, as a geophysicist in 1988, where he has worked in various jobs at the Geophysics and Petrophysics Research Department. Presently, he is employed as a Senior Geophysicist by NAM (Nederlandse Aardolie Maatschappij) in the quantitative interpretation team. His current research interests are data-driven inversion schemes for seismic data.

The title of his thesis is: *Boundary integral equations for the computational modelling of three-dimensional steady groundwater flow problems* (1988) Besides Professor De Hoop, also Professor J.C. van Dam of the Faculty of Civil Engineering was Van der Weiden's thesis supervisor. Problems concerning the flow of groundwater play an important role in the practice of civil engineering and groundwater hydrology. Solutions of these problems are generally based on the conservation of mass and on generalizations of Darcy's empirical law that incorporates the permeability characteristics of the subsoil. There is, however, a need for a more profound theoretical justification of these relations, as well as of the conditions under which they apply. Envisaging the soil as a fluid-saturated porous medium, it is shown that a suitable spatial (volume) averaging procedure leads consistently to the relevant macroscopic equations. Subsequently, these serve to formulate steady groundwater flow problems as (mathematical) boundary-value problems. The solution of these boundary-value problems has been investigated with the aid of the boundary-integral-equation method. The boundary-integral-equation formulation has been derived with the aid of a suitable reciprocity relation. A survey of the different boundary-integral-equation formulations has been presented. An efficient and straightforward scheme for their numerical handling, especially as far as the analytic evaluation of the (singular) integrals of Green's kernel functions over a triangular subdomain of the boundary is concerned, was discussed in some detail. Numerical examples have been presented for three-dimensional test flows in homogeneous, isotropic as well as anisotropic media.

Envisaging the soil in the earth as a fluid-saturated porous medium raises the question how transient acoustic waves propagate in such media. The answer to this question is certainly of great interest in seismics. The next thesis project deals with this question:

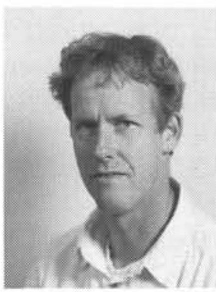

Sytze M. De Vries was born in Ylst, Friesland, the Netherlands on March 12, 1956. In 1978, he received a degree in electrical engineering of the Polytechnic School in Leeuwarden. After military service he was working at Philips Telecommunications and Data Systems in Hilversum from 1979 to 1980. In 1984, he received his M.Sc. in electrical engineering from the Delft University of Technology. In 1989 he obtained his Ph.D. in technical sciences from the Delft University of Technology. Since then, he has been working for Shell Research (former KSEPL, now SIEP-RTS), Rijswijk, the Netherlands). Within the Geophysics Department he joined several teams to develop new methods and algorithms for seismic processing. His areas of professional interests are seismic modelling and inversion. He is a member of "De Friesche Elf Steden Vereniging" and the SEG. He is the proud bearer of two "Elfstedenkruisjes" (1985, 1986) proving that he, twice, finished in the most gruelling, 200 km long skating tour in the world, organized when there is ice on the canals and lakes in Friesland. The title of his thesis is: *Propagation of transient acoustic waves in porous media* (1989, cum laude). Like in the previous thesis, a spatial volume averaging procedure applied to the microscropic structure leads consistently to the relevant macroscopic equations for the propagation of acoustic waves in the porous media. In the thesis a thorough discussion of the spatial averaging considerations has been presented. The resulting macroscopic relations are then used to introduce acoustic wave operators. Subsequently, the now well-known machinery of transform-domain wave equations, generalized-ray constituents and Cagniard-De Hoop technique has been applied to (an)isotropic fluid/porous medium configurations.

Besides all these geophysical problems, extensive research on optical fibers and other open waveguiding problems was conducted at our laboratory. One collaboration project was started up at the Eindhoven University of Technology during the period that Professor De Hoop was part-time professor there. The next thesis resulted from that.

Helena (Helmi) M. de Ruiter was born in Rhoon, the Netherlands on July 21, 1954. In 1978, she obtained her M.Sc. in electrical engineering in Delft, and in 1989, her Ph.D. from the Eindhoven University of Technology. From 1985 on, she was involved in software development with Philips Industrial Electronics Eindhoven as a software developer of the Lithography Department from 1985 to 1990; as a technical specialist of the Machine Tool Controls Department from 1990 to 1992. She was a participant to an EC funded research program on enhancement of static machine tool accuracy. This resulted in a co-supervision for the Ph.D. work of H.A.M. Spaan (Software error compensation of machine tools, Faculty of Mechanical Engineering, Eindhoven University of Technology, 1995). From 1993 on, she works as a technical specialist for Philips Industrial Automation Systems on software for embedded control. The title of her thesis is: *Transmission, reflection and radiation at junction planes of different open waveguides* (1989). The topic of this thesis, supervised by Professor J. Boersma (Applied Mathematics) and Professor A.T. de Hoop, deals with a canonical problem in guided wave optics. In the thesis, the junction problem has been formulated using the surface-source type integral formalism that involves appropriate Green's tensors. The resulting integral equations have been subjected to a transverse Fourier transformation. The resulting equations thus obtained have been solved numerically. Notwithstanding the advantage this Fourier-transform computational method has in that the spatial singularities in the Green tensors are more easily handled in the transform domain, the numerical solution of the resulting equations is not without its problems. Nevertheless, a number of important junction problem have been successfully solved.

Back again to the area of exploration geophysics, acoustic imaging and nondestructive testing. The next thesis was in the field of time-domain computations of three-dimensional acoustic wave fields, now not using integral equations as in Herman's thesis, but a finite-element approach. This research topic was inspired by the work that Professor De Hoop and Dr. G. Mur have performed with respect to the edge elements for a consistent description of the electromagnetic field vectors at discontinuous interfaces.

Hans Stam studied mathematics at the Delft University of Technology. After his graduation in 1986 he started a doctoral research at the Faculty of Electrical Engineering under the supervision of Professor A.T. de Hoop and Dr. G. Mur. In 1990, he obtained his doctorate with a thesis on the numerical computation of elastodynamic waves in inhomogeneous media. From 1990 to 1991 he served the army at the Physics and Electronics Laboratory TNO in The Hague. At the end of 1991 he joined Shell as a geophysicist/software engineer. Up to 1995 he has been greatly involved in the development of seismic processing software. Currently, his activities are in the area of interactive geophysical software. The title of his thesis is: *A time-domain finite-element method for the computation of three-dimensional acoustic wavefields in inhomogeneous fluids and solids* (1990). In this thesis a hybrid method has been presented that solves numerically space-time acoustic wave problems in a configuration that may consist of fluid and solid parts. In the time direction, a finite-element discretization has been chosen where the time weighting functions are equal to the time expansion functions ("hat" functions). The real problem now is the choice of local and global expansion functions in the discretization of the computational domain. After an extensive theoretical introduction, the problem of the strip load at a fluid and solid boundary has been addressed. In the numerical implementation a problem became visible. In case face elements were used, the symmetrization of the expansion of the stress became a problem. Because the individual local face expansion functions are not symmetric, this condition on the stress has to be enforced by supplementary local equations. How this is to be implemented is still an unsolved problem.

Apart from acoustic methods in the area of exploration geophysics, also electromagnetic methods were being investigated in the laboratory. The next thesis project is an example of that.

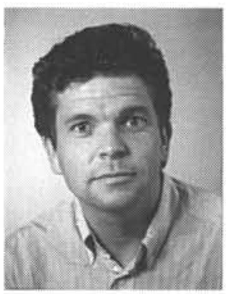

Leendert Combee was born in Amstelveen in 1963. He enrolled as a student in electrical engineering at the Delft University of Technology in 1981. In 1987 he received his master's degree on diffraction of electromagnetic waves in boreholes by bed boundaries. This research was carried out under the supervision of Professor H. Blok of the Laboratory of Electromagnetic Research. After this, Leendert Combee started his Ph.D. research on transient diffusive electromagnetic fields for electromagnetic prospecting under the supervision of Professor A.T. de Hoop. As part of this project, he joined the Electromagnetics Department of Schlumberger-Doll Research, Ridgefield, U.S.A. for four months in 1990. His professional career started off in 1992 at Schlumberger Geco-Prakla, from where he joined the Seismics Department of Schlumberger Cambridge Research in 1993. Here, he has been working on numerous problems involving acoustic and elastic wave-field scattering and propagation in unconsolidated surface layers. Part of his work has been presented at international conferences. The title of his thesis is: *Transient diffusive electromagnetic fields in layered anisotropic media* (1990, cum laude). In this thesis, the structural problem of the diffusion of transient electromagnetic fields into a plane-layered, arbitrary anisotropic earth has been investigated. This implies that on the time scale of interest it has been assumed that the electric displacement currents can be neglected with respect to the conduction currents. To solve the equations governing the behaviour of diffusive electromagnetic fields, a new analytic method has been developed based upon the Cagniard-De Hoop method. With this approach, closed-form analytical expressions in the form of well-behaved integrals are obtained for the time behaviour of the transient electromagnetic field at any point of the configuration. The approach discussed above applies equally well for arbitrary anisotropic and isotropic media.

The research of the next project has been carried out at the Koninklijke/Shell Exploratie en Produktie Laboratorium, Rijswijk, the Netherlands.

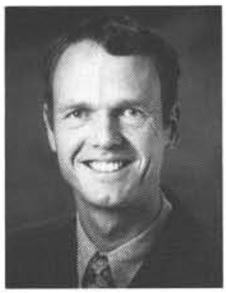

Maarten V. de Hoop was born in Delft, the Netherlands, on April 20, 1961. In 1984, he received his M.Sc. in theoretical physics from the State University of Utrecht. From 1985 to 1992, he was a research geophysicist at Koninklijke/Shell Exploratie en Produktie Laboratorium, Rijswijk, the Netherlands. At the end of this period, he received his Ph.D. from the Delft University of Technology. In 1992, he became program leader and senior scientist at Schlumberger Cambridge Research, Cambridge, U.K. From 1995 to 1996, he was a visiting and research professor at the Center for Wave Phenomena, Colorado School of Mines, Golden, Colorado, U.S.A. Recently, he is also appointed a research professor at the Department of Mathematical and Computer Sciences at the same school. Martijn's primary research experience includes: acoustic, elastic and electromagnetic wave propagation and modelling in anisotropic media; wave scattering in highly discontinuous and random media, as well as the development of multi-scale methods; and multi-dimensional imaging and (non-)linear inversion of scattering data with application to geophysical prospecting. The title of his thesis is: *Directional decomposition of transient acoustic wave fields* (1992, cum laude). Besides Professor De Hoop, this project was also supervised by Professors P.M. van den Berg and J.T. Fokkema. In this thesis an operator formalism has been developed to expand the transient acoustic wave field in a smoothly varying medium, generated by a source localized in space and time, into a superposition of constituents each of which can be interpreted as having travelled up and down with respect to a direction of preference a definite number of times. This is a generalization of the Bremmer coupling series. Both the existence and the convergence of the relevant series have been discussed. The pseudo-differential operator calculus that is the appropriate tool for this, leads to a natural generalization of the concept of slowness surface to multi-dimensionally smoothly varying media. Let the "vertical" direction be the preferred one, then the operator associated with the corresponding generalized vertical slowness induces the full "one-way" wave operator. The latter is loosely denoted as the "parabolic" wave operator. In this exact form, the decomposition reduces the scattering problem in n dimensions to a family of scattering problems in n - 1 dimensional hyperplanes, after which the corresponding results are used in a Neumann series to solve the remaining scattering phenomenon in the direction of preference. The decomposition introduced applies to media with smoothly varying properties. It is not known whether the operators involved can be defined in media with discontinuous properties. The theory leads to integro-differential equations that generate the different constituents (terms in the series). The kernel associated with the relevant integral operator can be approximated in such a way that the matrix representation in the corresponding numerical scheme becomes sparse. In the thesis, much attention has been devoted to this approximation, carried out on the left symbols of the associated pseudo-differential operator about the preferred direction of propagation. The underlying mathematical structure of the subsequent steps in the directional decomposition has been discussed in detail. In the last part of the thesis an extensive discussion of the formulation of an iterative acoustic inverse scattering scheme based on the reciprocity theorem of the time-correlation type has been presented. The thesis inspired a new research project on the directional decomposition of electromagnetic and acoustic wavefields in the laboratory.

The research project on magnetic recording in our laboratory has been terminated with the next thesis.

Dirk Quak was born in Rozenburg, the Netherlands, on September 9, 1942. In 1961, he received his first degree as navigation officer at the Nautical College in Amsterdam. In 1966, he became second mate at the Holland-America Line. After seven years on the high seas he started a study at Delft University of Technology and received his M.Sc. in electrical engineering in 1973. In 1973, he became a member of the scientific staff of the Laboratory of Electromagnetic Research. In 1992, he received his Ph.D. at the Delft University of Technology. The title of his thesis is: *Reproduction of digital signals in magnetic recording* (1992). In this thesis, he has described some fundamental aspects of the process of magnetic storage. In particular, there is a focus on the read process in magnetic recording theory. It has been assumed that the read process can be described by a quasi-static approximation of the electromagnetic field equations. Within this approximation, field integral relations for the magnetic field have been obtained for isotropic and multilayered anisotropic structures. The resulting theory has been applied to calculate the read EMF produced by a Karlqvist head in the two-dimensional approximation. Also, the read performance of single-edge sensitive, single-pole heads for perpendicular recording has been investigated. Much of the theory presented in the thesis comes together in the final problem that has been addressed: digital and harmonic response of two- and three-dimensional electric-current sheet heads.

Finally, the last thesis which, strictly speaking, has not formally been supervised by Professor A.T. de Hoop. However, his involvement and his own work on the topic of the thesis, that started as a research project at Schlumberger Cambridge

Research, Cambridge, U.K., made the formal thesis supervisor, Professor P.M. van den Berg, decide that this project should be discussed as the twenty-second thesis project, supervised by Professor A.T. de Hoop. The Ph.D. student in question fully agreed to this.

Bastiaan P. de Hon was born in Amstelveen, the Netherlands, on May 18, 1966. In 1991, he took his M.Sc. in electrical engineering from the Delft University of Technology. For his master's thesis he conducted research on wave propagation in anisotropic fluids. This research was carried out at the Laboratory of Electromagnetic Research under the supervision of Professor A.T. de Hoop. Under the supervision of Dr. A.L. Kurkjian he spent the summer of 1991 at Schlumberger Cambridge Research, Cambridge, U.K., where he continued the research started by Professor De Hoop on the crosswell space-time domain elastodynamic signal transfer. Caught by the beauty of this topic, he subsequently started his Ph.D. research at the Laboratory of Electromagnetic Research under the supervision of Professor P.M. van den Berg and Professor A.T. de Hoop. In June 1996, he took his doctoral degree from the Delft University of Technology. Presently, he is employed at the Eindhoven University of Technology in the Electromagnetics Group of Professor A.G. Tijhuis as an Academy Research Scientist installed by the Royal Netherlands Academy of Arts and Sciences (KNAW). In Eindhoven, his research is focused on the electromagnetic wave propagation in configurations involving waveguiding structures. The title of his thesis is: *Transient cross-borehole elastodynamic signal transfer through a horizontally stratified anisotropic formation* (1996, cum laude). A closed-form expression has been derived for the transient acoustic pressure in a borehole due to the action of a volume injection source in another borehole in a typical cross-well seismic setting with cased boreholes embedded in a horizontally stratified anisotropic solid formation. To account for the general anisotropy and the geometric complexity due to the occurrence of both vertical and horizontal structures, a modular and universal method has been developed. This method is based on the splitting matrix formalism by which the elastic wavefield in the anisotropic solid is decomposed in terms of its down- and upgoing wavefield constituents. The pertaining formalism comprises a unification of the theory on surface waves within the framework of the Barnett-Lothe tensor and the established theory concerning the down/up decomposition of wavefields in the complex horizontal-slowness plane. A numerically expedient implementation to the Cagniard-De Hoop method has been derived, and the existence and uniqueness of surface waves were discussed. The elastic-wave radiation from a fluid-filled cased borehole into an anisotropic formation is adequately evaluated in the quasi-static limit, leading to a tube-wave description of the wave motion inside the borehole fluid. Here, an elastostatic realization of the Barnett-Lothe tensor facilitates the application of vectorial conformal mapping, which has been used to handle general anisotropic formations. Further, the influence of a borehole casing on the elastic-wave radiation has been analyzed, and the scattering of tube waves at horizontal interfaces has been discussed. The wave motion inside a fluid-filled cased borehole, as it is induced by an incident elastic wavefield, has been evaluated with the aid of a fluid/solid reciprocity theorem. Upon assembling the modules, the transient crosswell Green's function thus constructed comprises a powerful tool in the identification of the distinct events. Through illustrative numerical examples involving both the Green's functions and the associated pressure responses to source wavelets, various physical phenomena have been discussed, such as wave conversion and multiples, secondary tube-wave source and receiver arrivals, triplication due to the anisotropy, Rayleigh waves, Stoneley waves and head waves travelling along horizontal interfaces, pseudo-conical waves emanating from a borehole at post-critical angles in case the tube-wave speed exceeds one of the wavespeeds in the formation, and tunneling-like phenomena for proximate boreholes in fast formations.

4. Conclusions

From the discussion from Adrian de Hoop's own contributions to wavefield science and the overview of that of his Ph.D. students a few things become clear. His work has ranged from rather abstract (general reciprocity theorems) to the applied (numerical computations), but a common thread through all his work has always been the search for physical insight in a rigorous mathematical approach. This thread is certainly visible in the work of his students. When Adrian de Hoop tackles a problem, it always becomes clearer and his solutions always seem more rigorous and intuitive than what had come before. Besides the element of intuition, certainly his more recent work breathes the quest for beauty. In example after example throughout his work and that of his students, he has shown how the most general principles - such as reciprocity and causality - can illuminate specific problems. Moreover, he has infected his students and colleagues with the same vision, the same high standards. His depth and breadth of knowledge and his willingness to discuss a wide variety of problems is extremely enriching. Wholeheartedly, I can agree with a statement made by one of his foreign colleagues: "Adrian is a joy to work with, and his work is a joy to study".

The last two words of the title of this paper are: "and beyond". Adrian, for many years to come there will be a place in your Laboratory of Electromagnetic Research. A place, where you can continue - and now without any formal obligations - to work on problems in one of the main passions in your life: wavefield sciences.

Adrian, I was most fortunate to be one of your students.

Acknowledgements

In writing this paper I have used and quoted from two letters evaluating Professor De Hoop's scientific qualifications. The writers of these letters are acknowledged.

List of books and journal papers of A.T. de Hoop

Schouten, J.P., and A.T. de Hoop, 1952, Huygens' principle in diffraction problems, Tijdschrift van het Nederlands Radiogenootschap", **17**, 45-62. (In Dutch.)

De Hoop, A.T., 1953, On the propagation constant in gentle circular bends in rectangular wave guides - matrix theory, Journal of Applied Physics, **24**, 1325-1327.

De Hoop, A.T., 1954, On the scalar diffraction by a circular aperture in an infinite plane screen, Applied Scientific Research, Section B, **4**, 151-160.

De Hoop, A.T., 1955a, On integrals occurring in the variational formulation of diffraction problems, Proceedings Koninklijke Nederlandse Akademie van Wetenschappen, **B58**, 325-330.

De Hoop, A.T., 1955b, Variational formulation of two-dimensional diffraction problems with application to diffraction by a slit, Proceedings Koninklijke Nederlandse Akademie van Wetenschappen, **B58**, 401-411.

Schouten, J.P., and A.T. de Hoop, 1957, Sur la rflection d'une onde lectromagntique plane par une surface rugueuse parfaitement conductrice, Annales des Telecommunications, **12**, 211-214.

De Hoop, A.T., 1958a, Representation theorems for the displacement in an elastic solid and their application to elastodynamic diffraction theory, Ph.D.-thesis, Delft University of Technology, Delft, The Netherlands, 84 pp.

De Hoop, A.T., 1958b, On the plane-wave extinction cross-section of an obstacle, Applied Scientific Research, Section B, **7**, 463-472.

De Hoop, A.T., 1959, A reciprocity theorem for the electromagnetic field scattered by an obstacle, Applied Scientific Research, Section B, **8**, 135-140.

De Hoop, A.T., 1960, A modification of Cagniard's method for solving seismic pulse problems, Applied Scientific Research, Section B, **8**, 349-356.

De Hoop, A.T., and H.J. Frankena, 1960, Radiation of pulses generated by a vertical electric dipole above a plane, non-conducting, earth, Applied Scientific Research, Section B, **8**, 369-377.

De Hoop, A.T., 1961a, Impulsive radiation from a vertical electric dipole situated above a plane, non-conducting earth, Simon Stevin, Wis- en Natuurkundig Tijdschrift, **35**, 49-52.

De Hoop, A.T., 1961b, Theoretical determination of the surface motion of a uniform elastic half-space produced by a dilational, impulsive, point source, C.N.R.S. Colloque 111 sur la propagation des ébranlements dans les milieux hétérogènes, Marseille, 21-32.

De Hoop, A.T., 1965, A note on the propagation of waves in a continuously layered medium, Applied Scientific Research, Section B, **12**, 74-80.

De Hoop, A.T., 1966, An elastodynamic reciprocity theorem for linear, viscoelastic media, Applied Scientific Research, **16**, 39-45.

De Hoop, A.T., 1968, A reciprocity relation between the transmitting and the receiving properties of an antenna, Applied Scientific Research, **19**, 90-96.

De Hoop, A.T., 1970, The surface line source problem in elastodynamics, De Ingenieur, Electronica en Telecommunicatie **1**, ET19-ET21.

De Hoop, A.T., 1972, Reciprocity in antenna theory, De Ingenieur, Electronica en Telecommunicatie **6**, ET71-ET74.

De Hoop, A.T., and G. de Jong, 1974, Power reciprocity in antenna theory, Proceedings IEE, **121**, 1051-1056.

De Hoop, A.T., 1975a, The N-port receiving antenna and its equivalent electrical network, Philips Research Reports, **30**, 302*-315*. (Issue in honour of C.J. Bouwkamp.)

De Hoop, A.T., 1975b, Electromagnetic field theory", Rotterdam, Delftse Universitaire Pers, 1975, 351 pp. (In Dutch.)

De Hoop, A.T., 1977, General considerations on the integral-equation formulation of diffraction problems, in: Modern Topics in Electromagnetics and Antennas, Peter Peregrinus Ltd., London, Chapter 6, 6.1-6.59.

De Hoop, A.T., 1979, Pulsed electromagnetic radiation from a line source in a two-media configuration, Radio Science, **14**, 253-268.

De Hoop, A.T., 1981, Theorem on the maximum absorption of electromagnetic radiation by a scattering object of bounded extent, Radio Science, **16**, 971-974.

Michielsen, B.L., G.C. Herman, A.T. de Hoop and D. De Zutter, 1981, Three-dimensional relativistic scattering of electromagnetic waves by an object in uniform translational motion, Journal of Mathematical Physics, **22**, 2716-2722.

De Hoop, A.T., 1982a The vector integral-equation method for computing three-dimensional magnetic fields, in: Integral Equations and Operator Theory, Basel, Birkhauser Verlag, **5**, 458-474.

De Hoop, A.T., 1982b, Motional influences on magnetic reproduction: an analysis based on the reciprocity theorem, IEEE Transactions on Magnetics, **MAG-18**, 758-762.

De Hoop, A.T., and J.H.M.T. van der Hijden, 1983, Generation of acoustic waves by an impulsive line source in a fluid/solid configuration with a plane boundary, Journal of the Acoustical Society of America, **74**, 333-342.

Van den Berg, P.M., A.T. de Hoop, A. Segal and N. Praagman, 1983, A computational model of the electromagnetic heating of biological tissue with application to hyperthermia and cancer therapy", IEEE Transactions on Biomedical Engineering, **BME-30**, 797-805.

De Hoop, A.T., 1984, A time-domain energy theorem for scattering of plane electromagnetic waves, Radio Science, **19**, 1179 - 1184.

Van den Berg, P.M., and A.T. de Hoop, 1984, Reflection and transmission of electromagnetic waves at a rough interface between two different media, IEEE Transactions on Geoscience and Remote Sensing, **GE-22**, 42-52.

De Hoop, A.T., and J.H.M.T. van der Hijden, 1984, Generation of acoustic waves by an impulsive point source in a fluid/solid configuration with a plane boundary, Journal of the Acoustical Society of America, **75**, 1709-1715.

De Hoop, A.T., 1985a, A time-domain energy theorem for scattering of plane acoustic waves in fluids, Journal of the Acoustical Society of America, **77**, 11 - 14.

De Hoop, A.T., 1985b, A time-domain energy theorem for the scattering of plane elastic waves, Wave Motion, **7**, 569-577.

De Hoop, A.T., 1985c, Time-domain far-field scattering of plane scalar waves in the Born approximation, Journal of the Optical Society of America A, **2**, 1961-1964.

De Hoop, A.T., and J.H.M.T. van der Hijden, 1985, Seismic waves generated by an impulsive point source in a solid/fluid configuration with a plane boundary, Geophysics, **50**, 1083-1090.

Mur, G., and A.T. de Hoop, 1985, A finite-element method for computing three-dimensional electromagnetic fields in inhomogeneous media", IEEE Transactions on Magnetics, **MAG-21**, 2188-2191.

Quak, D., and A.T. de Hoop, 1986, Time domain Born approximation to the far-field scattering of plane electromagnetic waves by a penetrable object, Radio Science, **21**, 815-821.

Quak, D., A.T. de Hoop and H.J. Stam, 1986, Time-domain far-field scattering of plane acoustic waves by a penetrable object in the Born approximation, Journal of the Acoustical Society of America, **80**, 1228 - 1234.

De Hoop, A.T., 1987, Time-domain reciprocity theorems for electromagnetic fields in dispersive media, Special Issue of Radio Science, **22**, 1171-1178.

De Hoop, A.T., 1988a Large-offset approximations in the modified Cagniard method for computing synthetic seismograms: a survey, Geophysical Prospecting, **36**, 465-477.

De Hoop, A.T., 1988b, Acoustic radiation from impulsive sources in a layered fluid, Nieuw Archief voor Wiskunde, Serie 4, **6**, 111-129.

De Hoop, A.T., 1988c, Time-domain reciprocity theorems for acoustic wave fields in fluids with relaxation, Journal of the Acoustical Society of America, **84**, 1877-1882.

De Hoop, A.T., and H.J. Stam, 1988, Time-domain reciprocity theorems for elastodynamic wave fields in solids with relaxation and their application to inverse problems, Wave Motion, **10**, 479-489.

De Hoop, A.T., and M.L. Oristaglio, 1988, Application of the modified Cagniard technique to transient electromagnetic diffusion problems, Geophysical Journal, **94**, 387-397.

Van der Weiden, R.M., and A.T. de Hoop, 1989, Boundary integral equations for the computational modeling of three-dimensional groundwater flow problems, Computational Mechanics, **4**, 283-291.

Quak, D., and A.T. de Hoop, 1989, Shielding of wire segments and loops in electric circuits by spherical shells, IEEE Transactions on Electromagnetic Compatibility, **31**, 230-237.

De Hoop, A.T., 1990a, Acoustic radiation from an impulsive point source in a continuously layered fluid - An analysis based on the Cagniard method, Journal of the Acoustical Society of America, **88**, 2376-2388.

De Hoop, A.T., 1990b, Reciprocity theorems for acoustic wave fields in fluid/solid configurations, Journal of the Acoustical Society of America, **87**, 1932-1937.

Stam, H.J., and A.T. de Hoop, 1990, Theoretical considerations on a finite-element method for the computation of three-dimensional space-time elastodynamic wave fields, Wave Motion bf 12, 67-80.

Tijhuis, A.G., and A.T. de Hoop, 1990, Report on R.C.P. 264: Rencontre Interdisciplinaire: Problèmes Inverses, IEEE Antennas and Propagation Magazine, **32**, 68-70.

Verweij, M.D., and A.T. de Hoop, 1990, Determination of seismic wavefields in arbitrarily continuously layered media using the modified Cagniard method, Geophysical Journal International, **103**, 731-754.

De Hoop, A.T., 1991, Convergence criterion for the time-domain iterative Born approximation to scattering by an inhomogeneous, dispersive object, Journal of the Optical Society of America A, **8**, 1256-1260.

De Hoop, A.T., 1991, Reciprocity, discretization, and the numerical solution of direct and inverse electromagnetic radiation and scattering problems, Invited Paper, Proceedings of the IEEE, Special Issue on Electromagnetics, **79**, 1421-1430.

De Hoop, A.T., and M.D. Verweij, 1991, Transient acoustic radiation in a continuously layered fluid-An analysis based on the Cagniard method, In: H.L. Bertoni and L.B. Felsen (Eds.), Directions in Electromagnetic Wave Modeling, Plenum Press, New York, 145-152.

De Hoop, A.T., 1992, Reciprocity, causality, and Huygens' principle in electromagnetic wave theory, In: H. Blok, H.A. Ferwerda and H.K. Kuiken (Eds.), Huygens' Principle 1690-1990: Theory and Applications, Elsevier, Amsterdam, 171-192.

De Hoop, M.V., and A.T. de Hoop, 1992, Scalar space-time waves in their spectral-domain first- and second-order Thiele approximation, Wave Motion, **15**, 229-265.

De Hoop, A.T., 1993, Similarity in wave propagation under a global relaxation law, In: R. Kleinman, T. Angell, D. Colton, F. Santosa, I. Stakgold (Eds.), Second International Conference on Mathematical and Numerical Aspects of Wave Propagation, 180-187.

Verweij, M.D., and A.T. de Hoop, 1993, Analysis of time-domain acoustic wave fields in arbitrarily continuously layered configurations based on the modified Cagniard method", In: Lau, R.L., D. Lee, A.R. Robinson (Eds.), Computational Acoustics, **1**, 399-409.

De Hoop, M.V., and A.T. de Hoop, 1993, Interface reflection of spherical acoustic waves in the first- and second-order rational parabolic approximations and their artifacts, Journal of the Acoustical Society of America, **93**, 22-35.

De Hoop, A.T., and D. Quak, 1993, Interference analysis of multichannel transmission lines-A system's analysis, In: Laven, F.J.H. (Ed.), Elektromagnetische compatibiliteit in theorie en praktijk, Holland Elektronika, Zoetermeer, 11 pp.

De Hoop, A.T., B.P. de Hon and A.L. Kurkjian, 1994, Calculation of transient tube-wave signals in cross-borehole acoustics, Journal of the Acoustical Society of America, **95**, 1773-1789.

De Hoop, M.V., and A.T. de Hoop, 1994, Elastic wave up/down decomposition in inhomogeneous and anisotropic media: an operator approach and its approximations, Wave Motion, **20**, 57-82.

Habashy, T.M., M.L. Oristaglio and A.T. de Hoop, 1994, Simultaneous nonlinear reconstruction of two-dimensional permittivity and conductivity, Radio Science, **29**, 1101-1118.

Olyslager, F., D. de Zutter, and A.T. de Hoop, 1994, New reciprocal circuit model for lossy waveguide structures based on the orthogonality of the eigenmodes, IEEE Transactions on Microwave Theory and Techniques, **42**, 2261-2269.

De Hoop, A.T., 1995, Similarity analysis of the elastic wave motion in a dissipative solid under a global relaxation law, In: J.L. Wegner and F.R. Norwood (Eds.), Nonlinear Waves in Solids, ASME Book **AMR 137**, 77-82.

De Hon, B.P., A.T. de Hoop and A.L. Kurkjian, 1995, Transfer of transient signals between two fluid-filled boreholes embedded in an elastic formation - a closed-form solution", In: J.L. Wegner and F.R. Norwood (Eds.), Nonlinear Waves in Solids, ASME Book **AMR 137**, 317-322.

De Hoop, A.T., S. Zeroug and S. Kostek, 1995, Transient analysis of the transmitting properties of a focused acoustic transducer with an arbitrary rim, Journal of the Acoustical Society of America, **98**, 1767-1777.

De Hoop, A.T., 1995, Handbook of Radiation and Scattering of Waves, Academic Press Limited, London, 1085 pp.

Das, U.C. and A.T. de Hoop, 1995, Efficient computation of apparent resistivity curves for depth profiling of a layered earth", Geophysics, **60**, 1691-1697.

De Hoop, A.T., 1996, The initial-value problems in acoustics, elastodynamics and electromagnetics, Wave Motion, **23**, 121-137.

De Hoop, A.T., M.L. Oristaglio, T.M. Habashy and C. Torres-Verdin, 1996, Asymptotic ray theory for transient diffusive electromagnetic fields, Radio Science, **31**, 41-49.

A Brief History of Electromagnetism

Douglas S. Jones
Department of Mathematics and Computer Science
University of Dundee, DD1 4HN, Scotland

While studies of electricity and magnetism separately go back over a millennium the investigation of their combination as electromagnetism has been undertaken only for a century or so. But in that comparatively short time tremendous developments have occurred and today it is difficult to realise what life would be like without the many applications of electromagnetism. Indeed many people are not aware that electromagnetism underpins the facilities which they take for granted: watching television, speaking on a mobile phone and using a credit card all made possible by electromagnetic waves.

Numerous scientists and engineers from different countries have been involved in the progress of electromagnetism from its early beginnings to its present state. The subject has required always a close interplay between theory and experiment. The theory is not simple - it needs a familiarity with sophisticated mathematical analysis plus, nowadays, a thorough knowledge of the capabilities of computers. Since the lecture is intended to be non-technical, most of the theoretical advances will be left undescribed. This will mean the omission of any tribute to eminent theorists and the important contributions which they have made in electromagnetism, but this is unavoidable and does not lessen our admiration for their achievement.

In fact, the starting point for theory today is the same as it was in the 1860's when a set of equations was devised by Maxwell. Maxwell showed remarkable insight in setting up the equations which have proved so long-lasting because at the time there was no way of checking them experimentally. It was not until near the end of the 1880's that verification was forthcoming in a superb series of experiments by Hertz. The magnitude of Hertz' feat in converting a theory into a practically useful tool cannot be overestimated; it is commemorated these days by the abbreviation Hz which appears in the description of radio stations, computers and the supply of electricity, to mention some examples.

After Hertz there was considerable theoretical activity but the 1920's were reached before the broadcasting of radio programs to the public commenced in Britain. Thereafter, the pace quickened. In the 1930's Baird transmitted pictures successfully. Voice communication with aircraft became feasible and radar was invented. By the 1960's television, in black and white, was commonplace and it was not long before the transmissions were in colour. This was also the decade in which signals from a laser were first sent along a thin glass wire - now known as an optical fibre. As a result cable television became feasible, though its adoption by the public has varied widely from country to country. One reason is that the cables have to be connected to each household and there is a competitor in television transmission from satellites. Other modern applications of electromagnetism will be referred to in this lecture.

Hertz' Experiments – Verification of the Unification

Martin D. Verweij
Laboratory of Electromagnetic Research, Faculty of Electrical Engineering
Centre for Technical Geoscience, Delft University of Technology
P.O. Box 5031, 2600 GA Delft, the Netherlands

Abstract

The historical context of the experiments by which Hertz showed the validity of Maxwell's theory of electromagnetism is sketched. The significance of several of these experiments is explained. Moreover, a description is given of a copy of the setup that was used by Hertz to manipulate beams of electromagnetic waves. With this setup it may be demonstrated, in the same way as more than 100 years ago, that electromagnetic waves behave in essentially the same manner as light waves.

1. Introduction

Electricity and magnetism, for thousands of years known to mankind as two seemingly independent phenomena, first showed their close relationship in experiments by Oerstedt (1820; attraction of a permanent magnet by an electric current) and Faraday (1831; induction of an electric tension due to a change of enclosed magnetic flux). Combining the theories of electricity and magnetism to account for these facts, a theory was arrived at that is now known as electrodynamics. In 1864, Maxwell proposed a theory that linked electricity and magnetism in a closer way than electrodynamics. Nowadays this theory is known as electromagnetics. It implied that electric and magnetic disturbances propagate in a combined fashion in the form of electromagnetic waves, and gave rise to the suggestion that light is an electromagnetic wave. Despite its elegance, many scientists doubted Maxwell's theory. The situation remained undecided until 1887/1888, when Hertz conducted several experiments that showed the existence of electromagnetic waves.

In this paper we will shortly explain the core of Maxwell's theory. Next, some early experiments of Hertz will be discussed. Finally, a description will be given of a demonstration setup, owned by the Faculty of Electrical Engineering, Delft University of Technology. Through this setup, Hertz' experiments with beams of electromagnetic waves may be repeated in the original fashion.

2. Maxwell's theory

A clear description of Maxwell's theory of electromagnetism may be found in his work 'A Treatise on Electricity and Magnetism' (Maxwell, 1873). Here we will present the most important equations in their original quaternion form (left), and their current form (right). The symbols and names of the quantities that appear in those equations are listed in Table 1.

Table 1. The symbols and names of the quantities that appear in the equations

Symbol (Maxwell)	Symbol (Present)	Name (Maxwell)	Name (Present)
$\mathfrak{A}$	$\boldsymbol{A}$	Electromagnetic momentum	Magnetic (vector) potential
$\mathfrak{B}$	$\boldsymbol{B}$	Magnetic induction	Magnetic flux density
$\mathfrak{C}$	$\boldsymbol{J}^{\max}$	Total electric current	Maxwell current density
$\mathfrak{D}$	$\boldsymbol{D}$	Electric displacement	Electric flux density
$\mathfrak{E}$	$\boldsymbol{E}$	Electromotive intensity	Electric field strength
$\mathfrak{G}$	$\boldsymbol{v}$	Velocity	Velocity
$\mathfrak{H}$	$\boldsymbol{H}$	Magnetic force	Magnetic field strength
$\mathfrak{K}$	$\boldsymbol{J}$	Current of conduction	Electric current density
Ψ	V	Electric potential	Electric (scalar) potential
C	σ	Conductivity	Conductivity
K	ε	Dielectric inductive capacity	Permittivity
μ	μ	Magnetic inductive capacity	Permeability

First of all, according to Maxwell the equation for the magnetic induction is

$$\mathfrak{B} = V\nabla\mathfrak{A} \quad \Longleftrightarrow \quad \boldsymbol{B} = \nabla \times \boldsymbol{A}. \tag{1}$$

The equation for the electromotive force, for a moving observer, is given by

$$\mathfrak{E} = V\mathfrak{G}\mathfrak{B} - \dot{\mathfrak{A}} - \nabla\Psi \quad \Longleftrightarrow \quad \boldsymbol{E} = \boldsymbol{v} \times \boldsymbol{B} - \frac{\partial \boldsymbol{A}}{\partial t} - \nabla \cdot \boldsymbol{V}. \tag{2}$$

Moreover, the magnetic induction is related to the magnetic force according to

$$\mathfrak{B} = \mu\mathfrak{H} \quad \Longleftrightarrow \quad \boldsymbol{B} = \mu\boldsymbol{H}. \tag{3}$$

Considering an observer with a velocity $\boldsymbol{v} = \boldsymbol{0}$, taking the rotation of Eq. (2), and substituting Eqs. (1) and (3), we arrive at

$$\nabla \times \boldsymbol{E} + \mu\frac{\partial \boldsymbol{H}}{\partial t} = \boldsymbol{0}. \tag{4}$$

This is nowadays called Maxwell's second equation. Further, Maxwell introduces the equation for the (total) electric current

$$4\pi\mathfrak{C} = V\nabla\mathfrak{H} \quad \Longleftrightarrow \quad \boldsymbol{J}^{\max} = \nabla \times \boldsymbol{H}, \tag{5}$$

the equation for the current of conduction (Ohm's law)

$$\mathfrak{K} = C\mathfrak{E} \quad \Longleftrightarrow \quad \boldsymbol{J} = \sigma\boldsymbol{E}, \tag{6}$$

and the equation for the electric displacement

$$\mathfrak{D} = \frac{1}{4\pi}K\mathfrak{E} \quad \Longleftrightarrow \quad \boldsymbol{D} = \varepsilon\boldsymbol{E}. \tag{7}$$

The important step Maxwell takes is to consider the (total) electric current as the sum of the conduction current and the time derivative of the electric displacement, thus

$$\mathfrak{C} = \mathfrak{K} + \dot{\mathfrak{D}} \quad \Longleftrightarrow \quad \boldsymbol{J}^{\max} = \boldsymbol{J} + \frac{\partial \boldsymbol{D}}{\partial t}. \tag{8}$$

If we combine these four equations, we obtain

$$-\boldsymbol{\nabla} \times \boldsymbol{H} + \varepsilon \frac{\partial \boldsymbol{E}}{\partial t} + \sigma \boldsymbol{E} = \boldsymbol{0}. \tag{9}$$

This is nowadays referred to as Maxwell's first equation. As explained further on in Maxwell's treatise, his theory implies the existence of electromagnetic waves that propagate with a velocity

$$V = 1/\sqrt{K\mu} \quad \Longleftrightarrow \quad c = 1/\sqrt{\varepsilon\mu}. \tag{10}$$

Moreover, he suggested that light is an electromagnetic phenomenon. After comparing the value of V with the velocity of light, both for air, he concluded that

> 'In the meantime our theory, which asserts that these two quantities are equal, and assigns a physical reason for this equality, is certainly not contradicted by the comparison of these results such as they are.'

Thus, according to Maxwell, light is a specific manifestation of the waves that logically follow from the unification of electricity and magnetism.

3. Hertz' experiments

By many scientists of those days, Maxwell's theory was regarded with doubt. A significant number of people believed that forces that act over a distance should propagate with an infinite velocity in order not to loose their grip on moving objects. This was in contradiction to the finite wavespeed that had been predicted by Maxwell. Another group of scientists, among which Helmholtz, had created a more elaborate theory of electromagnetism, from which Maxwell's theory could be arrived at by making three assumptions. These were (Hertz, 1893)

> 'first, that changes of dielectric polarization in non-conductors produce the same electromagnetic forces as do the currents which are equivalent to them; secondly, that electromagnetic forces as well as electrostatic are able to produce dielectric polarizations; thirdly, that in all these respects air and empty space behave like all other dielectrics.'

In 1879 the Berlin Academy of Science proposed a prize for an experimental proof of any of the first two assumptions. Helmholtz offered Hertz the possibility to work on the case, but Hertz soon came to the conclusion that with the methods available at that time, it was impossible to perform a decisive experiment. After finding, in 1886, a way of detecting very rapid electric oscillations by means of a tuned loop (resonator) with an adjustable spark gap, he soon found a method to prove the first assumption.

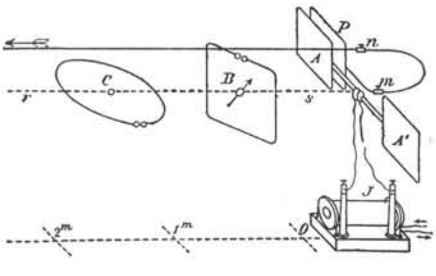

Figure 1. Hertz' first experimental setup for measuring the velocity of electromagnetic waves in air. (Reprinted with permission of Dover Publications, Inc.)

While working on a method for testing the second assumption, Hertz became convinced that only by proving the third assumption the full importance of Maxwell's theory would become clear. Observation of electromagnetic waves with a finite propagation velocity would show the validity of this assumption. Hertz' first experimental setup for measuring the velocity of electromagnetic waves in air is depicted in Figure 1 (Hertz, 1893). Through the primary winding of the induction coil J flows a current that is repeatedly interrupted. At the time of interruption, a very high tension is induced in the secondary winding, which results in a discharge over the spark bridge that is connected to the plates A and A'. Moreover, a current pulse starts to travel along a wire that is capacitively coupled with plate A by means of plate P. By choosing an appropriate orientation for the resonator B or C, the electromagnetic action that propagates through the air and the electromagnetic action that is due to the pulse along the wire, may be picked up in equal amounts. Moving the resonator along the line rs, Hertz observed an interference pattern. From the period of the interference pattern and the known velocity of the pulse along the wire, Hertz found a velocity of $320,000$ km/s for the electromagnetic action in air. In this way he had proved the third assumption, and the validity of Maxwell's theory. Unfortunately, the relative complexity of the experiment left open many points of doubt for the critics, and Hertz needed a more direct way of showing the existence of electromagnetic waves.

Following the behaviour of the electromagnetic action throughout his laboratory, Hertz discovered that the spark in his resonator became much stronger a small distance away from the walls and metal objects. He realized that this was caused by the interference between an incoming and a reflected electromagnetic wave. Soon, measurements in front of a zinc plate resulted in the interference pattern of Figure 2 (Hertz, 1893).This pattern revealed the wave character and the finite velocity of the electromagnetic action in a persuasive way. But Hertz went on with his investigations, and his attempts to form a beam of electromagnetic waves by means of a parabolic mirror resulted in an experimental setup by which he was able to show that in many respects electromagnetic waves behave in the same manner as light waves with a wavelength that is a million times smaller.

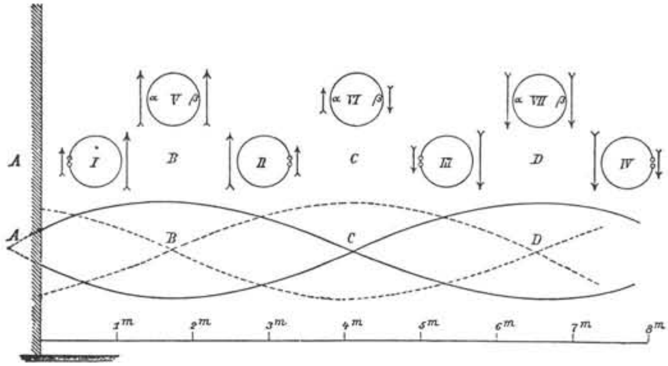

Figure 2. The interference pattern due to an incoming and a reflected electromagnetic wave at a zinc plate. (Reprinted with permission of Dover Publications, Inc.)

4. The demonstration setup

The Faculty of Electrical Engineering, Delft University of Technology, owns a working copy of this setup[1]. Its largest components are two parabolic mirrors, each of which has an antenna located exactly on its focal line and at half its height. One mirror is used for sending an approximately parallel beam of electromagnetic waves, the other for receiving it. Both mirrors have a height of 2.0 m, a breadth of 1.2 m, a depth of 0.7 m, and a focal length of 12.5 cm. The dimensions of these mirrors correspond to those of the originals, the sending version of which is depicted in Figure 3 (Hertz, 1893). At the sending side, an electromagnetic wave is generated by means of a spark discharge between the two halves of a dipole. This dipole is shown in Figure 3a. The wavelength of the dominant wave is approximately twice the length of the dipole, so $\lambda \approx 2 \times 26$ cm, which corresponds to a frequency of $f \approx 600$ MHz. The high tension that causes the spark comes from a large induction coil capable of generating several hundred kilovolt. The primary current is switched on and off by means of a rotary switch that has mercury covered contacts to avoid burn-in and that is immersed in alcohol to extinguish the sparks that occur at these contacts. At the receiving side, a dipole with a length of 1.0 m has been connected to an adjustable spark bridge. This construction may be seen in Figure 3b. The sparks at the receiver are always very weak. To increase the visible effects for demonstration purposes, the spark bridge is replaced by a small neon bulb. With this setup, most of the experiments described in the article 'On electric radiation' (Hertz, 1893) may be reproduced. In particular, using the sending mirror, a plane metal plate, and a resonator with a small neon bulb, it is possible to show the existence of the interference pattern near the plate. Further, using both mirrors, rectilinear propagation from one mirror to the other

[1]The author gratefully acknowledges the Working Group of the History of Electrical Engineering for the possibility to use this demonstration setup.

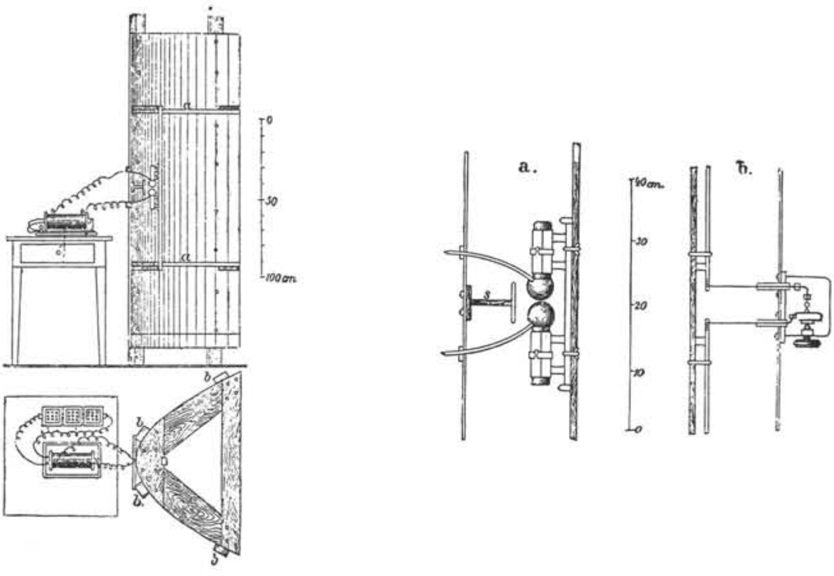

Figure 3. The sending mirror, the sending dipole (a), and the receiving antenna with the adjustable spark bridge (b).

may be demonstrated. Finally, by placing both mirrors under an angle and using the metal plate as a plane mirror, a reflection experiment may be performed.

5. Conclusions

By means of the experiments described above, Hertz has shown that electromagnetic waves exist and that they behave in principally the same manner as light waves. In this way he verified the validity of Maxwell's theoretical unification of electricity and magnetism. Maxwell's theory not only provides an elegant way for describing and predicting complicated phenomena, but it also constitutes a solid basis for powerful modelling tools like reciprocity theorems (De Hoop, 1995).

References

De Hoop, A. T., 1995, Handbook of Radiation and Scattering of Waves, Academic Press Limited, London.

Hertz, H., 1892, Untersuchungen über die Ausbreitung der Elektrischen Kraft, Johann Ambrosius Barth, Leipzig, English translation: H. Hertz, Electric Waves, Macmillan and Company, London, 1983.

Maxwell, J. C., 1873, A Treatise on Electricity and Magnetism, Clarendon Press, Oxford.

Acknowledgements

The editors express their gratitude to the following organizations who made the symposium possible by a generous financial support:

- Schlumberger-Doll Research, Ridgefield, Connecticut, U.S.A.
- Schlumberger Cambridge Research, Cambridge, U.K.
- Shell Nederland B.V., Rotterdam, the Netherlands
- KPN Research, Leidschendam, the Netherlands

Our special thanks go to the people of the Digital Graphics and Photographics Centre, Faculty of Electrical Engineering, Delft University of Technology, for their assistance in the lay-out of this symposium book; to Ms. Jane Zaat-Jones, for improving the English phrasing; and to Ms. Toke Hoek, who provided valuable assistance in the planning and organization of the symposium.